

I. AN EASILY ACCESSIBLE TOOLBOX OF FUNCTIONALIZED MACROCYCLES AND ROTAXANES

1. Purpose of Study

“...Ultimately, we can do chemical synthesis.... The chemist does a mysterious thing when he wants to make a molecule. He sees that it has got that ring, so he mixes this and that, and he takes it, and he fiddles around. And, at the end of a difficult process, he usually does succeed in synthesizing what he wants...”

*Richard Feynmann
from “There’s a plenty of room at the bottom”¹*

Technology is blooming and it seems to grow exponentially in the following decades. When we try to envisage the future of technology, it is probably easy to expect innovations like computer circuitry getting denser and faster or visualizations of smaller things with better-resolution microscopes. What about a swallowable surgical robot of which the hands are controlled by an operator’s hands? As this latter one, first two issues were once, but not long ago, just imaginary. Nowadays, they are a few of the many interests of nanotechnology².

One of the first and best known ideas on achieving nanosystems was initiated by Richard Feynmann (in his talk titled “There’s a Plenty of Room at the Bottom”, 1959) and established later by K. Eric Drexler. In his book *Nanosystems, molecular machinery, manufacturing, and computation*³, Drexler describes a range of molecular machines based on stiff, easily-modelled covalent structures. Construction of such machines will require programmable molecular assemblers (or special-purpose molecular mills) able to position reactive molecules with atomic precision, guiding chemical reactions to build up complex structures. Thus, such machines are beyond the reach of today’s laboratory synthesis capabilities, only within reach of today’s computational modelling techniques⁴. To represent the idea of such a machine, among many examples, we may look at a “fine-motion controller for molecular assembly” or so called a “molecular manipulator”. In his book, Drexler presented several designs of such machines one of which is supposed to contain an arm of 4 million atoms on a 100 nm-scale. He also presented a much smaller design of 2,596 atoms of which the picture can be seen below in Figure 1. The exciting feature of these designs is that they are designed to atomic precision - that is, the machine is designed atom-by-atom. Drexler described these machines (the molecular assemblers) as a machine containing an arm “that must be able to move his “hand” by many atomic diameters, position it with fractional-atomic-diameter accuracy, then execute finely-controlled motions to transfer one or a few atoms in a guided chemical reaction. Our arms use muscles and joints for large motions, but

more finely-controlled finger motions for precision. Assembler mechanisms will likely be designed along similar lines.”

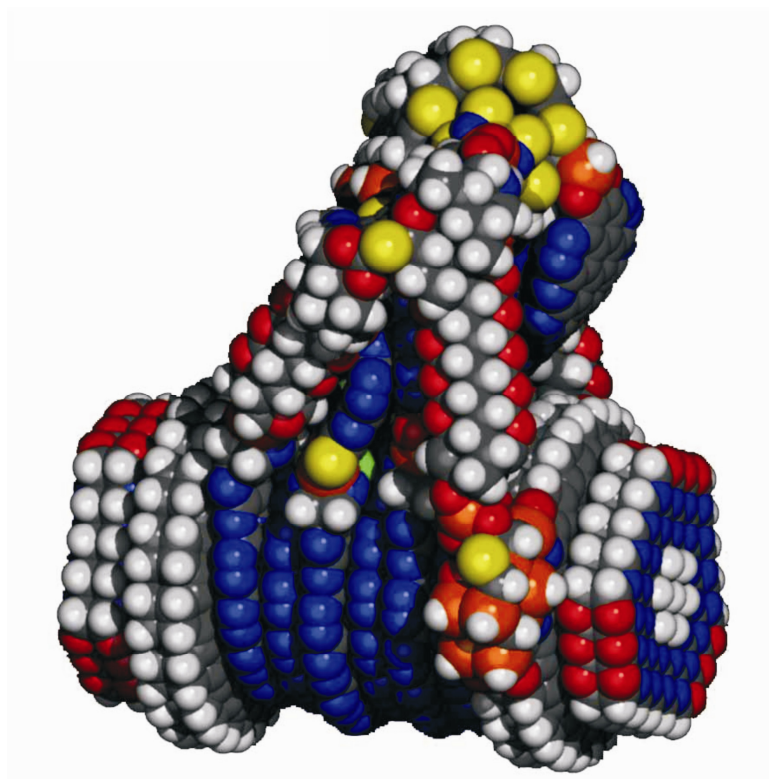


Figure 1. Drexler's atomic-precision “molecular assembler” of 2.596 atoms⁴.

As stated before, these molecular assemblers and many other theoretical artificial molecular machines that could facilitate manufacturing at the molecular size, act as a molecular gear or a pump, although very precisely described, are only computed models. Designing these machines atom-by-atom is quite appealing, though is an impractical way of production to our knowledge of chemistry and physics for today. This issue has caused a great debate between the Nobel Laureate Richard Smalley and Drexler himself, too. Smalley argued that chemistry is extremely complicated, reactions are hard to control, and that a universal assembler is science fiction. Drexler and colleagues, however, noted that Drexler never proposed universal assemblers able to make absolutely anything, but instead proposed more limited assemblers able to make a very wide variety of things. They challenged the relevance of Smalley's arguments to the more specific proposals advanced in *Nanosystems*. e.g. “More practical look to the subject is to design smaller parts that could be put together to yield in macro effects”.

At the “bottom” where “there is a plenty of room” according to Feynman, for production and assembly of such machines, there is a world with new rules differing from those of the macroscopic world. As the sizes get smaller, we have to redesign some tools because the relative strength of various forces changes. Gravity becomes less important, surface tension becomes more important, Van-der-Waals attraction becomes significant. These differences, which were mentioned by Feynman during his famous talk, are the issues that have vastly been studied by supramolecular chemistry - the chemistry of the “weak interactions”. Thus, supramolecular chemistry is one of the best candidates for achieving a practical way for the production of nanomachines⁵. The elements to create such machines or devices have been synthesized and studied by supramolecular chemists, though very new, many successful examples were given boosting others to work on synthesizing, property-studying, efficiency-tuning and assembling these machines.

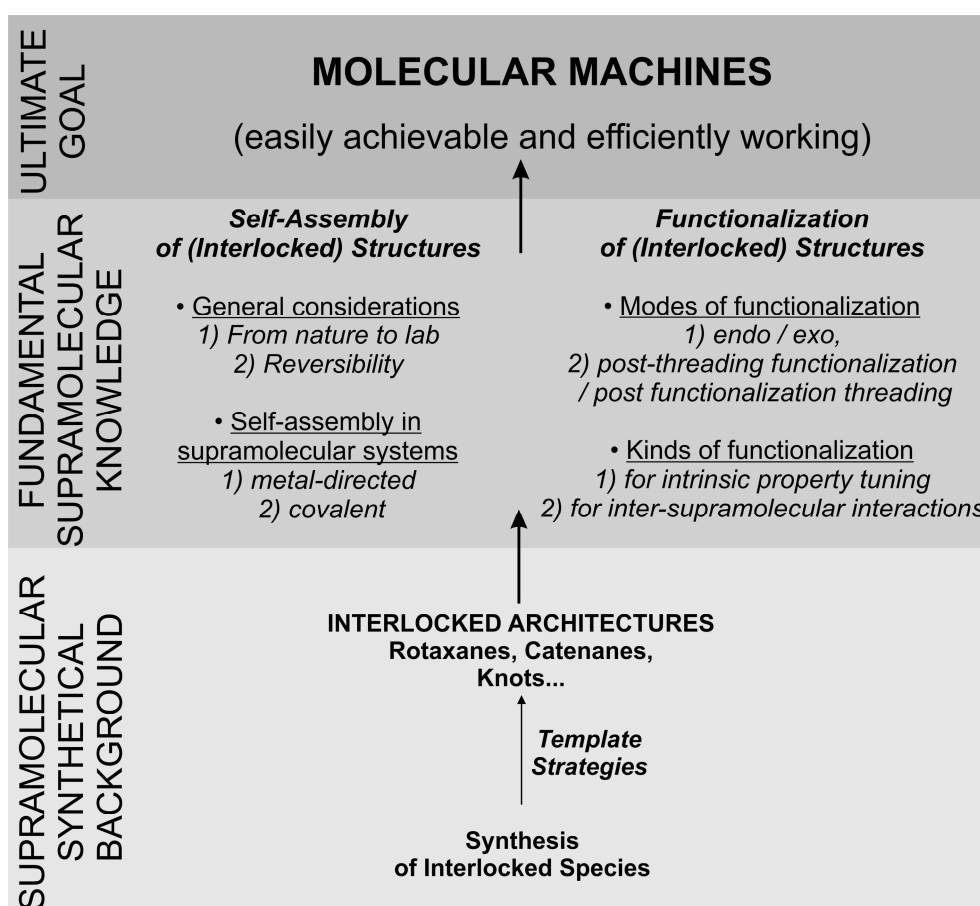


Figure 2. The schematical representation of the idea connecting molecular machines to interlocked architecture which are supramolecular species that can be candidates for efficient molecular machinery.

Figure 2 describes the idea of producing efficient molecular machines using knowledge on supramolecular chemistry and how synthetical work on interlocked architectures (also requiring “supramolecular experience” on template strategies) are connected to these. Throughout the following pages, obtaining supramolecular machines from their elements will be shown in general displaying the above mentioned links. The elements of supramolecular machines (the supramolecular architectures) are described concentrating on the interlocked species which is the focus of this study. How these elements are functionalized and how they can be assembled to yield in larger entities are then widely described and finally a practical way to obtain such functionalized architectures is proposed.

2. Introduction

2.1. Macrocycles, catenanes and rotaxanes: Functional supramolecular elements for molecular machines

From the work of Pedersen⁶ and Curtis⁷ on synthetic macrocyclic chemistry in 1960's, the supramolecular chemistry, chemistry of non-covalently linked multi-component systems emerged. Choosing a macrocycle instead of the open chain analogue had many advantages of which the most important one being the enhanced stability of the host-guest complexes. The first and most studied examples of these kinds of complexes were of ions and neutral guest molecules. From these primary studies, supramolecular chemists gathered fundamental knowledge on the intermolecular interactions which was then used for building interlocked and intertwined architectures through template synthesis and self-assembly⁸ (Figure 3).

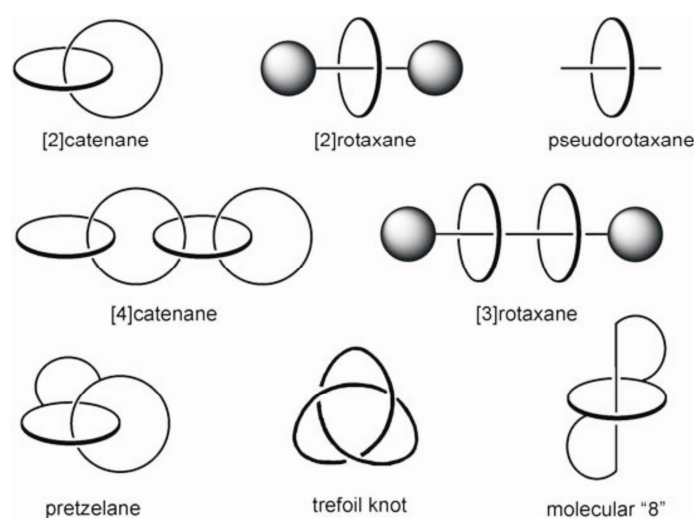


Figure 3. Various interlocked architectures. The numbers in the brackets represent the number of mechanically bound species in the supramolecule.⁸.

With the new pathways explored and optimized to produce these architectures and the utilization of new and powerful characterization methods to investigate them and the intramolecular motion within, supramolecular chemistry changed its focus recently from structure to function.⁹ The current studies on development of molecular devices for molecular electronics¹⁰, artificial photosynthesis¹¹ and the control of molecular motion¹² display the variety of approaches to develop functional supramolecular architectures and molecular machines.

Among these different architectures, rotaxanes and catenanes¹³ have been the most frequently synthesized and studied supramolecules. At first, these interlocked structures were of interest because of their aesthetical appearance¹⁴ and the challenge to synthesize such architectures. The studies to control the motion of the macrocycle with respect to the axle in a rotaxane, or with respect to the other macrocycle in a catenane resulted in molecular shuttles¹⁵. The interest on molecular shuttles that are built in the form the rotaxanes and catenanes has especially grown, because the motion within these structures is controllable by light (e.g. by photoisomerization)^{16,112b}, electrons (oxidation/reduction)¹⁷ or chemical signals (metal coordination, protonation/deprotonation)¹⁸. These shuttles can be called molecular machines, since the motion can be addressed and controlled by the mentioned inputs. Other than shuttles, according to the macroscopic devices they resemble, molecular machines¹⁹ were given different names: Molecular motors²⁰, molecules that are capable of unidirectional motion by external input; molecular propellers, molecules of which the motion resembles that of a propeller; molecular switches, molecules that can be reversibly shifted between two or more states; molecular tweezers, host molecules that can hold guests between their “arms” and so on. Molecular sensors²¹ that respond to analyte inputs and molecular logic gates²² that can output upon combinations of inputs can also be considered in the frame of molecular machines. The scope of this thesis does not cover the different kinds of molecular machines and physical studies²³ the motion within (the molecular machinery). However, it is important to know how the molecular machines function to fulfil the structural requirements, to increase the efficiency of such machines and to make better design for efficient synthesis. A few representative examples of interlocked compounds as molecular machines and motors²⁴ are given below in Figures 4 to 7: A shuttle²⁵, a molecular abacus²⁶, an operational nanovalve²⁷, a molecular elevator²⁸ respectively (for modes of working refer to figure captions).

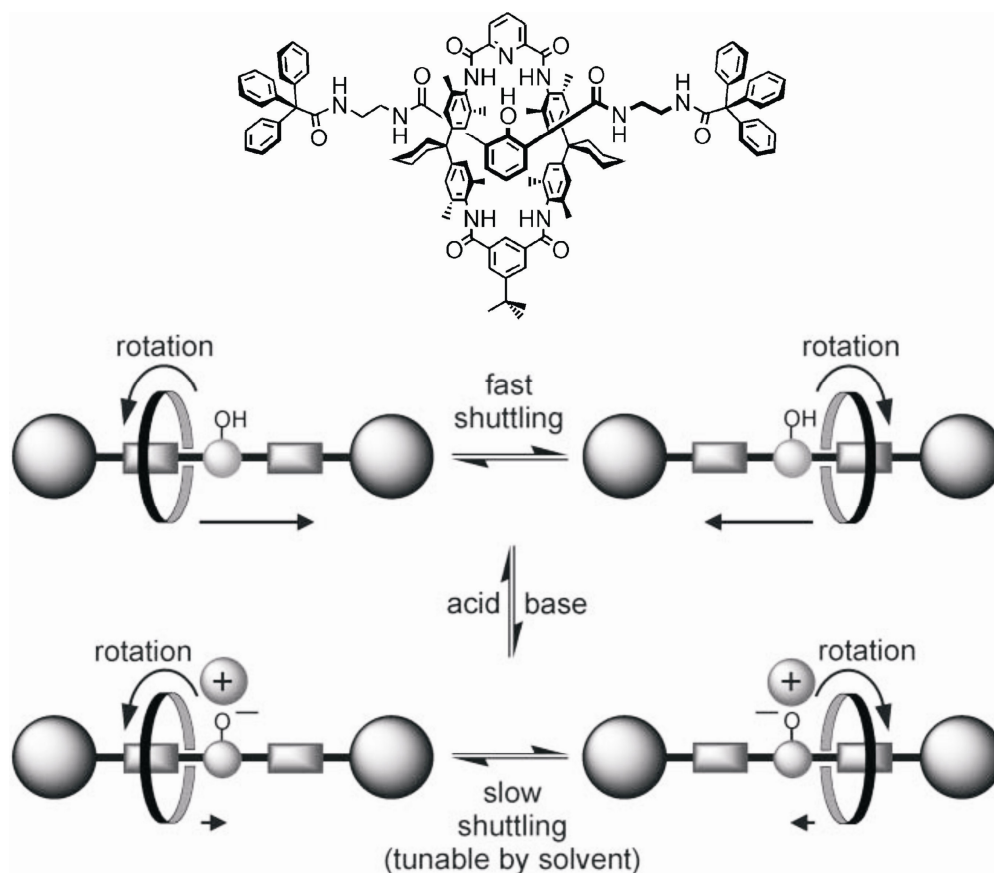


Figure 4. A molecular shuttle -- shuttling controlled by acid/base inputs and solvent. With the introduction of a base, phenol on the axle is deprotonated and a large cation sticks to it hindering the shuttling motion of the wheel between two stations. Acid input protonates the phenolate to phenol which can not keep the cation so, the fast shuttling is revived ²⁵.

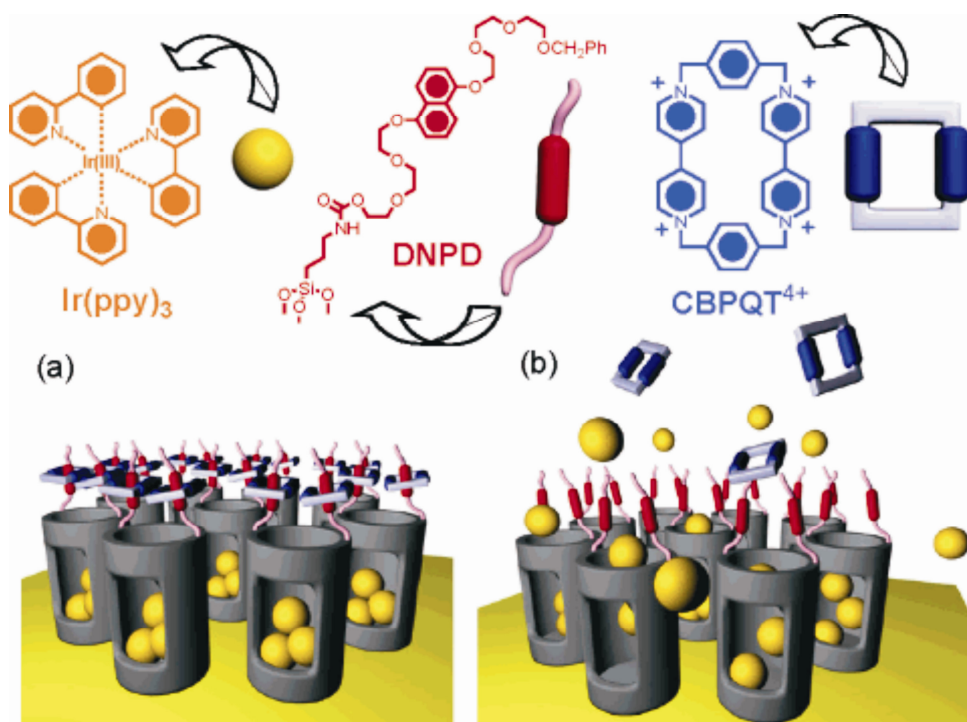


Figure 5. Graphical representations of operation of nanovalves. (a) The orifices of the nanopores (diameter 2 nm) are covered with pseudorotaxanes (formed between DNPd and CBPQT⁴⁺) which trap the luminescent Ir(ppy)₃ molecules inside the nanopores. (b) Upon their reduction, the CBPQT²⁺ bisradical dications are released and so allow the Ir(ppy)₃ to escape²⁷.

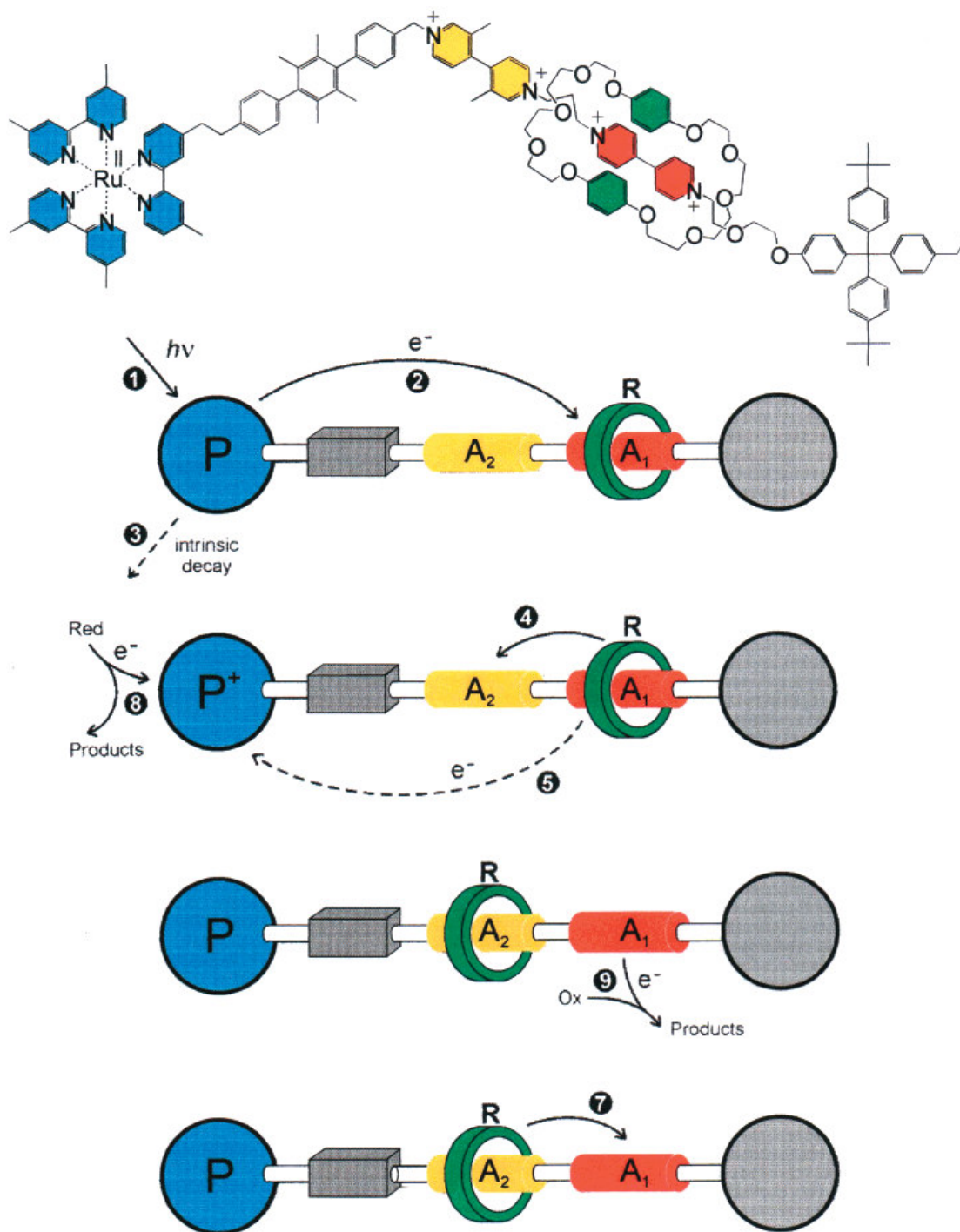


Figure 6. A molecular abacus: irradiation of the photosensitizer stopper provokes electron transfer to one of the two different bipyridinium units incorporated in the axle, thereby reducing this “station” and inducing ring motion to the second bipyridinium unit. A reductant is necessary to efficiently suppress back electron transfer. Reoxidizing the bipyridinium cation-radical to the dication induces back shift of the wheel²⁶.

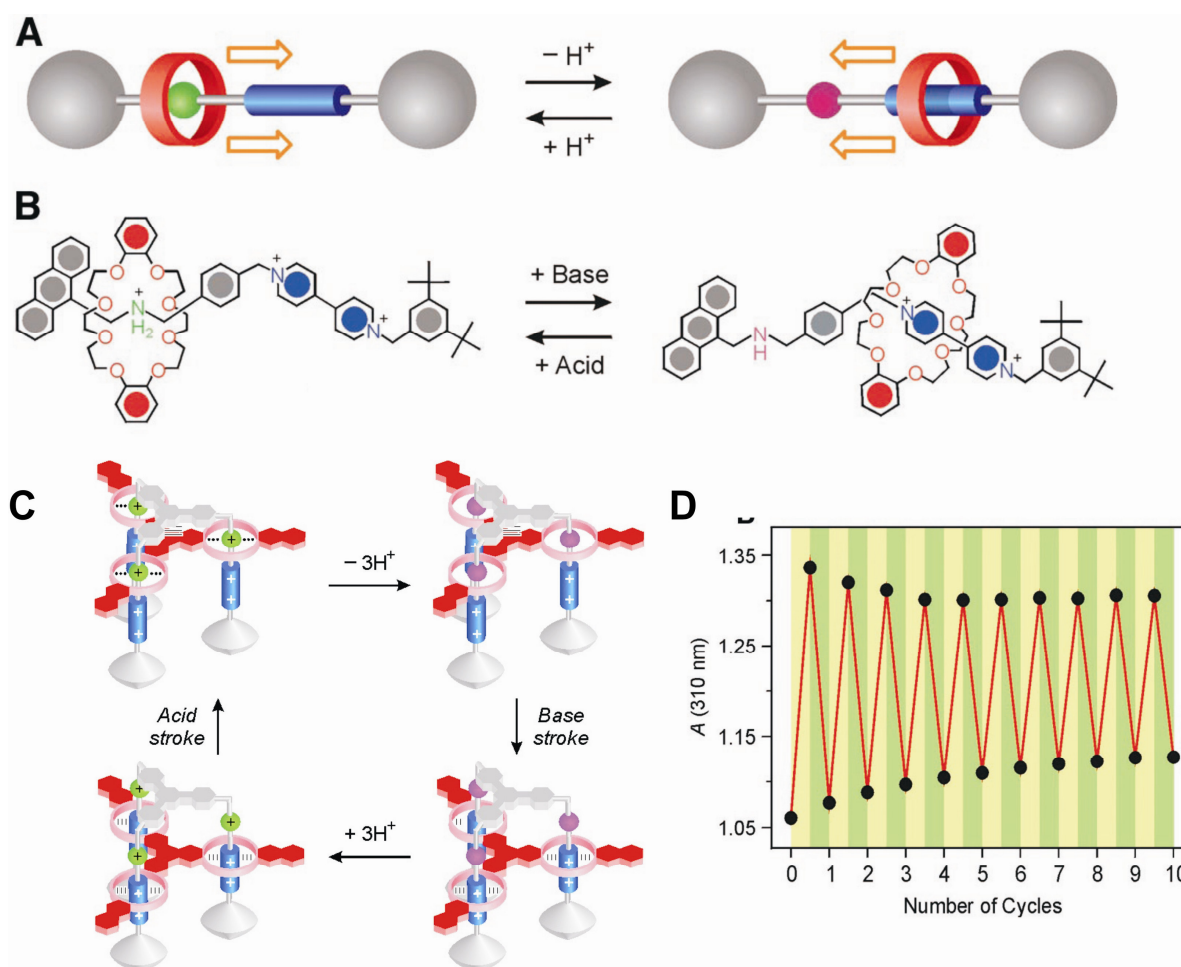


Figure 7. A) Schematic representation of a controllable, bistable [2]rotaxane that is controllable by pH change. B) The chemical shuttling. C) Same rotaxanes incorporated in a tris fashion to act as an elevator as a result of acid-base switching. D) Operating cycles of the elevator showing the reproducibility of motion²⁸.

As seen from the above examples the interlocked species form the basis of the molecular device or machine. The specialization of the molecular devices are based on the functional units on them- the parts that take place in intrastructural motion (acidic-basic groups), metal binding (intrastructural motion or interstructural assembly), fueling the machines (absorption of the energy or electrons) can be thought as the functional groups that can be modified for more efficient or different systems.

The tuning of the functional groups together with new strategies to synthesize and optimize these molecular systems may help solving the challenges that still exist in the world of molecular machines; the most important of which are in the areas of 1) unidirectional motion 2) efficient synthesis of molecular machines and the efficiency of work done by them

3) efficient fueling of the machines 4) incorporation of molecular machines to everyday nanotechnology e.g. assembling the molecular machines and immobilization of them.

Supramolecular chemists are still at the beginning of optimization of the efficiency and directionality of the motion in molecular machines. For the molecular motors, for example, unidirectional motion a question to be solved¹²: A system in which the direction of rotation is not well defined will not be productive, because the motors rotating clockwise will consume in the reverse process the work done by the motors running counter clockwise and vice versa. Considering that a clockwise sense of rotation is enantiomeric to a counter-clockwise rotation, it becomes immediately clear that an additional chiral element will render the two directionalities diastereomeric in nature; one can expect one of them to be more favourable than the other one. Consequently, chirality²⁹ is an important, if not necessary, prerequisite for defining unidirectionality. The approaches to synthesize chiral supramolecular architectures and molecular machines are discussed later in this chapter.

Concerning the efficient synthesis in the field of machines based on interlocked compounds, even the knowledge on template effects and synthesis of rotaxanes and catenanes³⁰ is explosively growing, and there are still problems in efficient synthesis of desired structures. The main concern of this thesis is to present such a method for straightforward and efficient achievement of variety of functionalized interlocked structures and displaying a few of the possible properties of these systems.

Beyond the single molecular machines, in order to obtain macroscopic effects, ordering of these machines should be realized. By ordering in membranes³¹, assemblies on surfaces³² or simply by self-assembly (discussed later in this chapter) larger, ordered, and complex species could be obtained. The synthesis and characterization of such complex structures are also different endeavours. Functionalization of interlocked species has given opportunity to control the scheme and geometry of such complex architectures as well as tuning other properties of these structures as shown in the next sections.

2.2. Macrocycles, catenanes and rotaxanes: Template Directed Synthesis and Functionalization

2.2.1. Template Directed Synthesis of Catenanes and Rotaxanes

Interlocked species became attractive as the basis for molecular devices and machines since 1980's, after when their syntheses were facilitated through new strategies⁹ other than the statistical syntheses³³ of these molecules. The most prominent and high-yield strategy to synthesize the interlocked structures, catenanes and rotaxanes is the template-directed

synthesis which involves non-covalent bonds that mediate the threading of one component into the other^{12a,34}. A variety of different template syntheses have been developed, using metal- coordination³⁵, π -donor- π -acceptor³⁶, hydrogen bonding³⁷ to ammonium cations^{8,38}, amides³⁹, or anions^{25,40}.

2.2.2. Anion and Amide Templated Synthesis of Catenanes and Rotaxanes

As stated above, various methods for the templated synthesis of rotaxanes exist. We will take a closer look to two template strategies that were used for synthesis of rotaxanes with the tetralactam macrocycle in this study. These rotaxane syntheses that utilize anion or amide templates are well-studied and the mechanisms leading to rotaxane is well-understood for the non-functionalized tetralactam in Figure 8.

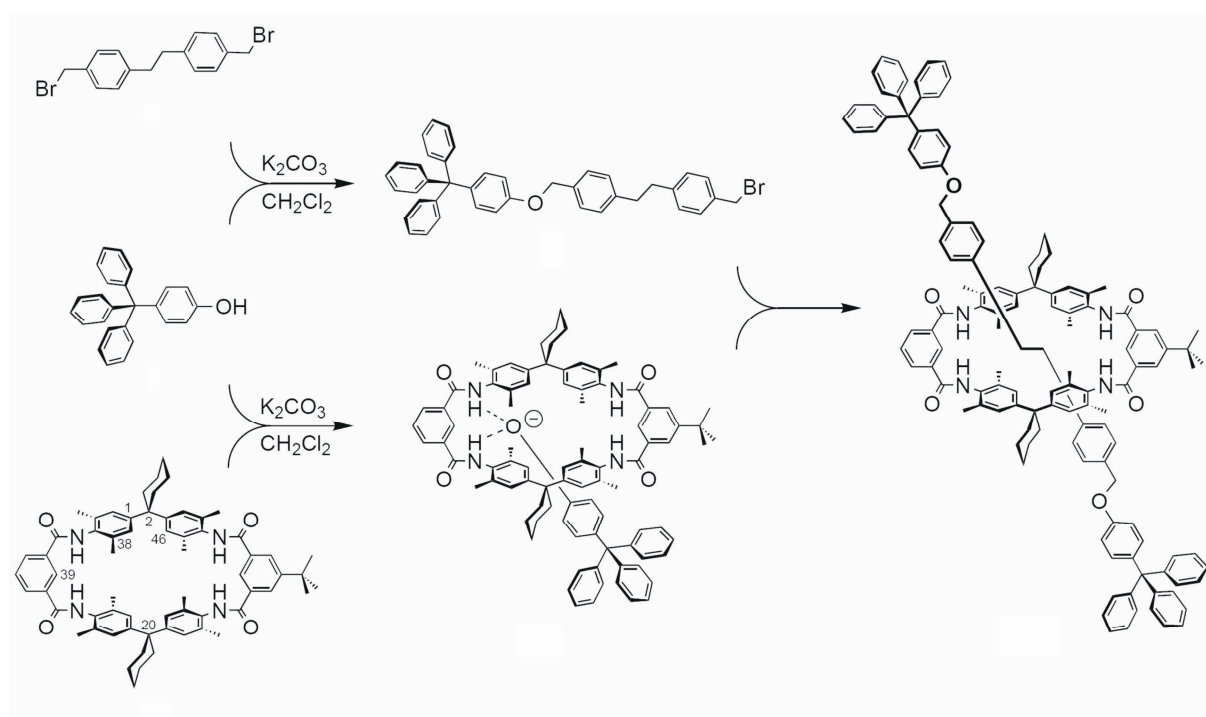


Figure 8. Template mechanism leading to the formation of an “ether” rotaxane.

The anion templated synthesis of a rotaxane was first reported by Vögtle and co-workers (Figure 8). The synthesis is based on the recognition of phenolate stopper within the macrocycle. The very high binding constant of this complex ($K > 10^5$ M)^{40c-e} is attributed to the two hydrogen bonds that form between the macrocycle and the stopper, that shifts the equilibrium to the complexed structure. The axle middle piece-stopper (semi-axle) formed in the reaction then reacts with this complex to form the rotaxane in very high yields (up to

95%). The mechanism is well studied and examined by later studies^{40f,g}. For example, the anion templation was tried to be improved by removing the template from the stopper to the axle middle piece. The anion template synthesis of rotaxane is very attractive because of its higher yields and neat purification procedures.

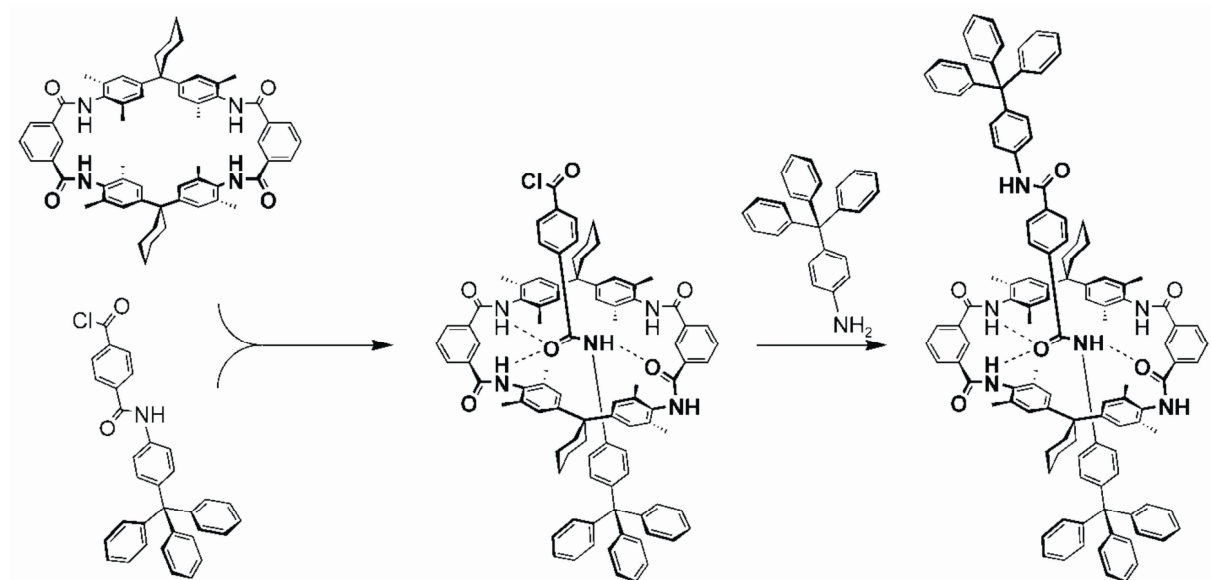


Figure 9. Template mechanism leading to the formation of an “amide” rotaxane.

The amide template rotaxane synthesis was studied by Vögtle^{39b-d} (Figure 9) and Leigh^{39e} and the mechanism of the templation was well examined and stated by Schalley^{39a}. In these studies it was shown that the reactants, i.e. the acid dichloride and the amine, do not form stable complexes with macrocycle, but the intermediate amide that forms from both can form three hydrogen bonds to coordinate the macrocycle and yield, in a second attack from a stopper, in a rotaxane.

Both template mechanisms are well known and the syntheses of rotaxanes through these syntheses is well-studied. Being clearly understood and high-yield processes make both anion and amide templates appealing reaction pathways for the studies on functionalization of the rotaxanes.

Beyond the practical experience from the synthetic works, the conformers of the tetralactam macrocycle and formation of interlocked structures were given insight with density functional calculations^{39a} (Figures 10 and 11).

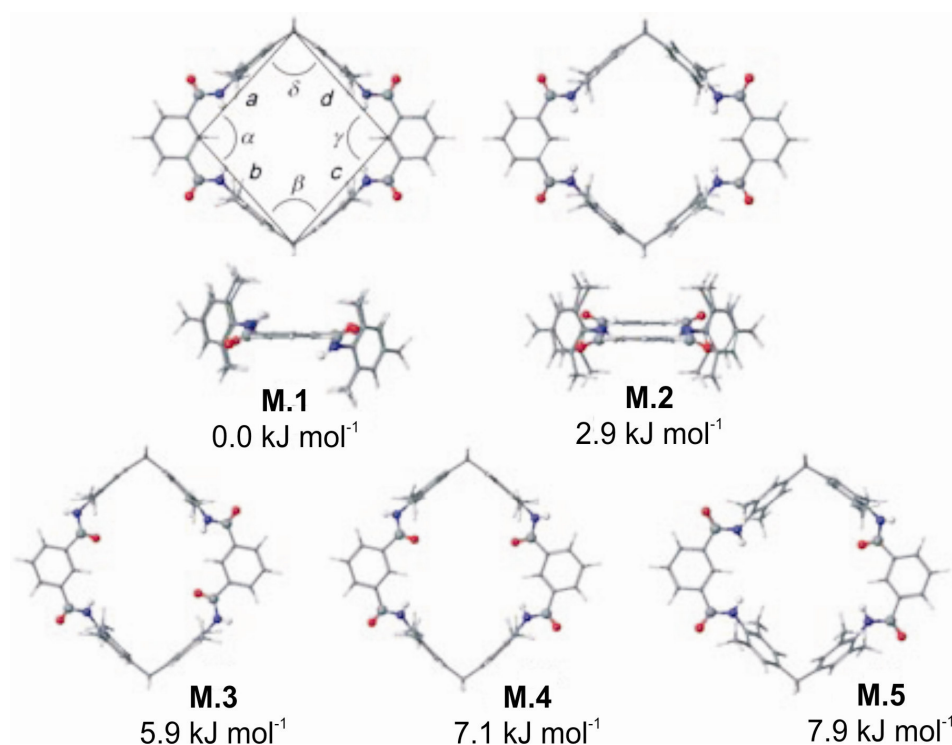


Figure 10. Five conformers of tetralactam macrocycle (non-functionalized, without cyclohexyl groups) used in the study optimized with the B3LYP density functional hybrid and DZP basis. **M.1** and **M.2** are also viewed from side to show the NH groups above and below the macrocycle plane. The energetically preferred (**M.1**) and least favourable (**M.5**) structures are less than 9 kJ mol^{-1} ^{39a}.

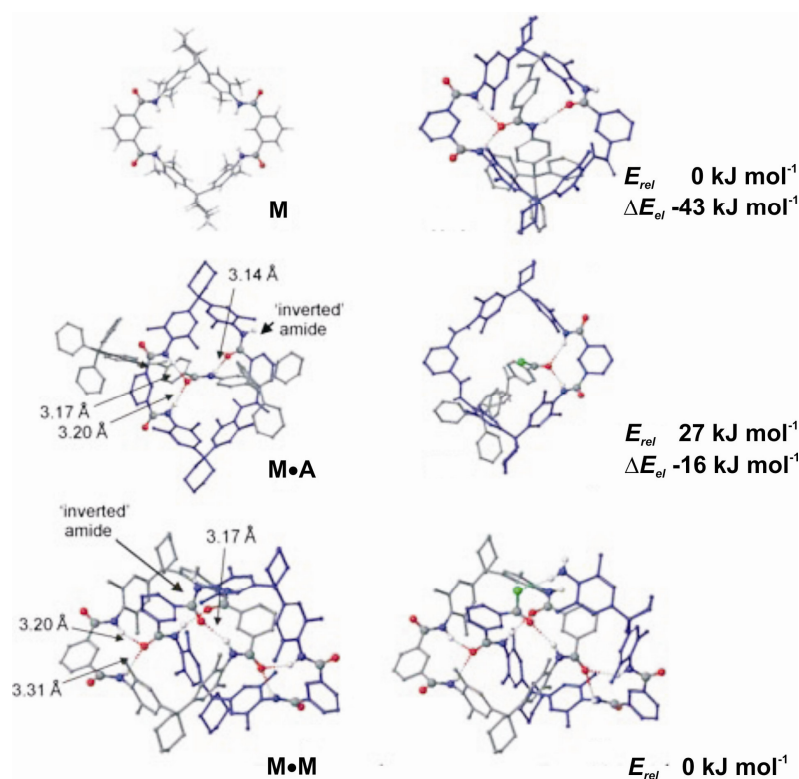


Figure 11. Left (top to bottom): the energetically most favourable structures of macrocycle *M*, rotaxane *M•A* and catenane *M•M*. Note the common hydrogen bonding pattern of each pair of macrocyclic host and guest. Right: intermediates immediately preceding the products in the template synthesis. The energies given are relative energies (E_{rel}) calculated at the AM1 level of theory and can be compared only pairwise for the structures of the same elemental composition. Electronic energy differences relative to the two components are denoted

$$\Delta E_{el}^{39a}.$$

2.3. Functionalization of Supramolecular Architectures

2.3.1. Early Considerations and Functionalization of Macrocycles for Sensor Design

Functionalization of the supramolecular architectures is as mentioned before, of great importance for establishment of utility for these structures and especially for their use as molecular machines. The first examples of the functionalized architectures are as old as the synthetic macrocyclic chemistry. The simple attaching some longer alkyl chains to the macrocycles, improved their solubility in organic solvents. Tuning of the cationic, anionic and neutral guest binding to crown ether macrocycles triggered the studies on functionalization of macrocycles: Adding additional arms that helped to stabilize the complex can be considered as an attempt to arm the macrocycle body with appropriate helper.

The more sophisticated functionalization on the macrocycles appeared when the guest binding phenomena motivated the idea of signalling of host-guest binding. There are a number of physical methods that could be used to detect the weak host-guest interactions. NMR spectroscopy is the most extensively investigated, where specific resonances of the nuclei belonging to either the host or guest are perturbed upon complexation. However, in most cases where the sample size is small, higher sensitivity and rapid detection are required, NMR is impractical and inappropriate. Alternative techniques such as detecting the optical or electrochemical response are more convenient and faster. Electrochemistry (voltametry and potentiometry) and optical spectroscopy (absorbance and luminescence) which are physical techniques that can be miniturized for fast and sensitive detection, can then be utilized for sensing of guests in the functionalized macrocycles. Sensor design of any kind requires simply, an entity that binds the guest and another that reports the binding. Thus attaching a reporter to a host macrocycle is an example of functionalization of the macrocycle⁴¹. Synthetic control over the binding site in host and stereochemistry and pertinent signalling of binding event are the goals of chemical sensor design. This was accomplished in exceedingly many examples so far.

Derivatization of some elegant macrocycles such as calixarenes⁴² and resocinarenes⁴³ and pyrogallerenes⁴⁴ give rise to different host-guest binding properties and interesting architectures such as capsules and higher assemblies that can accommodate guests, catalyze chemical reactions. Functionalized porphyrins can form assemblies through metal-coordination⁴⁵ or through different side-arm functionalization⁴⁶. A recent example of organic molecular nanowires obtained via functionalization of a tri- β -peptide that can self-assemble via the macrocycles and also through metal coordination shows many directions the functionalizations on macrocycles can lead to⁴⁷ (Figure 12).

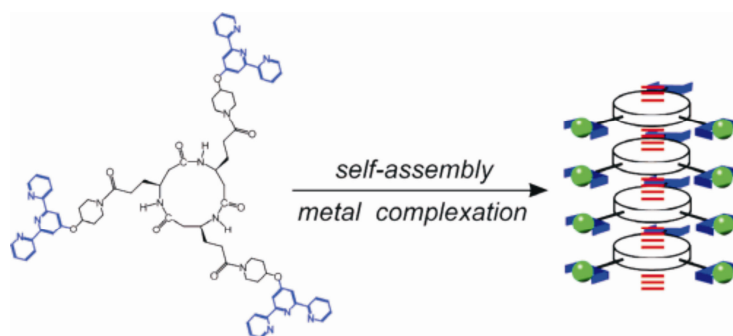


Figure 12. A molecular nanowire obtained by self-assembly into a peptide nanotube. The cyclic tripeptide is functionalized by terpyridines⁴⁷.

2.3.2. Functionalization of Supramolecules - Modes of Functionalization

As in the cases for macrocycles, rotaxanes and catenanes and supramolecules formed by self-assembly from the smaller parts can also be decorated with functional groups. In the interlocked architectures the functional entities can both be attached to the axles or macrocycles. The functionalization of the supramolecules can be done before the assembly (or threading for interlocked compounds) and the functionalized structures can be assembled afterwards, or, the assembly is obtained first and the structure is then functionalized with the desired groups. This change in sequence of the functionalization-assembly process is in some cases vital for the desired architecture⁴⁸. The choice of the right approach depends on many parameters, among which are the accessibility of the functionalization sites and the stability of the assembly.

2.3.2.1. Post-functionalization Assembling (Post-functionalization Threading) and Post-assembly Functionalization (Post-threading Functionalization)

The post-functionalization assembling or threading is the most favored way for obtaining functionalized self-assembled structures that are formed through metal coordination or covalent self-assembly: First the building blocks are functionalized, and then the assembly is formed as in the non-functionalized architectures. Some very striking examples of such assemblies were given by Fujita (Figure 13). The pyridine containing ligand that was known to form a nanoball was decorated once with PEG for endohedral functionalization (functional groups inside the ball) and in another example with porphyrin to obtain peripheral functionalization⁴⁹.

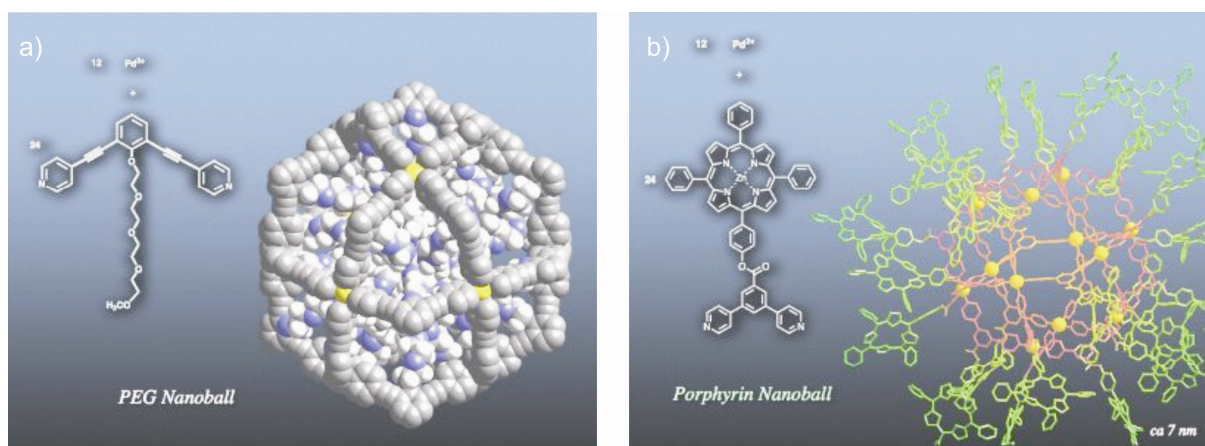


Figure 13. Self-assembly of functionalized building blocks to form a) endohedral and b) peripheral functionalized nanoballs. Both are examples of post-functionalization assembling⁴⁹.

The most favored way for functionalization of interlocked species is also to use the already functionalized building blocks and use the known template syntheses to form the final supramolecule. Post-functionalization threading for interlocked compounds is mostly preferred because of the ease of synthesizing such molecules, if only one compound is desired and studied. However, for the optimization of efficiency or change of functional groups this method is quite impractical as discussed in a separate section in this chapter.

Functionalization on the supramolecules can also be done after a supramolecule has formed which can be called as post-assembly functionalization or post-threading functionalization. This way, of course has some additional difficulties the most prominent one being the separation and purification of the final reaction products. Below is a representative study on the functionalization of Vögtle knots⁵⁰ (Figure 14).

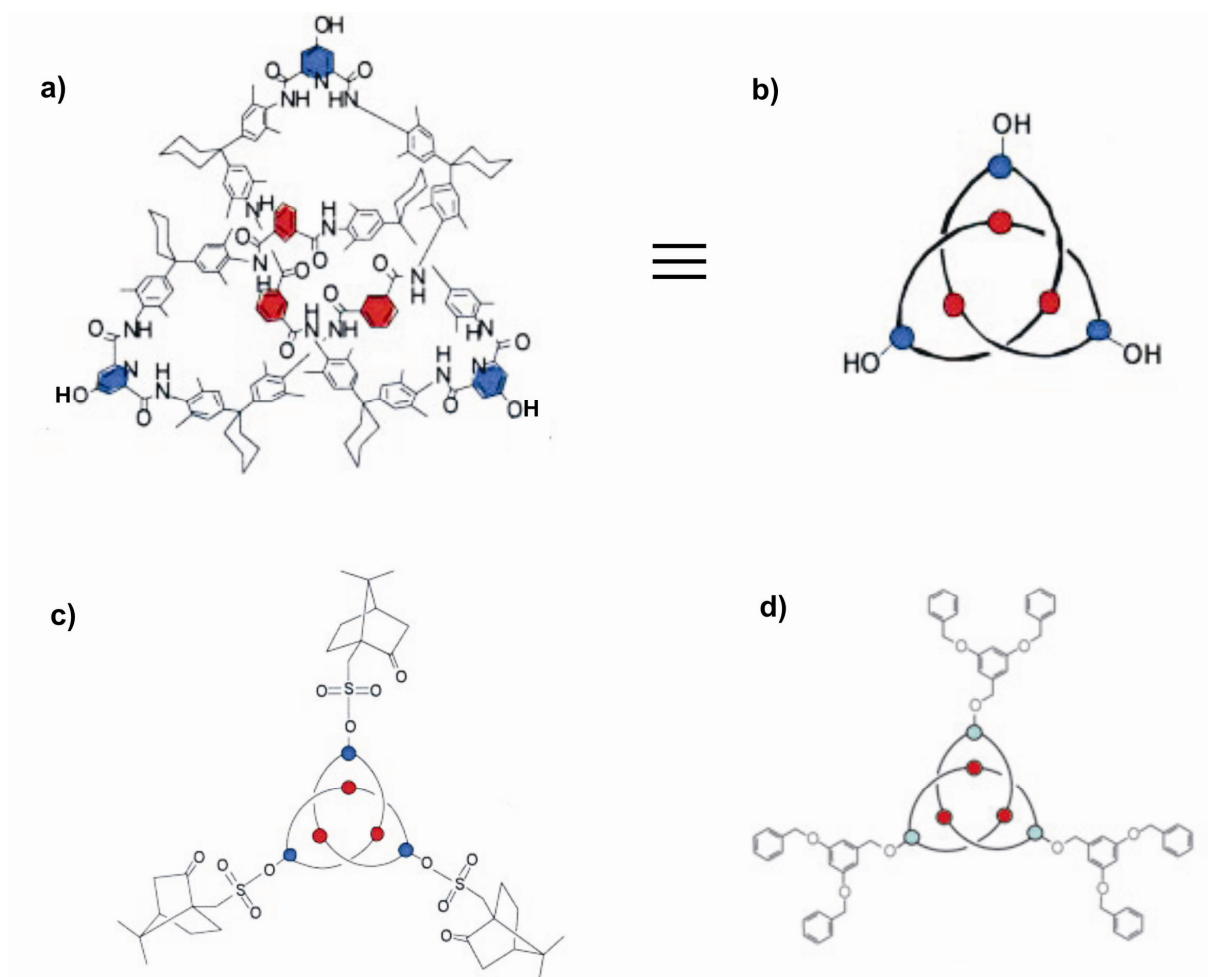


Figure 14. Functionalized amide knots. a) The nonfunctionalized knot and b) its schematical representation. c) Camphor functionalized knot for chiral separation of knot enantiomers⁵¹, d) knots can be selectively functionalized with dendrons and isolated as mono-di- and tris-products (shown here the tris- compound).

2.3.2.2. Endo- and Exo-Functionalization of Supramolecules

The functionalization of supramolecules or supramolecular assemblies can be also classified into two: endo-functionalization and exo-functionalization⁵². In endo-functionalization, the functional group is incorporated into the supramolecule body or is embedded in one or many of the building blocks forming the assembly. In contrary, with exo-functionalization, the initial architecture is retained but functionalized by attachment of the desired function on the body (Figure 15).

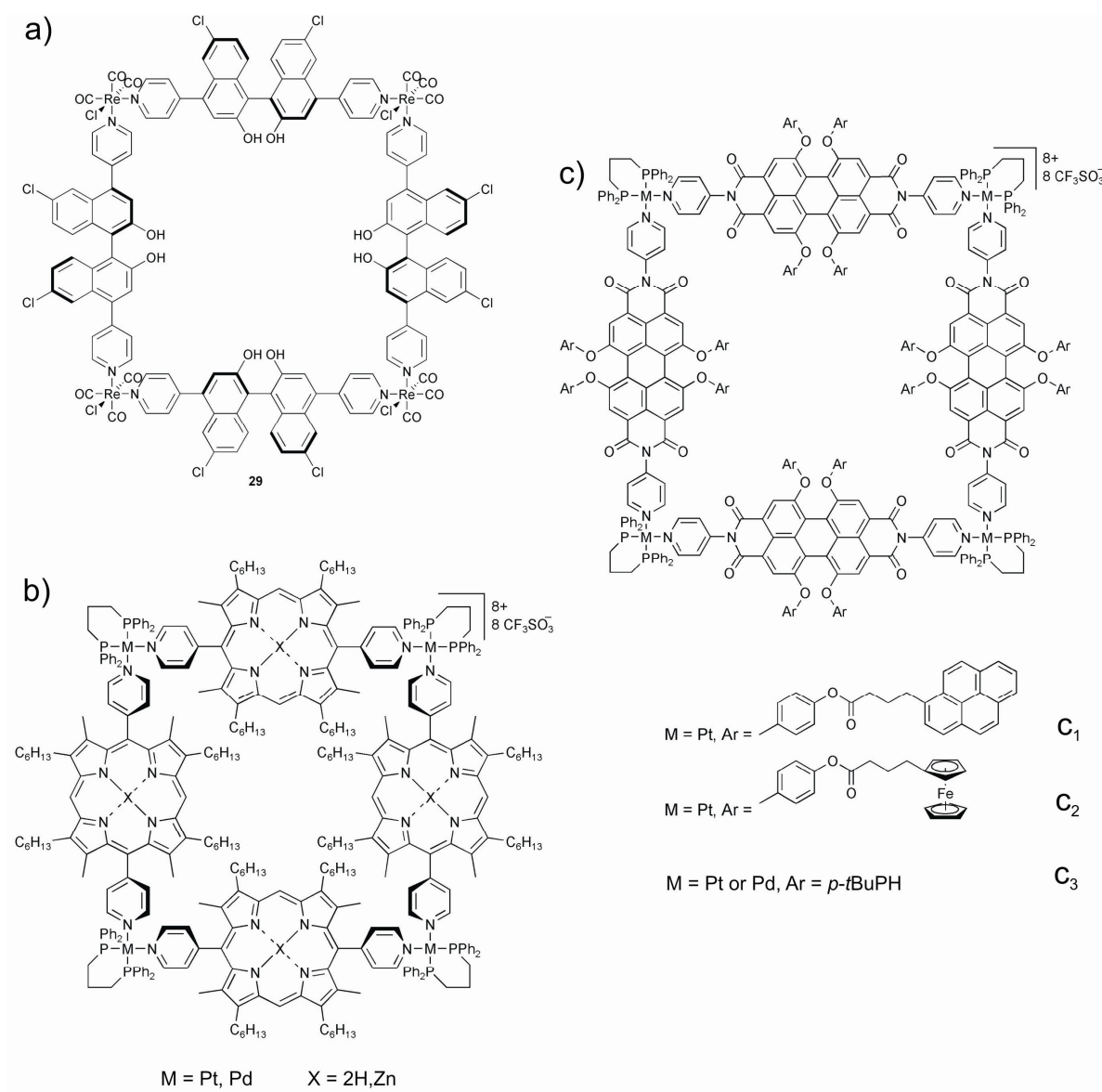


Figure 15. Different functionalization modes of supramolecular squares: a) endo-functionalization of the molecular square by incorporation of chiral units into the ligands,, b) endo-functionalization of squares with porphyrin and Zn-porphyrin complex incorporation, c) endo- functionalization of a molecular square with perylene incorporation to the ligand and exo- functionalization by attachment of pyrene (c₁) and ferrocene (c₂) arms⁵³.

Figure 15 shows the difference between endo- and exo-functionalization: In (a) a chiral unit is incorporated in the ligand, (b) has again an endo-functionalized ligand, (c) has both endo- and exo- functionalized assembly, that is, ligand is incorporated perylene units which are attached photo- or electrochemically active groups in an exo- fashion.

2.3.3. Functionalization of Supramolecules and Supramolecular Assemblies – Functional Groups

A great variety of functionalized supramolecular architectures can be imagined. However, functionalization on the structures can be recognized in two classes: Functionalization 1) aiming at changes of the intrinsic properties of the supramolecules or 2) initiating or improving supramolecule function or inter-supramolecular interactions. In the first kind, functionalizations done for increasing their solubilities in organic and aqueous^{54, 55}, for easy post-functionalization purification of the interlocked molecules⁵⁵ could be assigned. Functional groups for achieving or enhancing molecular recognition, for electrochemical response, for assembling the supramolecular structures in a desired fashion through ligand attachment⁵⁶ or attaching appropriate groups for photoluminescence and light harvesting⁵⁵ are of the second type.

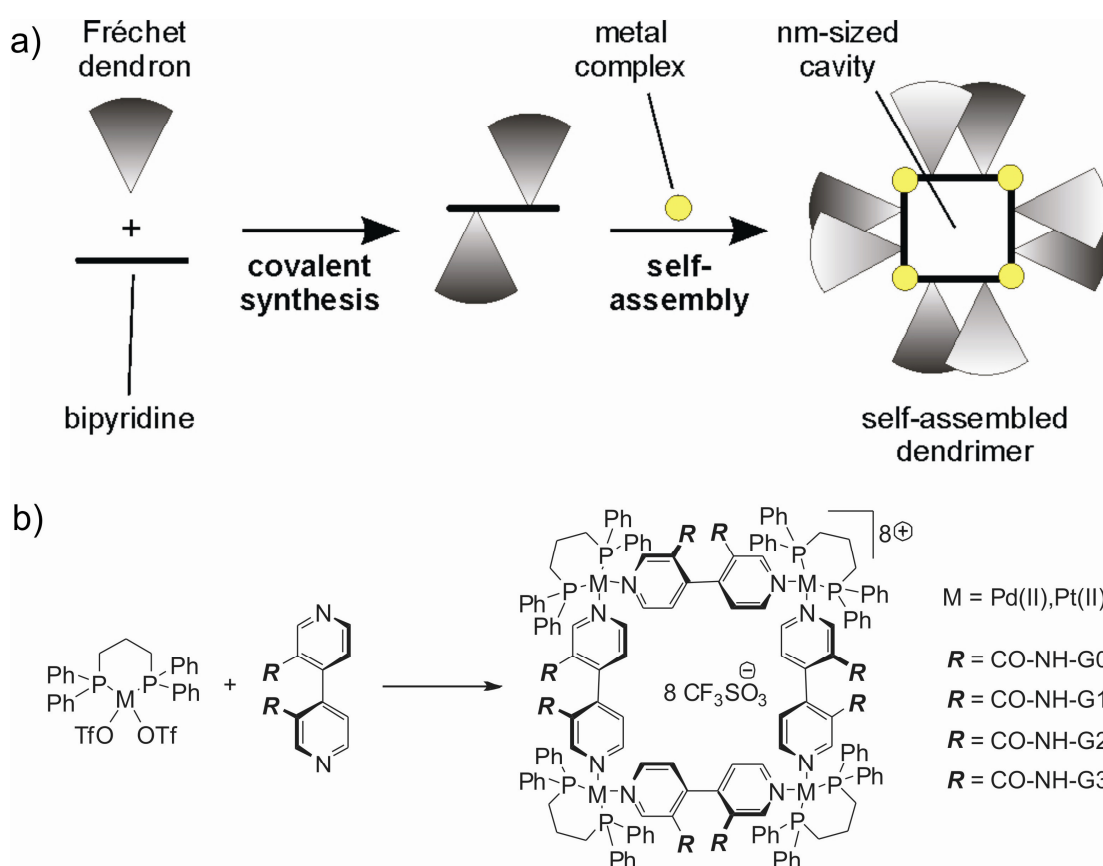


Figure 16. a) Schematical representation and b) the structure of a dendron-decorated square.

The functionalized building blocks assembled through metal-coordination enhance the molecular recognition and host-guest properties of the supramolecular square. The functionalized square can accommodate dyes; a phenomenon which is possible neither with the functionalized building block nor with the non-functionalized assembly⁵⁷.

Functionalization of a supramolecule or supramolecular assembly may result in interaction or combination of these functionalities that yield in different properties of the final structure (initiation of an intrinsic property). For example, metal-directed self-assembled squares were functionalized with dendrimer attachment on the assembling ligands⁵⁷ (Figure 16). These squares were found to extract dye molecules from aqueous solution into the organic solvent displaying a molecular recognition event which was not possible with functional building blocks or with non-functionalized squares.

Other than recognition property, many other functions can be incorporated into the supramolecules. As discussed earlier in the chapter, molecular machines need to be tuned up for everyday nanotechnology and the several problems in attaining this can be overcome by selective functionalization: Fueling of the molecular machines can be optimized by successful studies in photophysics or electrochemistry that require functionalization with such groups. The problem of ordered and addressed assembly of molecular machines can be connected by their self-assembly through metal-coordination and dynamic covalent bonds. The scope of solutions for these questions is quite broad. Here will be concentrated on the ways of efficient integration of photoactive units and groups for self-assembly as implied from the topic of the study.

The supramolecular architectures that bear ligands for metal-coordination, their metal complexes or functionalized with appropriate groups to covalently self-assemble have been studied extensively up to now. The interesting and important process of self-assembly is discussed in the following sections. Here will be shown only some examples of interlocked supramolecular structures decorated with ligands or functionalized in other ways to take place in assemblies. The ligand functionalized or ligand incorporated interlocked compounds are mostly found as examples of products from metal-templated synthesis and/or they are designed for studies on metal assisted intramolecular motion⁵⁸ (Figure 17).

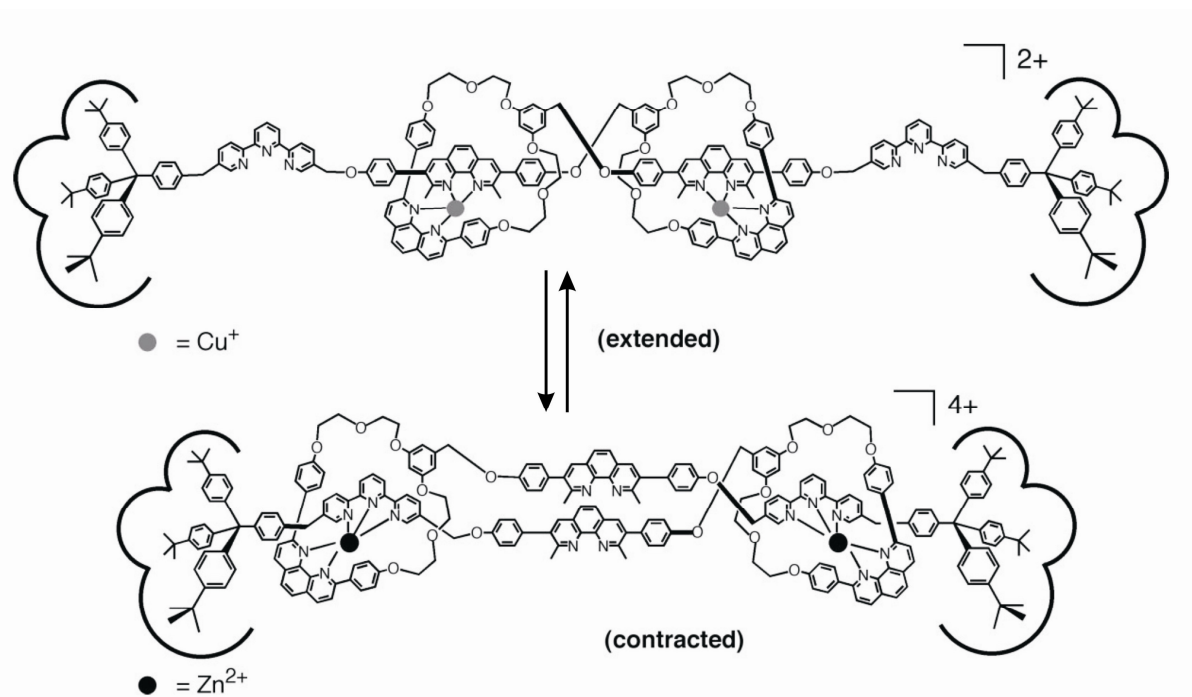


Figure 17. A molecular muscle⁵⁸ that can contract or extend by metal ion (Cu^+ and Zn^{2+}) inputs is an example of a [2]rotaxane which contains ligands for metal coordination is an example of a ligand decorated rotaxane for studying intramolecular motion.

The most appealing feature of the ligand-decorated interlocked species could be their ability to self-assemble into larger predefined architectures. For example, assemblies of rotaxanes or catenanes that display controlled motion of parts of the interlocked molecules, and thus are considered as molecular machines can be combined or detached by the assembly processes. The performance that is obtained from the combination of the small molecular machines can be a visual macro effect of the motion that is created at the molecular level⁵⁹ or depending on the nature and the geometry of the assembly something different than this motion.

Interestingly, only a few examples of making of ligand-decorated interlocked species such as catenanes and rotaxanes exist in the literature. Shown in Figure 18, Schalley's work on rotaxanes and catenanes having exocyclic biquinolines⁷⁷, Leigh's rotaxane functionalized at both axle and wheel for different metal coordination⁷⁸ and Stang's pyridine based ligand decorated with a crown ether to form pseudorotaxanes⁶⁰ are the most prominent examples. Loeb studied especially on the metal-assisted self-assembly of rotaxanes⁷⁴ and designed ligands for this purpose as will be discussed in the metal-directed self-assembly section.

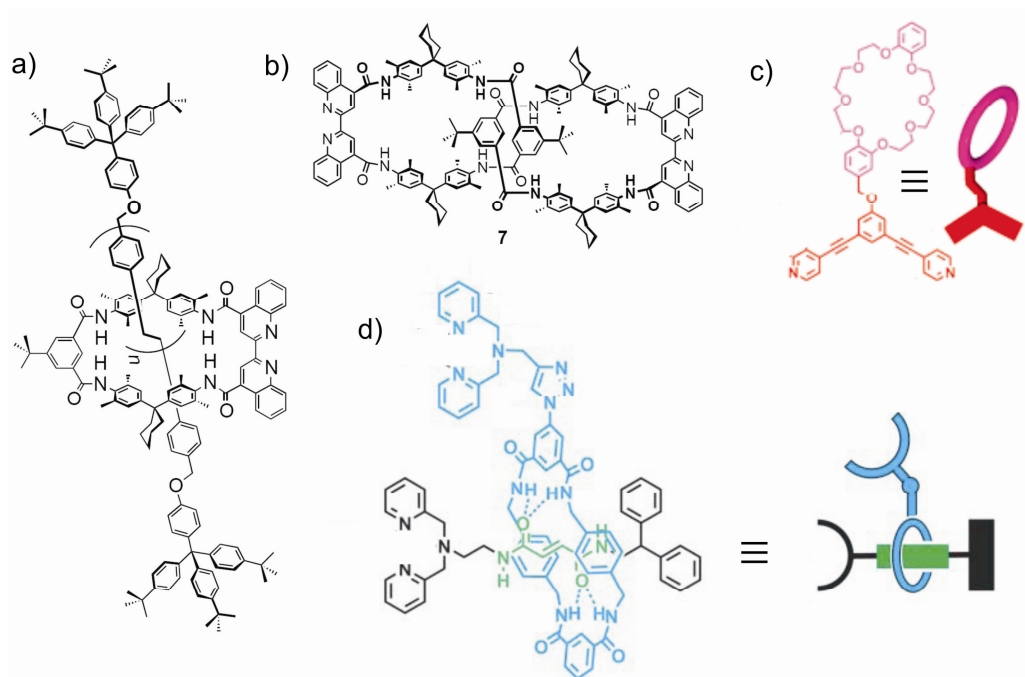


Figure 18. a) Biquinoline rotaxane and b) biquinoline catenane can form dimmers through Cu(I) coordination⁷⁷, c) pyridine ligand attached crown ether can assemble into a hexameric species with a kinked Pt(II) complex⁶⁰, d) two metal binding sites of a rotaxane can bind different metals selectively⁷⁸.

So far, most of the functionalization on the interlocked supramolecular architectures were done non-systematically⁶¹, target function-oriented point examples. Although there are plenty of examples of successful functionalization with the desired function or property of the final structure, the lack of studies to optimize the effects on the systems is overwhelming. The examples for elegant structures decorated with functional groups suffer the separation and purification procedures after the functionalization e.g. only the presence of these after the functionalization could be detected- in some cases no pure compound was obtained⁵⁵. Thus, optimizing the functionalization syntheses, exploring a straightforward way for achieving variety of functions and finding appropriate ways to achieve pure and appreciable amounts of functionalized architectures are of vital importance and are the main aims of this study.

2.4. Self-Assembly: Combining and Addressing the Molecular Motion

2.4.1. Self Assembled Systems, Reversibility and Supramolecular Chemistry

The most fundamental definition of self-assembly is the spontaneous formation of higher order structures from simpler building blocks⁶². Many complex architectures and phenomena in nature, from the smallest ones in a cell like folding of peptides into proteins,

formation of bilayers in lipids, folding of nucleic acids into their functional forms to the very complex (including the human body and mind⁶³) are examples of self-assembly, many of which have not been fully understood yet. Not more than 50 years ago, molecular biological studies on the viruses implied that cellular architectures like membranes or bacterial flagella are formed through a sequence of events of “fitting together” which can be called as molecular self-assembly. Later studies on light-harvesting antenna complexes of some bacteria revealed that these complexes are also self-assembled smaller units. These studies and many other studies on biological systems proved that self-assembly is a physical principle that rules nature. They also proved another thing: The tedious nature of isolation of the assemblies and the huge amount of effort to be taken to make systematic analyses on these systems. Thus, chemists have been trying to make smaller architectures, systems consisting of molecules that self-assemble to understand the fundamental physics of self-assembly and create complex structures as nature does⁶⁴. In fact, the systems that are build so far in this fashion are quite good candidates to study the complex systems in nature, depending on the fact that both are governed by the same intermolecular interactions such as Van der Waals bonds, hydrogen bonding, electrostatic interactions, π - π stacking etc. It should *also* be noted that mimicry of the nature’s elaborate and complex architectures combined with their highly efficient functional properties would be impossible by the aggressive nature of the total covalent synthesis and moreover, lack the two most important feature accompanied by the self-assembled structures: Reversibility and error correction⁶⁴.

The self-assembled systems show sensitivity to perturbations exerted by the environment. These fluctuations may alter the thermodynamic variables of the self-assembled sytems that may lead to marked changes in the self-assembled structures. The weak nature of interactions in these systems allows these perturbations to effect the system structure at any stage of the assembly process (and even after the assembly). If the effects on the thermodynamic variables are so that they are brought back to the starting conditions, the system goes back to the initial configuration⁶⁵. This means reversibility in the whole architecture which is not achievable by other synthetic techniques.

The new building blocks which can be programmed to assemble could be assigned function to act as “the atoms” or “the molecules” in the future materials, too. The nowadays approach to nanotechnology mostly uses the “top-to-bottom” path which uses a machine to manufacture complex structures. This process is far from reaching the complexity displayed by nature and does not allow the reversibility which is followed by error correction⁶⁴. As stated by Feynmann in the 50s, the “bottom-to-top” approach promises the nanotechnology

the properties it does not have so far. Evident from the almost exploding number, different sorts of chemical self-assembled systems that are synthesized, studied and analysed everyday, it may be possible to see in the near future, in many areas of nanotechnology, the building blocks that are programmed by the scientists to self-assemble and perform the desired functions. And it is not a science-fiction dream nowadays to expect them to reach a higher level of “intelligence”, to self-heal⁶⁶ and to self-replicate⁶⁷.

Molecular self-assembly is a key concept in supramolecular chemistry since self-assembly processes are governed by weak interactions. Numerous examples of self-assembled systems in supramolecular chemistry include self-assembled capsules⁶⁸, nanotubes^{64, 69}, vesicles⁷⁰, polygons⁷¹ etc. Self-assembly in supramolecular chemistry is so far mostly concentrated on two different approaches: Metal-directed self-assembly where the assembly is directed and mediated by metal ions or covalent self-assembly where the assembly is achieved by reversible covalent bonds.

2.4.2. Metal-Directed Self-Assembly of Pseudorotaxanes, Rotaxanes and Catenanes

Metal-directed self-assembly makes use of directional coordinative bonds between the ligands and the metals to achieve designed multi component architectures in one, two or three dimensions. Based on this coordination chemistry, successful strategies have been developed for construction of complex structures⁷¹. The advantages of the metal-directed self-assembly are the control over different geometries and bond strengths depending on the metal ions or complexes utilized in the assembly. The area of research on metal-directed self-assembly is vast; however the metal-directed self-assembly of interlocked structures is new and not so well-investigated.

Many interlocked compounds, pseudorotaxanes, rotaxanes, catenanes and knots containing metals in the structure have been synthesized⁷², thus the metal inclusion to such supramolecules is not a new topic. However, one must distinguish the metal-templated or ligand (or metal complex) bearing structures from the ligand functionalized ones and metal assisted motion in those structures from the real self-assembly processes (Figure 19). Below will be discussed only the latter.

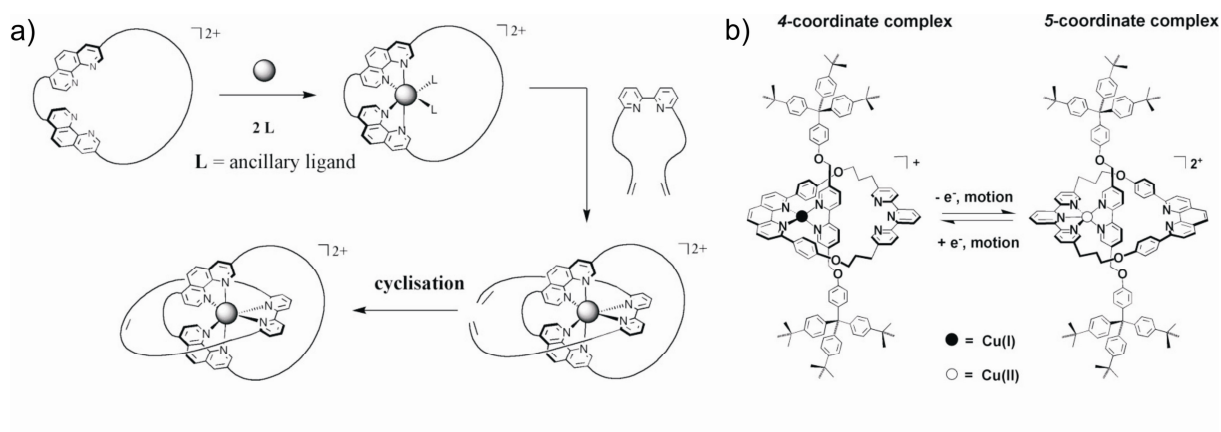


Figure 19. Metal ion can be incorporated into the interlocked compounds a) to act as a template, b) to control the intramolecular motion.

The simplest examples of metal complexation and self-assembly of macrocycles can be achieved by using crown ethers as shown in Figure 20: If the macrocycle of the rotaxane is small enough like a crown ether, any metal complex with a single open coordination site is bulky enough to effectively cap the axle of a pseudorotaxane and form [2]rotaxane⁵⁶ (Figure 20). This is also the case when the metal-complex stoppering the pseudorotaxane is big enough like an axially coordinated porphyrin to prevent the deslipping⁷³.

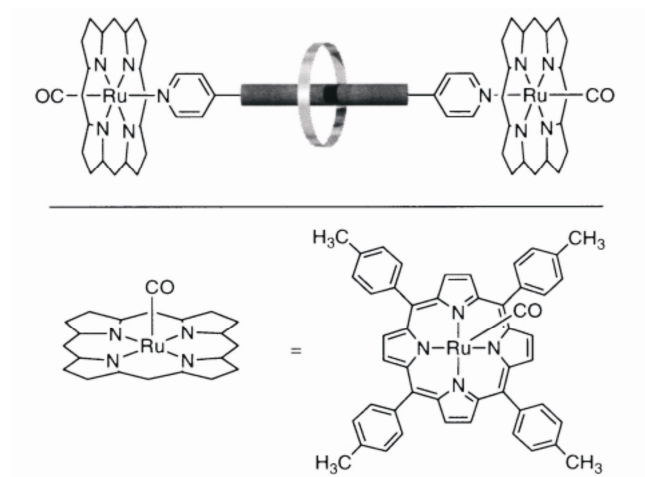


Figure 20. Axially coordinated porphyrin as a stopper of a pseudorotaxane. (macrocycle: Benzocrown[8], axle : 1,2-bis(4,4'-bipyridyl)ethane)

Maintaining the weak non-covalent interaction between the axle and the wheel decreases the yields of the rotaxanes and assemblies formed this way. Thus, threading of a

multidentate-ligand-incorporated axle and formation of the rotaxane prior to the metal-coordination is a preferred way. Under the conditions of Fe(II) ⁷⁴ and Ru(II) ⁷⁵, it was found out that the integrity of the supramolecular architecture was retained and the complexes could be formed successfully. The nature of the wheel was found the effect the photophysical properties of the Ru(II) complexes. Incorporation of different ligands and metal complexes into interlocked structure may give rise to new unique properties⁷⁶.

Going from the simple metal complexes of rotaxanes to the metal-directed self-assembly of rotaxanes, we encounter one, two and three dimensional networks by using the metal complexes of different types and geometries⁵⁶. Shown below in Figure 21 (a) is an Fe(II) templated self-assembly of terpyridine functionalized rotaxanes.

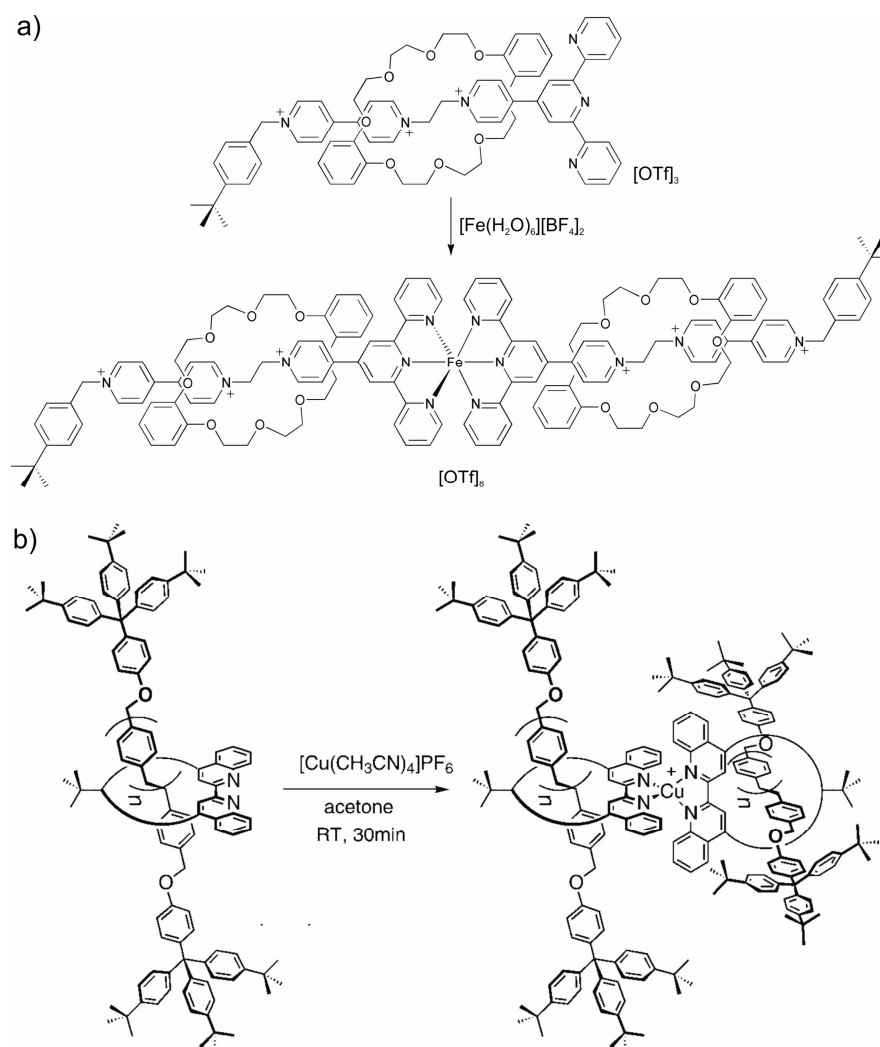


Figure 21. Assembly of rotaxanes a) through terpyridine functionalized axle by addition of Fe^{2+} (Loeb)⁷⁴ b) through biquinoline functionalized macrocycle by addition of Cu^+ at room temperature (Schalley)⁷⁷.

In our group, there was a successful attempt to form assemblies of tetra- and octalactam macrocycles and corresponding rotaxanes and catenanes⁷⁷, Figure 21(b). These rotaxanes contain macrocycles which bear biquinolines that point outwards (exocyclic site). Cu(I) complexes of both macrocycles and rotaxanes of this type could be obtained by straightforward syntheses at room temperature. A Ru(II) complex of the macrocycle using Ru(bpy)₂Cl₂ was also obtained and assigned use in anion sensing.

Others have contributed to metal-complexed rotaxanes by interesting examples: Leigh has made homo- and mixed metal complexes on the same rotaxane⁷⁸. Again, with the same system an allosteric control over the motion in the rotaxane was achieved⁷⁹. Although the goal of this study was not the self-assembly of rotaxanes, it was important to show that rotaxanes may be differently functionalized by ligands both on axle and on the macrocycle.

In Figure 22 another very appealing example in the field, the assembly of pyridine based ligand attached to a macrocycle or the corresponding pseudorotaxane through kinked Pt(II) complexes is shown. Threading into a pseudorotaxane can be achieved before or after the assembly displaying the flexibility of the approach.

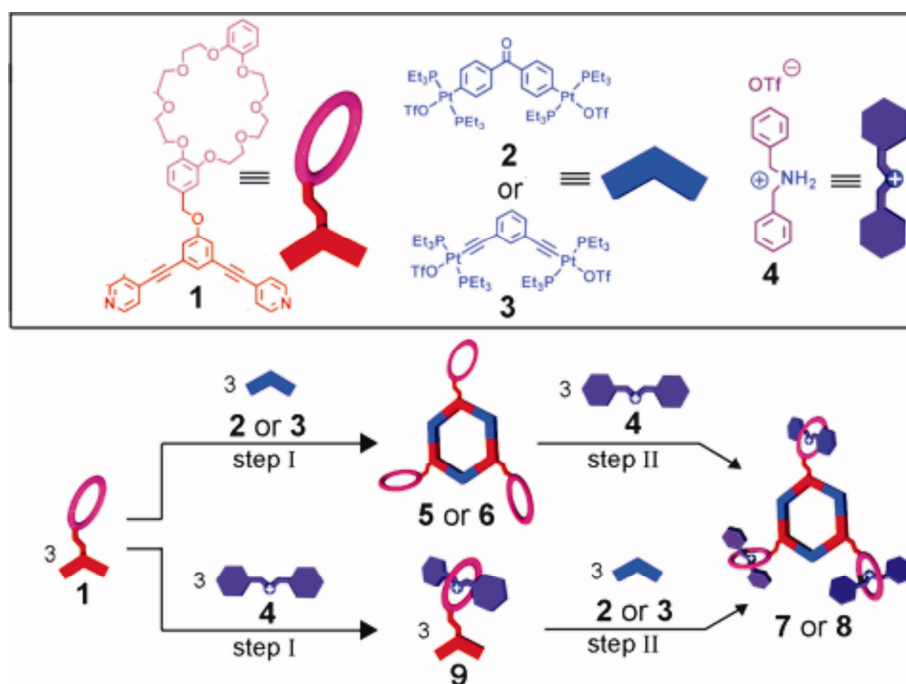


Figure 22. Ligand-attached macrocycle **1** can form hexameric assemblies with Pt (II) complexes **2** and **3** as well as thread **4** to form a pseudorotaxane. The assembly and the pseudorotaxane formation can be in any order displaying the flexibility of the approach⁶⁰.

2.4.3. Covalent Self-Assembly

Self-assembly in supramolecular chemical synthesis is not limited to metal-directed strategies. The chemistry of the covalent bond formation can be used in programmed self-assembly, too. Contrary to the natural sense of covalent synthesis being irreversible and the formed bonds being strong enough to keep the product intact under the reaction conditions, there is a growing interest for covalent bonds which may be broken and reformed under equilibrium controls⁸⁰. If the equilibria are fast enough, then the products can be obtained under thermodynamic control- this strategies of synthesizing compounds under thermodynamical control through covalent bonds are recently called as dynamic covalent chemistry⁸¹. Ring-closing metathesis, imine formation, disulfide bridges, transesterification are kind of reactions that were used in the synthesis of interlocked compounds through reversible covalent bonds⁸². The same reactions and methods can also be used in assembling the interlocked species to for example daisy chains⁸³ or other structures like bundles^{84a} or suitanes^{84c} (Figure 23).

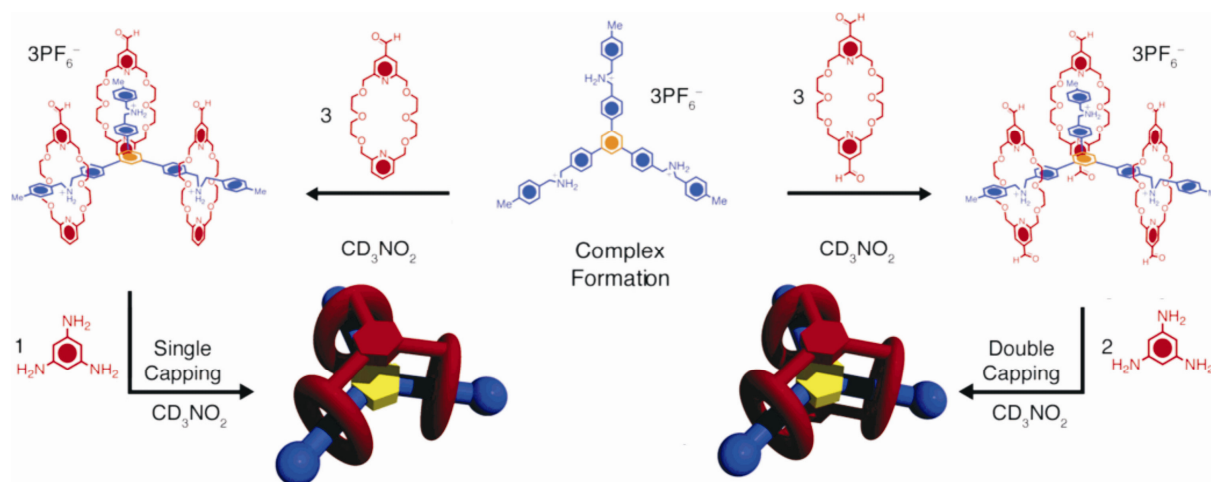


Figure 23. Covalent self-assembly through imine formation reaction to synthesize singly or doubly capped tris bundles^{84a}.

2.5. Covalently Bound Interlocked Architectures

Assembling the supramolecular or interlocked species is not only done by means of self-assembly. There are some examples in the literature that present the covalent bond formation between two or many interlocked species. Caprolactam stoppers on the rotaxanes were reacted with bisamines to yield network, side-chain and main chain polyrotaxanes in one case⁸⁵ (Figure 24). In another case, a tetrakis rotaxane and a biscatanene molecule were synthesized using linkers between the interlocked species⁸⁶ (Figure 25). Despite the beauty of the final products, the approach of synthesizing such systems covalently is non-fellexible because of irreversibility. Moreover, low efficiency and harsher conditions needed to achieve the systems are reported. However, the readers are here encouraged to compare the self-assembly approach with the covalent and imagine how these compounds could be formed through self-assembly strategies.

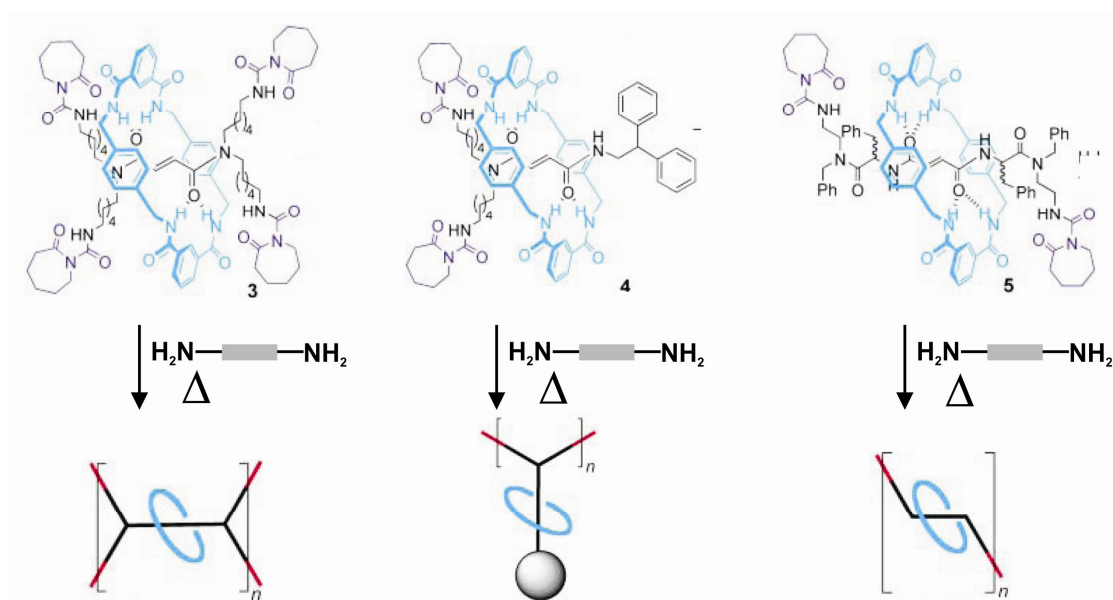


Figure 24. Polyrotaxanes: rotaxanes connected in different fashions to form polymers are examples of covalent assemblies of rotaxanes⁸⁵.

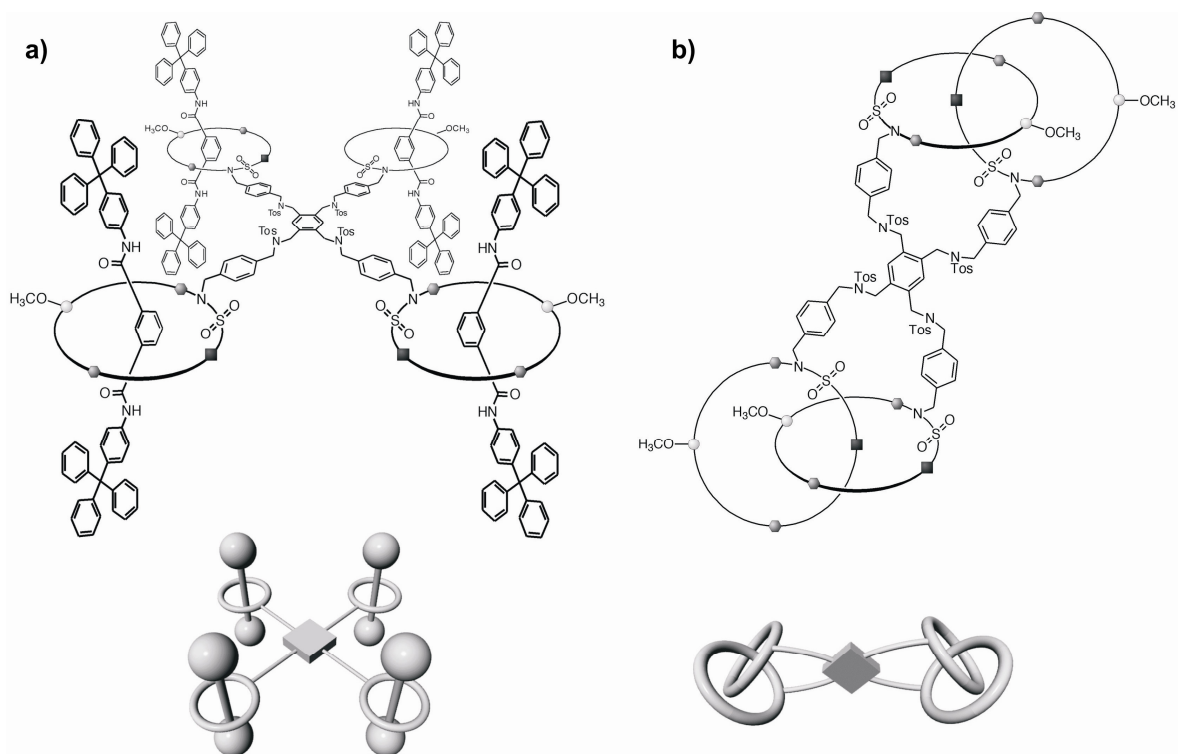


Figure 25. The covalently bound rotaxanes and catenanes⁸⁶.

2.6. Chirality in Supramolecular Systems: Topological Chirality in Interlocked Systems

As stated in the beginning of the chapter, to achieve unidirectional motion in molecular machines, chirality is a prerequisite (see section 2.1 for the discussion on unidirectional motion).

Chirality has long been an interesting topic for chemists. Chirality caused by a chiral center is one of the first things that chemistry students learn in their organic chemistry classes. However, chirality may exist even though there is a lack of chiral center (or stereocenter) in the molecule. This phenomenon, sometimes referred to as axial chirality, can be seen in unsymmetrically substituted allenes or biphenyls. Likewise, a supramolecular structure can possess chirality and exists as enantiomers without having a stereocenter in the structure. This phenomenon was first described in 1961 by Frisch and Wasserman⁸⁷. However, the first syntheses of such molecules, a topologically chiral knot and a catenane were first done by Sauvage and coworkers in 1980's⁸⁸.

One can realize the chirality in these molecules by reducing the structure to the simplest form (Figure 26). Thus, a macrocycle can be reduced to a flat circle. If two macrocycles are connected through a mechanical bond the result is a catenane, which has a

non-planar graph⁸⁹ and the topology is still achiral. The knot has a nonplanar graph and is topologically chiral because of the intertwining within the structure⁹⁰ and synthesized as racemic form.

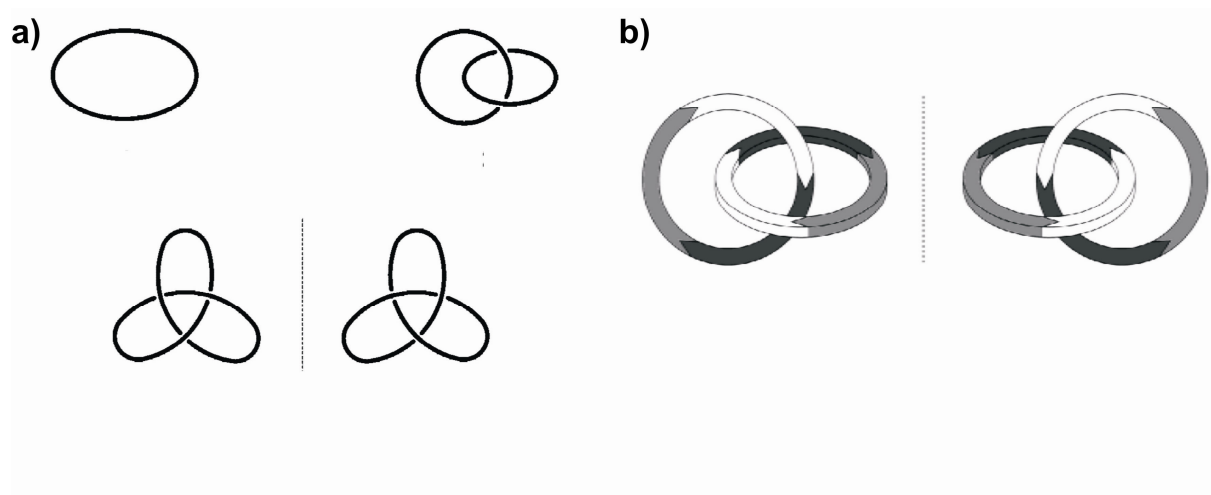


Figure 26. A macrocycle and a catenane has achiral topologies, whereas a knot is topologically chiral (a). Enantiomers of a topologically chiral catenane (b)⁹⁰.

Catenanes which consist of achiral macrocycles can be synthesized to be chiral by inducing an atom sequence giving the wheels directionality: The interlocked macrocycles in catenane have an orientation with respect to each other that may resemble the orientation of an allene, in which two double bonds stay perpendicular to each other. Like the unsymmetrically substituted allenes, if a substitution that causes the rings to be unsymmetrical is incorporated in the molecule, the resulting catenane is then, chiral. The idea of making small chemical changes in the macrocycle to obtain chiral structures was shown in some previous works⁹¹. Assemblies of supramolecular structures (e.g. knots) were also accomplished⁹². Many examples of chiral catenanes were synthesized by Sauvage⁹³, Vögtle^{90, 94}, Puddephatt⁹⁵ and Siegel⁹⁶. By the self-assembly of meso-macrocycles by palladium chiral catenanes were also obtained⁹⁷, as well as from chiral ligands by synthesis of Au(I) complexes⁹⁸. The catenanes which are made chiral starting with already chiral elements like binaphthyls⁹⁹ or enantiomeric 1,2-diaminocyclohexane¹⁰⁰ will not be discussed here.

As in the case for catenanes, if an unsymmetrical macrocycle is tied on an unsymmetrical axle, chiral rotaxanes can be obtained. The very few examples on chiral rotaxanes¹⁰¹ include a [2]rotaxane composed of an asymmetric wheel and axle for chiral sensing of amino acid derivatives¹⁰².

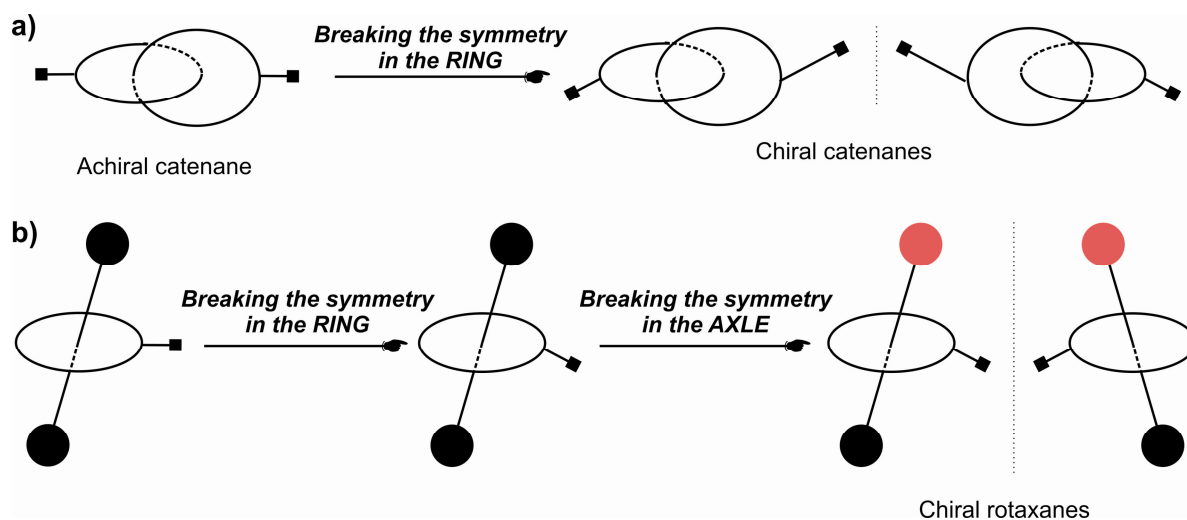


Figure 27. From achiral catenanes and rotaxanes to their chiral analogues: (a) For chiral catenanes ring symmetry must be broken to have directionality of rings that lead the interlocked structure to be chiral. In the case for a rotaxane (b) both ring symmetry and axle symmetry must be broken (a rotaxane may be thought as a one-ring opened-catenane) in order to achieve chirality in the architecture.

Topological chirality is not limited to catenanes, rotaxanes, and knots. Chiral rotaxanes can be fixed by covalent bonds between the macrocycle and the axle yielding in chiral pretzel-shaped structures^{94, 103}. These and other “pretzelanes”¹⁰⁴ and bis[2]catenanes formed on a calixarene template¹⁰⁵ are also chiral.

2.7. Energy Transfer in Interlocked Compounds

Fluorescence resonance energy transfer (FRET) is widely used to monitor association and dynamic processes of biological molecules¹⁰⁶, and has been used to monitor self-assembly of molecular capsules¹⁰⁷. However, there are only few systems featuring FRET across mechanically interlocked compounds¹⁰⁸⁻¹¹¹. As discussed in section 2.1, controlling¹¹² and addressing molecular motion is an important step in achieving efficient fueling of molecular machines. Figures 28 and 29 show some examples of related systems. The basic idea of such energy transfer systems is having a donor chromophore and an acceptor chromophore in which the donor in its excited state can transfer energy by a nonradiative, long-range dipole-dipole coupling mechanism to the acceptor in close proximity (typically $< 10\text{nm}$)¹¹³. In the interlocked systems, it is logical to attach the chromophores in different parts of the interlocked species. The efficiency of FRET which is monitored as increase in emission

spectrum of the acceptor upon excitation of the donor depends on the spectral overlap between the donor emission and the acceptor absorption and the distance between them.

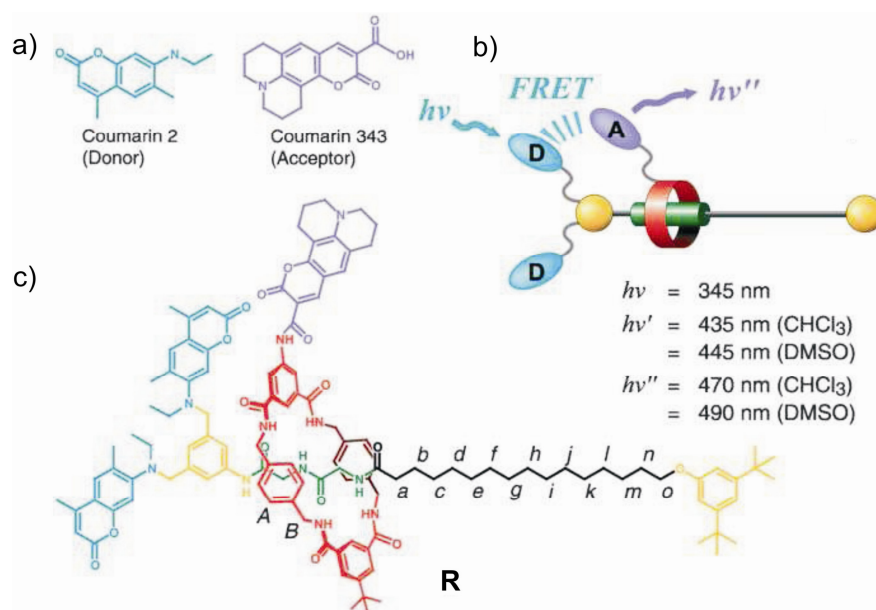


Figure 28. a) Donor and acceptor coumarins used in FRET study within the rotaxane **R**. b) Schematic and c) chemical structures of the rotaxane **R**^{110c}.

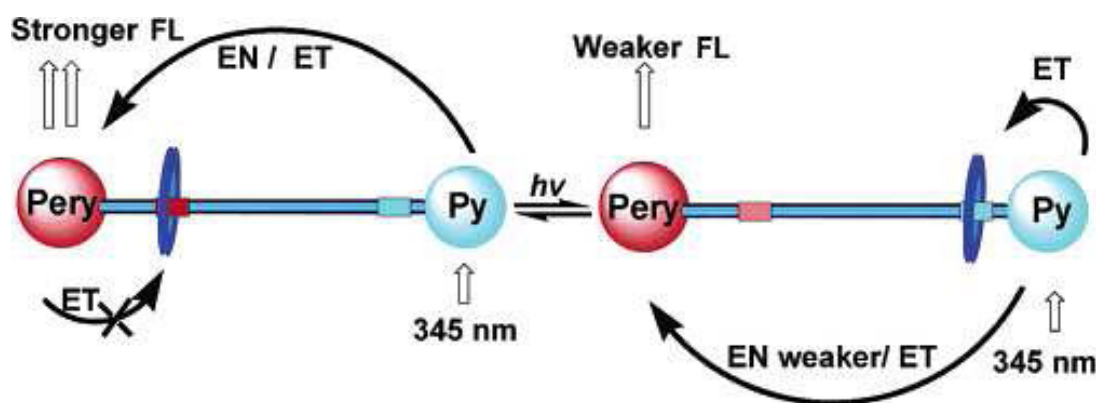


Figure 29. A bistable rotaxane containing pyrene and perylene bisimide as both stoppers and photoactive units. The shuttling of macrocycle switched the energy transfer from the pyrene to the perylene which results in change of fluorescence of the perylene moiety¹¹⁴.

2.8. An Easily Accessible Toolbox: Classical vs Toolbox-Oriented Synthesis

"Creativity, it has been said, consists largely of re-arranging what we know in order to find out what we do not know."

George Keller

Supramolecular chemistry, on the way to its unique architectures, developed new synthetical routes to create them. As stated before, the notion of supramolecular chemistry is the utilization of the self-assembly and template strategies as much as possible in producing complex systems with desired functions. In many cases with synthetic supramolecular chemistry, template and self-assembly strategies were quite efficient. The metal ion assemblies, in which the directionality of the interactions can be tuned very well, for example, display usually quantitative formation of the desired architecture; an amazing example to this is given by Fujita: 36 building blocks come together by metal-directed self-assembly to yield only one product¹¹⁵. Interlocked structures such as rotaxanes, catenanes, knots have profited very much from the efficient syntheses using these strategies as shown in previous section.

The missing link between the elaborately synthesized interlocked compounds and well-working molecular devices and machines was stated before in the beginning of this chapter as problems in 1) unidirectional motion, 2) efficient synthesis of molecular machines and the efficiency of work done by them, 3) efficient fuelling of the machines, and 4) incorporation of molecular machines to everyday nanotechnology starting with assembling the molecular machines.

Throughout the introduction chapter, these problems are addressed solutions from the efficient functionalization of the interlocked compounds were stated. Actually, functionalization of the supramolecular architectures is not a new topic in supramolecular chemistry and many examples, as displayed during the chapter, were given to the different modes of functionalizations with various functional groups for desired functionalities. However, effort to optimize the "point examples" was barely taken, most probably because of the lack of systematical approach in combination of threading (assembly) and functionalization of the structures.

Moreover, studies on the assembly (ordering) of molecular motion involving self-assembly and metal-directed self-assembly processes are quite new. The energy transfer through the mechanical bonds which is vital process in fuelling the machines is still to be

investigated in detail. All these require the right, efficient and straightforward functionalization techniques.

On the way to explore efficient, general use system for functionalized interlocked structures it is found that the minor changes in the modes of functionalization make large effects in efficiency of syntheses in the whole and efforts that are spent during the synthetical period.

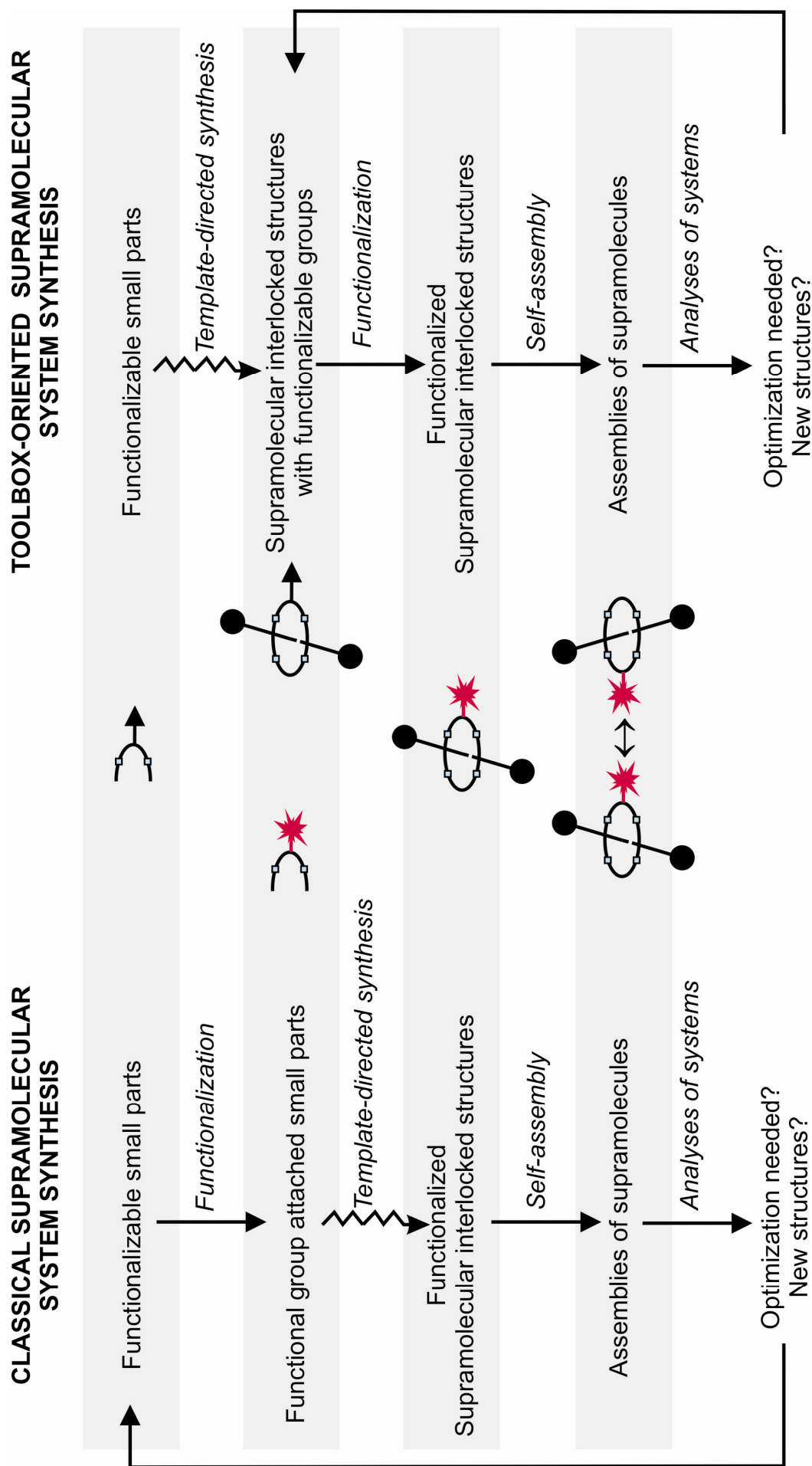


Figure 30. Classical vs. tool-box oriented supramolecular system synthesis. The effort is much reduced with the latter not only because the loop to a new architecture is smaller but also the effort-intensive template-directed synthesis step (shown with broken arrows) has to be run only once.

As stated before, the supramolecular chemists so far are working to achieve a particular desired structure and afterwards concentrate to analyze its function. So they usually start with the functionalizable small parts of the supramolecular building block, functionalize them and by the known (template directed) syntheses they form the supramolecular or interlocked structure which could then self-assemble or perform other functions. This approach what we called in the previous section as post-functionalization threading (or assembly) is the classical supramolecular synthesis which countless examples of functional structures were produced with success. However, the approach has a disadvantage that if a change in the functional group is needed, for example a fine-tuning in the fluorophore's wavelength (change of fluorophore) or altering of the metal-ligating part of the system is needed, the whole system should be resynthesized starting from the smallest parts, their functionalization, then the synthesis of the interlocked structure and the assembly. Each time when a need of change emerges, going back to the first step is required. Moreover, with every new compound the template-directed synthesis should be reoptimized. This includes optimization of the yield and the exploration of neat purification techniques (Figure 30).

The tool-box oriented supramolecular system synthesis which produces some supramolecular key compounds in the first step and postpones any kind of functionalizations to the latter steps, prevents the above-mentioned disadvantages by helping skip the template-directed synthesis of the interlocked structures every time when a change is needed. Briefly: **We do not need to produce the auto from the beginning to change the tyres.**

2.8.1. Practical Emergence of the Tool-Box Oriented Synthesis

The first sparks of the idea of having a tool-box oriented system which starts by the synthesis of key building blocks appeared after many unsuccessful or low-yield attempts to change the ligand incorporated in a rotaxane for metal-directed self-assembly synthesized previously by our group (Figure 31). The general synthetical way to obtain a tetralactam macrocycle of this type is first to prepare the Hunter's amine and one (when the macrocycle is symmetrically functionalized) or two (when it is asymmetrically substituted) acid dichlorides one of which is used to prepare the "extended diamine" in a reaction with excess Hunter's amine. The extended diamine and the acid dichloride are then separately prepared dichloromethane solutions and simultaneously dropped in a huge flask of dichloromethane. Under high dilution conditions, the macrocycle forms. Since the conditions are never ideal, higher cyclic or linear oligomers form together with the desired macrocycle which can be separated from the by-products by column chromatography.

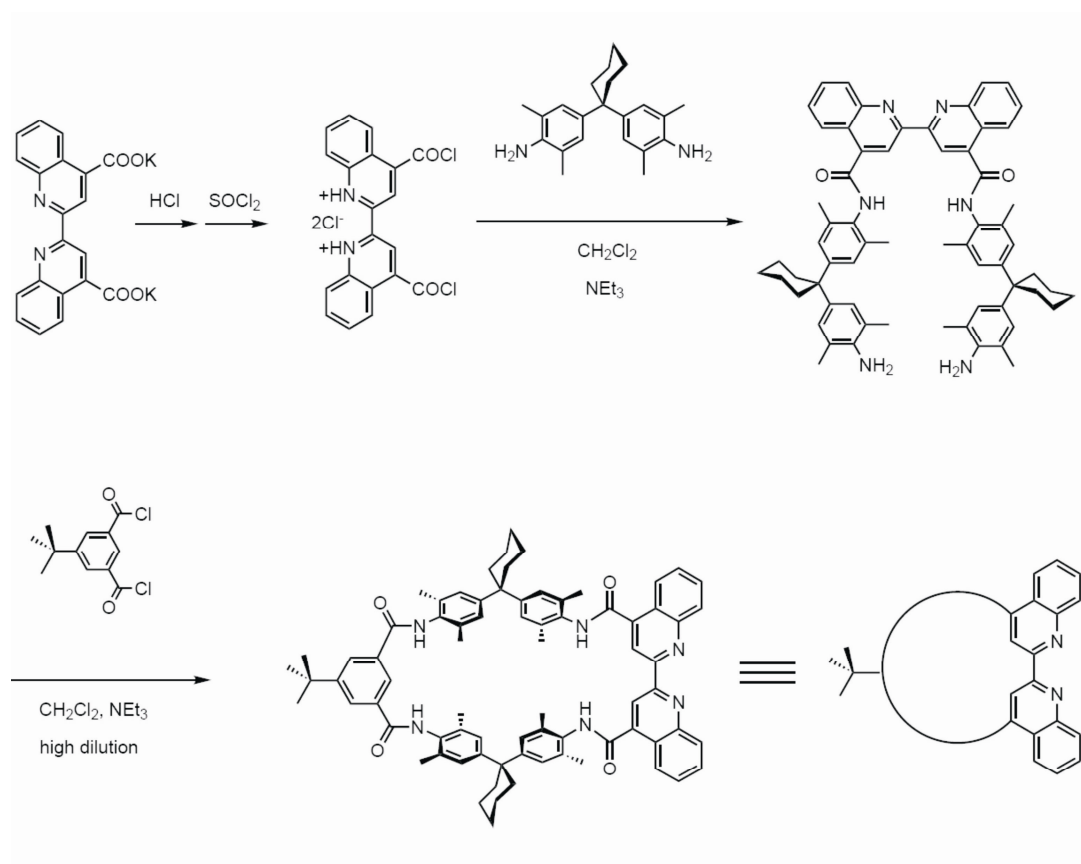


Figure 31. Synthesis of biquinoline macrocycle from its small parts.

To obtain a different macrocycle, first, every time a new acid dichloride had to be synthesized. Even at this very first step there were some problems for some ligands such as phenanthrolines. For the “mono-functionalized” macrocycles, macrocyclization step suffered from different solubilities of the acid dichlorides (solubility is one of the main factors that affect the yield in macrocyclization). Case for the 4,4'-dicarboxy 2,2'-bipyridine was harder because of the preferred trans orientation of the ligand which did not let any macrocycle to form. (The cis-trans barrier was smaller in 4,4'-dicarboxy 2,2'-biquinoline so the tetralactam macrocycle could be obtained in appreciable yield.) For the syntheses of macrocycle having two of these ligands in the structure requires the syntheses of the “extended diamines” of the corresponding ligands. This was in many cases also hard, because of the need to optimize the purification procedure for the extended diamines which form together with higher oligomers (Figure 32).

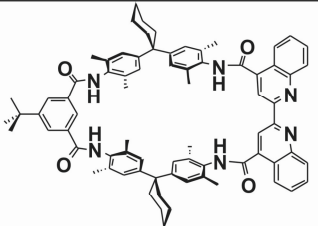
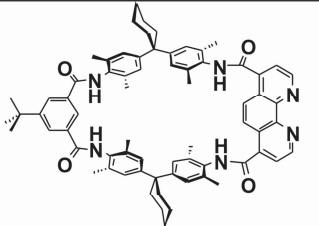
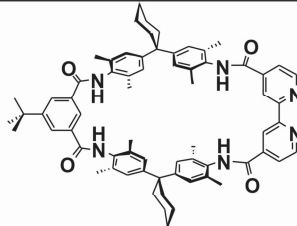
		
low cis-trans barrier	no cis-trans barrier problem acid dichloride	high cis-trans barrier low-solubility
Macrocycle yield: 10%	No macrocycle	No macrocycle

Figure 32. Change in the ligand incorporated in the structure causes different problems for each case.

Another way to obtain the macrocycles containing 2,2'-bipyridine-like ligands is to use a metal ion as a template in the synthesis to fix the cis-trans motion in the cis- geometry. This method was tried and for the low soluble bispyridine extended diamine the tris complex around Ru(II) was formed. In an other trial, a tris 2-2'-bipyridine 4,4'-carboxylic acid Ru(II) was synthesized. Forming the macrocycle following difficulties were encountered: 1) The extremely low yield in formation of the tris extended diamine Ru (II) complex, 2) The very low solubility of the both metal complexes in the solvent of macrocyclization reactions (Figure 33).

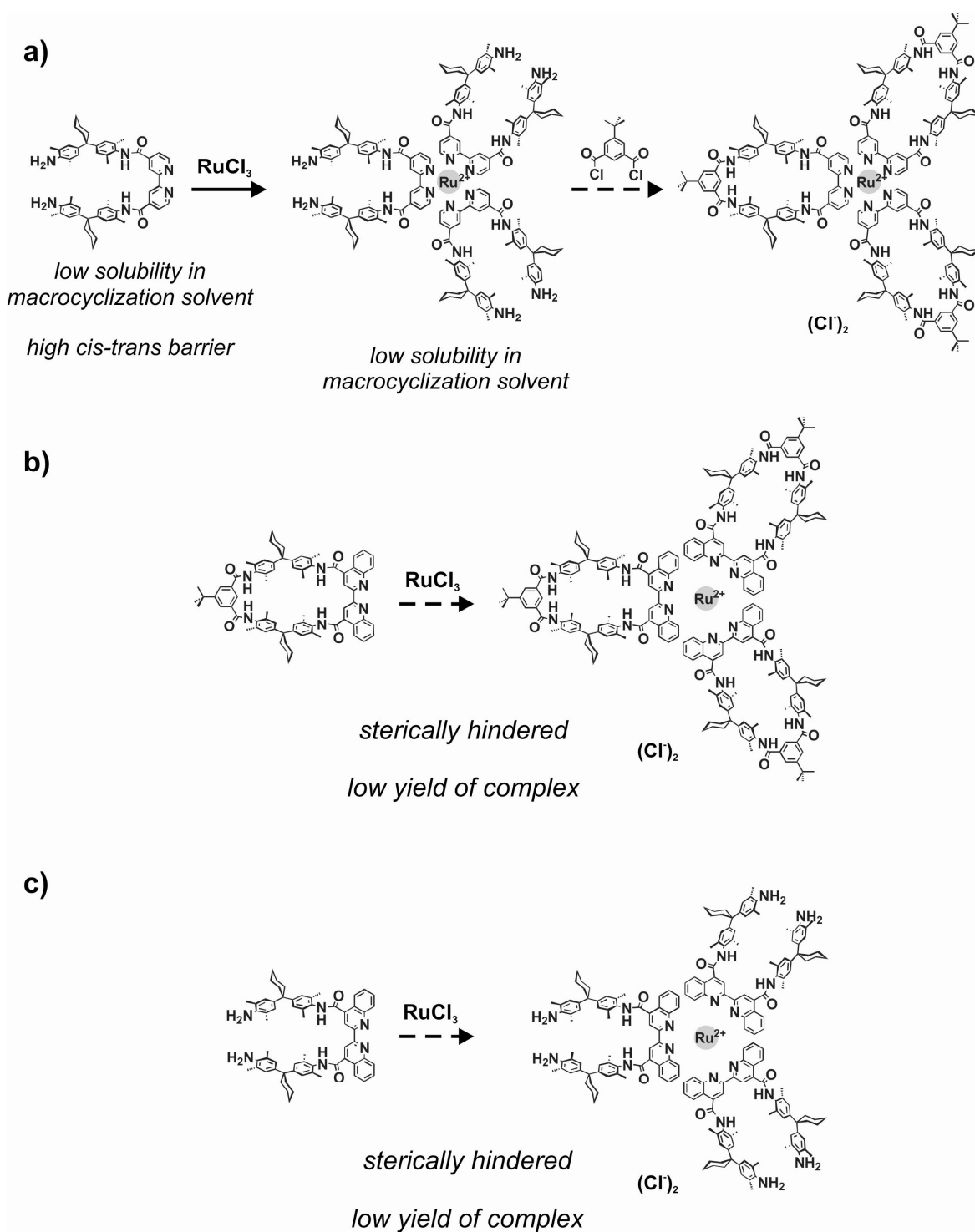


Figure 33. Problems encountered in making tris Ru^{2+} complexes of the biquinoline or bispyridine extended diamines, (a) and (c); and of the biquinoline macrocycle (b).

So far, a few of the problems encountered in some particular macrocycle syntheses were briefly stated. Work for optimization is also needed in the next step, rotaxane synthesis, where the macrocycle is used as a template. Since putting different-length functional groups

on the frame of the macrocycle alters the macrocycle shape, the positions of the templating amide groups are also affected. Thus, the rotaxane synthesis has to be studied (new axle design, determination of the binding constant for new axles and the host macrocycles etc.) for each new case.

2.8.2. *Applying the Tool-Box Oriented Supramolecular System Synthesis to Generate a Tool-Box of Tetralactam Macrocycle Based Functionalized Supramolecular Architectures*

For the generation of key compounds the most important factors that care should be taken are:

- Retention of the cavity's size, shape and hydrogen bonding scheme (utilization of the knowledge on template effects on unsubstituted tetralactam macrocycles, discussed in section 2.2)
- Straightforward access to a variety of macrocycles and rotaxanes from the same precursors
- High yields in obtaining the functionalized macrocycles and rotaxanes

For fulfilling these main requirements first of all the mode of functionalization was changed from endo-functionalization to exo-functionalization. That is the macrocycle body was retained and the functional groups were carried out of the macrocycle using of halo-isophthalic acid. Utilization of the obtained key macrocycle in template directed synthesis to obtain the supramolecular structures to prepare key interlocked compounds which then could be functionalized with the desired function is the application of *tool-box oriented supramolecular synthesis* displayed in this thesis (Figure 34).

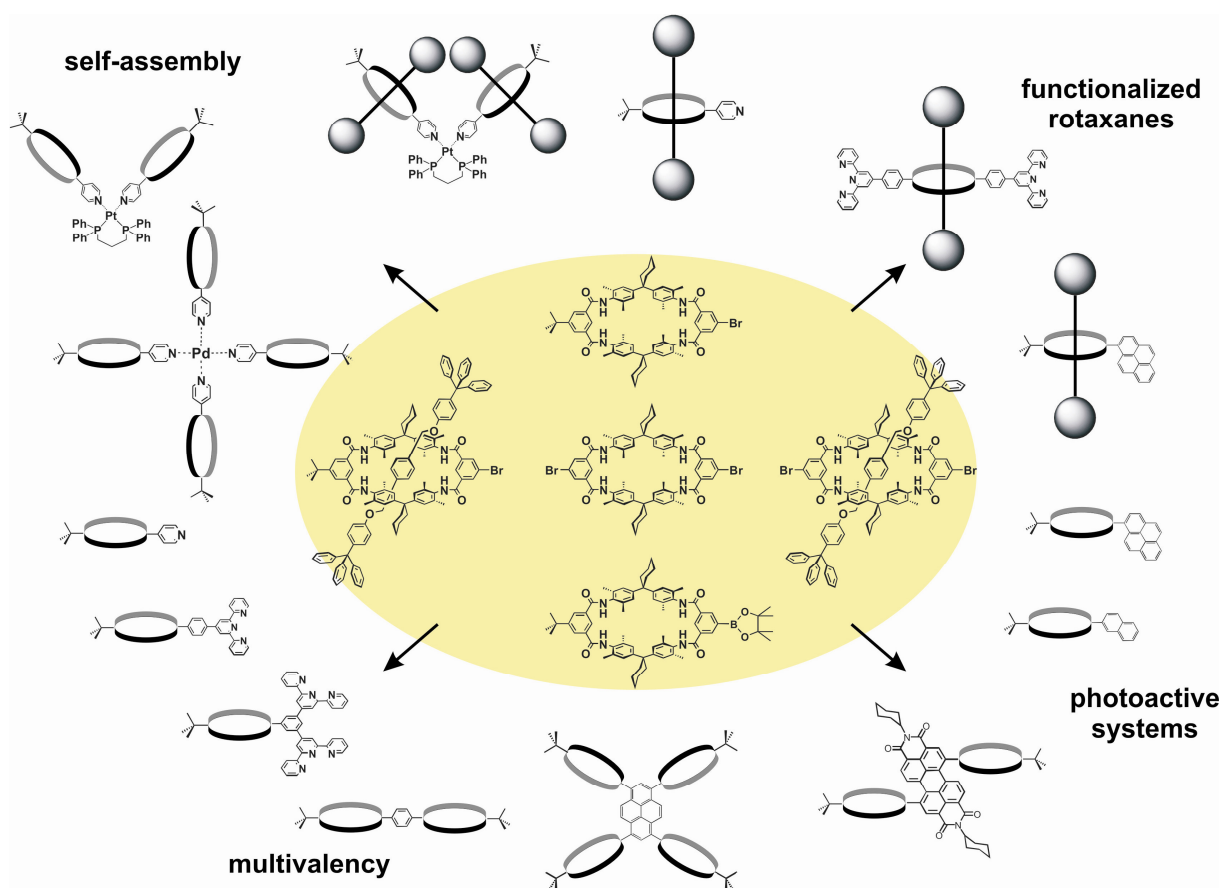


Figure 34. Representative examples of macrocycles, rotaxanes and assemblies produced by tool-box oriented supramolecular synthesis.

For the attachment of functional groups on the macrocycles, rotaxanes and catenanes, Suzuki¹¹⁶ and Sonogashira cross coupling and Click reaction¹¹⁷ procedures were chosen not only because of the higher yields in coupling reactions, but also of their mild nature which do not harm the already existing groups on the architectures. Moreover, for the structure flexibility coupling reactions are cross-coupling reactions fine-tune: The resulting structures have enough flexibility to allow the ring behave independently from the functional groups but are *rigid as desired for achieving directionality* (e.g. for metal-directed self-assemblies) (Figure 35).

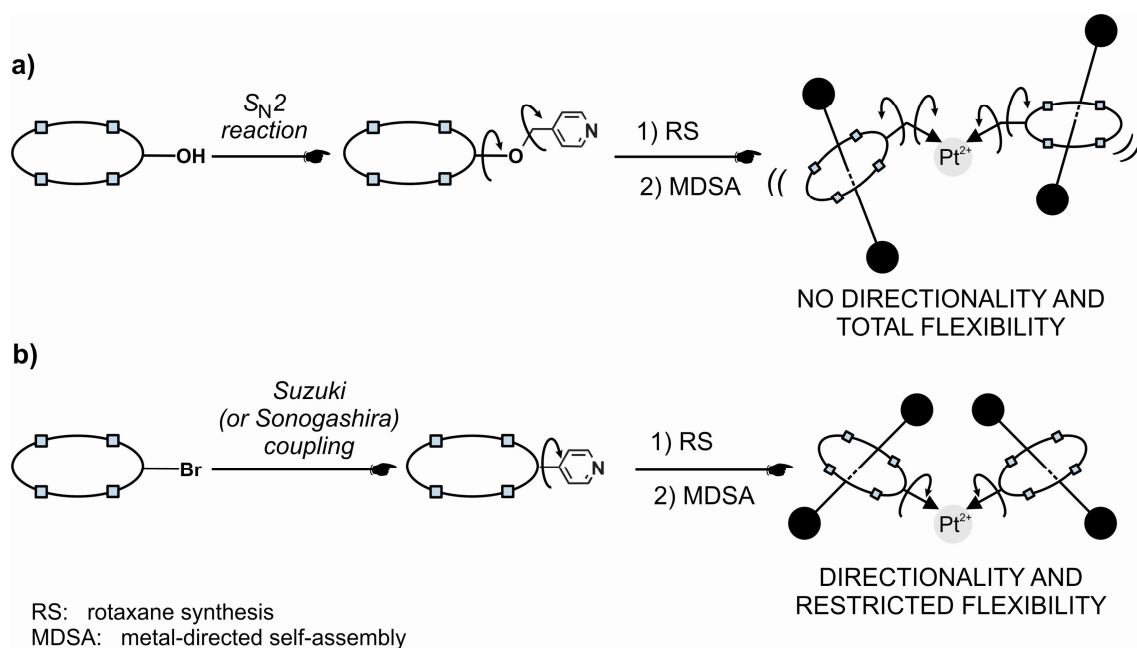


Figure 35. a) Total flexibility of the final architectures may be achieved by efficient S_N2 reactions. However the lack of directionality of the macrocycle units can be a problem for alignment in desired directions, b) Cross-coupled products have restricted flexibility, however directionality e.g. around a metal ion is kept as needed.

The success in obtaining great variety of compounds in an efficient way together with the examples of functional architecture for desired function are exhibited in the following part of this work.

3. Results and Discussion

3.1. Syntheses of the Key Compounds

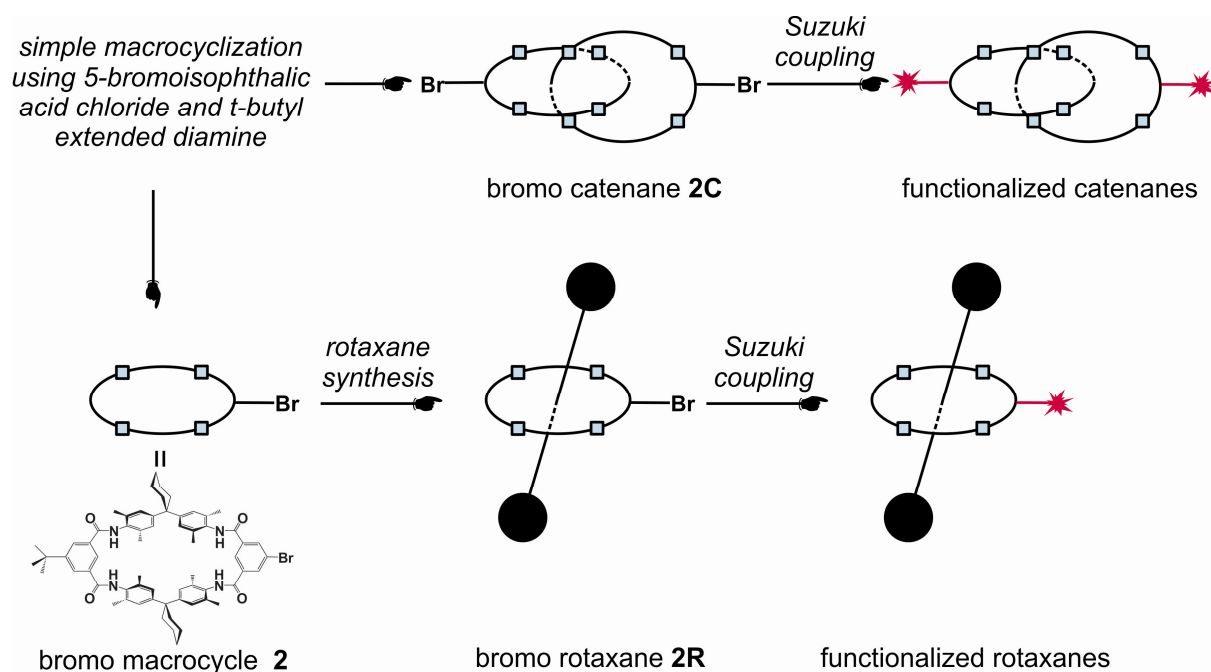


Figure 36. The schematic representation of the tool-box oriented synthesis on some of the key compounds: bromo tetralactam macrocycle **2**, bromo rotaxane **2R** and bromo catenane **2C**; and the strategy to obtain functionalized supramolecules (stars designate functional groups).

To have an easy access to a tool-box of supramolecular compounds, and since the rest of the functionalization was attempted to be Suzuki coupling reactions, first the syntheses of precursor (key) compounds, bromo **2** and dibromo **3** tetralactam macrocycles from the bromo-isophthalic acid dichlorides was the first step (Figure 36 and Figure 37). Previously, for key functionalization of the macrocycle, triflate **1**¹⁸⁸ was used, but because of the multi-step procedure to obtain this macrocycle, low yields both in obtaining the macrocycle and in further syntheses with the macrocycle turned our attention to the bromo macrocycles **2** and **3** which are rather easily achievable and functionalizable. Bromo catenanes need not to be separately synthesized, since they are by-products of the macrocyclization reaction. However, some effort was also spent on increasing the usual low-yields obtained for the catenanes since these interlocked species had not been fully investigated for further post-threading reactions. Key rotaxanes **2R** and **3R** were separately synthesized from the key macrocycles **2** and **3** for further functionalization which, also had not been studied previously.

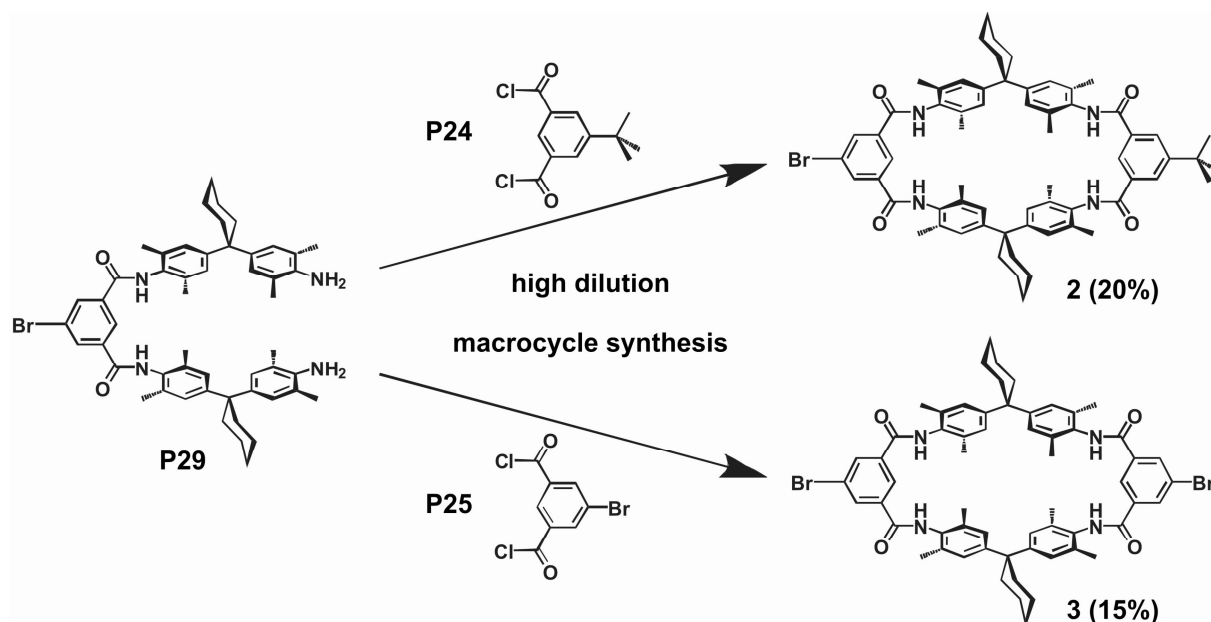


Figure 37. Synthesis of the key macrocycles from the extended diamines.

On the way to the bromo macrocycles the extended diamines is the usual first step (Figure 37). The extended diamine was synthesized from 5-bromo isophthalic acid dichloride **13** by using the general procedure¹⁹⁰. The extended diamine was then reacted in high dilution with either 5-*tert*-butyl isophthalic acid dichloride **P24** or 5-bromo isophthalic acid dichloride **P25** to form the starting macrocycles **2** and **3**, each time with moderate to low yields (20-25% for the bromo macrocycle and 15-20% for the dibromo macrocycle). In the case with dibromo macrocycle **3** low solubility of the extended diamine **P29** in dichloromethane prevents higher yields. For that reason, the synthesis of the bromo macrocycle **2** was done using the 5-bromo isophthalic acid dichloride **P25** and the dichloromethane-soluble *tert*-butyl extended diamine **P28**. In this case yield of macrocycle was increased by 5-10 %.

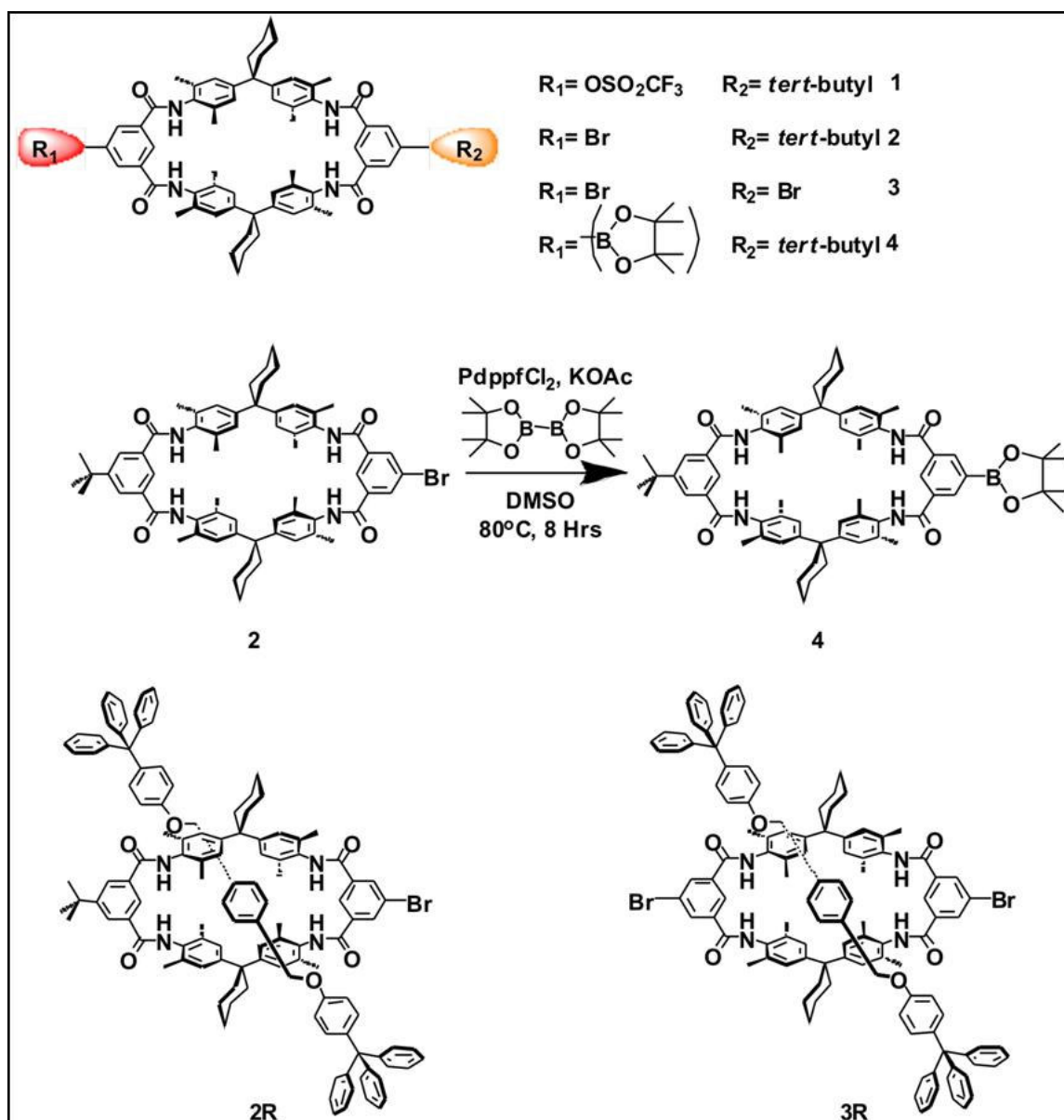


Figure 38. The key compounds synthesized in this work: bromo macrocycle **2**, dibromo macrocycle **3** and boronic acid pinacol ester **4** macrocycles and bromo **2R** and dibromo rotaxanes **3R**.

The boronic ester macrocycle **4** can easily be prepared from the bromo macrocycle in a standard Miyaura reaction¹¹⁸ as shown in the Figure 38. This compound was useful when the counterparts in the desired following Suzuki reactions were not readily available as boronic acids or esters, especially for production of multivalent hosts. The yields for the isolated boronic ester macrocycle usually were moderate around 75%. Higher solubility of the obtained macrocycle in the common organic solvents was an additional advantage for further reactions.

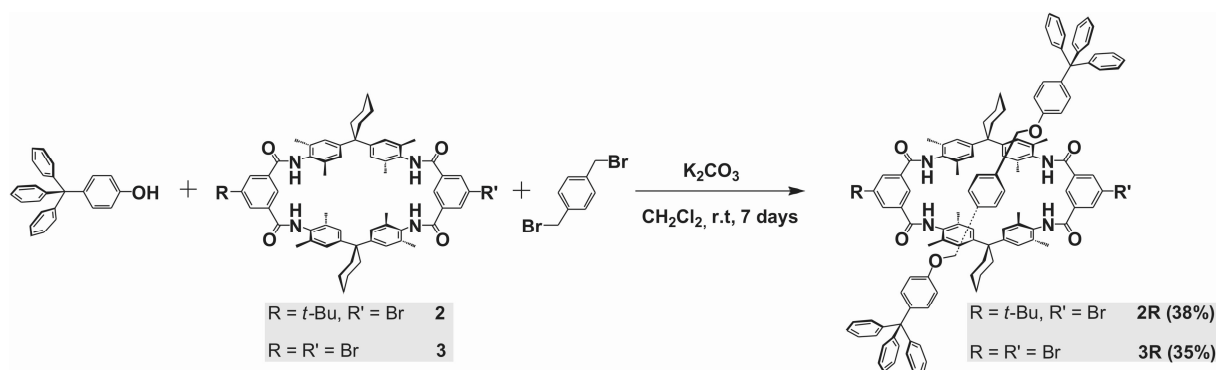


Figure 39. Synthesis of the key rotaxanes **2R** and **3R**.

Synthesizing a key rotaxane and functionalizing it with different groups is the reflection of the tool-box concept in the functionalized rotaxane synthesis. For that purpose, bromo rotaxane **2R** and dibromo rotaxane **3R** were synthesized using the anion template strategy (Figure 39). The choice of template and so of the axle was made according to the yield of the rotaxane synthesis known in the literature and from the previous studies in the group. Anion templated rotaxane syntheses are known⁴⁰ to have high yields (around 90%). In our case, the yields were lower (around 40%) probably due to the low solubility of the bromo and dibromo macrocycles in pure dichloromethane which was the solvent of the reaction. However, the rotaxanes could be obtained purely as evident from the negative mode FTICR-MS spectra and ¹H NMR spectrum (Figure 40 and 41).

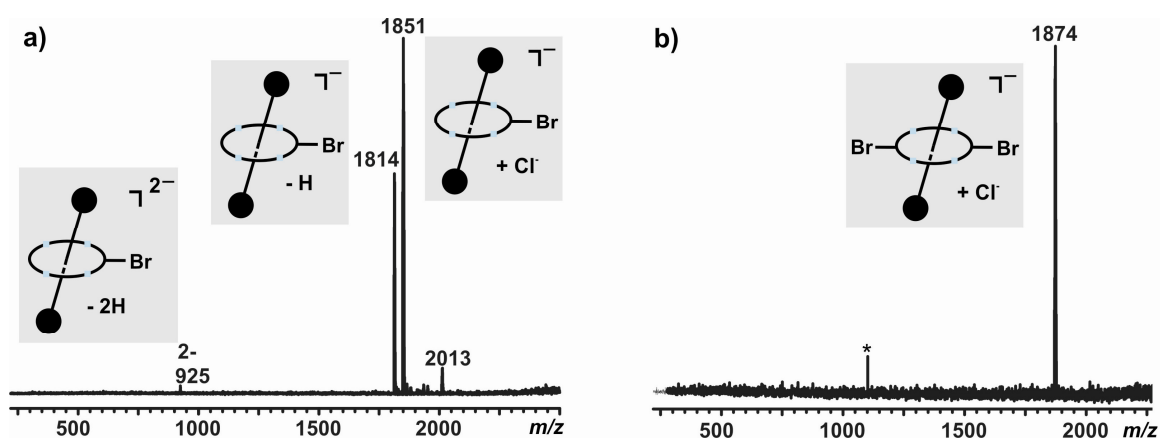


Figure 40. FTICR-MS of a) bromo **2R** and b) dibromo **3R** rotaxanes showing the rotaxanes can be obtained pure: Free macrocycle and free axle are not present in the spectrum.

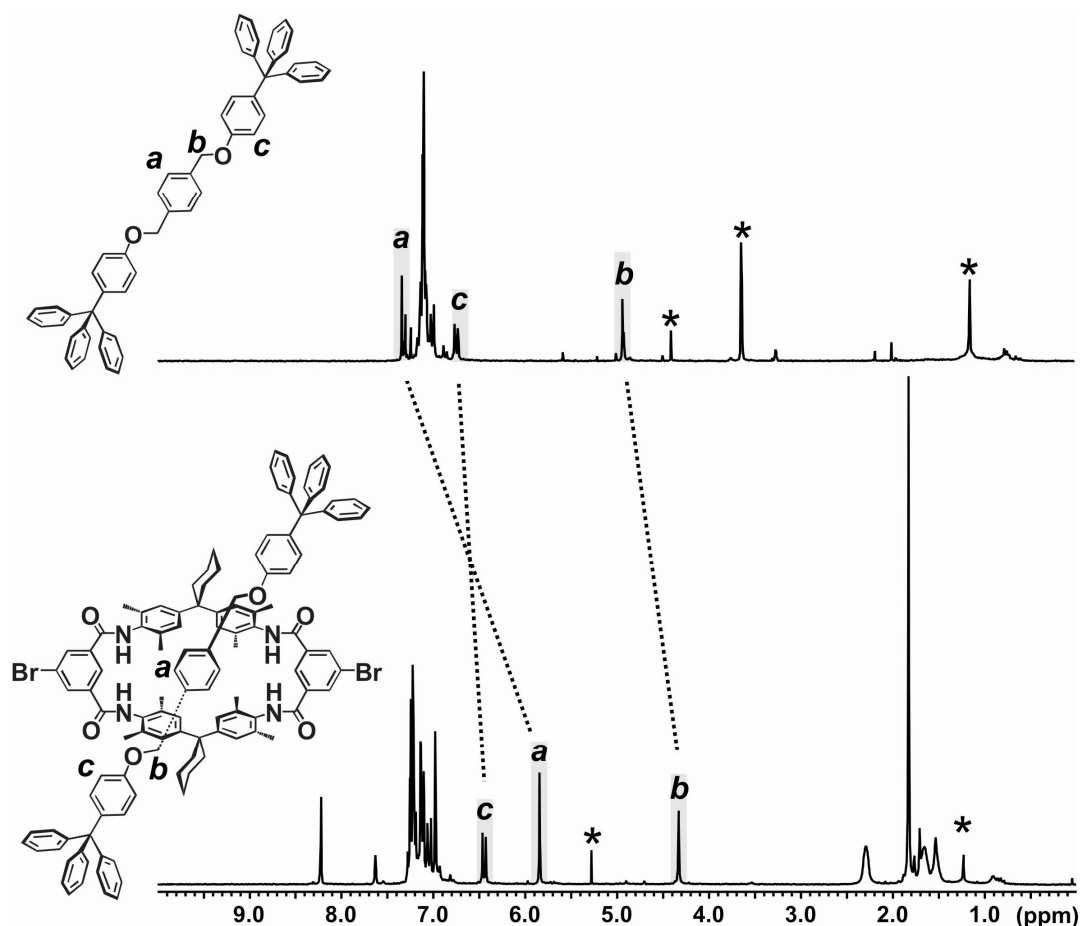


Figure 41. ^1H NMR spectra of free axle and dibromo rotaxane **3R**. The anisotropy of the phenyl rings in the macrocycle cavity causes the axle protons **a**, **b** and **c** to shift to upfield which is an indication of the interlocked structure.

As expected for rotaxanes the phenyl protons (**a**) of the axle middle piece were shifted around 1.5 ppm upfield because of the anisotropy effect created by the phenyl rings making up macrocycle cavity that they are in. A similar upfield shift was observed for the methylene protons (**b**) of the axle (-0.5 ppm) and the ortho protons of the phenyl (**c**) of the stopper (-0.3 ppm). The effect was more pronounced for the middle piece because it stays deeper in the cavity. The interlocked nature of the rotaxanes could be also proved by MS/MS experiments. A rotaxane may be differentiated from the isomeric 1:1 complex of macrocycle and free axle by the differences in MS/MS spectra: 1:1 complex should easily dissociate at lower energies whereas for the rotaxane higher energies must be given in order to cleave one bond on the macrocycle to release the free axle from the interlocked structure¹¹⁹. Unfortunately, this was not possible for the anion templated rotaxanes since the benzyl ether cleavage is a favoured process (even at lower excitation energies) that can compete with the dissociation of the

unthreaded complex. Nevertheless, clean NMR spectra displaying the high field shifts of the middle piece of the axle and the mass spectra showing the presence of the right m/z for the rotaxanes and absence of free components proved the rotaxane structure every time.

3.2. Functionalization of the Macrocycles

3.2.1. Functionalization of the Key Macrocycles by Suzuki Coupling Reactions

3.2.1.1. Syntheses of Macrocycles for Self-Assembly

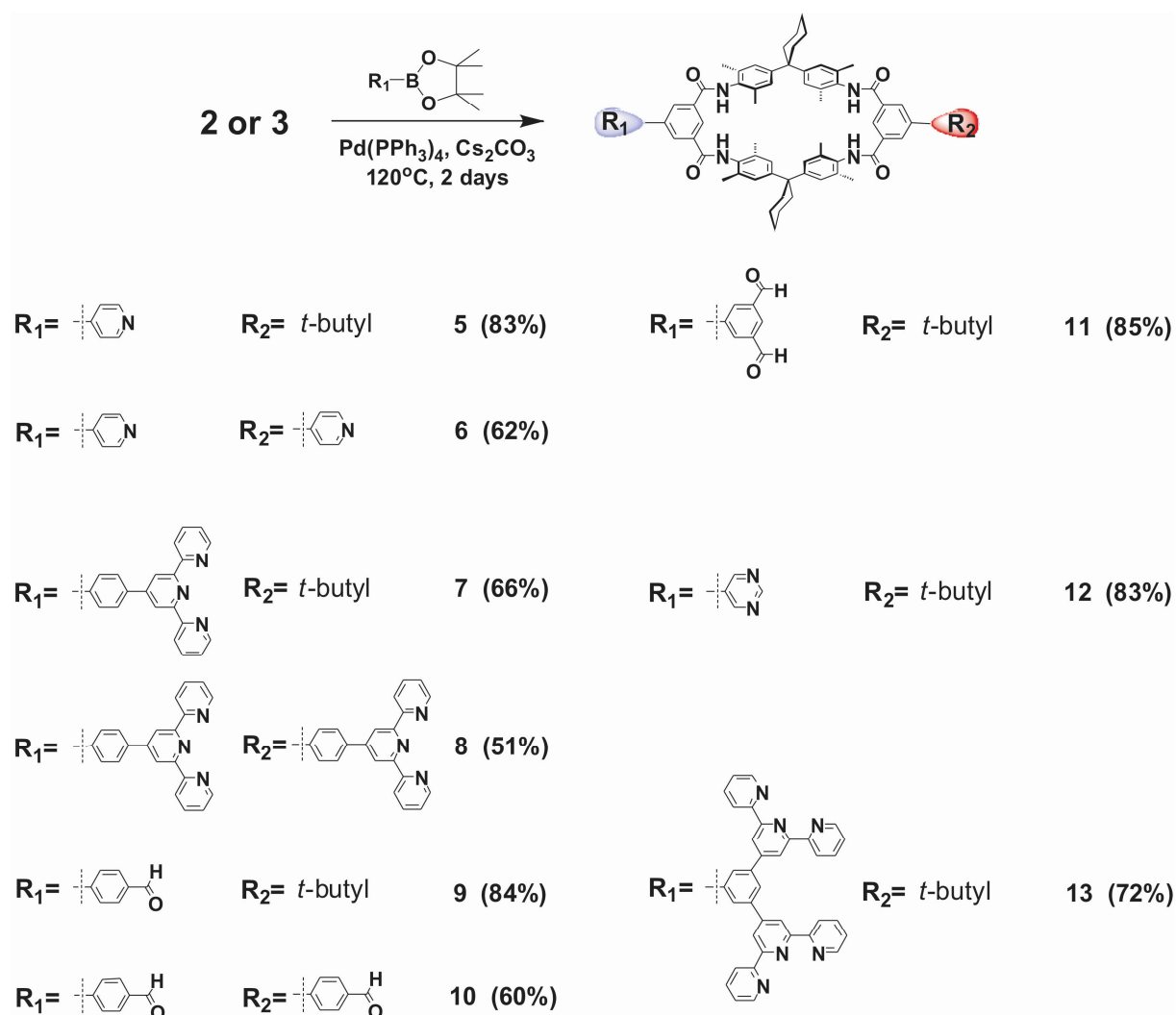


Figure 42. Functionalization of the key macrocycles with ligands by Suzuki coupling reaction: Products for metal-directed self-assembly and covalent-self-assembly.

The first group of compounds synthesized by using Suzuki coupling reaction on the key macrocycles were the ones containing functional groups for the self-assembly of the macrocycles: ligands for metal-directed self-assembly with metal ions (**5-8** and **12-13**) and

aldehydes for covalent self-assembly with amines (**9-11**) (Figure 42). A usual Suzuki coupling reaction on aromatic compounds has two counterparts: a halogen (or triflate) containing compounds and a boronic acid. Lately, it was shown that boronic acid esters can also be used¹²⁰. For a reaction with our macrocycles boronic acid pinacol esters were more attractive because of the higher solubility of these esters in organic solvents. Thus for the ligands of choice the pinacol esters were prepared from their boronic acids whenever the boronic acids were available. In the cases that the corresponding boronic acids were not commercially available, like the terpyridine ligands, pyrimidine and the 3,5-benzene dicarbaldehyde, boronic ester was synthesized either from boronic acid which was prepared from the bromide or in one step using Miyaura reaction.

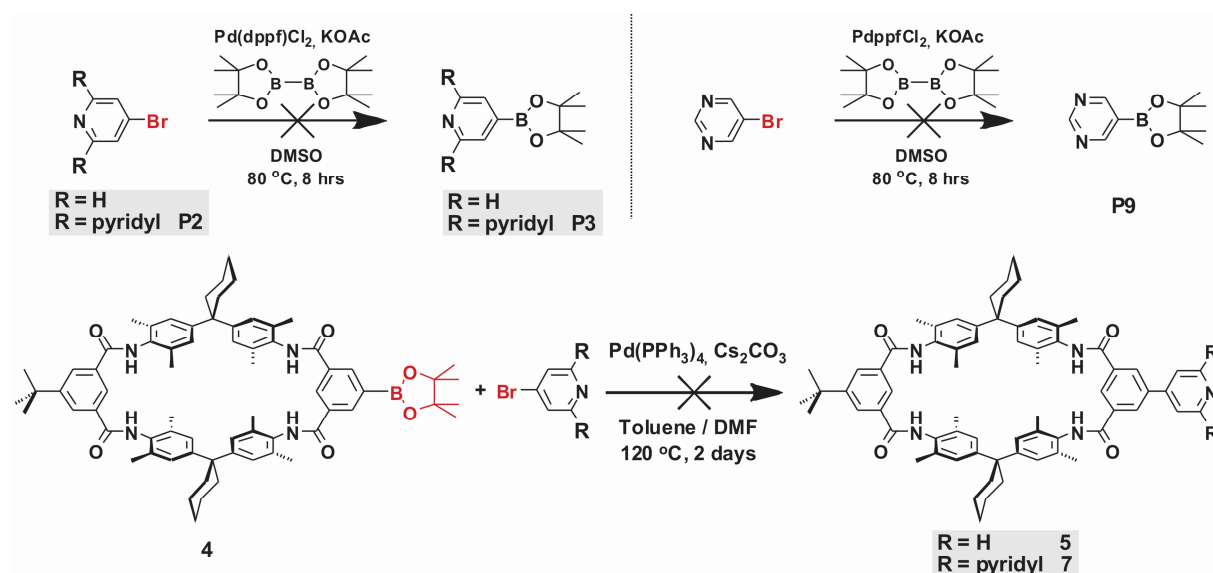


Figure 43. Limitations in preparations of the boronic esters of the nitrogen containing rings and the following Suzuki coupling.

It should be noted here that Miyaura reaction does not work directly on the nitrogen-containing aromatic rings, so this way could not be taken for pyridine, pyrimidine and for terpyridine¹²¹. Likewise, Suzuki coupling does not work when the bromides of these compounds are put into the reaction with aromatic boronic esters¹⁷⁹ (Figure 43).

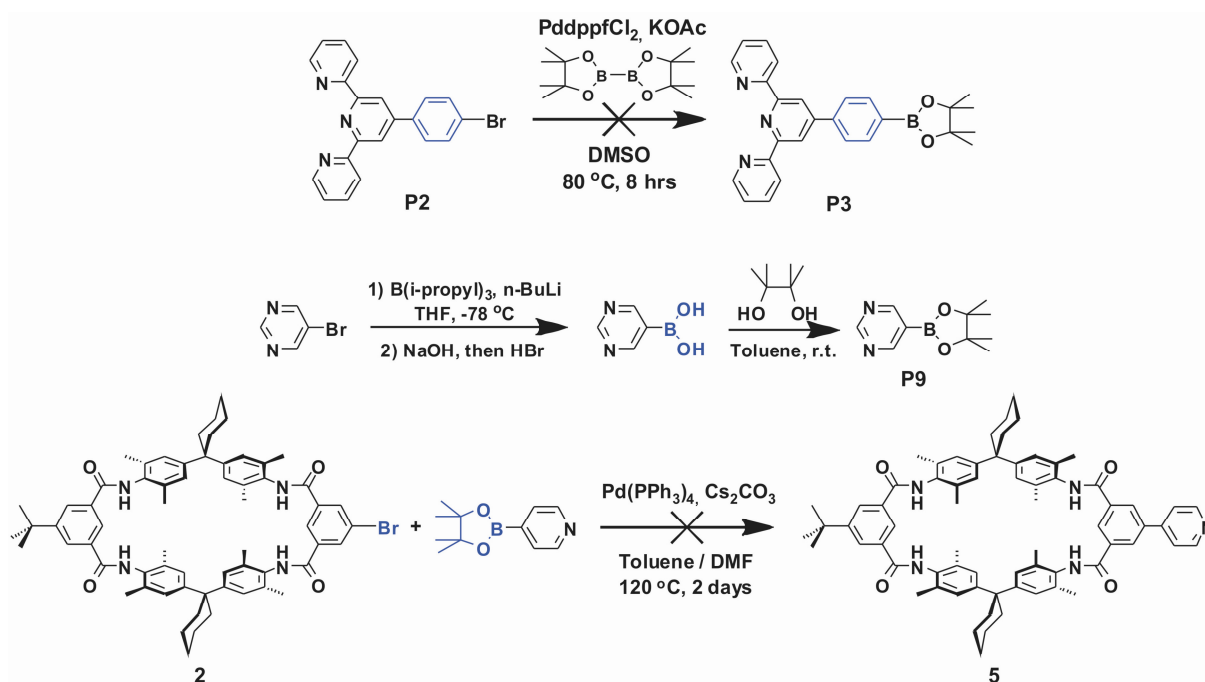


Figure 44. Some solutions to the problems encountered in the synthesis of ligand functionalized macrocycles.

To overcome these limitations,

1) the ligands were separated from the macrocycle by one phenyl unit. In this case, because there is lack of direct connection, the ligand could be attached the boronic acid pinacol ester function by Miyaura reaction. Terpyridine macrocycles were prepared using this method because of the additional advantage in the preparation of the starting bromo terpyridines which is a one-pot and high-yield synthesis. (The 4'-bromide terpyridines are usually synthesized through multi-step procedures which increases the effort) and

2) the step-wise procedure to obtain the boronic acid pinacol ester was used. If a direct connection between the ligand and macrocycle is needed and boronic acid could be obtained easily, this is the most advantageous way. Pyridine and pyrimidine macrocycles were prepared this way (Figure 44).

In all cases the coupling reactions were quite efficient, seeming to be quantitative on TLC. Purification with column chromatography on silica and alumina was quite straightforward, especially for the mono-functionalized macrocycles. Characterizations of all the functionalized compounds were made by ^1H NMR, ^{13}C NMR and ESI-MS. All of the compounds synthesized were used in appropriate self-assembly studies and/or rotaxane syntheses.

3.2.1.2. *Unsymmetrical functionalization on the tetralactam macrocycle: Pyrene-pyridine macrocycle*

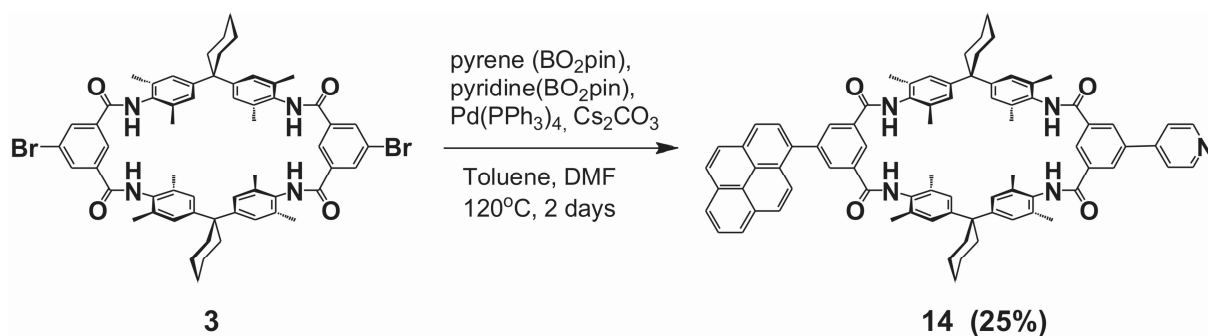


Figure 45. *Synthesis of differently substituted macrocycle 14.*

The symmetrical substitution on the macrocycle provides the same kind of connectivity or function on both sides of the macrocycle. Attaching different groups on the macrocycle may provide two functional groups for different purposes. As an example, a pyrene-pyridine macrocycle **14** was synthesized through a Suzuki coupling reaction using both boronic acid pinacol esters at in one pot (Figure 45). The reaction yielded statistically, the symmetrically substituted products, bispyrenemacrocycle and bispyridine macrocycle and the desired unsymmetrically substituted macrocycle in 25% (isolated yield). A step-wise procedure starting from dibromo macrocycle **3** and first obtaining mono-substituted pyrene or pyridine macrocycles was not taken to avoid the yield-reducing purification steps on column. The product was characterized by ¹H NMR and FTICR MS.

3.2.1.3. Syntheses of Macrocycles for Multivalency¹²² and Photophysical Studies

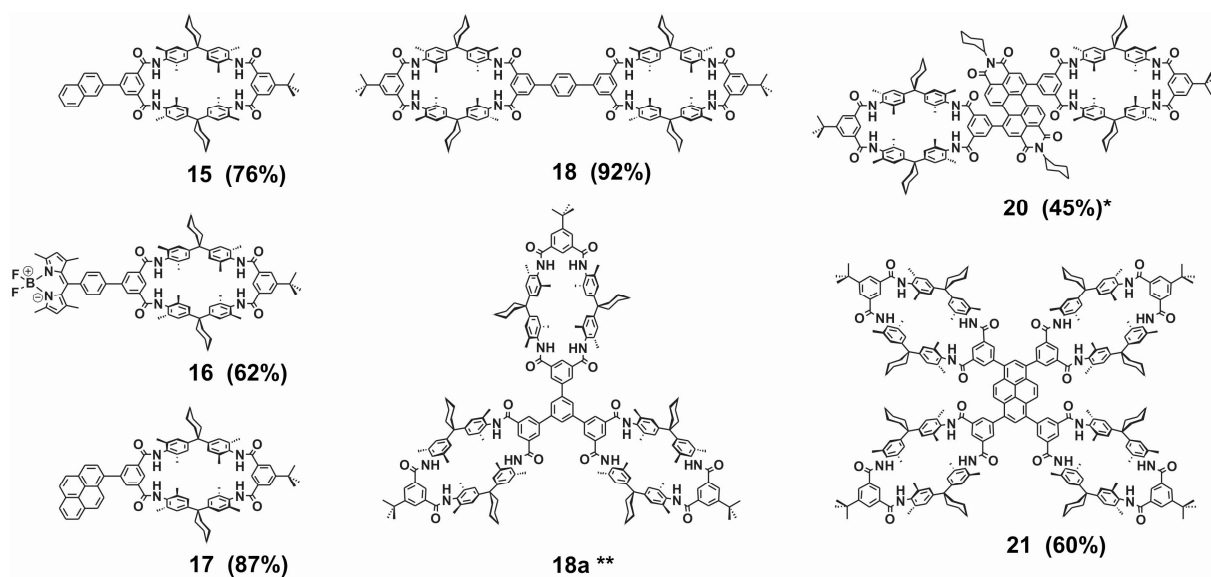


Figure 46. Photoactive macrocycles **15**, **16** and **17** (left), multivalent double and triple macrocycles **18** and **18a**¹²³ (middle), multivalent photoactive hosts **20** and **21** (right). The yields of isolated products are given in parentheses (*: yield after extensive purification steps, **: compound not isolated).

Functionalization of the macrocycle with photoactive groups were done

- to determine binding constants of the host complexation by spectroscopic measurements,
- to study the intra-rotaxane energy transfer,
- to operate future molecular machines built from these rotaxanes by light.

For obtaining a palette of wavelengths of absorption and emission and to obtain variety of systems with different macrocycles and guests (or rotaxanes), bromo macrocycle **2** was reacted with the boronic acid pinacol esters of the desired photoactive groups in Suzuki reactions. In all cases the coupling was quantitative on TLC and the isolated yields were high. Naphthalene **15** and pyrene **17** macrocycles were used later in studies for determination of binding constants and building energy transfer in rotaxane systems. The other macrocycles **16**, **18**, **20** and **21** were recorded UV-VIS spectra and - if applicable - fluorescence.

Multivalent interactions, which rely upon noncovalent bonds, are essential ingredients in the mediation of biological processes, as well as in the construction of complex structures for materials applications. A fundamental understanding of multivalency in supramolecular chemistry is necessary not only to construct motors and devices on the nanoscale but also to

synthesize model systems to provide insight into how biological processes work^{122c}. This study focuses only on some multivalent hosts, the problems and in their synthesis and characterization and the solutions for these. The multivalent hosts **18** and **18a** were synthesized with good to moderate yields. Comparing the two syntheses, it was seen that increasing the number of macrocycles around a small core like benzene the purification of the compound gets more complicated with column chromatographic methods. **18a** could not be obtained as a pure product, though the thin-layer chromatographic investigations showed that the coupling reaction was almost complete. Changing the core benzene with a larger molecule like perylene or pyrene (compounds **20** and **21**) gave better results. These compounds could be isolated with higher purity. The detailed discussion of these compounds will be given later in Section 3.3.

3.2.2. Functionalized Macrocycles by Other Methods Than Coupling Reactions

Other ways of attaching the photoactive groups on the macrocycle were also studied: A dansyl macrocycle was obtained from the amino macrocycle **25**¹⁸⁸ or a BODIPY (DIPYrromethene BOron difluoride) macrocycle **16** was synthesized in a one-pot reaction from the Suzuki coupled aldehyde macrocycle **9**.

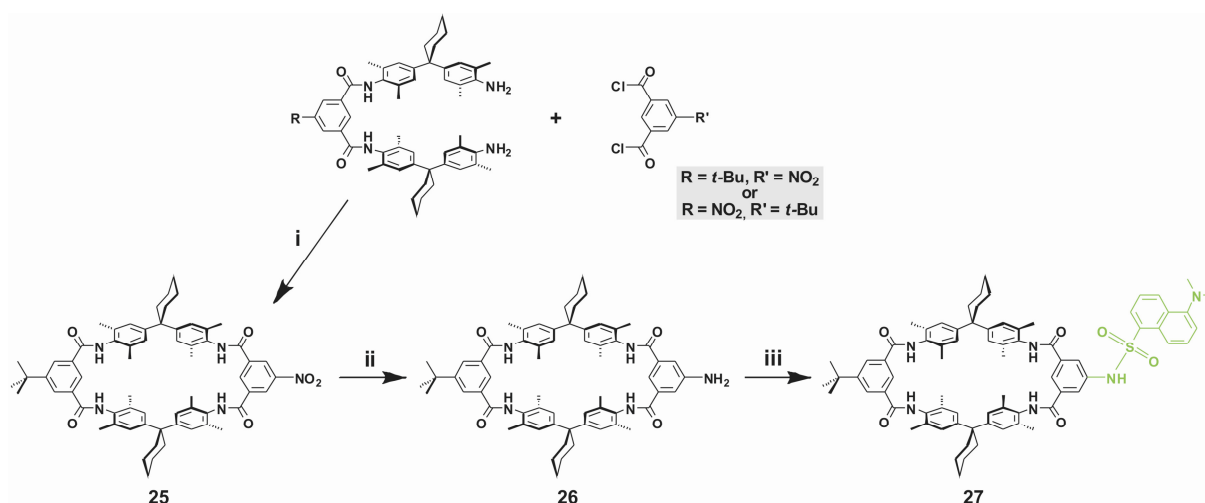


Figure 47. Synthesis of dansyl macrocycle using amino macrocycle: (i) High dilution, CH_2Cl_2 , NEt_3 , r.t. 25%. (ii) SnCl_2 , EtOH , reflux, 2 hrs, 51%. (iii) dansyl chloride, pyridine, $0^\circ\text{C} \rightarrow \text{r.t.}$, 2 days, 90%.

The functionalization on the macrocycles is not limited to Suzuki coupling reactions and the tool-box oriented synthesis. In some cases it was also advantageous to use the

previously investigated ways of functionalization. As an example, to synthesize a dansyl functionalized macrocycle, amino macrocycle **26** which was obtained by the reduction of the nitro macrocycle **25** was used (Figure 47). As shown by TLC, the reduction of nitro macrocycle **25** to the amino compound **26** was almost always a quantitative process when fresh SnCl_2 was used in the reaction. However, after purification on a silica column the yields were significantly diminished ($< 10\%$). This problem was solved either by using a very short filter column to obtain the product or the direct use of the product after the simple work-up, in the next step. In this case, next step was a straightforward reaction to obtain the dansyl functionalized macrocycle **27** in which the product could be obtained purely in high yields.

Making a BODIPY dye attached macrocycle was especially attractive because of the ease of synthesis, narrower absorption and emission bands, and very high quantum yields of members of this dye group that is of vital importance for energy transfer and sensing processes¹²⁴.

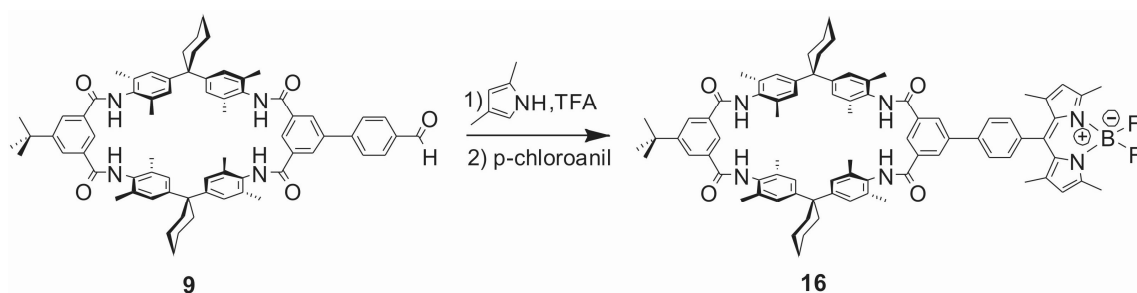


Figure 48. Synthesis of the BODIPY macrocycle **16** from the aldehyde macrocycle **9**.

BODIPY was built on the macrocycle using the aldehyde functionality as usually encountered in the literature¹²⁵. For synthesis of **16** first Suzuki coupling to obtain the aldehyde then making the BODIPY on the aldehyde is the only pathway since BODIPY can not survive the coupling conditions (Figure 48). The product was isolated in high yields (Suzuki coupling to aldehyde macrocycle (**9**) 84%, BODIPY reaction to (**16**) 64%) after the synthesis and characterized by ^1H -NMR, ^{13}C -NMR and FTICR-MS (Figure 49).

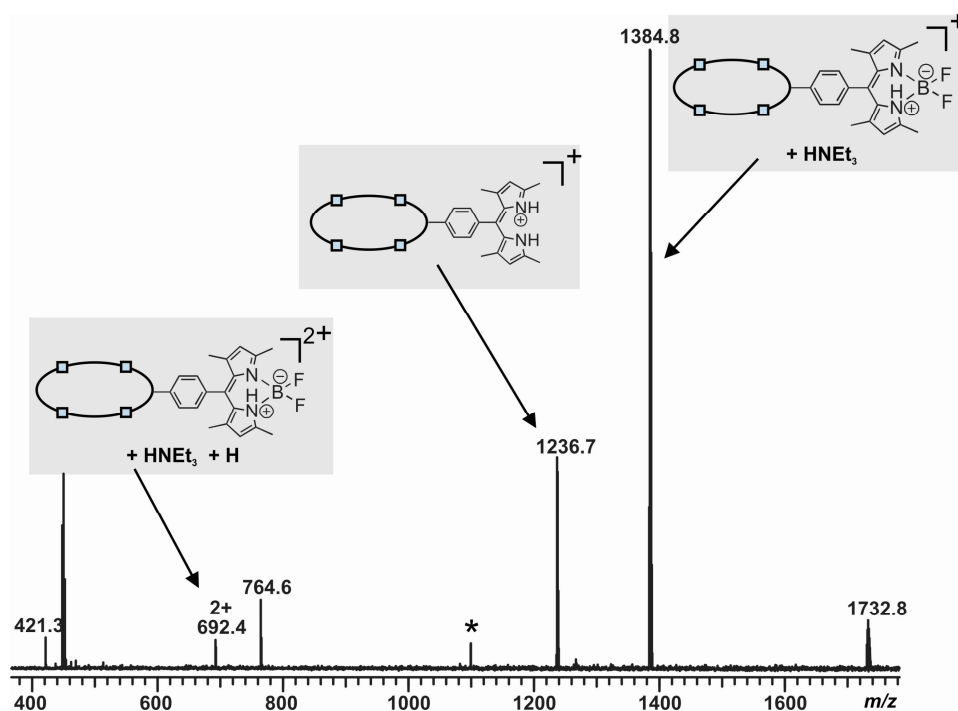


Figure 49. FTICR-MS of the BODIPY macrocycle. The spectrum shows the BODIPY macrocycle with triethylammonium (NEt_3 was added to increase the signal-to-noise ratio in the spectrum) as singly and doubly charged species and a fragment.

The positive mode FTICR mass spectrum of the compound showed the macrocycle as singly charged triethylammonium form, the BODIPY unit losing its BF_2 , and a doubly charged species. In the negative mode, deprotonated macrocycle could be seen both bare and with triethylamine. The absorption spectrum of the BODIPY macrocycle in dichloromethane has maxima at 206 and 498 nm of which latter is BODIPY absorbance. The extinction coefficient was found to be $67200 \text{ L mol}^{-1} \text{ cm}^{-1}$.

3.3. Studies on Functionalized Macrocycles

3.3.1. Studies on Macrocycles with Photoactive Groups: Host-guest chemistry

Decorating the macrocycles with photoactive groups (or in general rotaxanes¹²⁶) are interesting for finding more accurate binding constants for the guest binding processes in the macrocycle, since fluorescence studies are known to give better results especially when the binding constants are too high to be determined by NMR spectroscopy. In the case with tool-box strategy, since the cavity shape and nature is retained binding should not be affected from the introduction of any photoactive group outside the macrocycle. The binding may be monitored and the binding constant can be determined by energy transfer from guest to host

(or vice versa). In the first example studied, a naphthyl attached amide guest¹²⁷ was prepared to be complexed with pyrene macrocycle **17**. In ¹H NMR spectra of the host pyrene macrocycle, the guest and the 1:1 mixture of both, showed that the shifts of the axle protons moved upfield because of the anisotropy of the macrocycle rings, so the expected complexation took place (Figure 50).

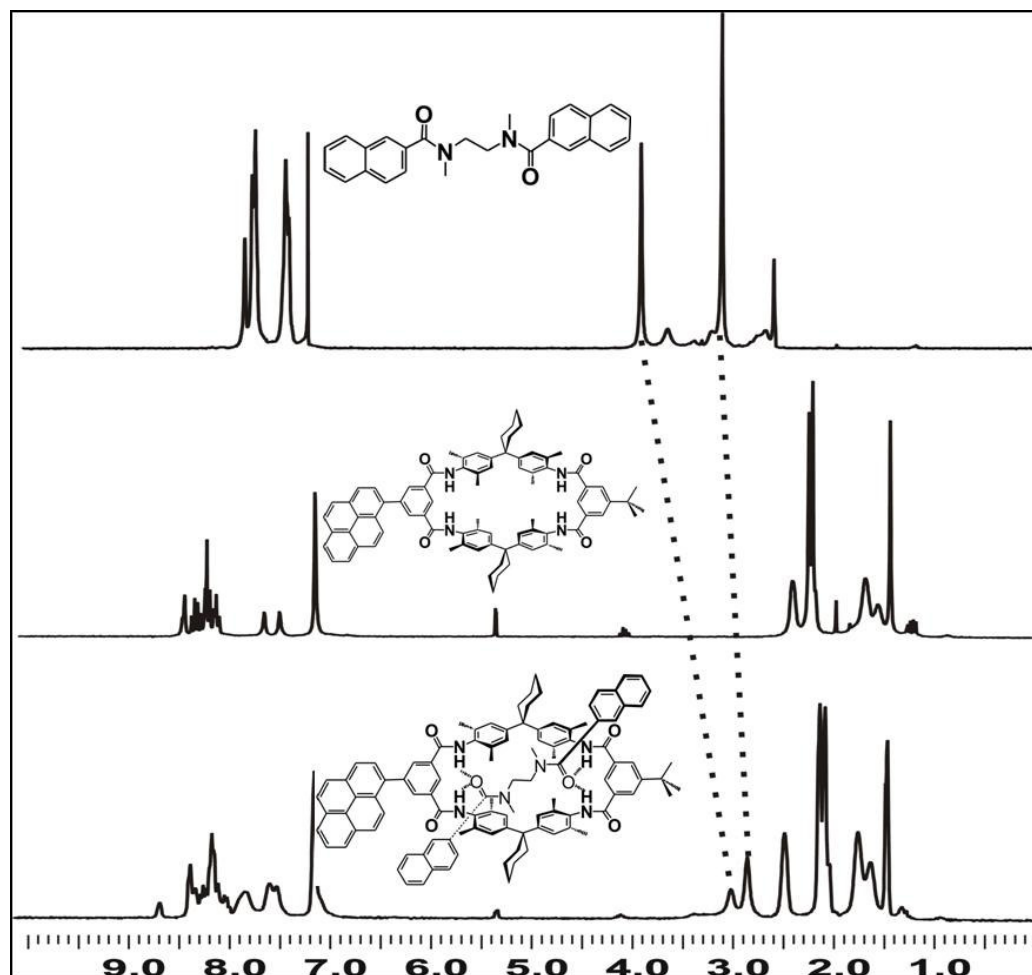


Figure 50. The ¹H-NMR spectra of the guest axle, pyrene macrocycle **17** host and the complex of axle@**17** showing the shifts of the axle protons moving upfield upon complexation.

Although the complexation was almost quantitative in the concentration of NMR studies (10^{-2} - 10^{-3} M), it was seen that the pseudorotaxane dissociated into the free host and guest, when the sample was diluted to concentrations around 10^{-6} M for the determination of binding constant by fluorescence studies (Figure 51).

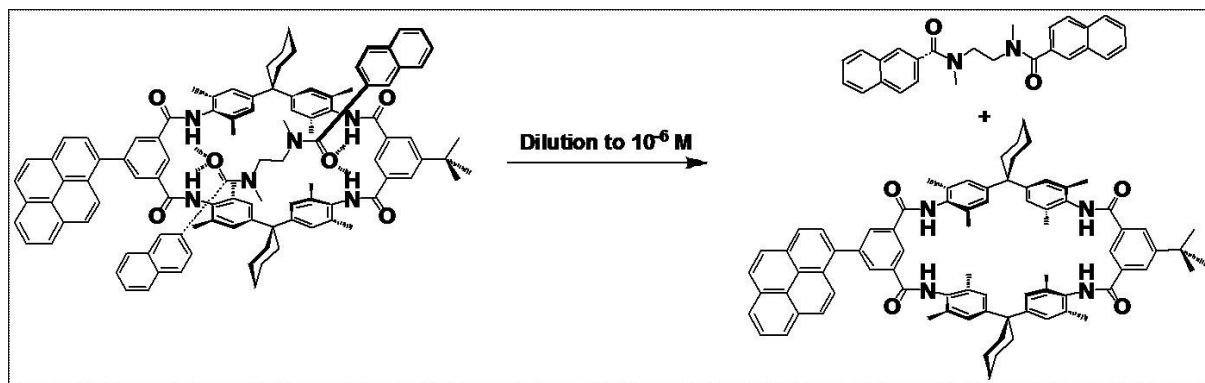


Figure 51. Deslipping of the naphthyl axle from the pyrene macrocycle **17** in higher dilutions.

The latter determination of binding constant by the ^1H -NMR measurements showed that the value for the binding constant¹²⁸ was 750 M^{-1} which was not enough to maintain the pseudorotaxane in higher dilutions. To have an intact assembly, attention was turned into the rotaxanes and catenanes. Utilisation of interlocked compounds may give insight to fluorescence studies, more importantly, increase the efficiency of energy transfer within the system, which may then be applied to the host-guest systems and pseudorotaxanes with high binding constants. The synthesis of these rotaxanes will be described in section 3.7.

3.3.2. Studies on Macrocycles with Photoactive Groups: Absorbance Measurements

Recording absorbance spectra of macrocyclic hosts is important to find out the changes upon host-guest binding or to pick out the right macrocycle for intrarotaxane energy transfer. Shown below in Figure 52, the absorption spectra of BODIPY macrocycle **16**, pyrene macrocycle **17** and 1,7-bisperylenylene macrocycle **20**.

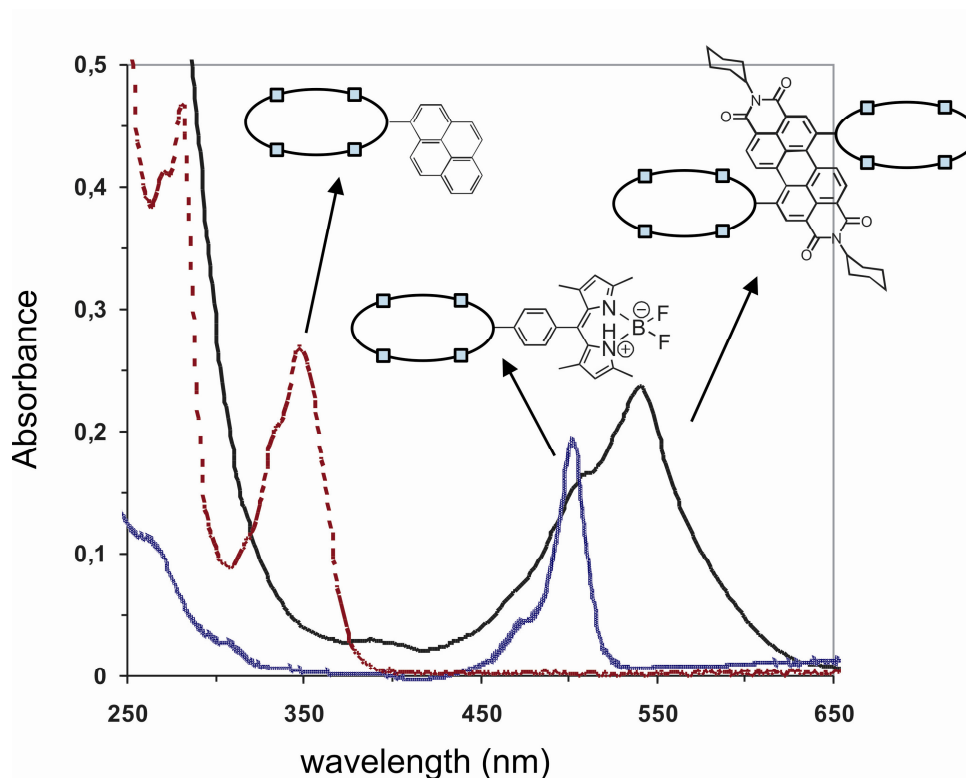


Figure 52. UV-spectra of a) pyrene macrocycle (1×10^{-6} M) (multiplied by 10) b) BODIPY macrocycle (5×10^{-6} M) c) 1,7-bismacrocyclic perylene (1.6×10^{-5} M) in CH_2Cl_2 .

In Figure 52, it is clearly seen that the typical absorbance patterns for the photoactive groups are retained in the hosts. Up to 300 nm the macrocycle body absorbs because of the phenyl rings in the molecule (typical range is around 200 nm). In the case of pyrene and perylene macrocycles absorbance maxima are 348 nm and 548 nm respectively. The former maximum is not effected when the solvent was changed from CH_2Cl_2 to acetonitrile, whereas the latter shifts about 10 nm which was again expected from the solvatochromic behaviour of 1,7-substituted perylene dyes¹²⁹. The BODIPY macrocycle has the highest extinction coefficient ($67200 \text{ M}^{-1}\text{cm}^{-1}$ at 498 nm) with the sharpest peak shape, the typical absorbance properties are kept within the macrocyclic host.

These data helped us in designing intrarotaxane FRET systems (section XX): The pyrene macrocycle **17** was chosen as the acceptor of such a system where the axle was decorated with naphthyls as the donor group. The spectral overlap of naphthalene emission maximum (338 nm, excitation at 270 nm) and the pyrene macrocycle absorption maximum (348 nm) was ideal for achievement of the desired energy transfer.

3.3.3. Studies on Macrocycles with Photoactive Groups: Multivalent hosts

Tool-box approach can also be used to obtain multivalent hosts where the tetralactam macrocycles are the hosts as shown before. Incorporating photoactive groups as the “body” of the multivalent systems may help the systems to be analyzed by absorption and fluorescence studies. For that purpose, bromo macrocycle **2** or the boronic acid pinacol ester macrocycle **4** were reacted in Suzuki coupling reactions with multi-functionizable core molecules like 1,4-benzene bisboronic acid pinacol ester, tribromobenzene, 1,7-dibromoperylene tetracarboxylic anhydride **P16**, 1,3,6,8-tetrabromo pyrene **P13** and 1,3,6,8-tetraethynylpyrene **P15**. The choice of the place of the boronic ester group was made depending on the ease of having boronic acid pinacol ester functionality on the compounds. In most cases (and especially keeping the “tool-box approach” in mind) it was easier to have one boronic ester macrocycle to react with the commercially available or easily achievable bromides of the core molecules. In all cases the reaction was complete according to TLC analysis after the reaction. The simple purification on silica columns were very successful for smaller products like the bismacrocyclic compound **18**, however for the larger systems (for example **21**) even after consecutive columns and preparative TLCs the products could not be obtained with high purity. Nevertheless, $^1\text{H-NMR}$ and FTICR-MS showed that the desired products are obtained.

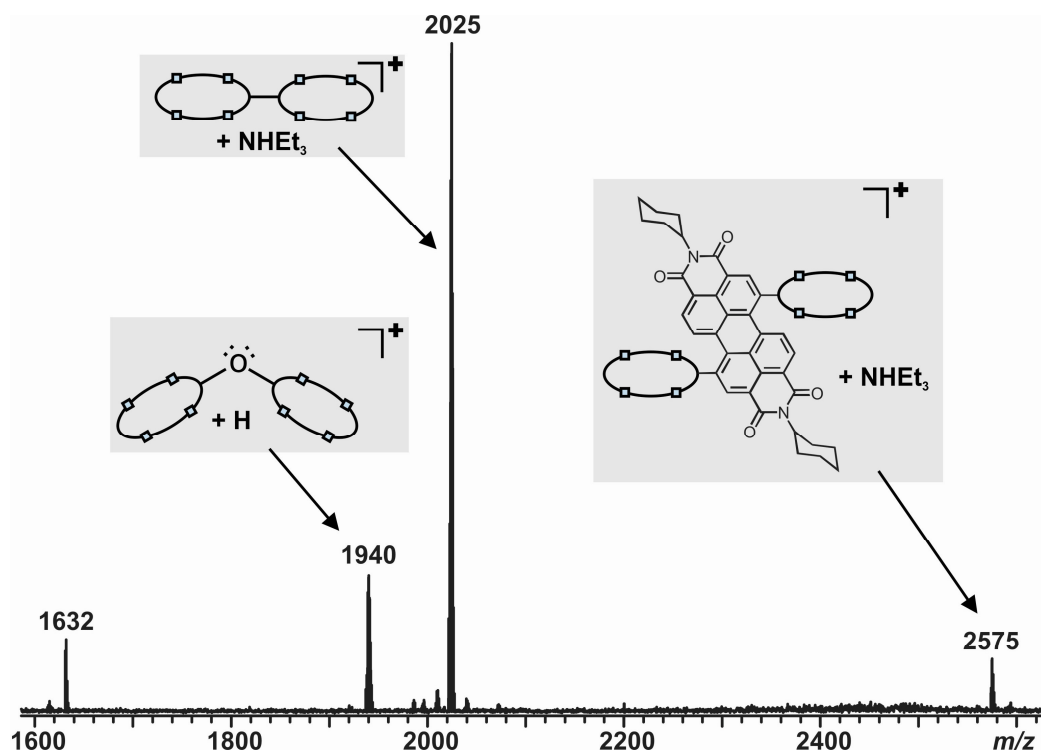


Figure 53. FTICR-MS of 1,7-bismacrocycleperylene **20**. Even after consecutive columns, **20** is associated with some bismacrocycles as by-products.

One can make a comparison of the ease to obtain and purify the alike bis-compounds 1,4-bismacrocyclebenzene **18** and 1,7-bismacrocycle perylene **20**: Both of the compounds are isolated from the reactions where TLC showed complete consumption of the starting bromo or boronic acid pinacol ester macrocycles. However, one could obtain very clean product and neat spectra after a short silica column for the former compound, where the latter was still impure after many columns and PTLCs with different solvent mixtures. The major impurities were the bismacrocycle that may have formed by the coupling of trace amount of bromo macrocycle with the boronic ester macrocycle, and the bismacrocycle ether which may have formed from a very small amount of hydroxyl macrocycle in the reaction mixture. In every case, these side products were not visible on the TLC plates, even when the mixture was applied very concentrated on the plate. Thus, one might conclude that they are exaggerated by the ESI-MS. (NMR is not a useful tool to discuss the purity in these cases since the desired compounds and the by-products give similar peaks in NMR spectra) (Figure 53).

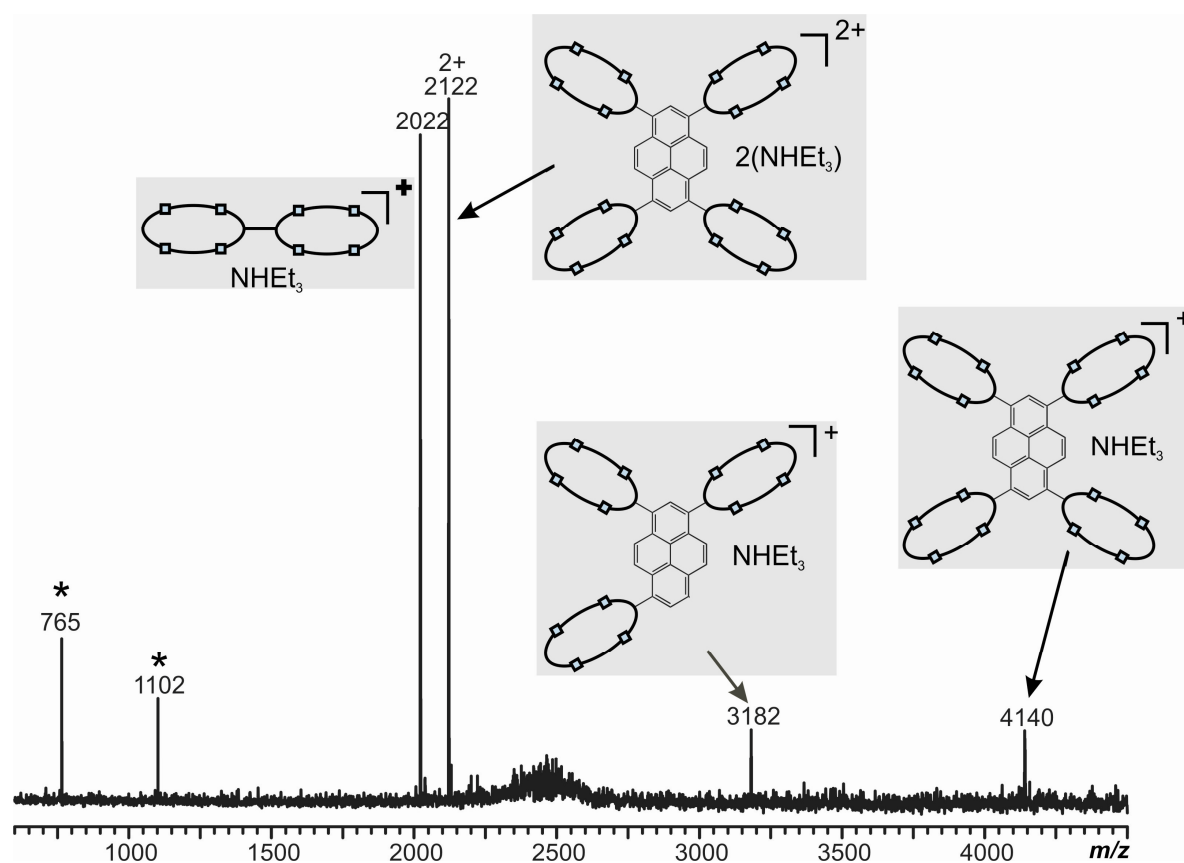


Figure 54. FTICR-MS of tetramacrocyclepyrene **21**. Even after consecutive columns, the tetra compound is associated with triply substituted product and the bismacrocycle.

Similarly, for the tetramacrocyclepyrene **21** system, the mixture obtained after many columns and TLCs were analyzed by FTICR-MS which showed that the desired product was formed together with the trismacrocyclepyrene and bismacrocycle (Figure 54). It must again be noted that the signal intensity ratios in the mass spectrum do not refer to the real product distribution in the mixture. The contribution from the side-products tris- and bis- compounds may be overestimated, since it is known that it is harder to get the signal from higher m/z . Nevertheless, better purification technique must be employed to isolate the tetrakis-compound, as well as the interesting by-products.

The not-straightforward purification of the tetrakis-macrocyclepyrene and the structural considerations about the bulkiness around the core and the restricted rotation of the macrocycles around the core pyrene turned our attention to the more flexible ethynyl bridged system **21a**. The attempts to synthesize the ethynyl bridged tetramacrocyclepyrene system can be described as follows (Figure 55):

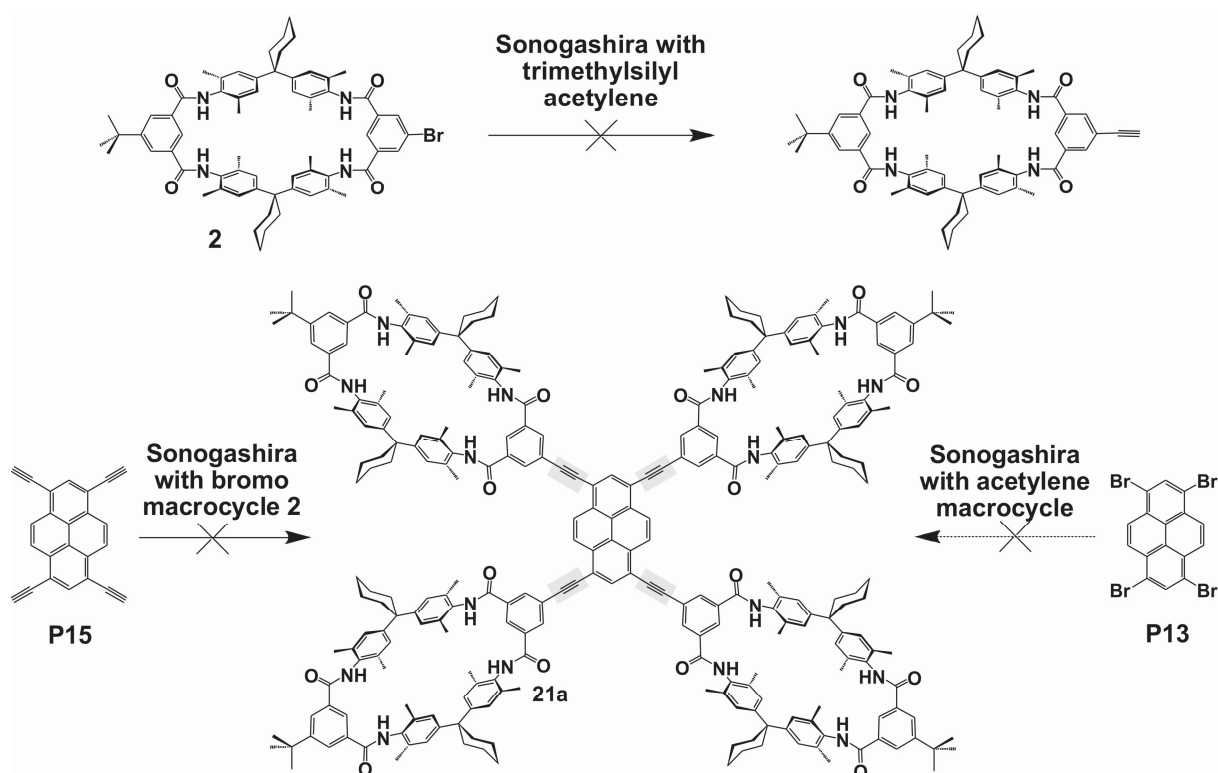


Figure 55. The attempts to synthesize tetraethynylmacrocycle from bromo compounds.

1) The easily achievable tetraethynylpyrene **P15** was subjected into a Sonogashira reaction with bromo macrocycle **2**.

2) Acetylene functionalized macrocycle was tried to be obtained from the bromo macrocycle **2** and this was thought to react with tetrabromopyrene **P13** in a Sonogashira reaction to yield in tetraethynyl macrocycle pyrene.

Both of these attempts were unsuccessful and it was figured out that the bromo macrocycle **2** can not be substituted in Sonogashira reactions with trimethylsilylacetylene to later produce acetylene macrocycle. It was also not successful to let it react with tetraacetylene pyrene **P15** under same conditions. Following studies done in our group¹³⁰ suggested that the use of iodine instead of bromine in the key macrocycle changed the reactivity in Sonogashira reactions drastically. Iodine macrocycle can be substituted with both trimethylsilylacetylene for further functionalization to ethynyl-bridged compounds and in a reaction with tetraethynylpyrene **P15**, to yield the desired tetraethynylmacrocyclepyrene **21a**. The purification of the latter product was again not so straightforward and the product was obtained with the tri-substituted pyrene.

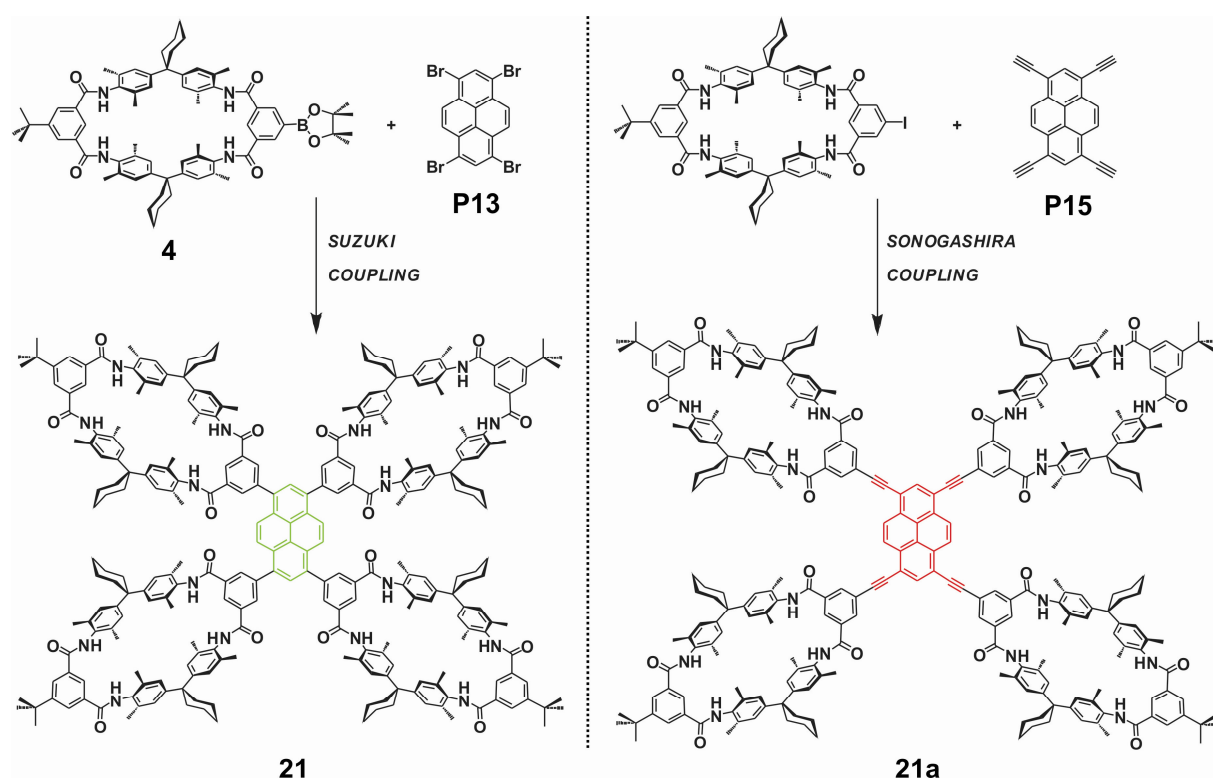


Figure 56. Sonogashira and Suzuki coupling with the tetralactam macrocycle to obtain the tetramacrocyclopirenes **21** and **21a**¹³⁰.

Both of the tetramacrocycles can be used multivalent hosts, serving as a template for [5]rotaxanes and the rotaxane antenna¹³¹ systems, therefore their isolation from the side-

products, especially from the tris- product is an important issue. Figure 57 shows how the linker nature affects the final architecture and the (estimated) reactivity of the two compounds. Shown on the left, tetramacrocyclepyrene **21** has direct links between the macrocycles and the pyrene body which restrict the free rotation around the C-C bond connecting the both. Thus in the low-energy state, the macrocycles are not coplanar. A planar tetravalent guest is hard to thread in and so is the formation of [5]rotaxane. In contrast, with this conformation, it can be possible to thread one axle going through all four (or at least two) of the macrocycles more efficiently than the flexible ethynyl-bridged compound (right). For the antenna systems, since bulky axle-stoppers are considered to achieve higher energy transfer efficiency within the system, the better choice seems the ethynyl-bridged pyrene system.

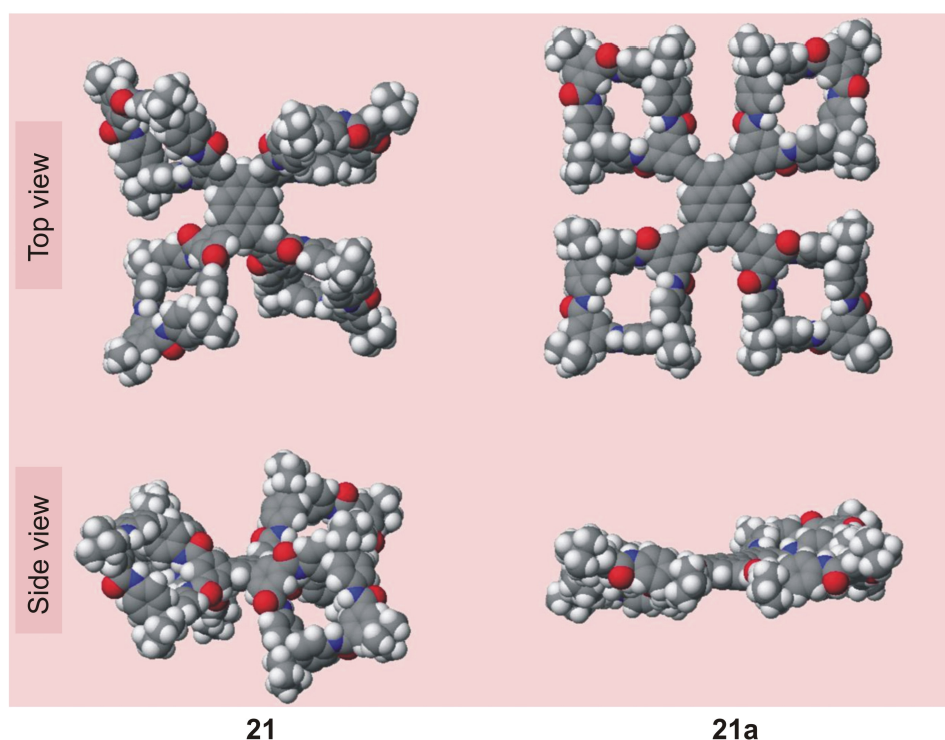


Figure 57. Energy-minimized structures of tetramacrocyclepyrene **21** with no linker (left) and with ethynyl linker **21a** (right). While the ethynyl-linked compound can adopt a planar conformation, direct attachment of the macrocycle to the pyrene causes bulkiness around the chromophore so that a planar structure is not possible.

3.4. Syntheses of Functionalized Rotaxanes

3.4.1. Post-threading Functionalization of Key Rotaxanes by Suzuki Coupling

Post-threading functionalization (Figure 58) on the key rotaxanes **2R** and **3R** was tried using Suzuki coupling reaction which was successful for the corresponding macrocycles. Under the same conditions used for the macrocycles the bromo and dibromo rotaxanes failed to yield in appreciable amount of functionalized rotaxane (less than 10%).

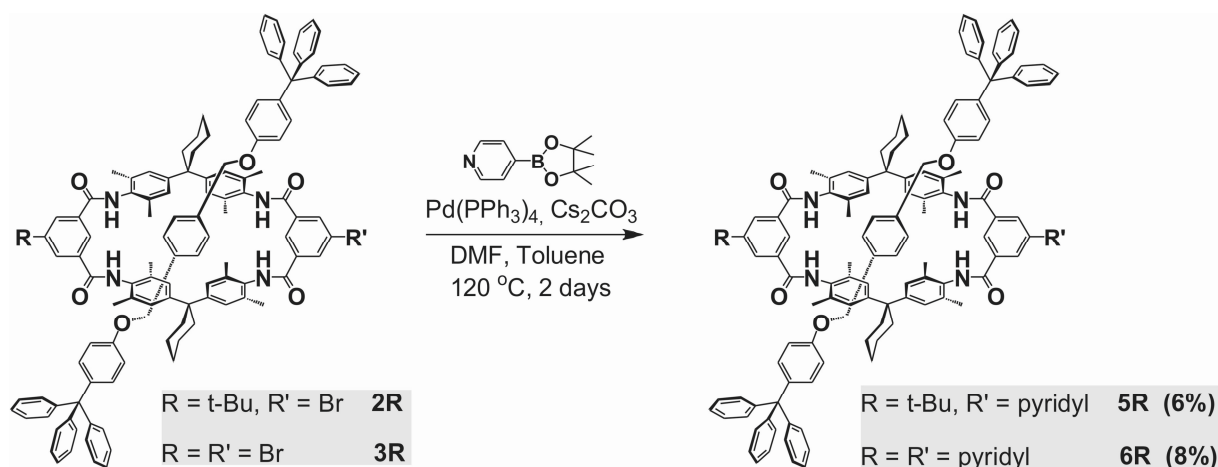


Figure 58. Suzuki coupling on the key rotaxanes **2R** and **3R**.

When the resulting product mixtures were analyzed it was seen that the major products were the functionalized macrocycles **5** and **6** and the free axle. These results implied that the Suzuki coupling was indeed working on the expected position. The surprising result was that the interlocked compound was detaching and reattaching into the free components: the macrocycle and the axle. Since amide bonds on the macrocycle are relatively stronger than the benzyl ether linkages of the axle, it was concluded that the axle was breaking and reforming in the reaction. This process was assisted by 120 °C (standard reaction temperature) and Pd catalyst. In order to suppress this process either temperature must be lowered or the catalyst must be changed. However, both of these ways are time and effort intensive. Since the nature of the linkages on the axle was not important for our final goals, we switched to the synthesis of the key rotaxanes through an amide template (Figure 59). For this purpose trityl aniline stopper was added dropwise into a solution of bromo macrocycle and the isophthalic acid dichloride and reaction was let 5 days until the total consumption of the stopper. The resulting rotaxanes was purified on a silica column and characterized by MS and NMR. Functionalization by Suzuki coupling was performed at the same conditions as for the anion-

templated rotaxanes. Even though the product has not been isolated yet, it was evident from the TLC analysis that the rotaxane structure was retained.

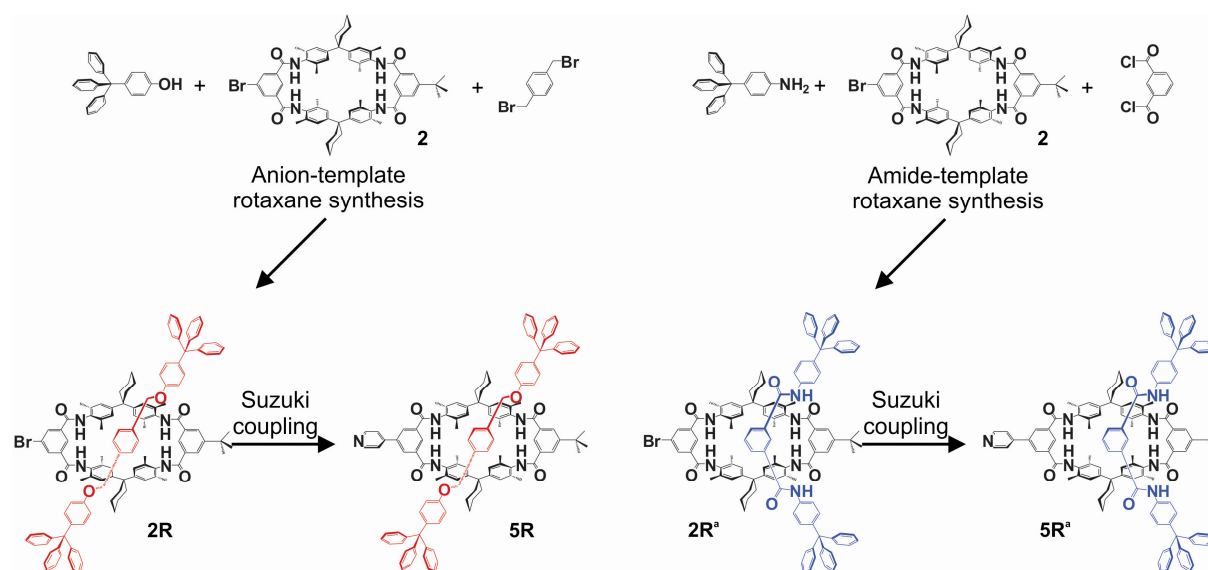


Figure 59. Anion **2R** and amide templated **2R'** rotaxanes synthesis and post- threading functionalization to **5R** and **5R'**.

For the amide template rotaxane synthesis isophthalic acid dichloride was chosen as axle middle piece because of the previous experience on the ease of purification of the rotaxanes obtained using this middle piece. As expected the amide-templated rotaxanes unlike the anion-templated ones have kinked axles and one must keep in mind that the axle in the amide-templated rotaxanes can make four hydrogen bonds to the macrocycle different to the anion rotaxane, in which after the synthesis there is no hydrogen bonding between the axle and the macrocycle (Figure 60).

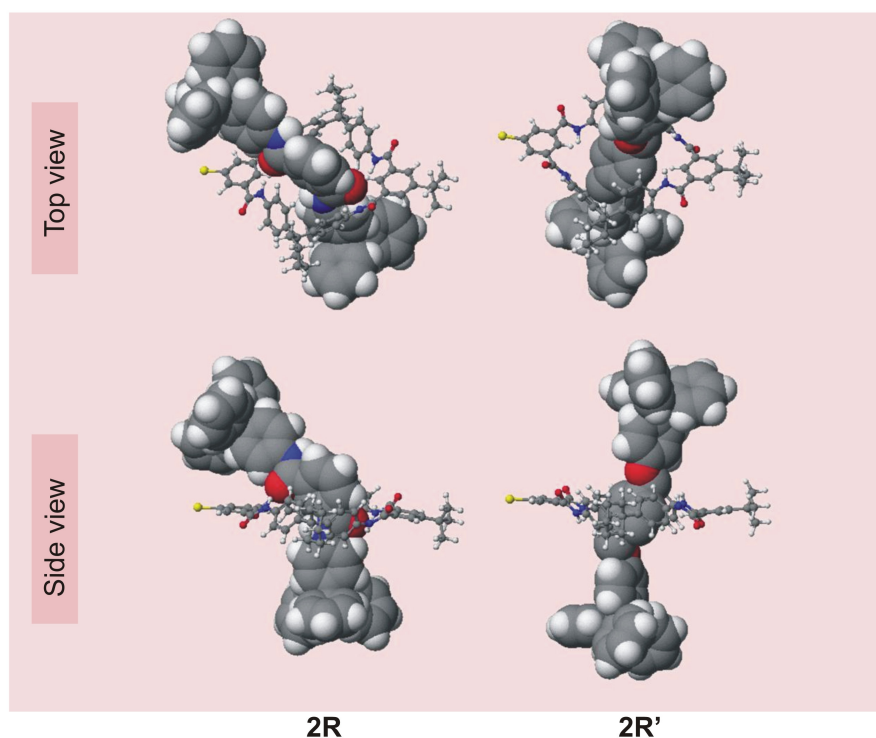


Figure 60. Energy minimized structures of bromo amide-templated rotaxane **2R** (left) and bromo anion-templated rotaxane **2R'** (right).

3.4.2. Direct Synthesis of Rotaxanes From Functionalized Macrocycles

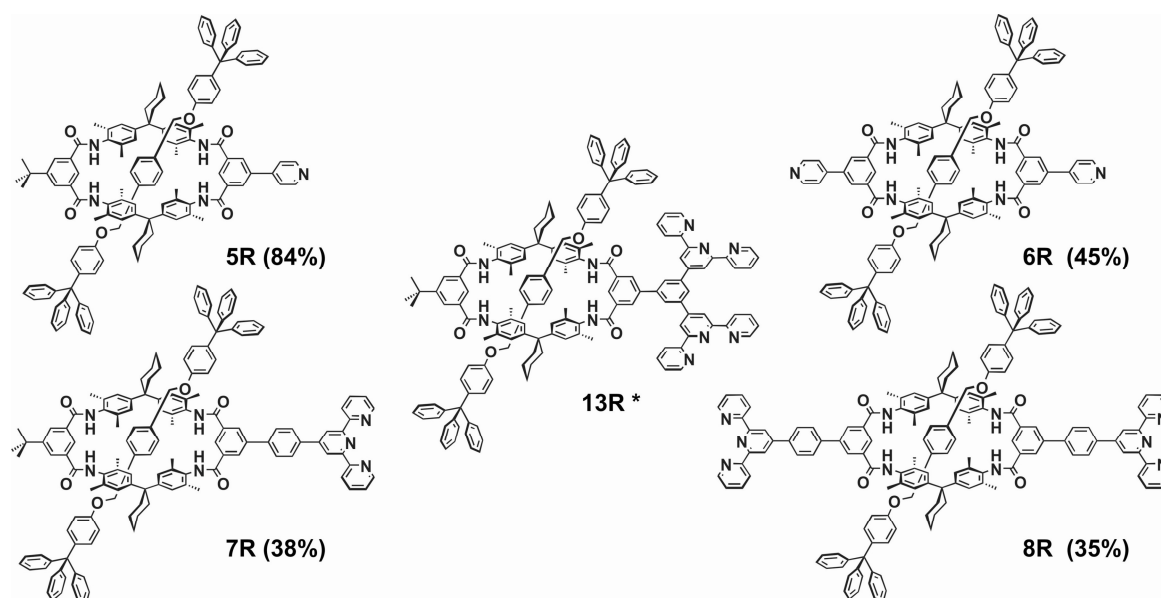


Figure 61. Rotaxanes obtained by post-functionalization: **5R**, **6R**, **7R** and **8R** are achieved with appreciable yields. *: **13R** is not isolated but Suzuki reaction was quantitative leaving no starting compound.

The direct syntheses of the rotaxanes from the already functionalized macrocycle and the axle pieces in anion template rotaxane syntheses were employed to obtain the corresponding rotaxanes in higher yields since the anion-templated key rotaxanes were not intact in the following Suzuki coupling reactions (Figure 61). The yields of these syntheses were higher than the ones for the post-threading rotaxane syntheses, yet lower than the literature examples of same kind^{40c-h}. This is due to the poor solubility of some macrocycles (**6** and **8**) in the solvent of reaction, which was found out to be the major factor affecting the yield in the anion-template rotaxane synthesis.

3.5. Synthesis of a Functionalized Catenane

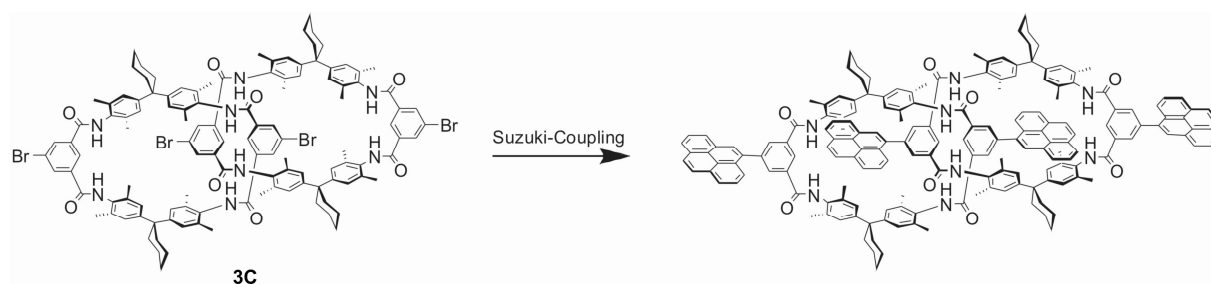


Figure 62. Post-threading functionalization of a catenane: Suzuki coupling reaction with $\text{Pd(PPh}_3)_4$, Cs_2CO_3 , 1-pyrene boronic acid pinacol ester.

Catenanes as well could be functionalized through post-threading synthesis. As an example, the catenane of the dibromo macrocycle **3C** was subjected to Suzuki coupling with pyrene boronic acid pinacol ester (Figure 62). The TLC after 2 days showed that all the starting catenane was consumed and there are new fluorescent spots on the TLC plate. However, the purification of the products turned out to be a tedious process and requires diligent separation more than offered by conventional techniques. At this point only preliminary positive result may be concluded.

3.6. Synthesis of Chiral Rotaxane and Catenane From an Achiral Macrocycle

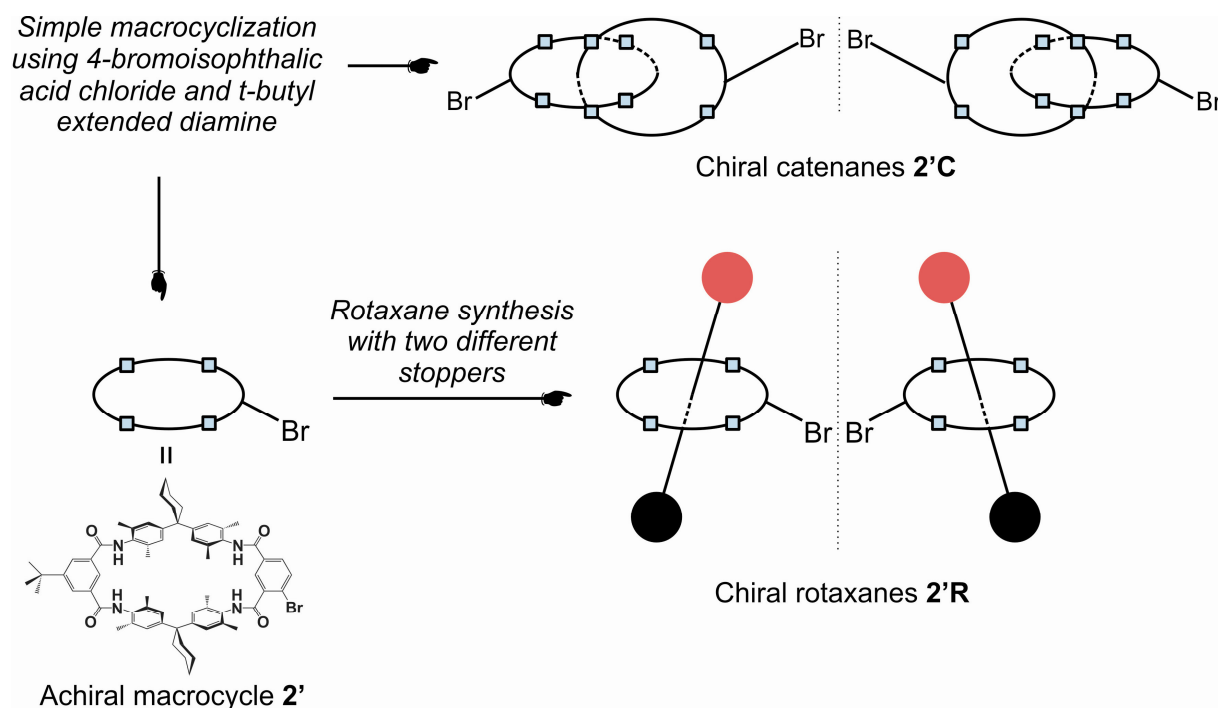


Figure 63. Schematic representation of the synthesis of chiral catenanes **2'C** and chiral rotaxanes **2'R**.

Changing the position of bromide in the isophthalic acid from 5- to 4- a very small but important change is made on the catenanes and rotaxanes which can be obtained in the usual syntheses applied previously for the 5-bromo isomers. Unlike the macrocycle **2'** obtained in the macrocyclization that is achiral, the by-product catenane **2'C** forms as a mixture of two enantiomers that are topologically chiral (Figures 63 and 64). In our macrocycle syntheses these catenanes are isolated as a racemic mixture and characterized by NMR and FTICR-MS.

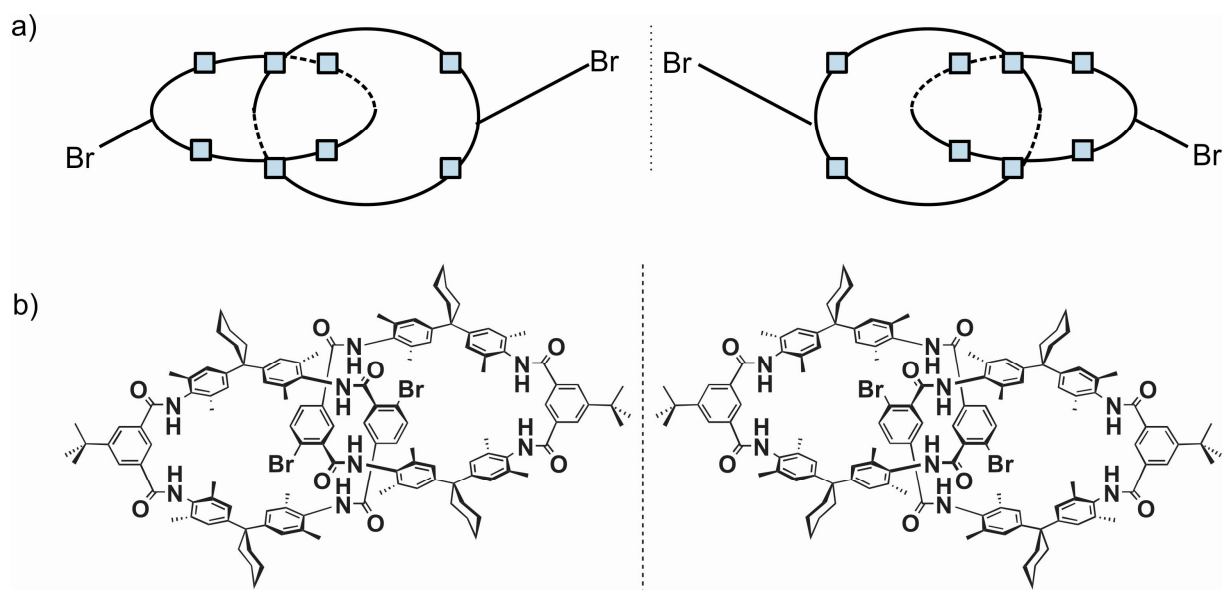


Figure 64. (a) Schematic representation and (b) structure of chiral catenane. The molecule consist of two topological enantiomers which can be obtained easily as a enantiomeric mixture which gives rise to complicated NMR signals.

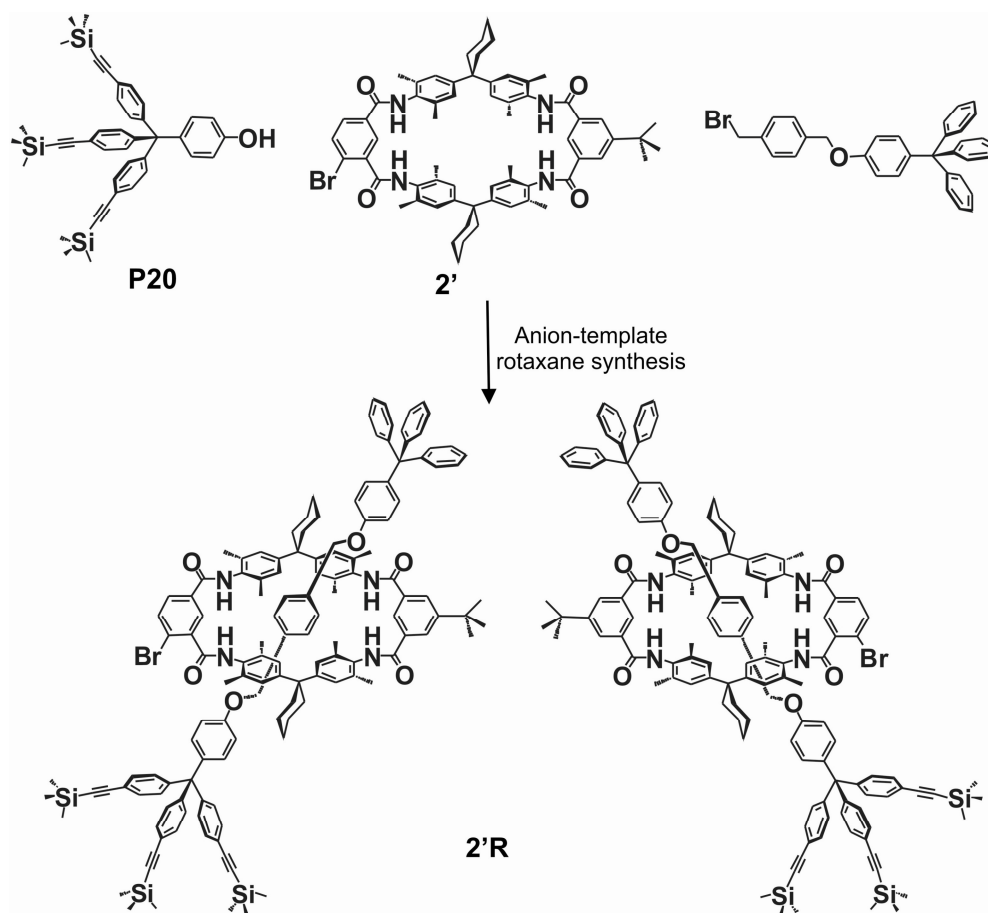


Figure 65. Synthesis of chiral rotaxanes **2'R** using two different stoppers.

In the same manner, using different stoppers in the rotaxane synthesis should lead to chiral rotaxanes. When two different stoppers are to be used in the reaction directly, 3 kinds of products could be expected with respect to the nature of the stoppers: [Stopper A-Axle-Stopper A], [Stopper A-Axle-Stopper B] and [Stopper B-Axle-Stopper B] rotaxanes. For reducing the amount of products forming in the reaction and getting only the [Stopper A-Axle-Stopper B] type of product, one of the stoppers were reacted with axle in 1:1 ratio to form the stopper-axle compound and put into the rotaxane synthesis with the other stopper (Figure 65)¹⁸⁸. The anion-template synthesis using the 4-bromo macrocycle produced the rotaxanes in high yield. The purification of the compounds were done on a silica column and the rotaxanes were characterized by NMR and FTICR-MS. (See section 3.1 for discussion on how to prove rotaxane structure without tandem MS experiments). The functionalization of the achiral macrocycle **2'** was successful using the standard Suzuki coupling procedure¹⁹¹. The chiral separation and further functionalization of the catenanes and rotaxanes are left as a part of the future work.

3.7. Energy Transfer Systems

3.7.1 Synthesis of Functionalized Stoppers for The Energy Transfer Systems

Energy transfer in interlocked molecules is of great interest because of the adjustability of the energy transfer efficiency with respect to the shuttling motion. The intrarotaxane energy transfer systems display energy transfer between the parts of a rotaxane: Stoppers, axle and the macrocycle. The most interesting of these is the one between the stopper and axle because this is the one between the interlocked parts of a rotaxane as presented in the introduction part.

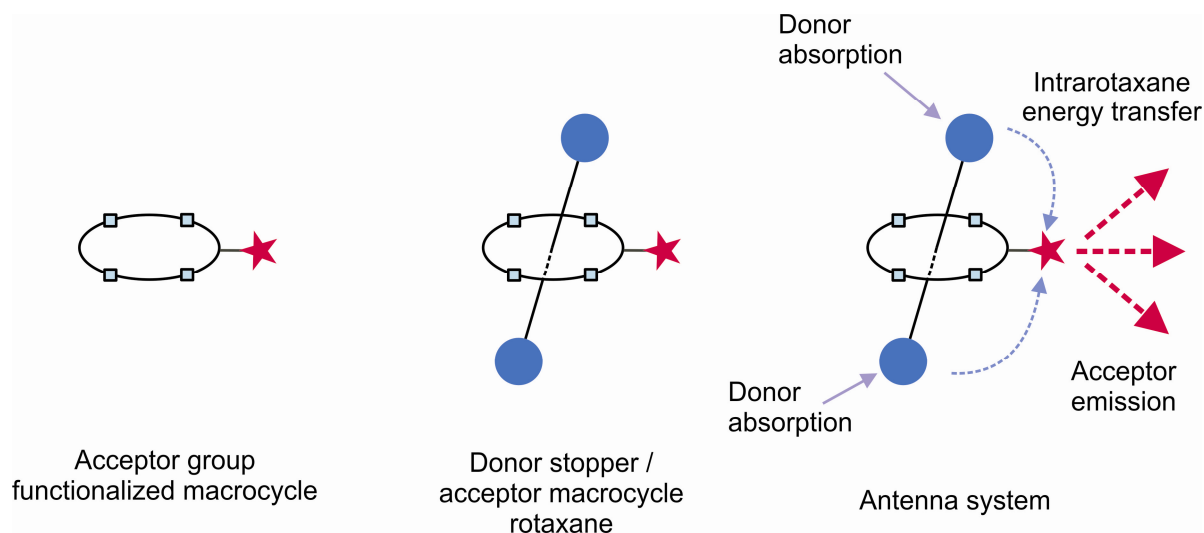


Figure 66. The schematic representation of intrarotaxane energy transfer consisting of donor attached stopper and acceptor attached macrocycle.

As an energy transfer candidate system we planned to synthesize a system with naphthyl stoppers and the previously obtained pyrene attached macrocycle **17** first. The reason for such a design was that the naphthyl-pyrene is a known donor-acceptor couple for such systems. Decorating the stopper with donor naphthyl groups and using the acceptor pyrene on the macrocycle provide the chance to have an antenna system since on the final rotaxane there are six of the donor groups and one acceptor group. The emission from the naphthyl groups can be absorbed by the pyrene, resulting in an appreciable enhancement of the pyrene emission: The result is an antenna effect (Figure 66).

The most direct way to a naphthyl stopper is the one that uses naphthyl instead of phenyl. To obtain such a stopper¹³² Grignard or BuLi reactions can be employed first to have the trinaphthyl methanol (Figure 67). Then by the acid catalyzed reaction of a phenol with this alcohol, the desired stopper may be produced. In our case, Grignard reaction did not work, so BuLi reagent was taken to produce the tertiary alcohol. The desired tertiary alcohols of the 2-naphthyls were prepared with moderate yields. Unfortunately, the second step, reaction with phenol failed to give the desired stopper in good yields.

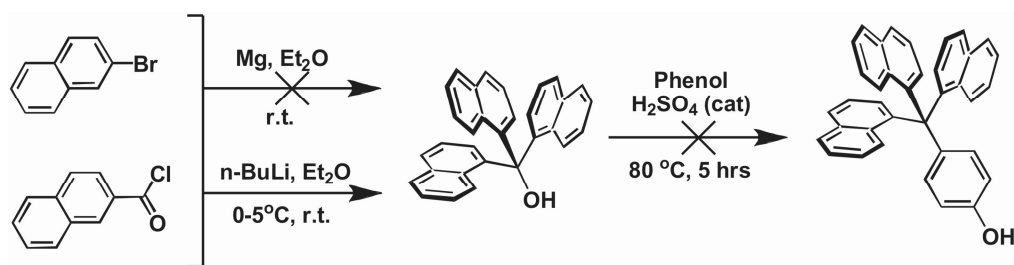


Figure 67. Direct synthesis of the naphthyl stoppers.

The synthetical problems and the low-yields in achieving appreciable amounts of stoppers with the direct approach lead us to think whether it would be possible to synthesize functionalized stoppers via “tool-box” strategy, which means, producing a key compound that could be obtained once and in high yields, and then attaching the functional group of desire.

The rotaxanes that we had used in our group so far had the trityl phenol or trityl aniline as stoppers as shown in previous studies in our group. The stoppers of this kind are bulky enough to prevent the slipping of the axle from the macrocycle and to stabilize the interlocked molecule¹³³. Functionalization of the phenyl groups on these stoppers may result in functionalized stoppers which may be used to attach the rotaxanes on a surface, produce different stoppers to have unsymmetrical axles without much synthetic effort¹⁸⁸, use the asymmetry in producing chiral rotaxanes and as well (as shown in previous section), used in building energy transfer rotaxanes.

The synthesis of functionalizable stopper is more straightforward when three of the phenyl rings are substituted, not only one. (That is also advantageous for our goals of having an antenna system within a rotaxane!) It is reasonable to substitute the hydrogen on the para position with a halogen atom, e.g. iodine. Iodine is chosen because of the literature known procedure to obtain the tris-(4-iodophenyl)-methanol and also the previous experience on Sonogashira and Suzuki couplings that could be done using this compound. Previously¹⁸⁸, a trimethylsilylethynyl stopper was synthesized using this route, in our group. Following the same procedure, through iodo stopper, trimethylsilylethynyl stopper was obtained in good yields (Figure 68).

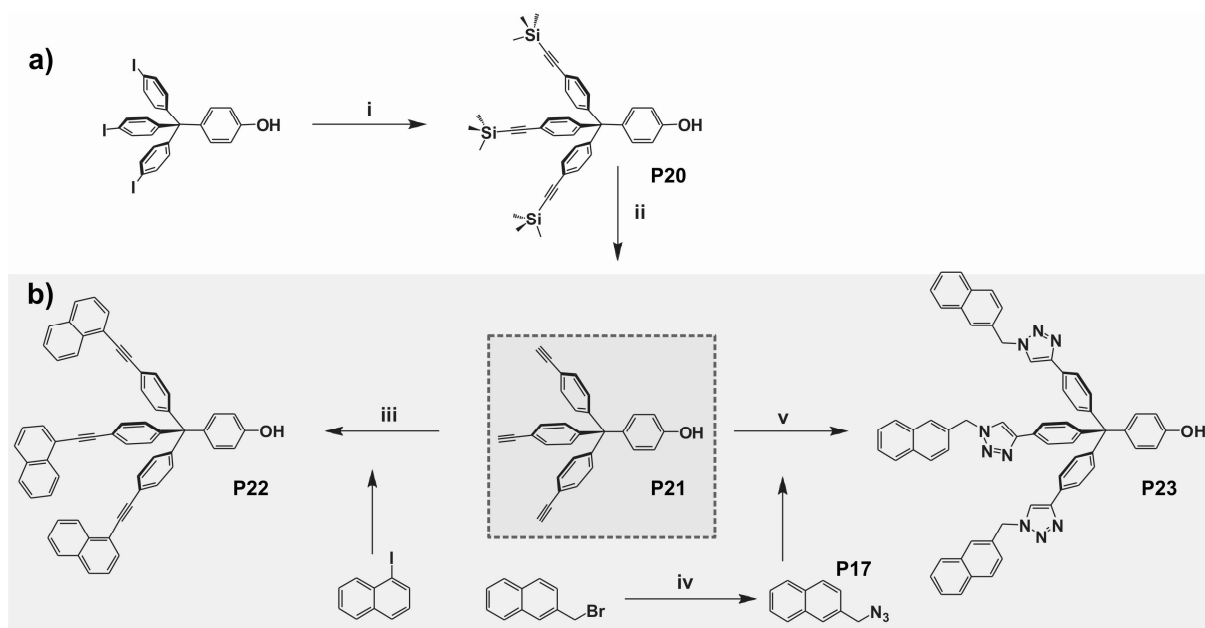


Figure 68. a) Removal of the trimethylsilyl groups from the previously synthesized trimethylsilylethynyl stopper **P20** to obtain a „key stopper“ **P21** (i) $\text{Pd}(\text{PPh}_3)_2\text{Cl}_2$, TMSA, CuI , NEt_3 , DMF, 40°C , 4 hrs. (ii) KOH , $\text{MeOH}/\text{H}_2\text{O}$ b) Functionalization of stopper using Sonogashira reaction (iii) $\text{Pd}(\text{PPh}_3)_2\text{Cl}_2$, CuI , NEt_3 , DMF, r.t., 21 hrs; and using click chemistry (iv) NaN_3 , DMSO, 45°C , overnight (v) $\text{CuSO}_4\cdot\text{H}_2\text{O}$, sodium ascorbate, $\text{H}_2\text{O}/\text{THF}$, r.t. 2 days.

Trimethylsilylethynyl groups were removed by base treatment and the resulted acetylene stopper was used in two different ways: In a Sonogashira coupling to obtain the triple bond bridged compound and in a click reaction¹³⁴ to obtain a different connectivity between the stopper body and the functional group. The Sonogashira reaction produced only one and desired product in high yield. The purification of the compound was done smoothly on a silica column. For the click reaction, the needed azide was prepared according to the literature procedures in almost quantitative yield and used in the reaction utilising the standard conditions. The click chemistry as well, produced only one and desired product in high yield. After the extraction into the organic solvent, the purification of the compound was done on a silica column.

3.7.2. Synthesis of Rotaxanes for Studies of Intrarotaxane Energy-Transfer

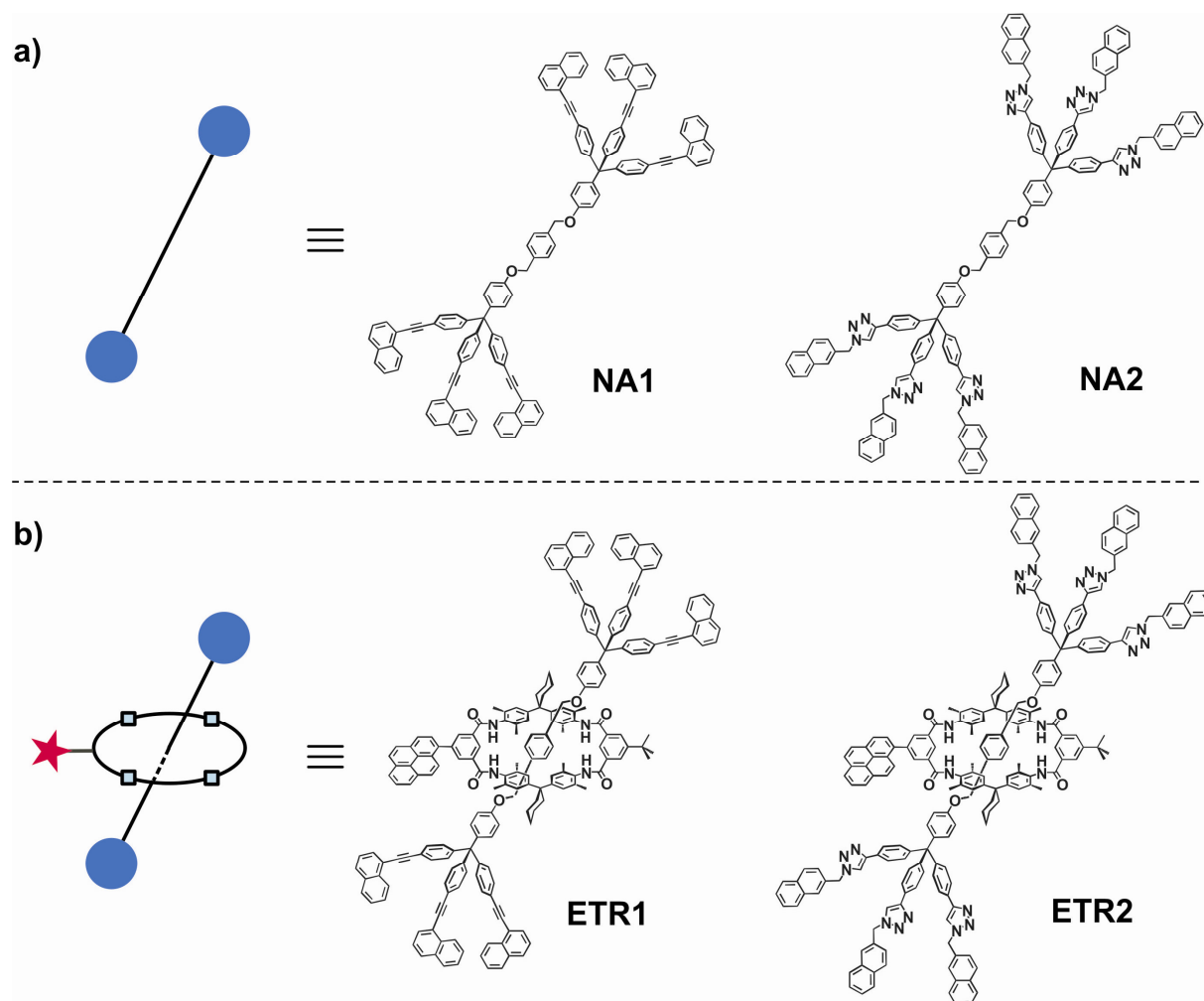


Figure 69. a) The free axles **NA1** and **NA2** and b) the energy-transfer systems **ETR1** and **ETR2**, which are obtained through anion template syntheses (the axles are side-products).

As shown before, the intrarotaxane energy transfer systems consist of two parts: The part where the donor molecule is incorporated and the part where the acceptor is attached. In rotaxanes, it is more interesting and functional to put one of these on the [axle-stopper] and the other on the macrocycle. For our future work on antenna systems, we functionalized the stoppers with naphthyl groups (synthesis was described in previous section). The standard anion-templated synthesis with the functionalized stoppers **P22** and **P23**, and the previously prepared pyrene macrocycle **17** lead to the **ETR1** and **ETR2** in good yields (85% and 82% respectively) (Figure 69). The characterizations of the rotaxanes are done with ^1H NMR and FTICR-MS to conclude that the final structure is a rotaxane without any free macrocycle and free axle. The side products of anion-templated syntheses are the unthreaded axles. In this case, axles are also important molecules, because they are one sort of the control compounds

that are used in energy transfer studies. Thus **NA1** and **NA2** were obtained as pure compounds from the above-mentioned columns and kept for the further studies. It is quite advantageous to obtain the control compounds together with the energy-transfer rotaxanes in the same syntheses, since in most cases these products should be separately synthesized. Nevertheless, because the yield of **NA2** was quite poor (less than 3%), to obtain appreciable amount of compound a separate reaction was employed (87%).

3.8. Self-Assembled Systems with Functionalized Macrocycles and Rotaxanes

3.8.1. Metal-Directed Self-Assembly of Macrocycles and Rotaxanes

Ligand-decorated macrocycles and rotaxanes were synthesized with good to excellent yields from their precursors and isolated, previously (section 3.2). The following step is the study of their assemblies. Different geometries of the macrocycles and rotaxanes around the metal centers can be obtained as shown in the examples in the introduction part. This provides a way to geometry-controlled self-assembly of macrocycles and rotaxanes. The differences in the strength of the metal-ligand interaction tune the degree of reversibility in the assemblies and allow error correction. Both of these phenomena were given the examples using pyridine **5** and terpyridine **7** macrocycles and rotaxanes **5R** and **7R** as follows (Figure 70):

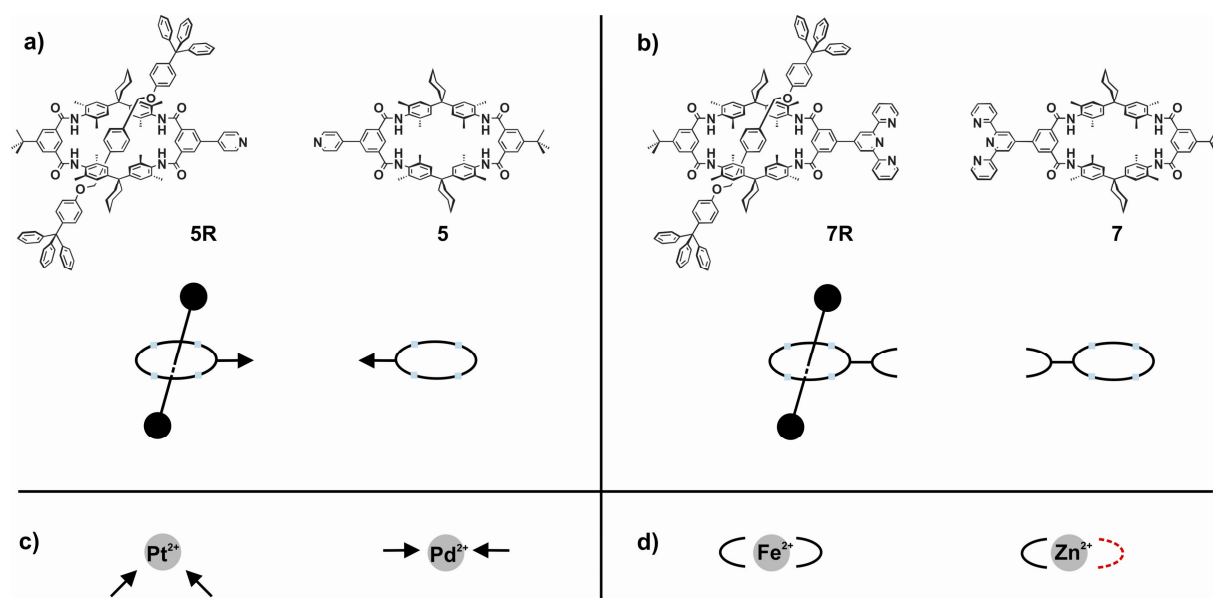


Figure 70. a) Pyridine rotaxane and pyridine macrocycle can be assembled reversibly around Pt^{2+} or Pd^{2+} so as b) terpyridine rotaxane and terpyridine macrocycle around Fe^{2+} or Zn^{2+} where the coordination geometry ensures directionality of the final assembly. c) cis- or trans-orientations cause different assembly geometries and d) strength of the metal-ligand bond determines reversibility.

Two examples orienting two pyridine macrocycles **5** in different geometries namely cis- and trans- around Pd^{2+} and Pt^{2+} were already described in a previous study¹²⁷. The cis- and trans- complexes were formed when two equivalents of the pyridine macrocycle **5** were mixed with Pd(dppp)(OTf)_2 or Pt(dppp)(OTf)_2 and $\text{Pd(PhCN)}_2\text{Cl}_2$ respectively. The complex formation was monitored by ^1H NMR, ^{13}C NMR and ESI-MS, and was seen that both of the complexes formed quantitatively.

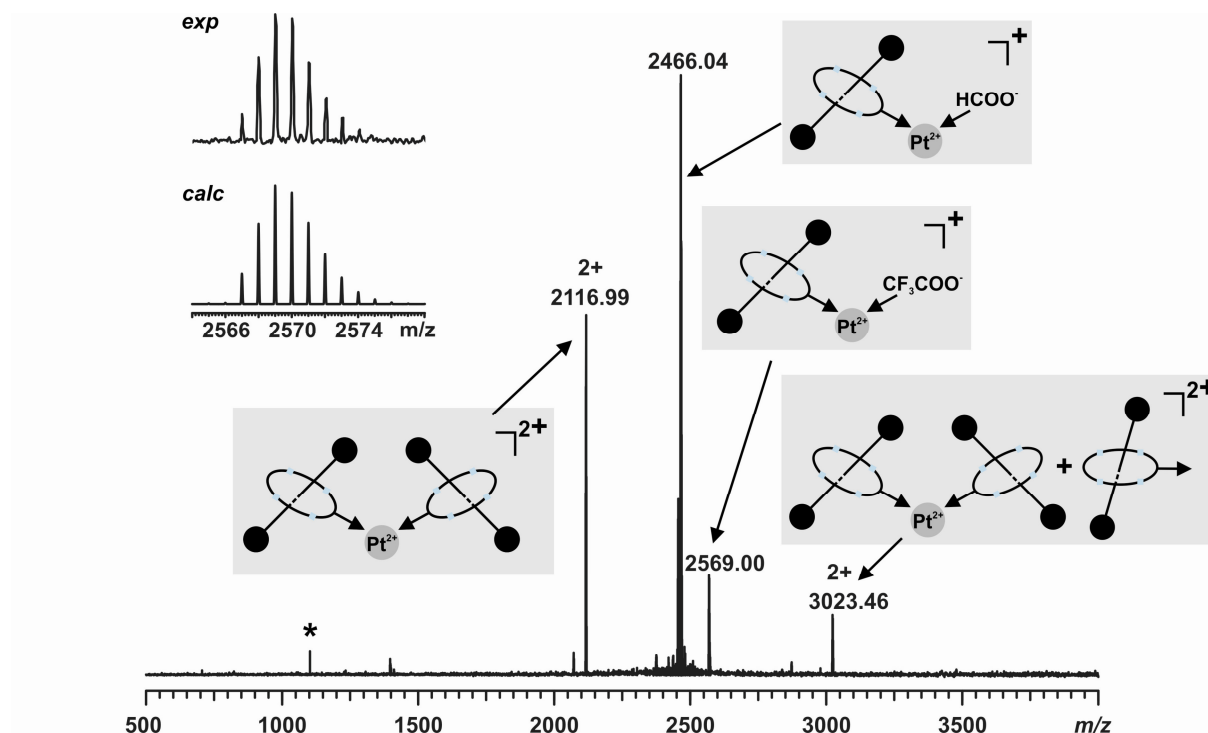


Figure 71. FTICR-MS of $\text{Pt(5R)}_2(\text{OTf})_2$, Pt^{2+} complex of pyridine rotaxane **5R**.

The metal complexation with Pt(dppp)(OTf)_2 or $\text{Pd(PhCN)}_2\text{Cl}_2$ were extended to rotaxanes. As an example cis- complex may be shown in detail: Two equivalents of pyridine rotaxane **5R** were added one equivalent of Pt(dppp)(OTf)_2 in DMF and the complex formation was monitored by ^1H NMR, ^{13}C NMR and ESI-MS (Figure 71). The quantitative formation of the expected divalent complex by displacement of weakly coordinating triflate and replacement with the ligand rotaxanes were evident from the shifts in the ^1H -NMR spectrum for the ortho protons of the pyridine and from the above shown mass spectrum. In this mass spectrum, which was obtained by spraying the mixture directly without the isolation of the complex, the complete consumption of the rotaxane **5R** can be seen. The 2:1 complex can be detected as its doubly charged form and 1:1 complex that may be the fragments of the 2:1 species, in singly charged form with a triflate or formate (formic acid is used to analyze

uncharged species in FTICR-MS. Formate is thought to be remaining from such a previous sample injection). The doubly charged 2:1 complex can also accompany a non-complexed rotaxane which may form hydrogen bonds to the complex through the pyridine on the macrocycle. In the figure, the experimentally obtained isotope pattern for the triflate species is shown together with the calculated one, which is an absolute match.

Whether the 1:1 is a fragment of 2:1 complex in the gas phase or is present individually in the solution can be verified from the pyridine peaks in ^1H NMR spectrum. If the pyridine peaks are shifted completely to low field, we can state that the assembly is complete and exclusively 2:1 complex is formed in the solution, which is the case, and one may conclude that 1:1 complex is just a gas phase species.

Trans complex with $\text{Pd}(\text{PhCN})_2\text{Cl}_2$ is a similar case, therefore it will not be discussed in detail. Replacement of the weakly bound benzonitrile with the pyridine rotaxane **5R** takes place quantitatively as shown by ^1H NMR and FTICR-MS.

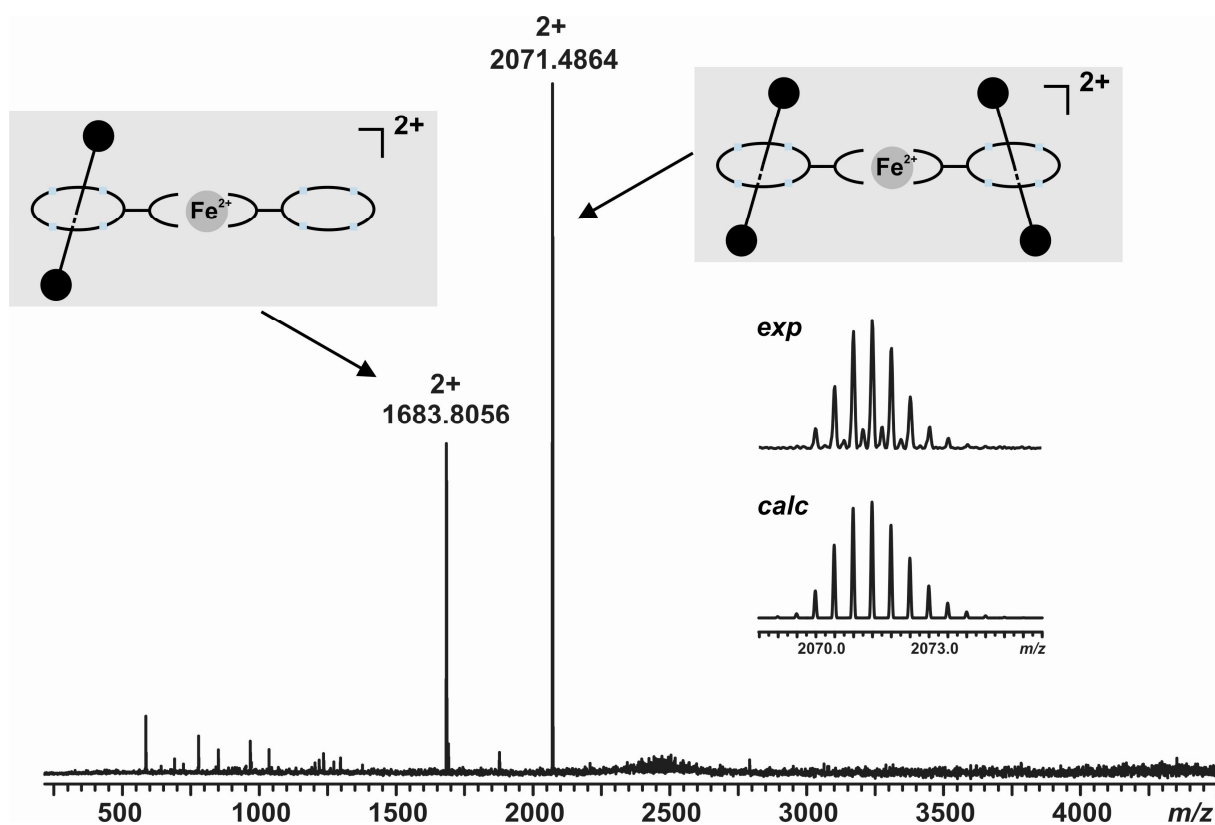


Figure 72. FTICR-MS of $\text{Fe}(\mathbf{7R})_2(\text{BF}_4)_2$, Fe^{2+} complex of terpyridine rotaxane **7R**.

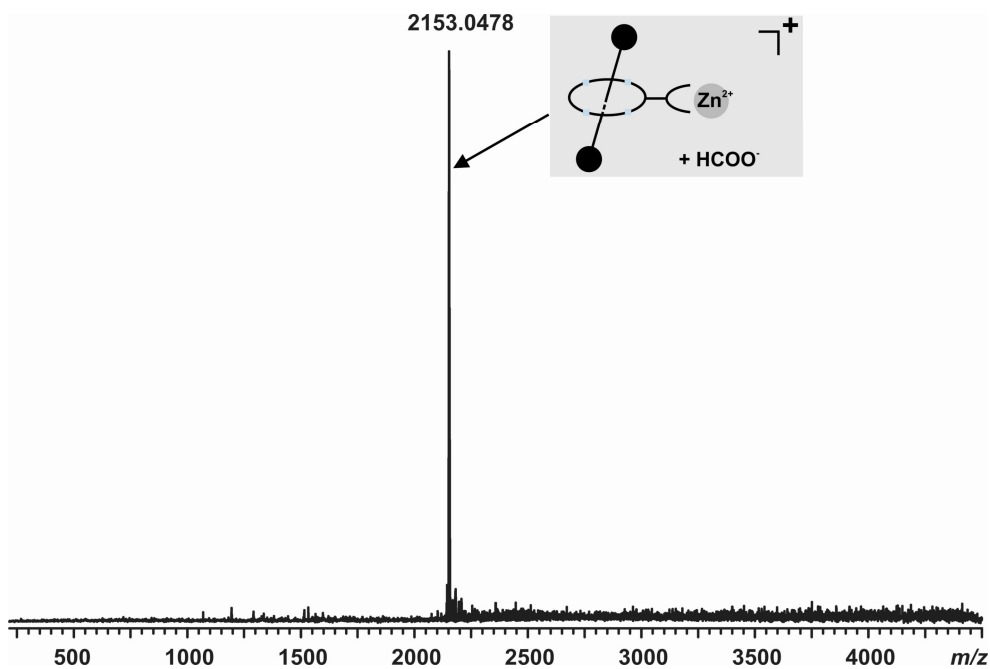


Figure 73. FTICR-MS of $\text{Zn}(\mathbf{7R})_2(\text{ClO}_4)_2$, Zn^{2+} complex of terpyridine rotaxane $\mathbf{7R}$.

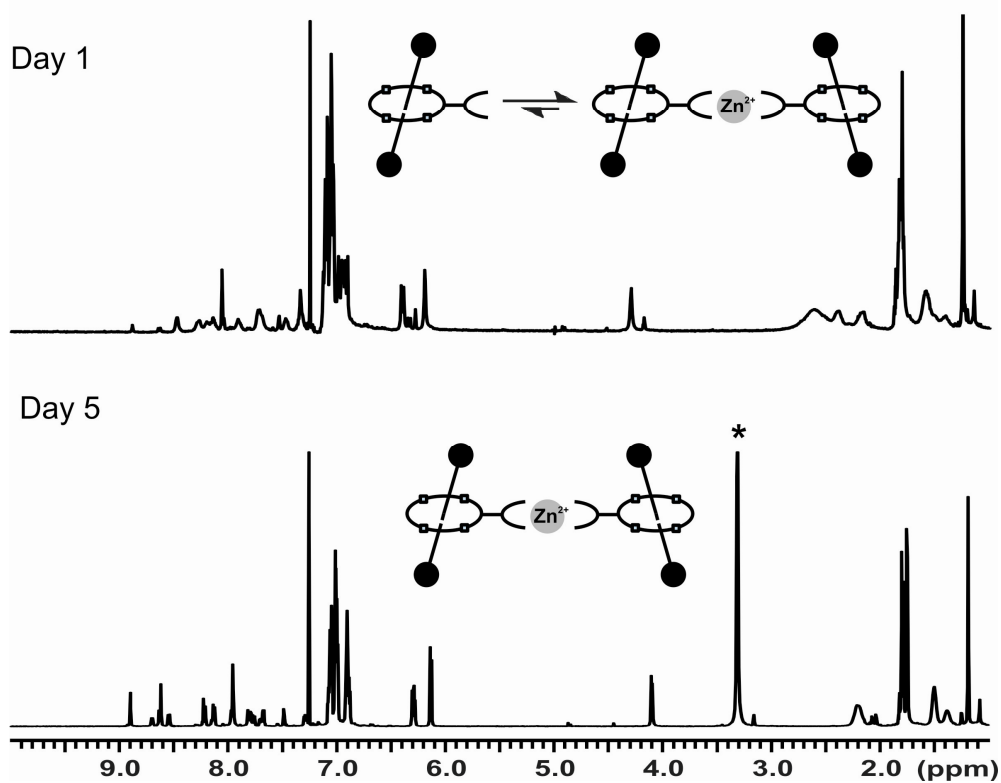


Figure 74. ^1H -NMR Spectra of $\text{Zn}(\mathbf{7R})_2(\text{ClO}_4)_2$, Zn^{2+} complex of terpyridine rotaxane $\mathbf{7R}$: After the first day the complex is formed incompletely. After 5 days, equilibrium is obtained and complex is formed quantitatively (* indicates CD_3OD added one drop to sharpen the spectra).

The strength and thus the reversibility of the assemblies with terpyridine rotaxane **7R** were studied with two examples: The rotaxane was let to mix separately with half equivalents of $\text{Zn}(\text{ClO}_4)_2 \cdot 6\text{H}_2\text{O}$ and $\text{Fe}(\text{BF}_4)_2 \cdot 6\text{H}_2\text{O}$ in deuterated acetonitrile/chloroform mixtures at room temperature. To obtain sharper signals in NMR spectra the solutions were then added two drops of deuterated methanol. The mixtures were then analyzed by ^1H NMR, ^{13}C NMR and FTICR-MS. Spraying both solutions into the mass spectrometer after dilution with acetone resulted in above spectra shown in Figures 72, 73 and 74.

It is clearly seen that with Fe^{2+} , rotaxane forms quantitatively the 2:1 complex; the signals for 1:1 complex or free rotaxane are totally missing. The smaller peak for the complex of one macrocycle and one rotaxane around the metal center is a fragment of the two rotaxane complex, as evident from the clean mass and ^1H -NMR spectra of the starting rotaxane and of the final complex. ^1H -NMR supports also the complete formation of the 2:1 complex by the single set of signals for the formed species and the high-field shifts of the terpyridine protons upon complexation¹³⁵. Mass spectrum showing the fragment complex of a macrocycle is an evidence of rather strong metal-terpyridine bond.

In case of Zn^{2+} , mass spectrum shows no 2:1 complex even at very soft ionization conditions. This shows in comparison to the iron complex, Zn^{2+} has a lower binding energy which is in agreement with literature on mass spectrometry of such complexes¹³⁶. In the ^1H NMR spectrum (Figure 74) two sets of signals are present for terpyridine protons, for the 2:1 complex and the uncomplexed rotaxanes. This case is a rather known phenomenon of Zn^{2+} complexes of similar type¹³⁷. Although the coordination of Zn^{2+} to terpyridines is reversible, the exchange is slow at room temperature giving rise to two separate sets of signals. (Usually, the equilibrium is achieved in a few minutes¹³⁷ but in our case the large ligands took 5 days to reach the equilibrium). The rise of a third set of signals is possible when excess of ligand is added, implying the formation of the 1:1 complex). This assures in many cases reversibility and error correction in the assemblies. Higher rotaxane assemblies with Zn^{2+} may equilibrate into the thermodynamically most stable and entropically most favourable one, which may be advantageous when easy, quantitative synthesis of high-molecular weight, complex assemblies of rotaxanes are considered. The work on complexes of the other terpyridine rotaxanes with more than one terpyridine ligand per rotaxane is being investigated at the time being.

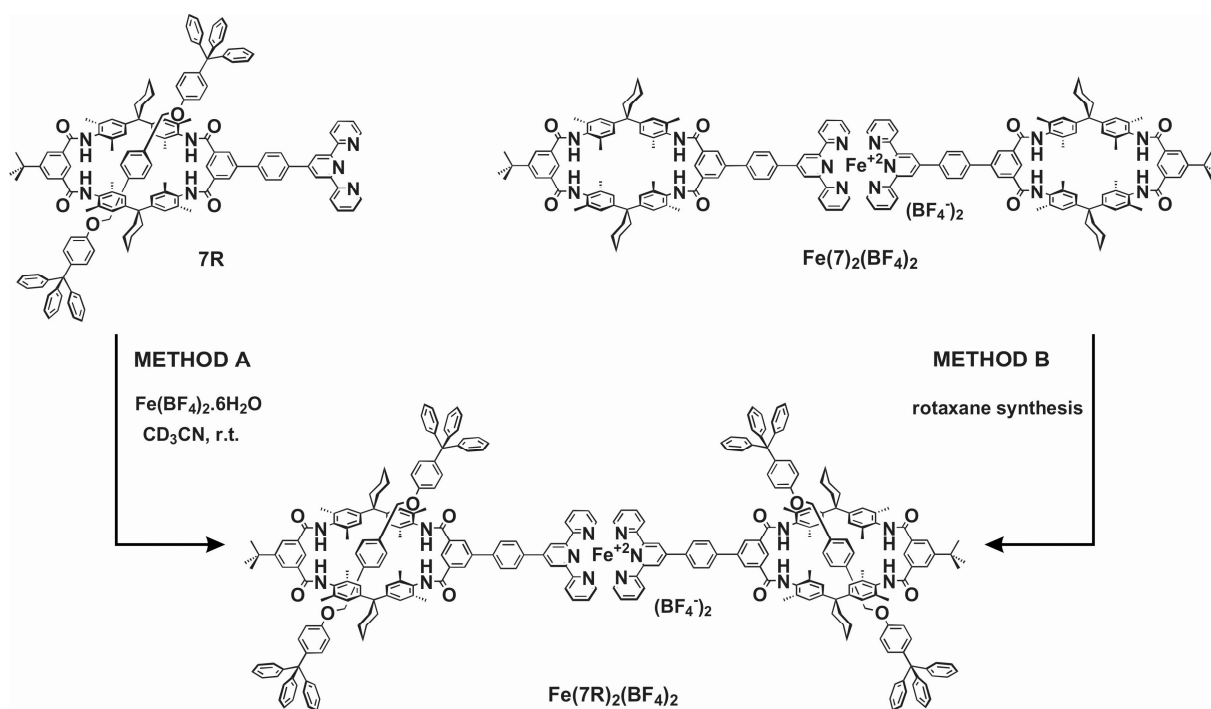


Figure 75. Two ways to synthesize the Fe^{2+} complex of terpyridine rotaxane **7R**: Starting with terpyridine rotaxane **7R**, Method A; starting with Fe^{2+} complex of terpyridine macrocycle **7**, Method B.

The order of synthesis with rotaxane metal complexes was also studied on the example with Fe^{2+} (since this ion forms strong complexes that can survive the threading reaction to form rotaxanes). The iron complex with terpyridine rotaxane can be formed in two ways as shown in Figure 75: The conventional way starting with $\text{Fe}(\text{BF}_4)_2 \cdot 6\text{H}_2\text{O}$ and terpyridine rotaxane as shown previously (method A); or using the iron complex of terpyridine macrocycle and performing a rotaxane synthesis on this compound. It was shown that the first way leads to the desired complex quantitatively. The yield of the rotaxane reaction on the terpyridine macrocycle iron complex is more restricted. However, retention of complex structure and successful threading reaction can be concluded (FTICR-MS shows only the threaded compound) which is quite important for further studies especially under topic of multivalency.

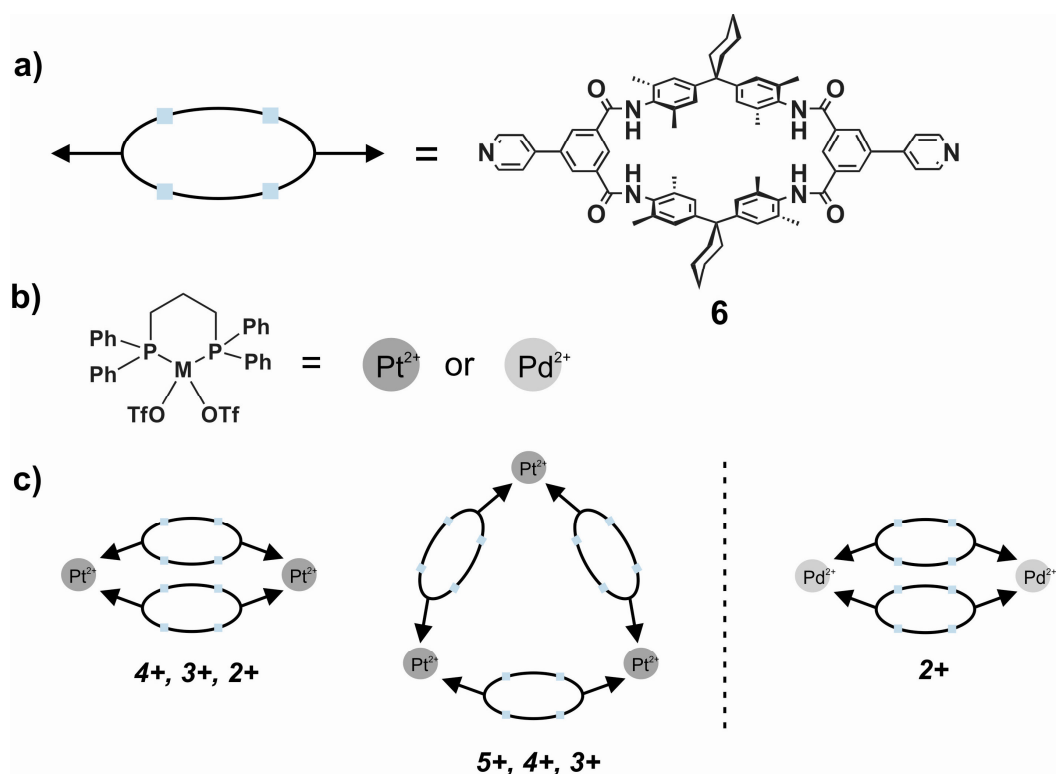


Figure 76. An equimolar mixture of a) bispyridine macrocycle **6**, b) Pd^{2+} or Pt^{2+} Stang's corner complexes display, c) 2:2 and/or 3:3 assemblies depending on the metal ion used in the assemblies. The observed charged states in the FTICR-MS analyses of the systems are given below the hypothetical structures.

Higher assemblies can be simply achieved by mixing the $\text{Pt}(\text{dppp})(\text{OTf})_2$ and $\text{Pd}(\text{dppp})(\text{OTf})_2$ complexes ("Stang's corners") with bispyridine macrocycle **6** and rotaxane separately (Figure 76). The assemblies of such complexes are well-studied by others⁷¹ and also in our group⁵⁷. Such systems are achieved as stated in the literature, by introduction of pyridine ligands in the "metal corner" solutions e.g. in DMF, triflate is replaced by pyridine and the complexation equilibria continues until the thermodynamically most stable and entropically most favoured species is formed. For platinum, equilibria are slower than palladium due to the stronger metal-ligand bond⁵⁷. Many different assemblies were obtained using different ligands with various geometries and lengths. For our studies, firstly, the bispyridine macrocycle **6** was chosen for forming the assemblies since the resulting species are of rather lower molecular weight than the ones with rotaxanes, and easier to analyze with FTICR-MS. The incredibly low-solubility of the bispyridine macrocycle **6** in common organic solvents was found not to hinder the assembly formation process, since the formed species are more soluble in the solvent of assembly. Mixing the bispyridine macrocycle with equimolar

Pt(dppp)(OTf)₂ in DMF resulted in formation of 3:3 and 2:2 complexes evident from mass spectrometric analysis of the mixture. For exact determination of structures, whether they are cyclic or not, ³¹P NMR spectra must be measured: only singlets showing all phosphorous protons are equal can prove the cyclic structures. Nevertheless, cyclic architectures are expected structures, since the long and flexible ligands may allow formation of such assemblies^{138, 139}. A very close example to this case was already stated in the literature using small macrocycles¹⁴⁰. With Pd(dppp)(OTf)₂ only smaller 2:2 complex was formed probably due to the weaker metal ion-ligand bond which is more reversible compared to the Pt²⁺ analog, that lets the system reach the entropically most favored state quicker.

3.8.2. Covalent Self-Assembly of Macrocycles

3.8.2.1. The Functionalized Macrocycles in Covalent Self-Assembly

For assembly of the macrocycles (or rotaxanes) via imine bonds, 4-formylbenzyl **9**, bis 4-formylbenzyl **10** and 3,5-diformylbenzyl **11** macrocycles were synthesized, in each case from the bromo macrocycle **2** in Suzuki coupling reactions with moderate to good yields (Figure 77). The aldehyde macrocycles were purified with column chromatography on silica prior to assemblies.

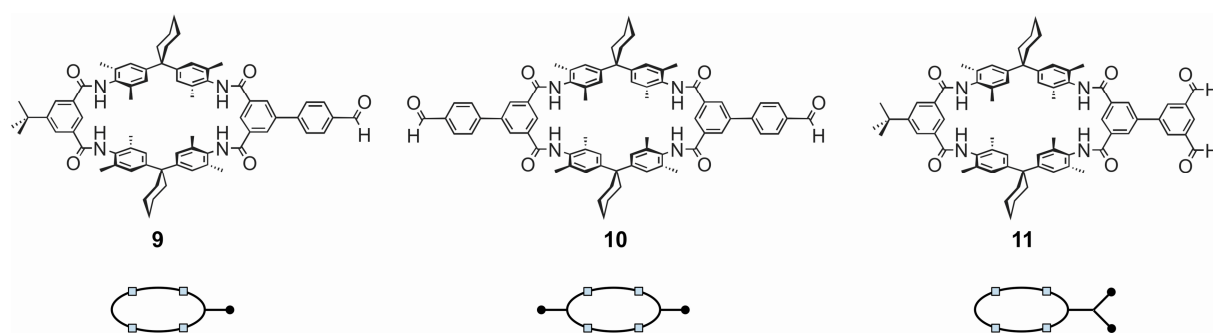


Figure 77. The macrocycles **9**, **10** and **11** having aldehyde groups and the schematical representation showing the directionality modes.

A preliminary experiment was made to check if there is some imine bond formation between an amine and our aldehyde macrocycle at room temperature. A solution of aldehyde in CDCl₃ was added an excess amount of benzylamine. The peak at 10.03 ppm for the aldehyde proton vanished and a new signal at 4.75 ppm emerged which was an evidence of

imine formation. This was a sign that the aldehyde macrocycle is suitable and available for our target assemblies.

3.8.2.2. The Template for Covalent Self-Assembly of Macrocycles

The macrocycles could be assembled with the help of different templates. An interesting and easily accessible template for imine assembly was thought to be 1,3,5-tris(aminomethyl)-2,4,6-triethylbenzene **P12** with a D_{3d} symmetry¹⁴¹. This compound has been used in self-assembly and molecular recognition events¹⁴² and has an advantage over its non-ethylated analog by the restricted position of the amine groups. All the amine groups in compound are proven to be on the same side of the plane of the benzene ring. Thus, the macrocycles can form assembly only on this side and because of the restricted rotation, this assembly is a nice template for a triple axle.

3.8.2.3. The Covalent Assembly with Aldehyde Macrocycle and a Trisamine

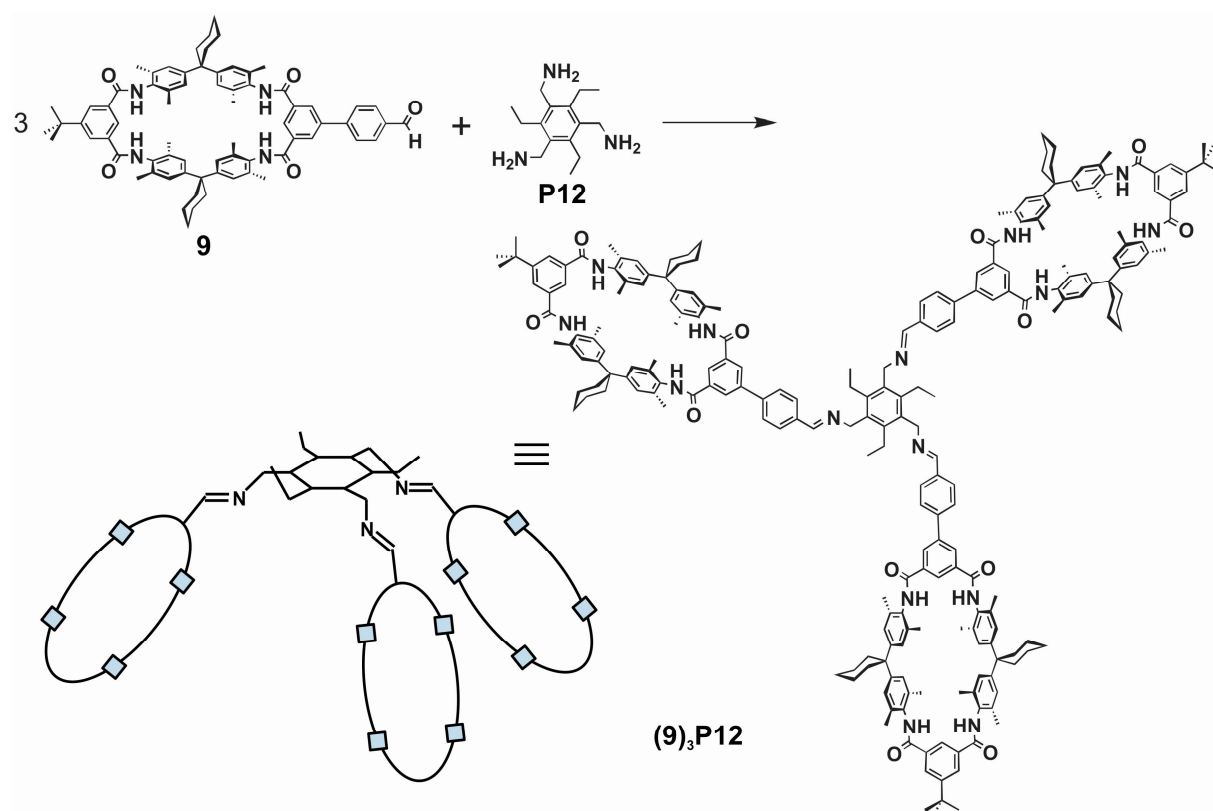


Figure 78. The self-assembly of the aldehyde macrocycle **9** around **P12** to form a trisimine.
(Here only one isomer of the final structure is shown.)

Trisamine **P12** for the covalent assembly with the aldehyde macrocycles was synthesized from its bromo derivative **P10**. The assembly to the trisimine was let to occur by mixing the two compounds in CDCl₃ in an NMR tube in 3:1 ratio (Figure 78). In the ¹H-NMR spectrum the aldehyde peak disappeared and the spectrum became more complex as expected from the cis and trans isomers that can be formed when imine bonds are made. ¹³C NMR also proved that the mixture of **9** and **12** does not contain any aldehyde. To have a clearer insight into the assembling process that is not possible from the NMR spectra, mass spectrometry turned out to be a useful tool. In the mass spectrum of the mixture that was obtained after direct mixing of the aldehyde and amine, the highest signal was obtained from the trisimine assembly. Although the spectrum is quite unexpectedly complicated, one may see the vanishing of the aldehyde macrocycle and co-appearance of monomacrocycle, bismacrocycle and trismacrocycle assemblies.

4. Conclusion and Outlook

4.1. Toolbox Synthesis

Although there are uncountable examples of supramolecular compounds and at least that much ingenious studies in assembling small building blocks to lead functional supramolecular architectures, the gap between supramolecular chemistry and nanotechnology is still wide. Making molecular machines, may it be using interlocked compounds or not, chemist encounter a number of problems in efficient and flexible synthesis, and as well, in achievement of unidirectional motion, fuelling, assembly and immobilization of these machines. In this study, it was shown that

- By reorganizing the sequence of reactions leading to a functional architecture, a bunch of products with different functionalities (ligands, photoactive groups and other functions for self-assembly and further reactions).
- The diversity of products is accompanied with high efficiency in the synthesis, purity of the final architectures, and moreover, with less effort to achieve both.
- The ligand decorated macrocycles and rotaxanes can be assembled with appropriate metal ions to obtain higher architectures with control of geometry and strength. (The latter plays an important role in the reversibility of the systems)
- The macrocycle-functional group bond flexibility is an important issue in achieving efficiency in the synthesis and as well, in the desired rigidity for final architecture e.g. organization of macrocycles or rotaxanes around a metal ion.

- Multivalent hosts can be prepared by using a core molecule in high efficiency; the core molecule can be chosen from a variety of molecules including photoactive ones.
- The sequence of rotaxane synthesis-functionalization is vital for ether-axled rotaxanes when Suzuki coupling is used in functionalization. Amide rotaxanes are more robust and sequence does not matter.
- Both macrocycles and rotaxanes can be decorated with photoactive groups, they may be used in FRET studies which are important in determination of binding constant of guests, fuelling rotaxane shuttles and co-centering the energy in one point (antenna effect).
- Chiral structures which are musts for unidirectional motion, can be obtained by very simple modifications on axles and macrocycles of rotaxanes and catenanes, with high yields.

4.2. Outlook: Energy Transfer Systems and Layer-by-layer Self-Assembly

The above stated points already opened a new and a straightforward way to obtain functionalized macrocycles and rotaxanes and variety of different architectures as a result of assembling them in our group. The studies with multivalent hosts, for example has expanded into a topic on its own covering whole aspects of investigations on interactions of these hosts with mono- and multivalent guests. The photoactive cored multivalent hosts are planned to be tied with axles stoppered with other photoactive units of suitable absorption and emission for antenna effect (Figure 79).

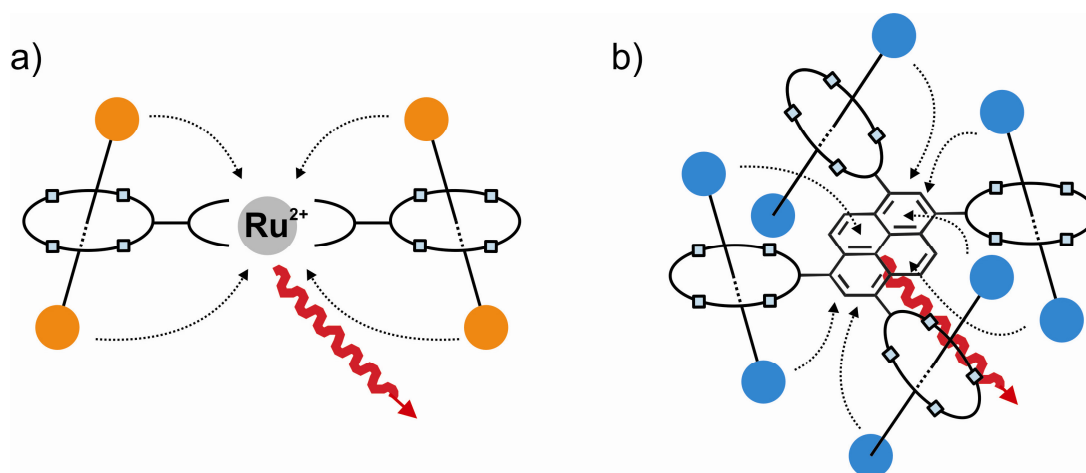


Figure 79. Possible energy transfer (or antenna) systems through toolbox strategy.

Ligand decorated macrocycles have shown in this study to form expected higher structures in metal-directed assembly processes. These assemblies may also be further

“functionalized”. For example, by decorating the iron complex of terpyridine rotaxane with photoactive groups FRET (Fluorescence Resonance Energy Transfer) or PeT (Photoinduced electron transfer) to the metal ion core may be achieved. These processes can further be coupled with shuttling motion of a rotaxane.

Apart from energy or electron transfer systems presented above that may help the efficient energy transfer (fuelling) of the nanosystems, another problem in feasibility of such nanosystems may be solved by ordering and addressing the individual parts. The assemblies of rotaxanes in solution have only a few examples. In the same manner, assemblies of rotaxanes on solid surfaces¹⁴³ have been studied for only one type of rotaxane in each case. However, assembling different kinds of individuals in an ordered manner and studying the interactions of these with each other and with surface can open a new era in nanotechnology. Thus, using our toolbox of ligand decorated macrocycles and rotaxanes, different architectures may be sequentially built on a surface utilizing a concept which is known as layer-by-layer self-assembly¹⁴⁴ (Figure 80).

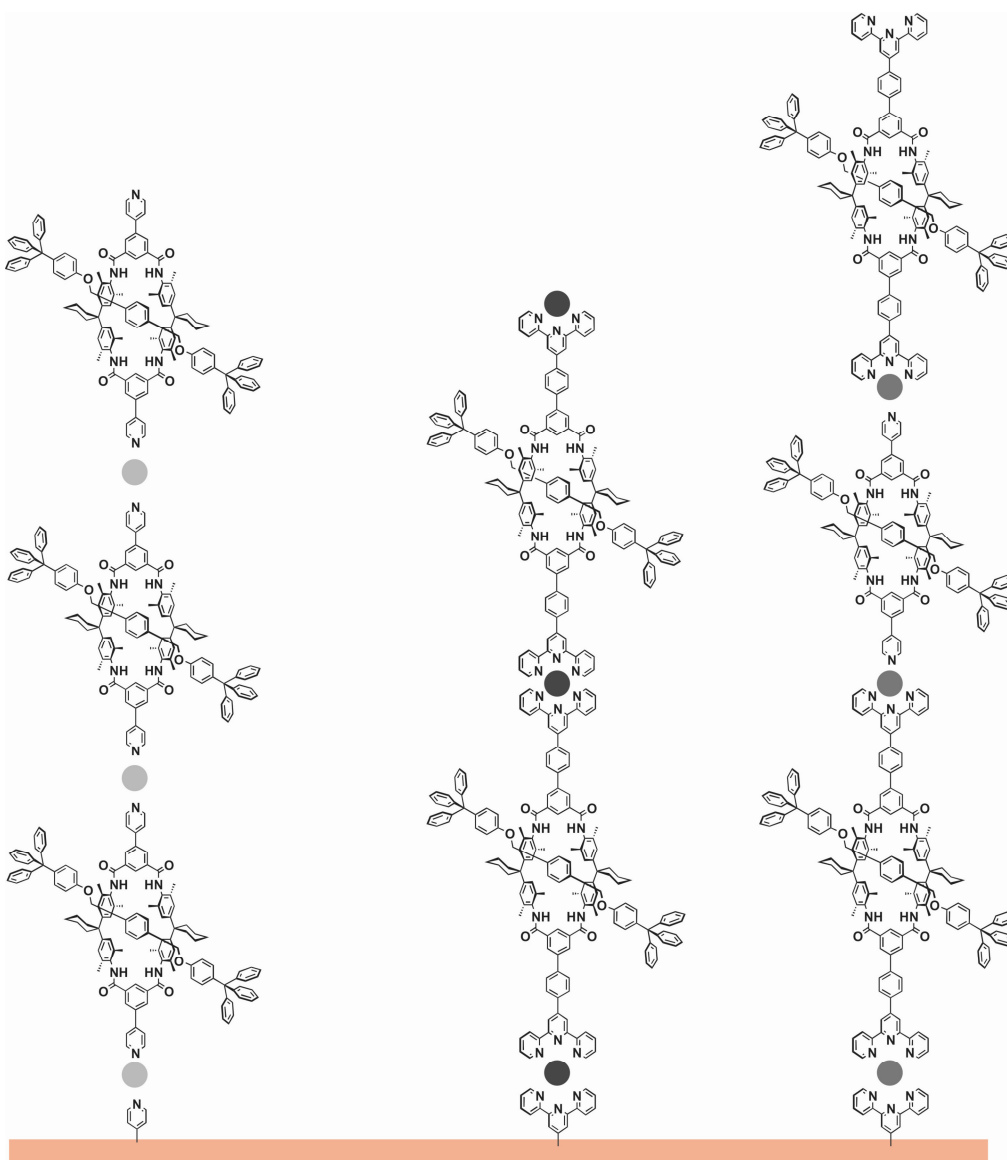


Figure 80. Layer-by-layer assembly of rotaxanes: The alternating additions of ligand and metal ions can yield in a controlled growth of rotaxanes (and rotaxane shuttles) on a surface; each layer can be separately and freely chosen.

Like a box of LEGO which gives innumerable possibilities for building architectures, the things that can be accomplished with our “toolbox” are only limited by imagination. Moreover, our toolbox consists of building block which may be altered by small changes on the blocks to obtain new blocks. So our toolbox may be considered as a LEGO set in which the building blocks can be used to generate the desired ones. This way, the problems in contemporary supramolecular chemistry/nanotechnology border may be solved in a straightforward way.

II. A (TANDEM) ESI-FTICR MASS SPECTROMETRIC STUDY ON FRÉCHET-TYPE DENDRIMERS WITH AMMONIUM CORES

1. Purpose of the Study and Introduction

Dendrons and dendrimers¹⁴⁵ are highly branched, ideally monodisperse and regularly shaped macromolecules with a significant impact on biomedical¹⁴⁶ and materials sciences¹⁴⁷. They are particularly interesting with respect to their nano-sized quantized structures and their aufbau principle in generations¹⁴⁸. Dendrimer research has been accelerated significantly by the development of analytical methods that permitted to characterize their structures, analyze their purity, and characterize their properties as a function of increasing generation number. Among these methods are nuclear magnetic resonance (NMR), size exclusion chromatography (SEC), high performance liquid chromatography (HPLC) and, more recently, scanning probe methods (SPM). However, since the development of the so-called soft ionization methods, mass spectrometry has proven to be a most valuable tool, because it provides detailed information on defects and impurities¹⁴⁹. Dendrimers have thus been ionized by fast atom bombardment (FAB-MS),¹⁵⁰ matrix-assisted laser desorption/ionization (MALDI),¹⁵¹ and electrospray ionization (ESI).¹⁵² The two latter techniques involve very gentle ionization methods that minimize the fragmentation of the analyte molecules, although there are examples for the destruction of dendrimers during the MALDI process¹⁵³.

The utility of mass spectrometry in dendrimers chemistry is not limited to the determination of molecular masses of dendrimers and their purity. Their chemistry in gas phase is an as well interesting and novel area of research¹⁵⁴. Mass spectrometry may provide even more information, for example on the self-assembly of dendrimers,¹⁵⁵ or on weak, non-covalently bound host-guest complexes of dendritic species¹⁵⁶. These results demonstrate the power of mass spectrometry for a detailed characterization of dendrimers without which the fast pace of development in this field would not have been possible.

Fréchet dendrons are synthesized in a convergent way¹⁵⁷ and can be attached to a core molecule in the final step. Here, the mass spectrometric characterizations of Fréchet dendrons which bear benzylic alcohols and benzylic ammonium groups at the focal point are presented. Finally, collision-induced decay (CID) experiments provide interesting and surprising insights into the fragmentation mechanisms of the dendrons.

2. Results and Discussion

2.1. ESI Mass Spectrometric Characterization of Fréchet Dendrons

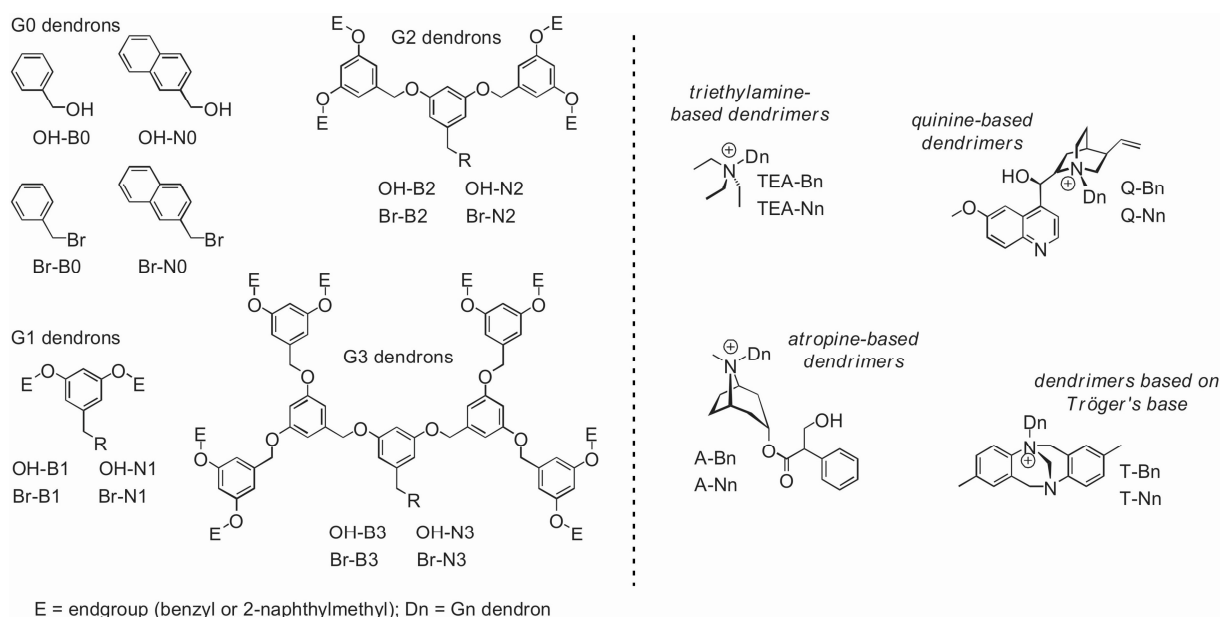


Figure 1. Dendrons and dendrimers under study, which bear a benzylic alcohol, a benzyl bromide or an ammonium ion at the focal point. The nomenclature consists of three labels: First, the focal point is characterized by a shortcut (“OH”, “Br”, “TEA” etc.), then “B” and “N” denote benzyl and 2-methylnaphthyl as peripheral endgroups E, and finally, the number indicates the generation of the dendron.

Figure 1 shows the dendrons and dendrimers under study which at the focal point bear either a benzylic alcohol, a benzyl bromide, or one of the four tertiary amines, which provide the necessary charge for ionization. The benzylic alcohols can be easily characterized by negative-ion ESI mass spectrometry. Deprotonation of the OH group during the electrospray process easily occurs, when methanol is used as the spray solvent. Interestingly, an intense signal for the dimeric species bridged by an $\text{O}^- \cdots \text{H-O}$ hydrogen bond is observed. The fact that the dimer survives even quite harsh ionization conditions can be rationalized by the strength of the hydrogen bond (ca. 130 kJ/mol) which includes an anionic donor atom and under the environment-free conditions in the gas phase does not compete with any solvent molecules.

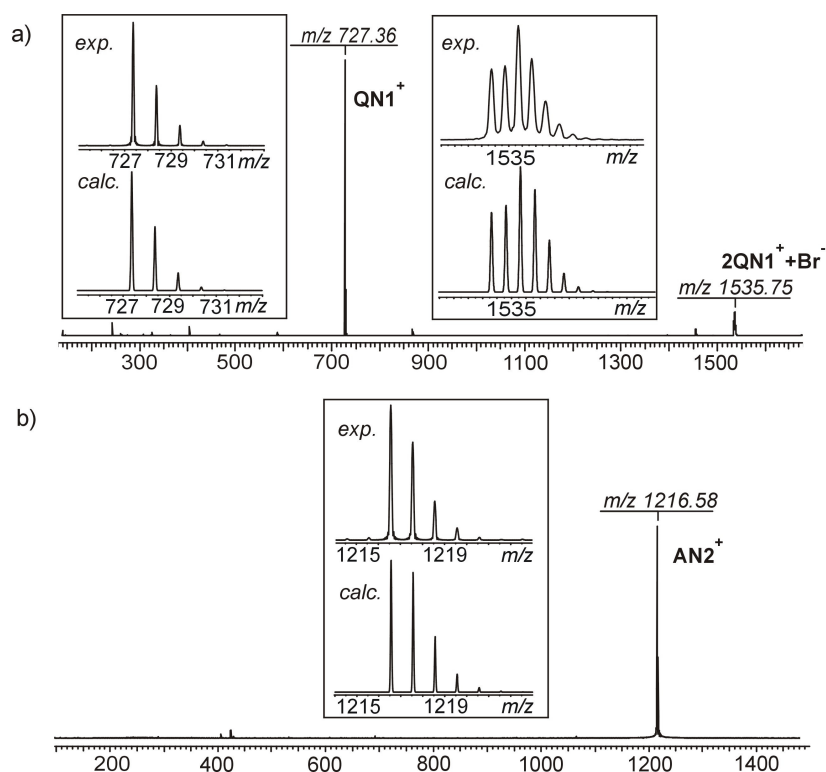


Figure 2. Two representative examples for positive-ion ESI-FTICR mass spectra of dendrimers bearing an ammonium cation at the focal point: a) **Q-N1**, b) **A-N2**. For **Q-N1**, a bromide bridged dimer is also observed under soft ionization conditions. The experimental isotope patterns match the calculated ones nicely.

The corresponding benzyl bromides are difficult to ionize with electrospray ionization, because they neither carry a charge, nor bear any groups which can easily be charged. All attempts to characterize them directly by ESI mass spectrometry yielded more intense signals of some traces of impurities which are much more easily ionized than the dendritic benzyl bromides. For example, the sodium adduct of triphenyl phosphine oxide was observed as one of the major signals. This compound stems from the conversion of the benzylic alcohol into the benzyl bromide using CBr_4 and Ph_3P as the reagents. It was the major ion seen in the mass spectra, although we were unable to detect it in the NMR spectra of the dendrons which proves that it is a trace component in the sample. Consequently, we added 1 eq. of triethylamine to the sample solutions of the benzyl bromide dendrons in methanol, thus generating **TEA-Bn** and **TEA-Nn** *in situ*. Each of these solutions gave excellent results with the parent ion being the most intense signal. Since this approach turned out to be successful, other, more complex tertiary amines, i.e. atropine, quinine, and Tröger's base were used instead of triethylamine. These compounds were isolated before the mass spectrometric

experiments. For all dendrimers bearing an ammonium cation at their focal point, clean mass spectra with excellent signal-to-noise ratio could be obtained. As shown in Figure 2 for **Q-N1**, dimers bridged by one counterion (bromide in all cases) and held together by electrostatic forces can be seen with low intensity, as long as they are small enough to appear within the mass range of the instrument. The exact masses and isotope patterns determined by experiment are in excellent agreement with those calculated.

The picture differs somewhat for the third generation compounds. A series of defects are observed in the ESI mass spectra which appear in the spectra at mass distances of $\Delta m = 212$ below the parent ions for the benzyl terminated dendrimers (Figure 3) and of $\Delta m = 264$ for the 2-naphthylmethyl terminated ones. These mass differences correspond to the masses of one branching unit plus a peripheral endgroup. The defect structures are shown in Figure 3. Since the corresponding second generation dendrimers do not show any signals for defects, the defects in the third generation dendrimers must originate from the last steps in the convergent synthesis. During the conversion of the benzyl alcohol into the benzyl bromide with PBr_3 traces of acids may induce rearrangements of the benzyl ether linkages. While it is easy to separate the analogous defects from the intact parent ion for the lower generations, the chromatographic separation of the intact dendrons becomes increasingly difficult for higher generations. Using $\text{CBr}_4/\text{PPh}_3$ for the production of the bromides, which is also advantageous because of higher yields obtained, no defects were observed in the mass spectrum of the compounds. Consequently, the defects that prevail in the samples even after chromatography are easily seen by ESI mass spectrometry. The examination of the fragmentation patterns described below makes sure that the signals assigned to defects do not correspond to fragments originating from the ionization procedure (see below).

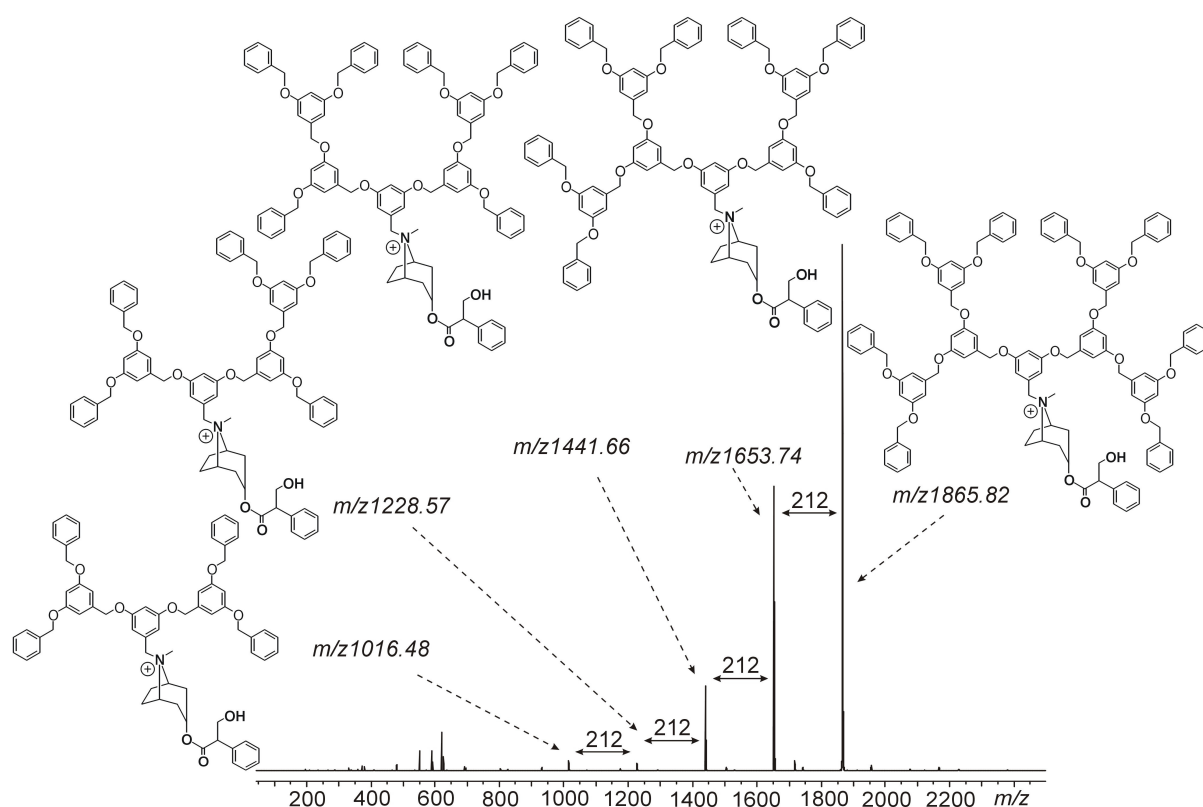


Figure 3. ESI-FTICR mass spectrum of the third generation dendrimer **A-B3**. Defects become visible at regular spacings of 212 Da below the parent ion of the intact dendrimer.

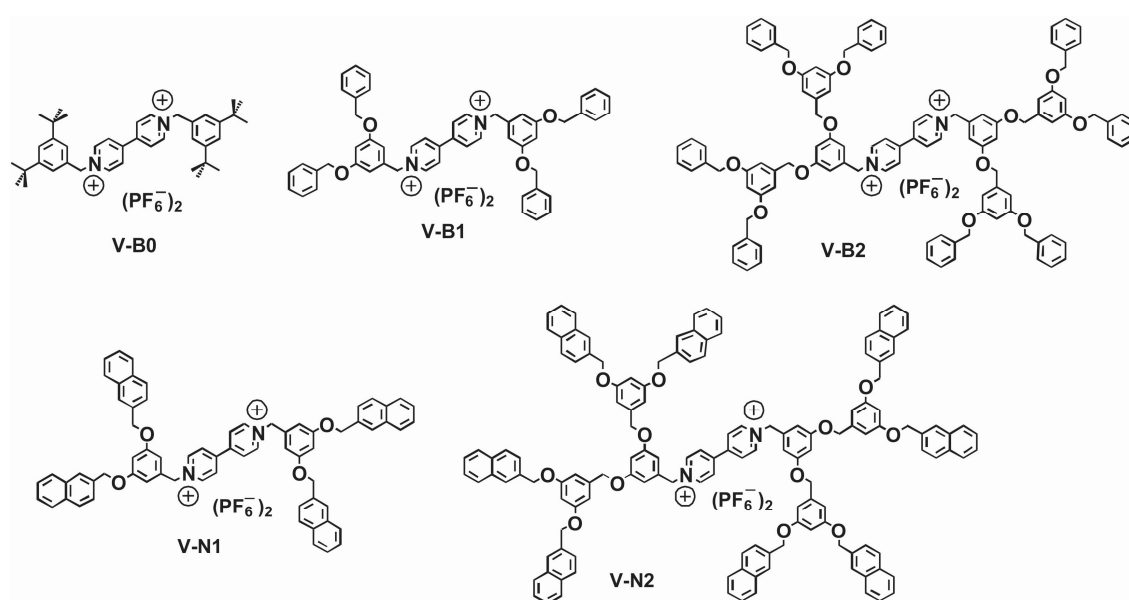


Figure 4. Dendritic viologens. **V-B0** is substituted with *t*-butyl groups in order to increase the solubility of the salt. For the same reason, the counterion is PF_6^- instead of bromide.

2.2. Dendritic Viologens: The Effect of Dendron Size on Dication Stability

Quite different from the ammonium salts discussed so far are the dendritic viologens shown in Figure 4. These compounds have been examined by mass spectrometry before with respect to their host-guest chemistry and they represent excellent guests for Klärner-type molecular tweezers¹⁵⁸. The dications are quite stable in solution, although in the long run, they decompose, when the solvent is nucleophilic to some extent. Due to the short distance between the two charges, significant charge repulsion effects can however be expected to affect their gas-phase behavior. Figure 4 shows the ESI-FTICR mass spectrum of **V-B0**. Most remarkably, we did not succeed in generating the dication in its bare form (asterisk in Figure 4) irrespective of the ionization conditions used. Instead, two series of clusters are formed: Singly charged $(M^{2+})_n(PF_6^-)_{2n-1}$ with $n = 1 - 3$ and doubly charged $(M^{2+})_n(PF_6^-)_{2n-2}$ with $n = 3 - 6$. In these clusters, the high positive charge can be compensated by the counterions and thus the compounds are significantly stabilized.

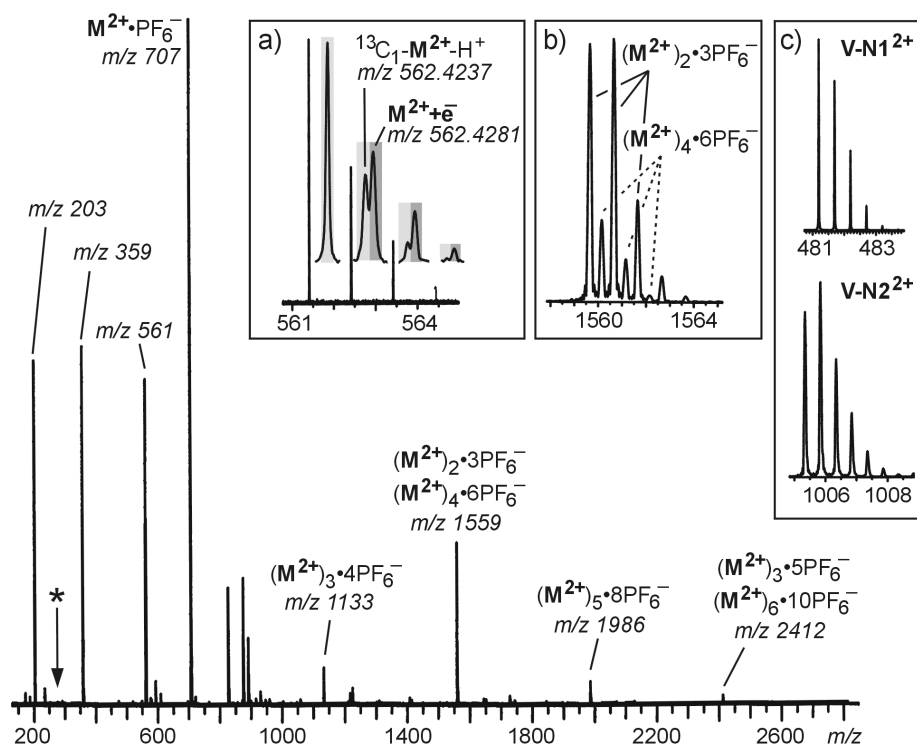


Figure 5. Positive-ion ESI-FTICR mass spectrum of a methanol solution of **V-B0**. Besides fragmentation into the two monocations at m/z 203 and m/z 359, the dication forms singly and doubly charged clusters with the PF_6^- counterions. The asterisk indicates the position, at which the bare dication is expected to appear. Insets: a) High resolution isotope pattern of the signal at m/z 561 revealing that both electron capture and proton loss overlap. b) Isotope pattern of the signal at m/z 1559 providing evidence for a superposition of singly and doubly charged clusters. c) Experimental isotope patterns of the bare dications of **V-N1** and **V-N2**.

Other signals also speak of a strong tendency to avoid bare dications: Signals at m/z 203 and m/z 359 are due to fragmentation of the dication by cleavage of one of the benzylic C-N bonds. A benzyl cation is then created together with a mono-substituted, singly charged bipyridinium. Charge repulsion is thus avoided by the separation of the two charges onto two independent ions. Interestingly, a signal at m/z 561 showed an isotope pattern in the broadband mode of the FT-ICR instrument, whose intensities changed with the ionization conditions. This pointed to the fact that two overlapping isotope patterns are observed that were not resolved. Changing the ionization conditions also changed the relative amounts of the two species contribution to the pattern. A high-resolution mass spectrum confirmed that. Two ions differing by only 1 Da correspond to a one-electron reduction occurring during the ionization process (m/z 562) and the loss of a proton from the dication (m/z 561). Since the proton has a mass differing from the exact difference between ^{12}C and ^{13}C , both patterns can be resolved and independently seen (inset (a) in Figure 5). Likely, the proton loss occurs at the benzylic position adjacent to one of the nitrogen atoms yielding a zwitterionic structure, which nevertheless is well stabilized by conjugation of the anion with the aromatic ring. Consequently, four different ways exist for a cation to avoid the charge repulsion within the dication: Compensation of positive charges by counterions, proton loss, or one-electron reduction, and fragmentation leading to the separation of two singly charged ions.

With the larger dendrimers **V-B1**, **V-B2**, **V-N1**, and **V-N2** the same experiments gave similar results. However, one significant difference was observed: Substitution with dendrons of the Fréchet-type stabilizes the bare dications so that signals for them can be observed in the ESI-FTICR mass spectra (Figure 5, inset (c)). A clear ranking of stabilities with increased dendron generations was observed depending on the harshness of the ionization conditions. In particular, the capillary exit voltage can be tuned in our instrument. This accelerates the ions to different velocities with which they then undergo collisions with residual gas molecules. At higher settings of this voltage, only **V-B2** and **V-N2** gave clearly observable signals for the corresponding dications, but no dications of the smaller generations were observed. By softening the conditions, all four dendritic viologens of first and second generation gave signals for bare dications, while **V-B0** did not yield any bare dications irrespective of the ionization conditions. This ranking was confirmed by other experiments with the Klärner-type tweezer complexes which showed a pronounced dendritic effect on their gas-phase reactions¹⁵⁸.

2.3. Collision-Induced Decay of Dendrimers Bearing Ammonium Ions at Their Focal Points

Chemical intuition would predict that the primary fragment formed upon collisional activation of mass-selected n^{th} generation dendrimer ions in the mass spectrometer would correspond to the loss of the tertiary amine giving rise to the corresponding benzyl cation of n^{th} generation. The tertiary amine is a good and stable leaving group and the benzyl cation is stabilized by the aromatic ring next to it.

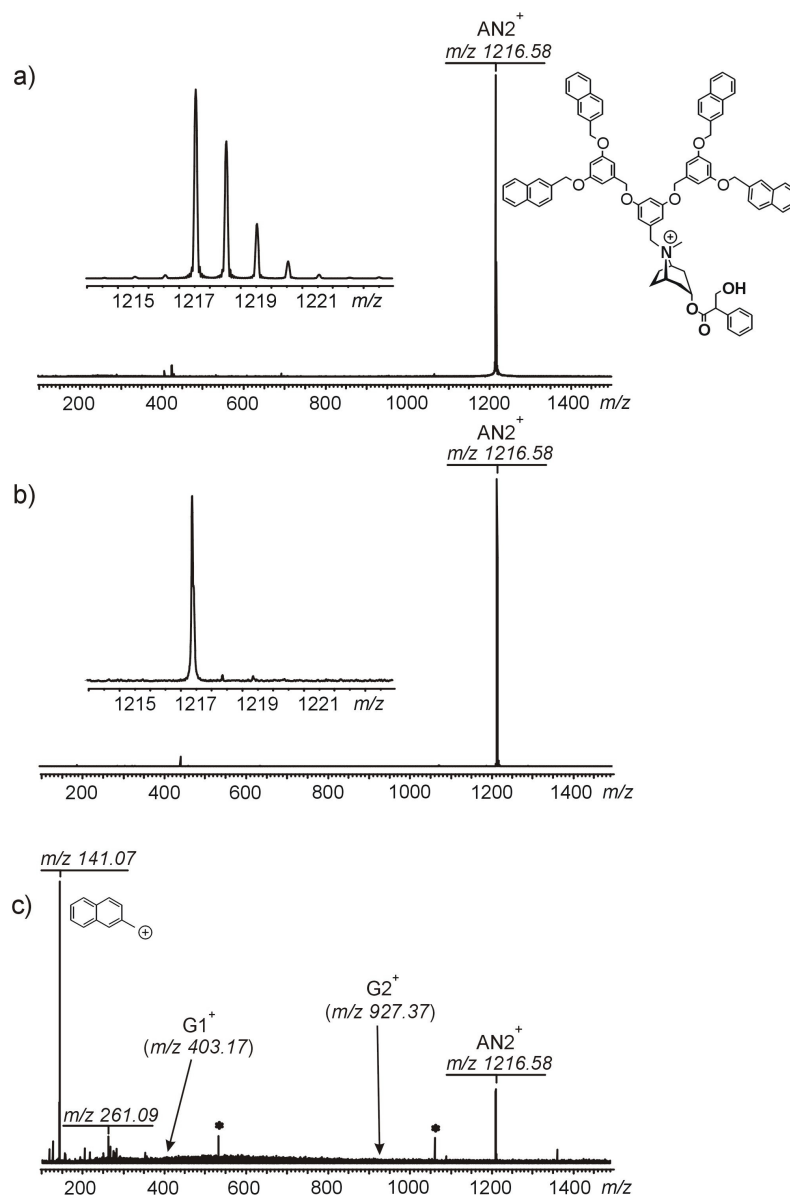


Figure 6. a) ESI-FTICR mass spectrum of A-N2. b) Isolation of the monoisotopic molecular ion. c) Collision-induced decay (CID) experiment. The most significant path leads to the 2-naphthylmethyl cation at $m/z=141$. The positions, at which the intermediate 2nd and 1st generation benzyl cations are expected are marked. Artifacts are denoted by asterisks.

For an analysis of the fragmentation behavior, the monoisotopic ions of interest, i.e. the first signal of the isotope pattern, was mass-selected in the FTICR cell and collided with argon as the collision gas. Figure 6 shows the spectra of **A-N2** as a representative example. Interestingly, the experimental result differs from expectation quite significantly. Regardless of the generation number, the most intense signal in all CID mass spectra corresponds to either benzyl or 2-naphthylmethyl depending on the peripheral endgroup incorporated in the dendrimer. Signals for the expected benzyl cations of 1st to 3rd generation are instead either not seen at all (G2 and G3) or hardly exceed the noise (G1). The question arises, which mechanism might account for this unexpected fragmentation behaviour. In the following chapters, five different mechanisms are presented and experiments are discussed which are in favor of them or rule them out.

2.3.1. Direct Peripheral Cleavage Mechanism

The simplest mechanism that can be imagined involves direct cleavage of the peripheral benzyl ether bonds. However, it is not likely to take place because of the following reasons: First of all, it is hard to imagine that it could energetically compete with the expected amine loss, if one considers that it would require a charge separation through formation of the benzyl or 2-naphthylmethyl cation and the corresponding anionic phenolic oxygen, which would compensate for the charge on the ammonium group of the neutral fragment. A second argument against such a mechanism is the fact that no other dendritic benzyl cations are observed, although for example the first generation Fréchet dendron is connected to the next branching unit in the G2 dendrimers through the same benzyl ether bond. Another evidence against such a mechanism comes from the CID experiments on viologens¹⁵⁸. Here the cleavage of the benzyl-bipyridine bond leads to two fragments which are both singly charged and thus can be detected, showing that such a cleavage is more favored than direct cleavage of the end groups of the dendrimer.

2.3.2. In-to-Out Benzyl-Tropylium Rearrangement Cascade

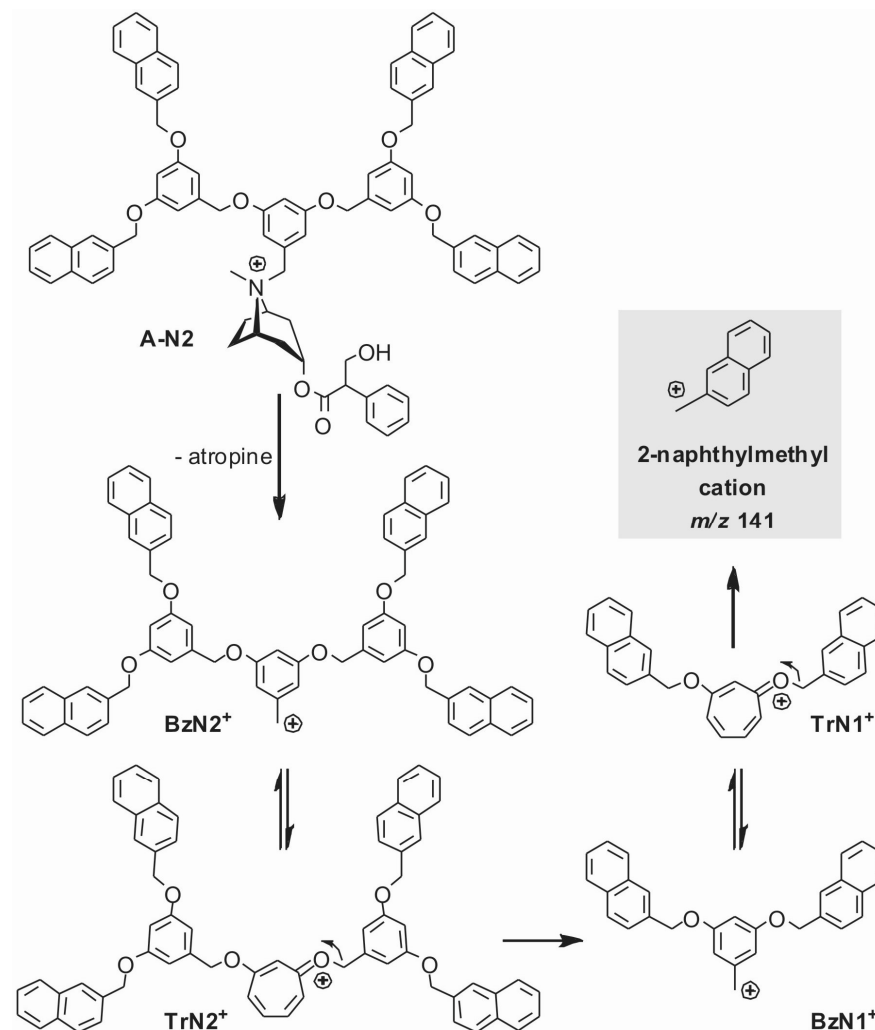


Figure 7. The fragmentation cascade shown for **A-N2** as a representative example. It is initiated by the loss of atropine and involves several quick rearrangement and fragmentation steps that finally lead to the 2-naphthylmethyl cation stemming from the periphery.

In order to resolve the mechanistic problem, the mechanism shown in Figure 7 was proposed exemplarily for **A-N2**. As the first step, it indeed involves the liberation of the neutral amine concomitant with the formation of the corresponding dendritic benzyl ion. As shown in Figure 7, the benzyl ion is stabilized by a total of four mesomeric structures. However, due to the *meta*-arrangement between the CH₂ group and the two oxygens attached to the aromatic ring, the lone pairs of the two ether oxygen atoms do not take part in the

mesomeric stabilization. Consequently, a benzyl-tropylium isomerization step (Figure 7) is energetically favorable and leads to a tropylium ion which has a total of nine mesomeric structures including two in which the oxygen lone pairs contribute to the stabilization of the cation. According to the literature on the benzyl/tropylium rearrangement, the barrier for this process is low and the unsubstituted tropylium is already energetically more favorable than its benzyl analogue¹⁵⁹. The participation of the two oxygen substituents in our case makes the rearrangement energetically even more favorable. It is important to note that an isolated ion or molecule in the gas phase does not exchange energy with its environment¹⁶⁰. Consequently, the reaction energy generated during the benzyl-tropylium rearrangement is stored in the ions as internal energy and remains available for further fragmentation reactions. For completeness, a second benzyl cation is shown in Figure 8, in which the two oxygen atoms can contribute to the stabilization of the charge. It cannot be excluded that this benzyl cation and the tropylium analogue interconvert freely and that the original benzyl cation can also rearrange into the latter benzyl cation. The next step shown in Scheme 1 uses the good leaving group properties of the tropone ring. In view of the amount of vibrational energy gained in the rearrangement, it is very likely that the next fragmentation produces another benzyl cation of the next lower generation in a fast process. If this process is fast enough, the intermediate will not be observed in the CID mass spectra. The same rearrangement/fragmentation reaction is repeated, again driven by the energy liberated in the benzyl/tropylium rearrangement. Finally, the peripheral benzyl or 2-naphthylmethyl cation is formed and the fragmentation cascade ends here, because a benzyl/tropylium rearrangement does not yield any products which could easily continue fragmentation.

It is quite difficult to obtain additional evidence for such a cascade mechanism, if the intermediates do not appear and thus cannot be isolated and examined in additional experiments. Elimination of the intermediate dendritic benzyl cations was attempted by expelling them from the ICR cell in a double resonance experiment. Ejection of an intermediate in such an experiment should result in the absence of all consecutive fragment ions. However, this experiment does not give clear results for intermediates which undergo further fragmentations at high reaction rates, since they can undergo fragmentation before being completely ejected. Consequently, this experiment failed in line with the energetic considerations above that predict the fragmentations to be very fast.

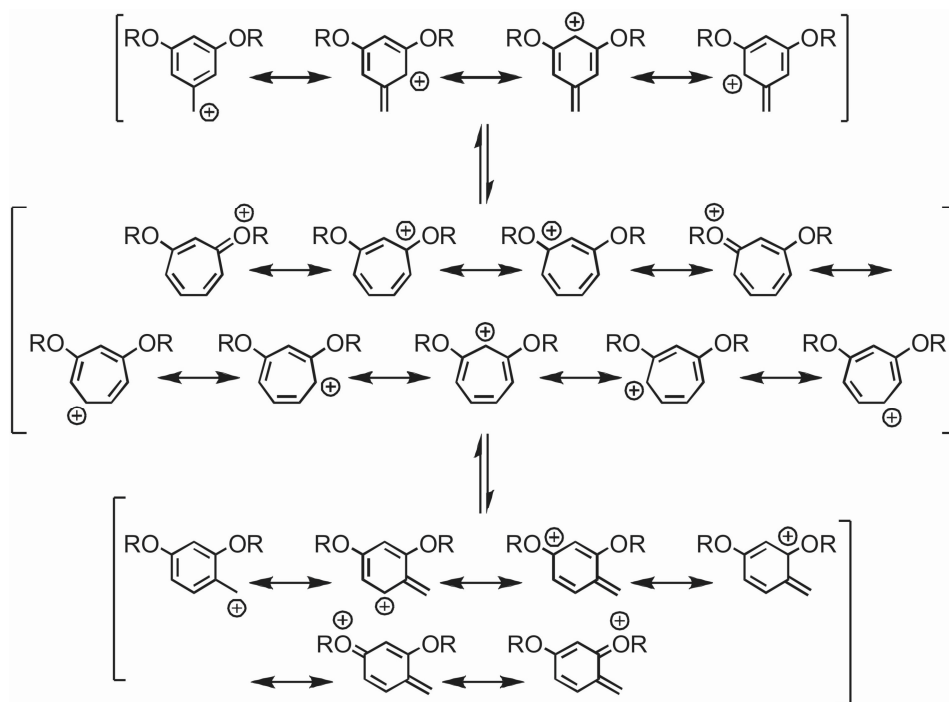


Figure 8. The benzyl and tropylium ions benefit from different amounts of mesomeric stabilization so that the rearrangement to tropylium is energetically quite favorable.

Several indications in favor of the cascade mechanism come from some other findings: Although amine loss and the subsequent cascade reaction occurs for all dendritic ammonium ions under study here, it is not the exclusive fragmentation pathway observed. Other pathways can sometimes compete to a certain extent. In the case of dendritically substituted atropin derivatives, a *syn*-periplanar 1,2-elimination within the bicycle is observed as shown in Figure 9 (top). Also, low-intensity fragment ions are observed, which are due to a 1,2-elimination of a neutral dendron yielding iminium ions. All quinine derivatives reveal water losses that compete with the loss of the amine. Apparently, 1,2-eliminations are the only reactions energetically favorable enough to compete with the fragmentation cascade. This is an additional indication that the formation of benzyl and 2-naphthylmethyl cations from the dendron periphery is not a high-energy process thus ruling out direct formation of these ions by cleavage of the peripheral benzyl ether bonds.

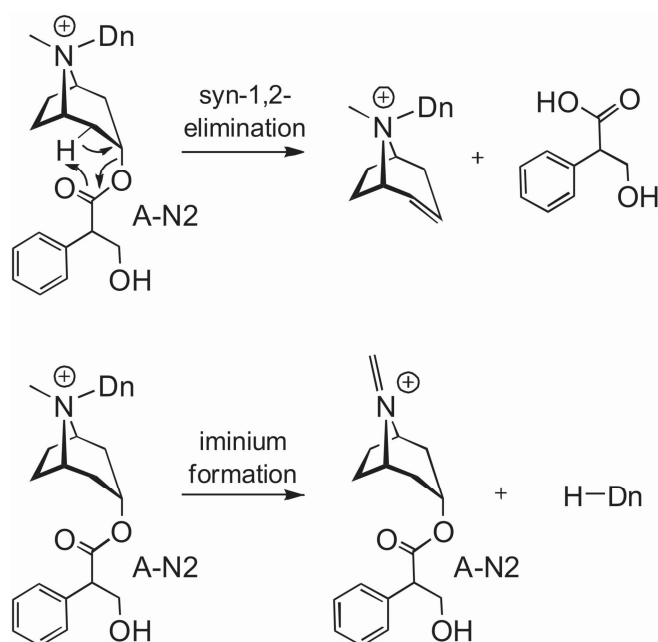


Figure 9. Top: Concerted syn-periplanar 1,2-elimination in analogy to ester pyrolysis. Bottom: 1,2-elimination of a neutral dendron generates iminium ions. Both reactions compete with the fragmentation cascade in Scheme 1 for atropine derivatives.

Finally, the viologen derivatives support the assumption that the cascade fragmentation is initiated by the loss of an amine. Since they are dications, the amine lost initially still bears a charge and is observed in the CID mass spectra. This provides evidence for the formation of dendritic benzyl cations, even though they are not seen in the CID mass spectra. In all other respects, the CID spectra of the viologens resemble closely those obtained from, for example, the dendronized triethylammonium derivatives. Again, no second generation benzyl cation is observed and the intensity of the first generation benzyl cation hardly exceeds the noise level. The most intense signals stem from the peripheral benzyl and 2-naphthylmethyl cations formed through the cascade mechanism.

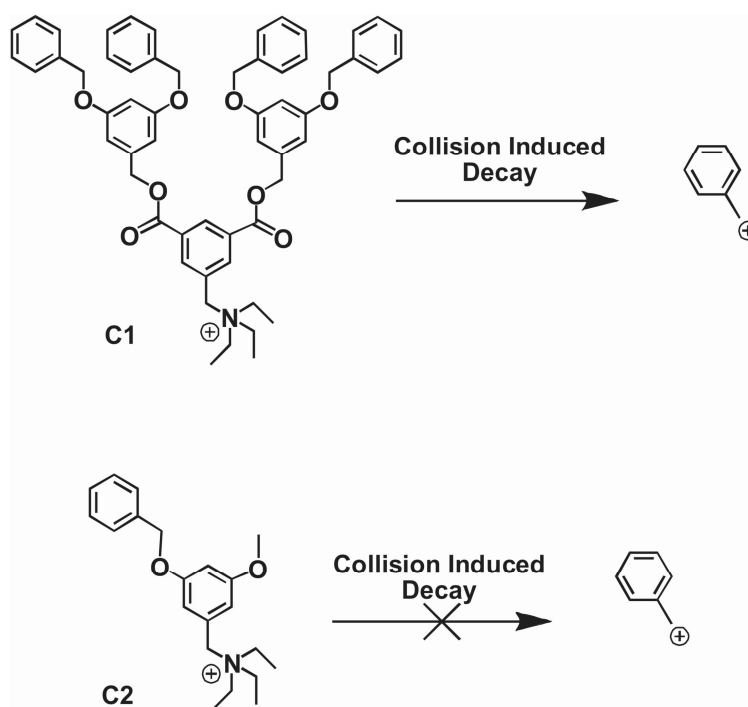


Figure 10. The control compounds (**C1** and **C2**) synthesized and their unexpected CID behaviour.

To find a mechanistic evidence for the in-to-out benzyl tropylium cascade mechanism, two different compounds were synthesized. The first dendrimer synthesized differs from the usual G2 dendrimer by additional carbonyl groups in the structure. This should prevent the cascade decay once the dendrimer is subjected to CID. Unexpectedly, this was not the case and the fragmentation obviously produced benzyl cation. The second compound in which the benzyl group in the periphery was changed to methyl, the expected formation of the benzyl cation as a result of cascade fragmentation was not detected. This points out that the second arm, without which energy demanding transition structures are formed, is definitely involved in the fragmentation process. Finally, it is seen clearly that both of these results were not in favor of the benzyl-tropylium cascade mechanism.

2.3.3. Cyclophane Formation Mechanism

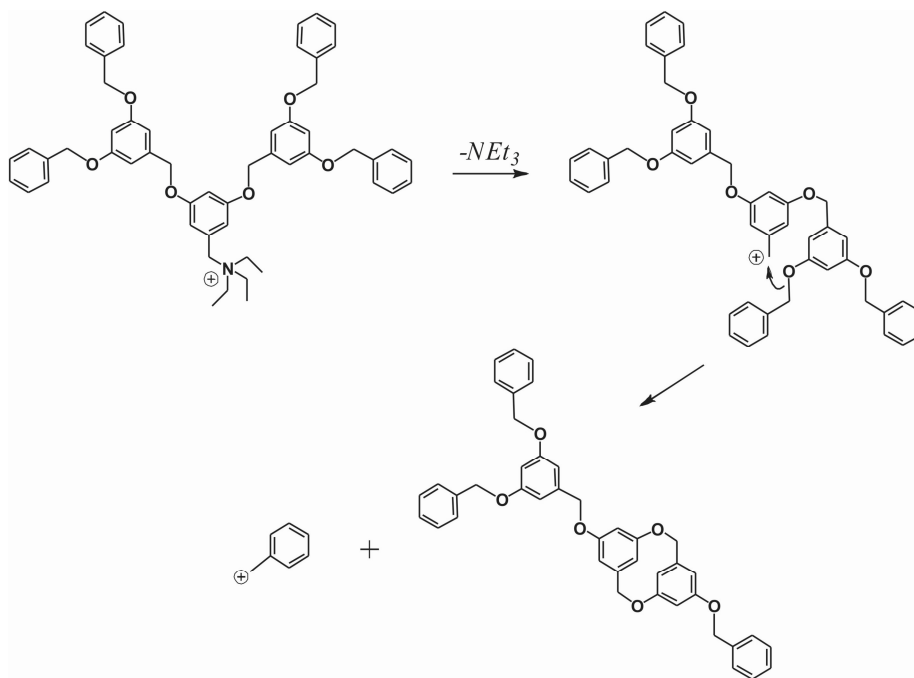


Figure 11. A cyclophane as a possible neutral fragment in the fragmentation process.

Another mechanism that may be proposed is the one which creates a non-strained dioxo-[2.2]metacyclophane as the neutral fragmentation product. However this mechanism maybe eliminated with careful investigation of the stepwise fragmentation: If this was the mechanism or one of the pathways, no fragmentation would be expected from the first generation benzyl cation; third generation dendrimers would generate first-generation benzyl cations as the fragmentation product, not the peripheral benzyl that are observed by experiment.

2.3.4 In-to-Out S_E^{ar} Cascade Mechanism 1

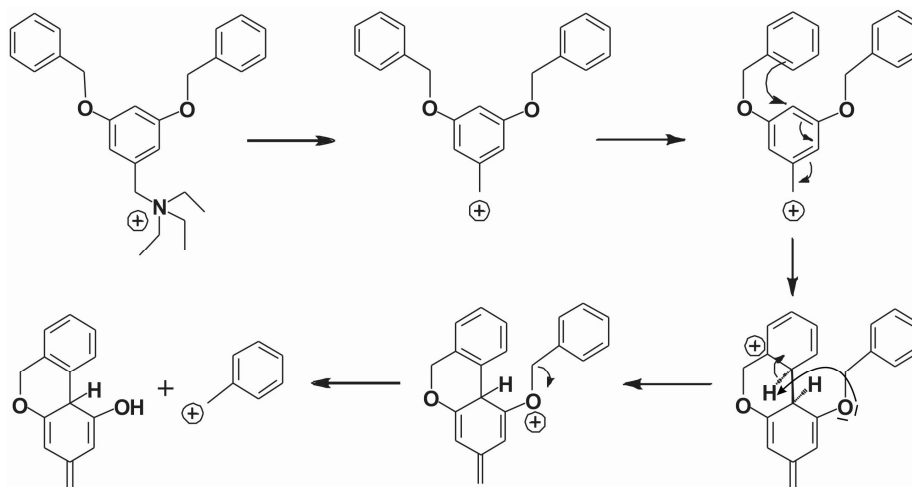


Figure 12. In-to-out cascade mechanism 1 involving an electrophilic aromatic attack and the following rearrangements leading to formation of a stabilized neutral.

A second mechanism could be proposed counting the fact that a second benzylic arm is of vital importance to generate benzyl in the collision induced decay processes. This mechanism should start with the loss of triethylamine followed by an attack from one of the benzylic arms of the first generation to the ring of the benzyl (or tropylium) cation that immediately forms after the dissociation. After some rearrangements, a neutral fragment that contains an aromatically stabilized ring can be eliminated together with the benzyl cation. The aromaticity in this neutral fragment could be thought as the driving force for this path. In each step a benzyl cation of lower generation is created, all intermediate benzylic cations decay through the same cycle and the process can again be addressed as a cascade fragmentation.

Although the proposed cascade mechanism seems reasonable and is in good agreement with experimental observations, theoretical calculations (DFT) predicts high-energy intermediates and barriers.

2.3.5. In-to-Out S_E^{ar} Cascade Mechanism 2

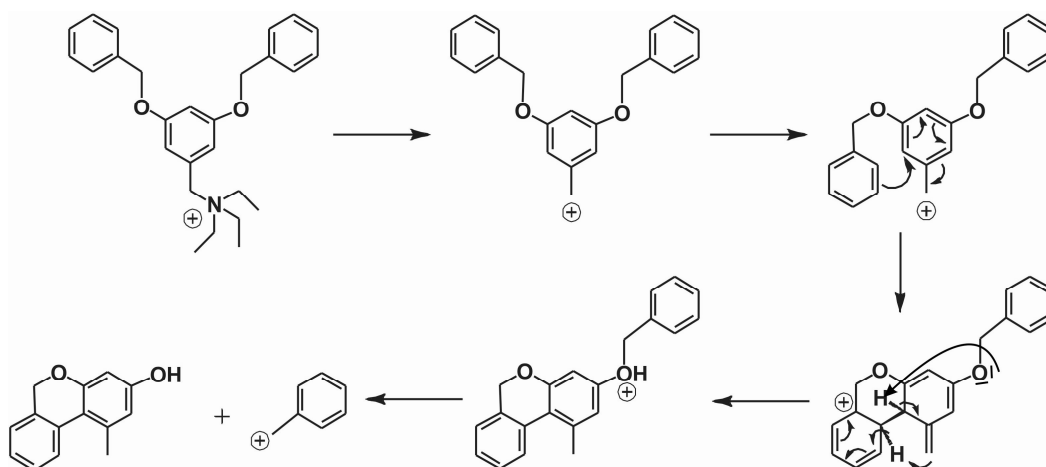


Figure 13. In-to-out cascade mechanism 2 involving an electrophilic aromatic attack and the following rearrangements producing a lower-energy neutral fragment.

In-to-out cascade mechanism may be favored if the rearrangements that take place after the dissociation of triethylamine lead to better-stabilized, lower-energy neutrals. Figure 13 shows how the formed dendritic benzyl cation may rearrange to yield a neutral fragment which is stabilized by the establishment of two aromatic rings. This extra stabilization may provide a way for the dendritic benzylic cations to decay in an energetically favored way until they form the final benzyl cation.

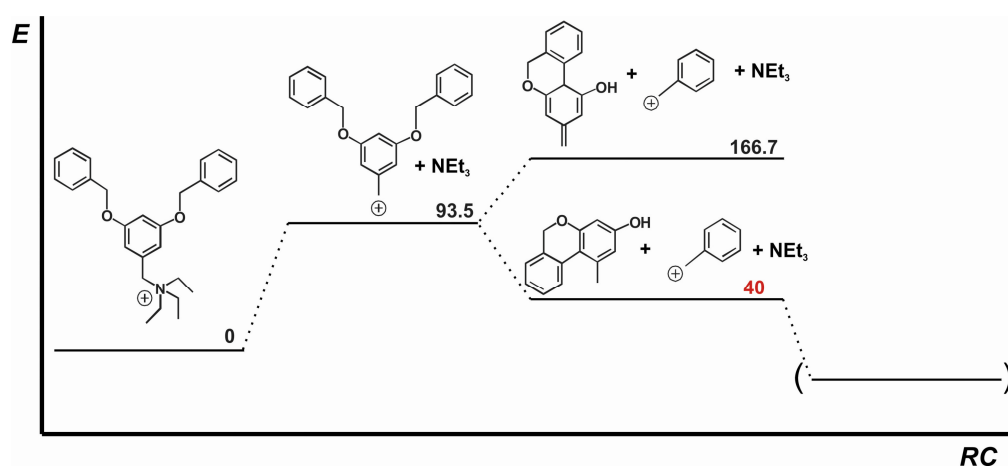


Figure 14. The energies (figures in kcal/mol) of the individual steps in in-to-out cascade mechanisms comparing the energies of two different neutrals that may form after rearrangements.

2.3.6. Investigations on the Mechanism with Different Peripheral Groups

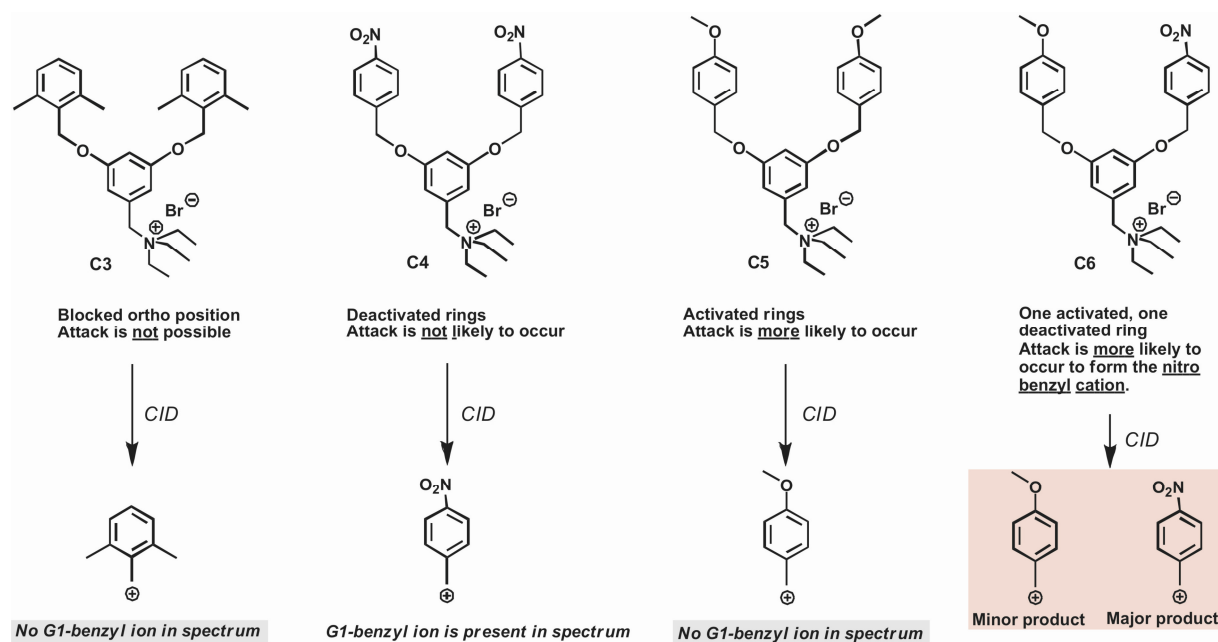


Figure 15. The dendritic compounds having differently substituted peripheral groups, the expected behaviour and summary of the result in CID experiments.

To have better insight to the fragmentation pathway that the dendritic benzyl cations decay, some first generation dendrimers with different peripheral benzyl groups were synthesized using the usual dendrimer syntheses (Experimental Section). The choices of the peripheral groups were made to change the reactivity of the peripheral aromatic ring in electrophilic aromatic attack that is thought to occur in in-to-out-cascade mechanisms. In the first compound, **C3**, the ortho positions of the aromatic ring are blocked to prevent the electrophilic aromatic attack whereas the reactivity is tried to be tuned by the nitro and methoxy substitutions on the ring in compounds **C4** and **C5**. In **C6**, this reactivity difference should give rise to a product ratio of the benzyl cations other than 1.

Interestingly, ortho blocking does not cease the fragmentation. Neither ring activation, nor deactivation affects the formation of the benzylic fragments. Parent dendrimer becomes visible in the CID spectra when deactivating groups are on the peripheral benzyls implying a slow-down in the cascade. As expected, in the unsymmetrically decorated **C6**, leads to different amounts of nitro and methoxy substituted benzyl cations. From these results, it can be concluded that final product stability to determine the fragmentation pattern and thermodynamics governs the whole process.

3. Conclusions

ESI-FTICR mass spectrometry proved useful for the ionization and characterization of dendrimers equipped with Fréchet-type dendrons. Not only the exact masses could be determined, but a sensitive detection of defects is possible without generating additional fragments during the ionization which would complicate the analysis. The benzylic alcohol dendrons were easily detectable in the negative mode by deprotonation and give rise to quite stable hydrogen-bridged dimers. The benzyl bromides are best characterized by addition of a tertiary amine which generates an ammonium ion at the focal point and thus provides the charge necessary for ionization. For doubly charged dendritic viologens, a pronounced effect of the dendron size on the stability of the naked dication in the gas phase was observed.

Collision-induced decay (CID) experiments provided insight into a surprising fragmentation cascade initiated by the loss of the neutral amine. Through several rapid reaction steps of energetically highly favorable rearrangements of the intermediate benzyl cations into tropylium ions and subsequent formation of the benzyl cation of the next lower generation, finally, the peripheral benzyl or 2-naphthylmethyl cations are generated as the most prominent signals in the CID mass spectra. Instead, no signals are observed for the intermediate benzyl or tropylium cations. (This cascade mechanism is particularly fascinating in view of the first name given to dendritic species by Vögtle et al., the so-called “cascadanes”¹⁶¹). The cascade mechanism is also governed by the final product stability e.g. the substitution pattern of the formed benzyl cation, energetically and kinetically.

III. HIERARCHICAL SELF-ASSEMBLY OF METALLO-SUPRAMOLECULAR NANO-SPHERES

1. Purpose of the Study and Introduction

Self-assembly is an attractive bottom-up approach to complex architectures⁶⁶ and nano-materials, because it reduces the synthetic effort and reversibility ensures error correction. A variety of nano-objects, e.g. nanotubes,^{64,69,162} vesicles,^{70,163} or micelles¹⁶⁴ have been prepared (see Part I section 2.4 for broader discussion on self-assembled systems). Vesicles and micelles form *inter alia* from synthetic amphiphilic block copolymers,¹⁶⁵ porphyrin¹⁶⁶ or terpyridine complexes,¹⁶⁷ and β -cyclodextrin inclusion complexes.¹⁶⁸ Liu et al. recently described the vesicle formation from metallo-supramolecular cages.¹⁶⁹ The final result of the self-assembly process depends on 1) the nature of the binding sites and their positions suitably programmed into the building blocks, 2) subunit rigidity, and 3) the environmental conditions. In this part, a novel coordination polymer synthesized by metal-directed self-assembly and their characterization by ESI mass spectrometry and NMR spectroscopy are presented. Evidence for the formation of vesicles from these metallo-supramolecular oligomers comes from (cryogenic) transmission electron microscopy (TEM, cryo-TEM).

2. Results and Discussion

2.1. Synthesis of self-assembled metallo-supramolecular polymers and preparation of metallo-supramolecular nano-spheres and vesicles

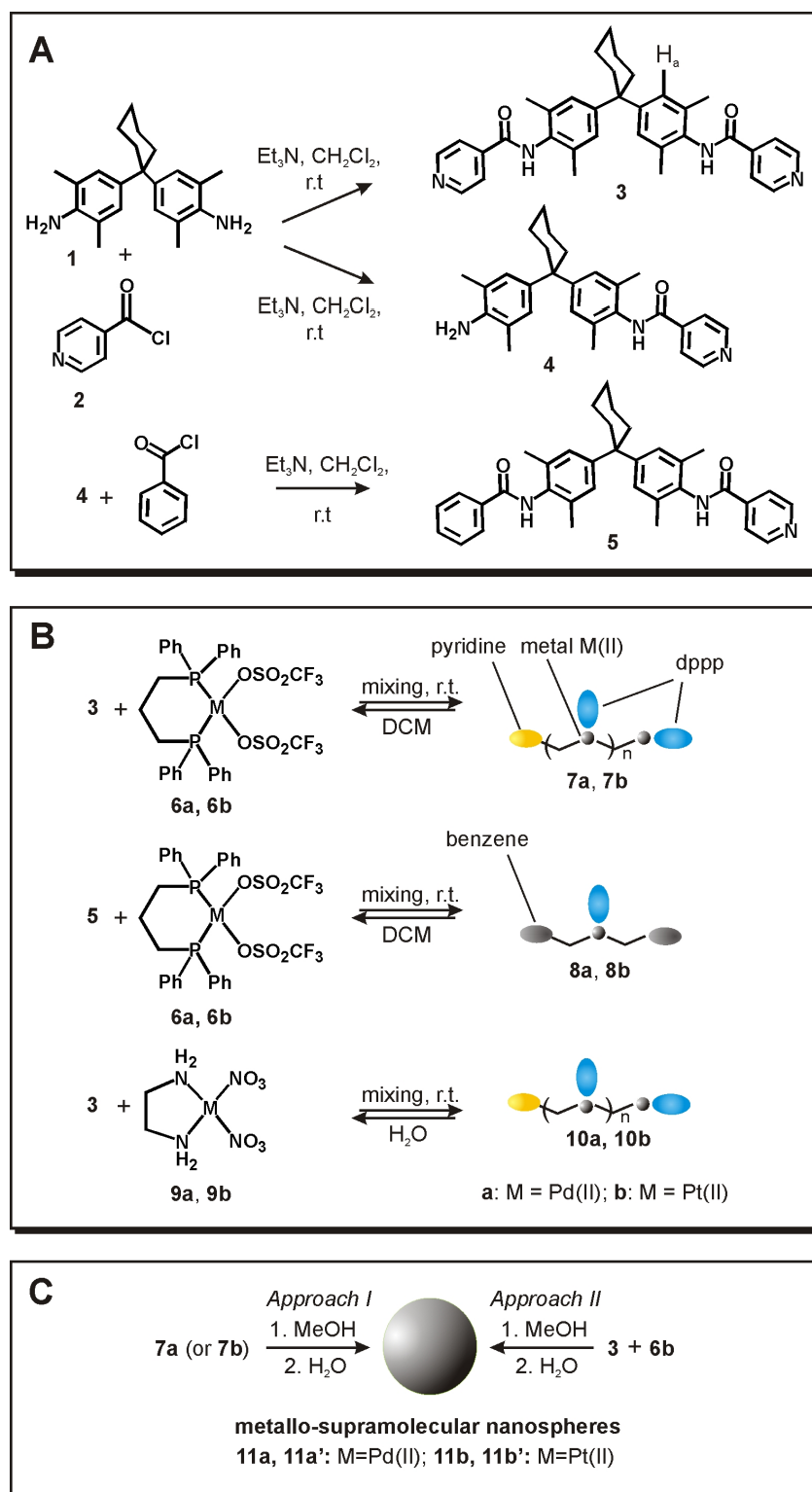


Figure 1. Synthesis of self-assembled metallo-supramolecular polymers and preparation of metallo-supramolecular nano-spheres and vesicles.

Standard amide-bond formation between Hunter's diamine¹⁷⁰ **1** and isonicotinoyl chloride **2** yields the bent bidentate dipyridyl-substituted ligand **3** (Figure 1),¹⁷¹ which bears two diverging coordination sites. For the preparation of coordination polymers,¹⁷² equimolar amounts of the (dppp)M(OTf)₂ precursor complexes (dppp = bis-(diphenylphosphino)-propane, OTf = triflate; M = Pd(II) (**6a**) or M = Pt(II) (**6b**))¹⁷³ and of ligand **3** were mixed in dichloromethane and stirred for 2 hours. Finally, slow addition of diethyl ether to the reaction mixture resulted in white precipitates of **7a** or **7b**, respectively, with yields of 95% and 90%.

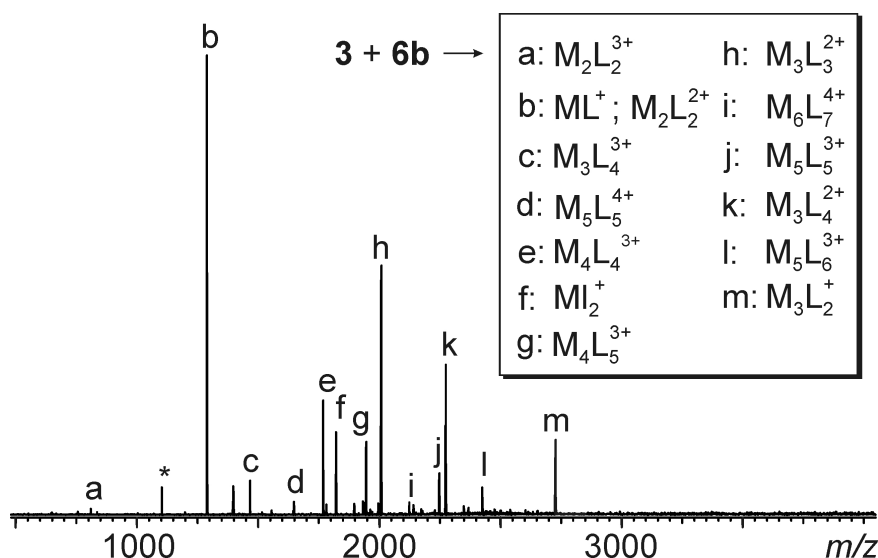


Figure 2: ESI-FTICR mass spectrum of a 150 μ M solution of ligand **3** and metal complex **6b** sprayed from acetone. The asterisk indicates an instrument artifact from stray radiation.

According to molecular modeling, the ligand's curvature is not ideal to form a small macrocycle from 2 corners and 2 ligands and some strain is likely generated upon its formation. Consequently, one might expect to obtain a mixture of coordination oligomers avoiding the strain. This is confirmed by electrospray-ionization Fourier-transform ion-cyclotron-resonance (ESI-FTICR) mass spectrometry⁵⁷: If **7b** is sprayed from acetone, a quite complex mass spectrum is obtained (Figure 2), from which three main conclusions can be drawn: 1) Oligomers are observed up to the $M_6L_7^{4+}$ complex. Assembly formation is thus not restricted to small cycles; 2) All signals except signal "m" in Figure 1 (likely a fragment) either correspond to complexes with the same number of corners and ligands (M:L = 2:2, 3:3, 4:4, 5:5) or they bear one ligand more than metal corners (M:L = 1:2, 2:3; 3:4, 4:5, 5:6, 6:7). The first series can be assigned to cyclic, the second to linear oligomers terminated at both

ends by a ligand - in line with the fact that the second pyridine binds more strongly to the corner than the first^{71u}; 3) Since some fragmentation usually occurs upon ionization¹³⁹, the average oligomer chain length is likely higher in solution than that observed in the mass spectrum.

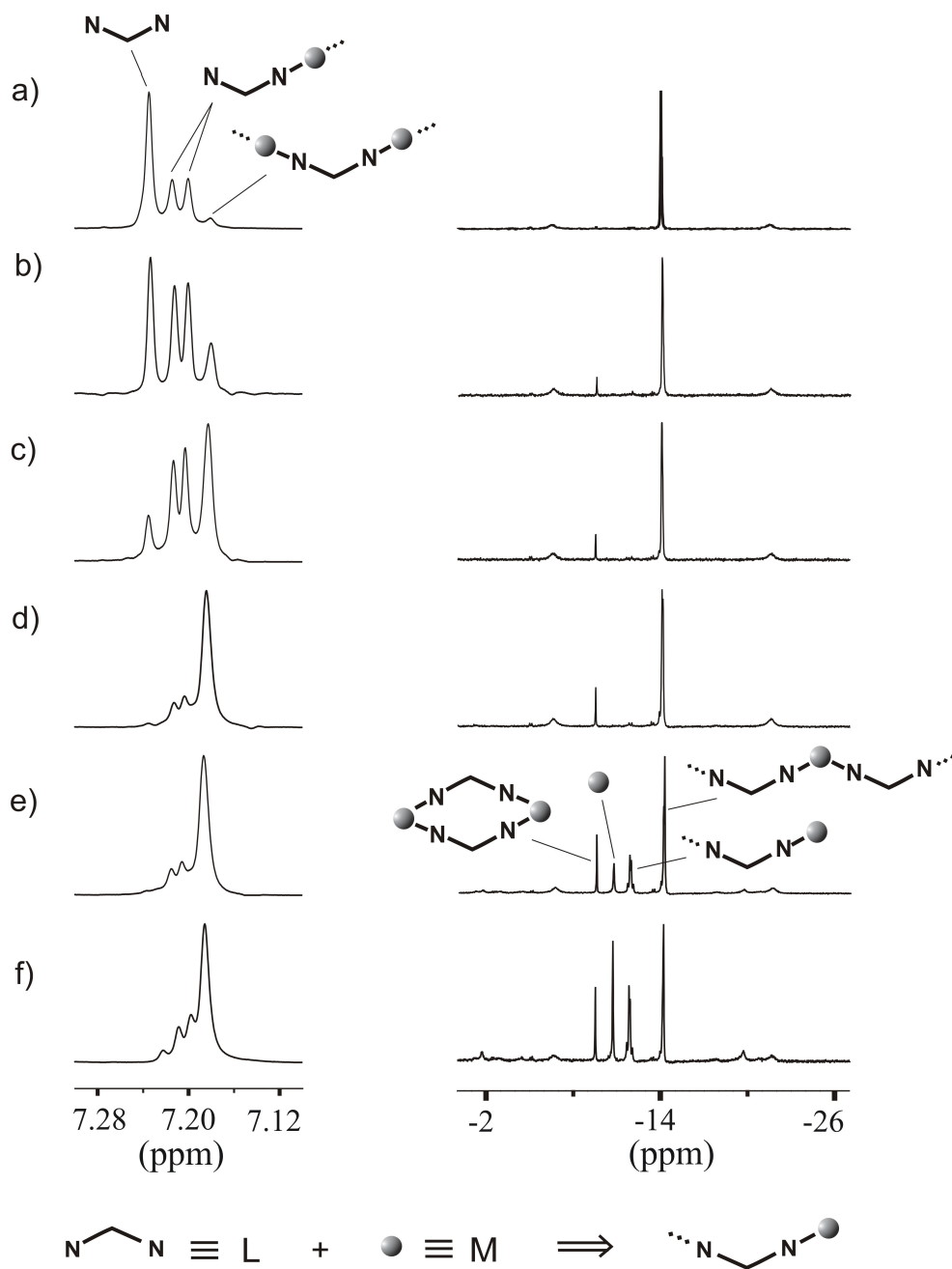


Figure 3. Left: Partial ¹H NMR spectra of mixtures of ligand **3** with increasing amounts of **6b** (a: 0.25, b: 0.50, c: 0.75, d: 1.00, e: 1.50, f: 2.00 equivalents relative to **3**) in [D₇]-DMF at 298 K. Right: ³¹P NMR spectra of the same samples

The mass spectral data is complemented by an NMR titration of corner **6b** into a solution of ligand **3**. Assembly formation can be monitored by following the signal for the aromatic dimethyl aniline C-H proton H_a and that of the P atoms of the corner (Figure 3). At low corner concentrations (Figure 3a), free ligand (1 ¹H NMR signal) is observed next to two signals for singly coordinated and thus unsymmetric ligand (2 signals, 1:1 ratio). All corners are doubly coordinated rendering the P atoms equivalent; only one signal is observed in the ³¹P NMR spectrum. Pyridine coordination is confirmed by a ¹J_{P-Pt} coupling constant of 3041 Hz ((dppp)Pt(OTf)₂ precursor: 3647 Hz). Upon increasing corner concentration, an additional ¹H NMR signal appears which grows to become the major one at a corner: ligand ratio of 1:1. It is a signal for doubly coordinated ligand as appearing in cyclic or along the middle of the chains in linear oligomers. For a corner:ligand ratio of 1:1, all corners are still doubly substituted in line with the mass spectra and binding energies. A small, somewhat strained cyclic 2:2 assembly may be responsible for the additional small peak appearing downfield from the major one in the ³¹P NMR spectrum. If the corner concentration is higher than that of the ligand, singly substituted corners appear as double doublets (the two P atoms at these corners are inequivalent and couple with each other). A singlet for the free corner becomes also visible. Mass spectrometry and NMR spectroscopy thus agree with each other indicating coordination polymers to be formed. In line with earlier data, ligand exchange is fast on the NMR time scale at r.t. for **7a** and only one averaged set of signals is observed.

2.2. Imaging of metallo-supramolecular nano-spheres and vesicles

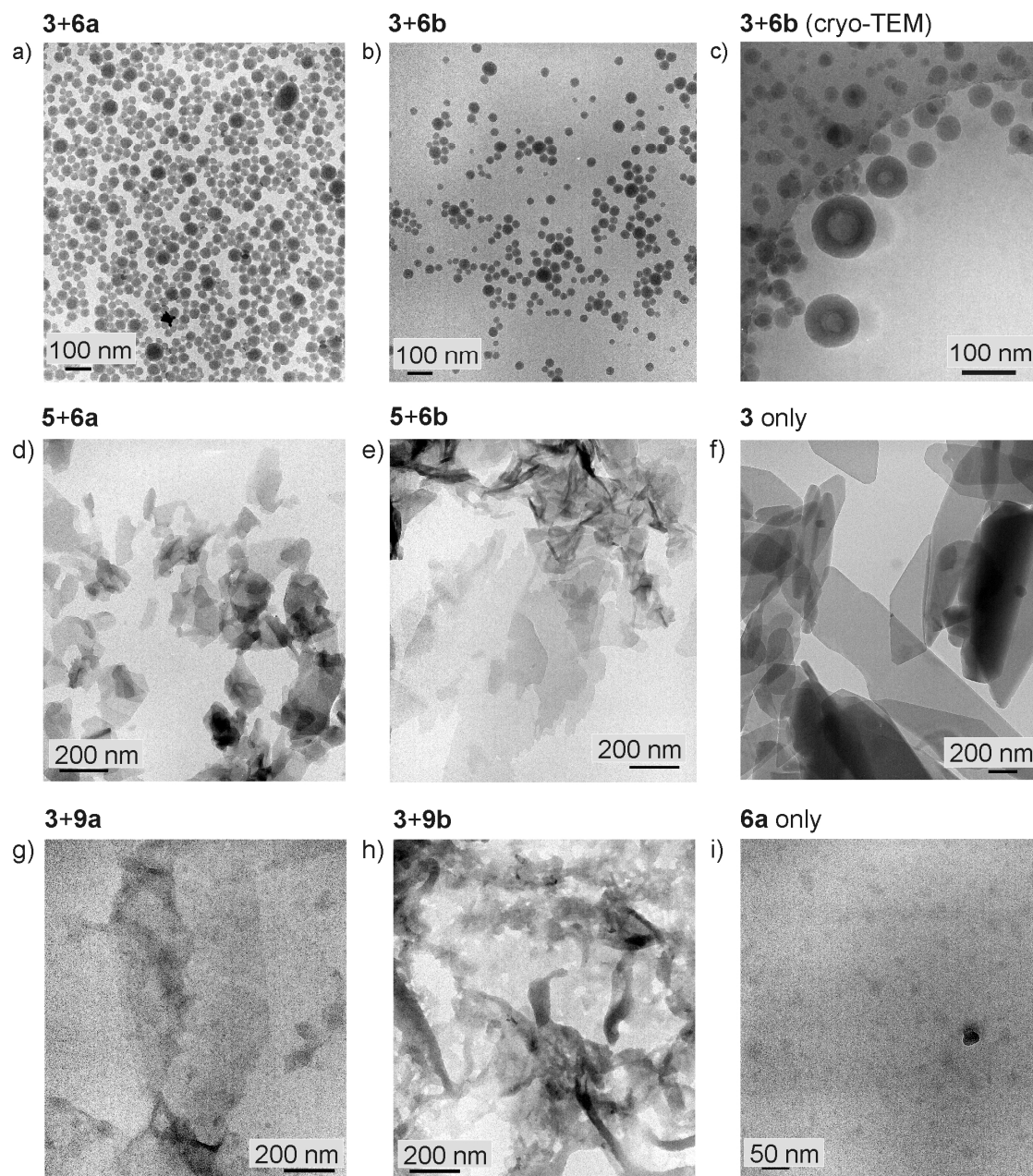


Figure 4. Representative TEM images of a) **9a'** (2 mg/mL) in 40 % MeOH/H₂O after sonication for 15 min; b) **9b'** (1 mg/mL) in 40 % MeOH/H₂O after sonication for 15 min; and c) cryo-TEM image of **9b'** (1 mg/mL) in 40 % MeOH/H₂O after sonication for 15 min. d) - i) Control experiments (all 1 mg/mL of the compounds indicated above the image). For details see text. All of these metallo-spheres were prepared using approach II.

When pre-assembled coordination polymers **7a** or **7b** are dissolved in methanol and heated to 50°C followed by cooling to r.t. and dropwise addition of deionized water, a cloudy suspension is obtained (Figure 1c, approach I). The same happens, when the building blocks are treated in the same way without intermediate isolation of the coordination polymers (approach II). Since we suspected vesicles or micelles to form, TEM images were recorded. After blotting the Pd(II) assemblies on a collodium-coated copper grids surrounded with a carbon-film, the TEM images revealed round-shaped objects to form (Figure 4a). The corresponding Pt(II) complexes form similar objects, which are somewhat smaller in diameter and more homogenous in size (Figure 4b). Sonication of the samples did not change the result much regardless of the metal cation used. A cryo-TEM image (Figure 4c) reveals two different kinds of spherical object to be present: Small ones with diameters of 40 - 50 nm that do not show contrast differences between the interior and the outer shell are completely filled. Much larger nano-spheres with diameters greater than ca. 100 nm have distinctly lower contrast at the center implying the formation of vesicles with wall thicknesses of ca. 40 nm.

The following control experiments have been performed (Figures 4d-i): 1) Ligand **3** alone leads to monolayer formation, when treated the same way. 2) Pt(II) corner **6b** gave much smaller black dots in the TEM images - probably nano-crystals. 3) Metal complexes **8a,b** formed from monodentate ligand **5** result in crystalline mono-layered structures. 4) The use of ligand **3** together with water soluble Fujita-type (en)M(II)(NO₃)₂ metal complexes,¹⁷⁴ (**9a**: M = Pd; **9b**: M = Pt) as the corners did not lead to the formation of round-shaped objects. Consequently, the nano-spheres require a bidentate ligand such as **3** and the use of Stang-type corners **6a,b**. Both building blocks are obviously required and the formation of coordination oligo- or polymers is likely a prerequisite for vesicle formation, because no vesicles are observed with the much shorter 2:1 complexes **8a,b**. The ancillary ligand (dppp vs. en) on the metal center also plays an important role by adjusting solubilities just right for aggregation to occur.

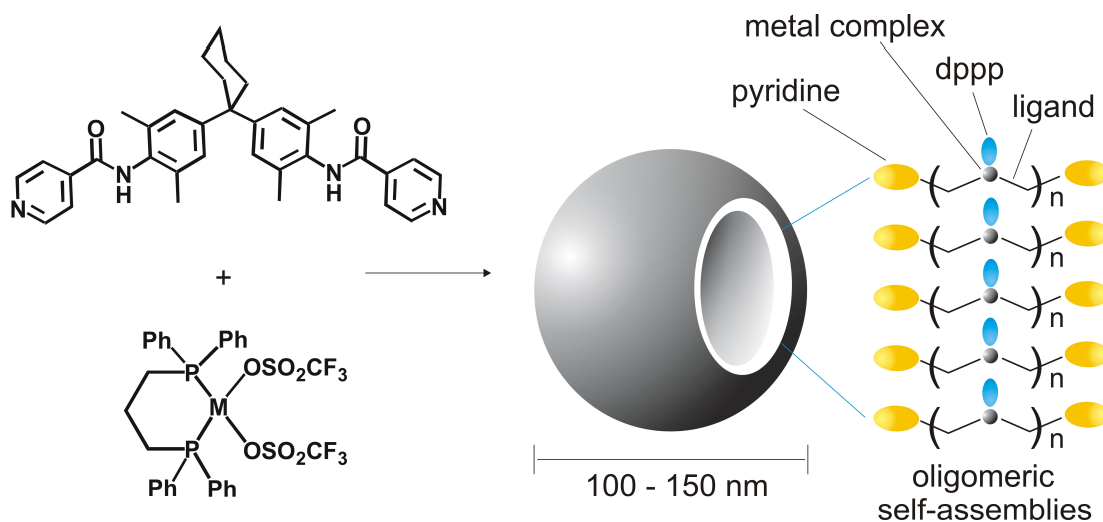


Figure 5. Schematic representation of vesicle formation from self-assembled oligomeric coordination compounds.

Based on these results, we suggest the structural model shown in Figure 5. Coordination oligomers cross the vesicle wall and can be connected among each other by 1) electrostatic interactions between the cationic metal centers and intermittent counter ions, 2) hydrogen bonds between the amide groups,¹⁷⁵ 3) Van-der-Waals and hydrophobic interactions between the backbones.¹⁷⁶ On both ends, the coordination oligomers have basic pyridines which are at least partially protonated and form hydrogen bonds to the surrounding water thus leading to the formation of a wall which is solvated on both sides by water - inside the vesicle and outside.

3. Conclusion and Outlook

An extraordinary formation of a nanovesicle from a coordination polymer was displayed in this part of the study. The characterization by means of different conventional techniques supported by clear TEM images proved the vesicles to which a model of formation was proposed. The future work on these vesicle systems can be concentrated on studying the host-guest properties of them, transportation possibilities and controlled release of guests by disassembly. Decoration of vesicles by functional groups (e.g. on the cyclohexyl chain) may help to improve their intrinsic or non-intrinsic properties like size-distribution, selectivity in guest-binding or straightforward signalling of the binding processes. Moreover, the idea of obtaining vesicles from coordination polymers may be extended to utilization of different ligands making use of properties of these ligands as shown in Figure 6.

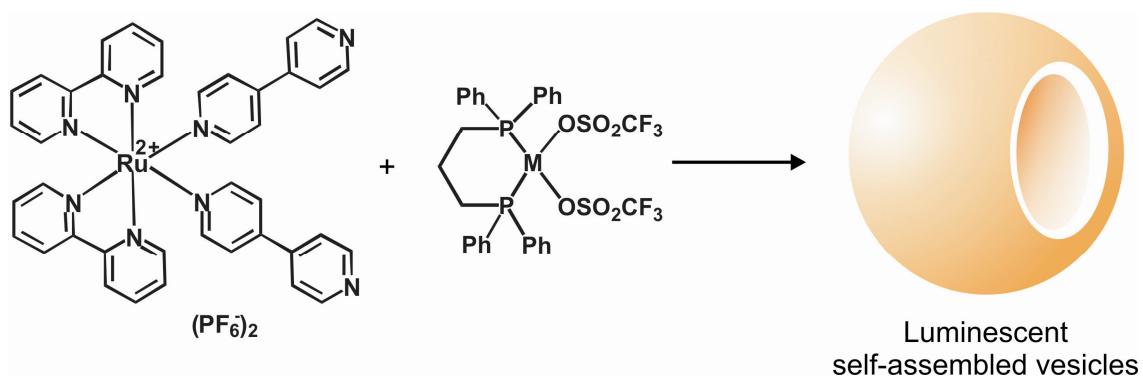


Figure 6. Luminescent vesicles may form through self assembly of “Stang’s corner” and a ligand that itself is a Ru(II) complex.

Experimental

E.1. Analytical Techniques

NMR Spectroscopy

- ¹H NMR: AC 250 and AM 270 SY (250 MHz), AM 400 (400 MHz), AMX500 (500 MHz) Bruker, Analytische Messtechnik GmbH, Karlsruhe, Germany.
- ¹³C NMR: AC 250 and AM 270 SY (250 MHz), Bruker, Analytische Messtechnik GmbH, Karlsruhe, Germany.
- ¹⁹F NMR: AM 400 (470 MHz) Bruker, Analytische Messtechnik GmbH, Karlsruhe, Germany.
- ³¹P NMR: AM 400 (202 MHz) Bruker, Analytische Messtechnik GmbH, Karlsruhe, Germany.

All data are given as δ (ppm) values. ¹H and ¹³C chemical shifts are calibrated with solvent signals or internal standard tetramethylsilane (TMS). ³¹P chemical shifts are provided in ppm relative to external 86% H₃PO₄ (0 ppm). ¹⁹F chemical shifts are reported relative to external CFC₃ (0.00 ppm). The coupling constants, *J* are given in Hertz (Hz). All spectra are measured at room temperature. The following abbreviations were used to express the multiplicities:

- s* Singlet
d Doublet
t Triplet
q Quartet
m Multiplet
br unresolved multiplets

Mass Spectrometry

ESI-FTICRMS: *for PART I.* Samples were measured on an Ionspec QFT-7, Varian Inc., Lake Forest, CA, equipped with a 7 T superconducting magnet and a Micromass Z-Spray ESI-Source, Waters Co., Saint-Quentin, France. Solvent flow rate was adjusted to 4 μ L/min, spray voltage was set to 3.8 kV. All other parameters were adjusted for a maximum abundance of the relative [M+H]⁺ ([M+Cat]⁺ or [M-H]⁺, respectively). *for PART II.* ESI mass spectra were recorded on a Bruker APEX IV Fourier-transform ion-

cyclotron-resonance (FT-ICR) mass spectrometer with an Apollo electrospray ion source equipped with an off-axis 70° spray needle. Typically, acetonitrile served as the spray solvent and 30 – 50 μM solutions of the analytes were used. Analyte solutions were introduced into the ion source with a syringe pump (Cole-Parmer Instruments, Series 74900) at flow rates of ca. 3 - 4 $\mu\text{L}/\text{min}$. Ion transfer into the first of three differential pumping stages in the ion source occurred through a glass capillary with 0.5 mm inner diameter and nickel coatings at both ends. Ionization parameters - some with a significant effect on signal intensities - were adjusted as follows: capillary voltage: -4.1 to -4.4 kV; endplate voltage: -2.8 to -3.5 kV; capexit voltage: +200 to +300 V; skimmer voltages: +8 to +12 V; temperature of drying gas: 200 °C. The flows of the drying and nebulizer gases were kept in a medium range (ca. 10 psi). The ions were accumulated in the instrument's hexapole for 0.5 - 1 s, introduced into the FT-ICR cell, which was operated at pressures below 10^{-10} mbar and detected by a standard excitation and detection sequence. For each measurement 16 to 512 scans were averaged to improve the signal-to-noise ratio.

Tandem MS experiments. For MS/MS experiments, the whole isotope patterns of the ions of interest were isolated by applying correlated sweeps, followed by shots to remove the higher isotopes. After isolation, argon was introduced into the ICR cell as the collision gas through a pulsed valve at a pressure of ca. 10^{-8} mbar. The ions were accelerated by a standard excitation protocol and detected after a 2 s pumping delay. A sequence of several different spectra was recorded at different excitation pulse attenuations in order to get at least a rough and qualitative idea of the effects of different collision energies on the fragmentation patterns.

ESI-TOF: Samples were measured on an Agilent 6210 ESI-TOF, Agilent Technologies, Santa Clara, CA, USA. Solvent flow rate was adjusted to 4 $\mu\text{L}/\text{min}$, spray voltage set to 4 kV. Drying gas flow rate was set to 15 psi (1 bar). All other parameters were adjusted for a maximum abundance of the relative $[\text{M}+\text{H}]^+$.

EI-MS: Samples were measured on a MAT 711, Varian MAT, Bremen. Electron Energy for EI was set to 80 eV unless stated otherwise.

FAB-MS: Samples were measured on a CH-5, Varian MAT, Bremen. Glycol was used as matrix.

Transmission Electron Microscopy

Measurements were carried out using a Philips CM12 instrument operated at 100 kV accelerating voltage. Exposures were made at the low-dose mode ($< 100 \text{ e}/\text{\AA}$). For the cryo-TEM images, the sample preparation procedure was used as described before¹⁷⁷. Briefly, a G-200 mesh copper grid covered with a porous foil was used as obtained from Quantifoil Micro Tools (Jena/Germany). After deposition of the sample, the grid is propelled into liquid ethane (90 K). The vitrified sample is then transferred under liquid nitrogen into the transmission electron microscope. Microscopy was carried out at a temperature of 94 K.

Melting Point

Melting points were obtained with a Büchi-SMP-20 and were not corrected.

E.2. Solvents and Other Chemicals

All solvents were distilled and dried before use by using standard methods. Starting materials (compounds which appear without numbers or reference numbers in the procedures) were purchased from Fluka, Merck, Riedel de Haën, Acros Organics, Lancaster and Aldrich and used without further purification.

For chromatographic separation the following material were used:

Thin Layer Chromatography: TLC aluminium sheets silica gel 60 F₂₅₄, Merck

Aluminium oxide 60 F₂₅₄, neutral, Merck

Column Chromatography: Silica gel 60 (63-100 μm), Merck

Aluminiumoxid S, active neutral, Riedel de Haën

E.3. Abbreviations

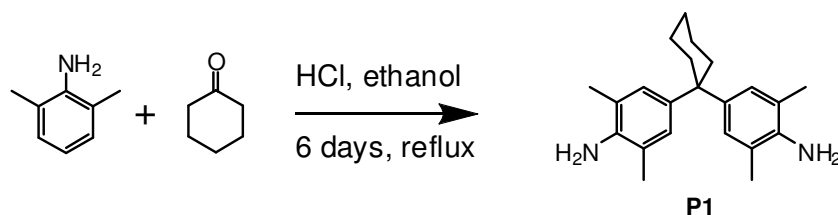
Ar	Aromatic substituent
d	day
conc.	concentration
Cy	cyclohexyl
DMF	<i>N,N</i> -Dimethyl formamide

DMSO	Dimethyl sulfoxide
EI	Electron Ionization
ESI	Electrospray Ionization
FT	Fourier-Transformation
h	hours
HPLC	High performance liquid chromatography
Hz	Hertz
ICR	Ion Cyclotron Resonance
Isophth	isophthalic acid or amide
<i>J</i>	Coupling constant
M ⁺ and M ^{+•}	molecular ion and molecular ion radical
MALDI	Matrix Assisted Laser Desorption/Ionization
MHz	Megahertz
mp.	Melting point
MS	Mass Spectrometry or mass spectrum
NEt ₃	Triethyl amine
NMR	Nuclear Magnetic Resonance
Ph	Phenyl
R _f	retention factor
<i>t</i> -Bu	<i>tert</i> -Butyl
tpy	2,2';6'2"-terpyridine
Trityl	Triphenyl methyl
TLC	Thin Layer Chromatography

E.4. Synthetical Procedures

E.4.1. Preliminary Compounds for the Tool-Box

1,1-Bis(4-amino-3,5-dimethylphenyl)cyclohexane (Hunter's amine) (P1)¹⁷⁸



126 ml 2,6-dimethylaniline, 53 ml cyclohexanone, 84 ml hydrochloric acid (37%) and 15 ml ethanol was refluxed for 6 days. After the reaction was cooled to room temperature 100 ml of

10 M NaOH solution was added to the solution and the basic solution was extracted with dichloromethane. The organic phases were washed with water, dried over MgSO₄ and the solvent was evaporated until only some dichloromethane was left. At this point, 500 ml ethanol was added and the evaporation was continued so that the remaining dichloromethane was fully evaporated. The precipitation of crystals of Hunter's amine could then be seen in the flask at this stage. If not, the flask was left in a fridge overnight for precipitation of Hunter's amine. The precipitate was collected on a large glass filter and washed with fridge-cold ethanol. The filtrate was treated the same way (evaporation, addition of some more ethanol, precipitation, filtration) until there is no appreciable amount of precipitation in the flask. After drying, white or cream colored solid was obtained. Yield: 35-45%. mp= 185°C.

C₂₂H₃₀N₂

322.49 g mol⁻¹

MS (ESI-FTCIR)

m/z (%) = 323.25 (100) [M+H]⁺.

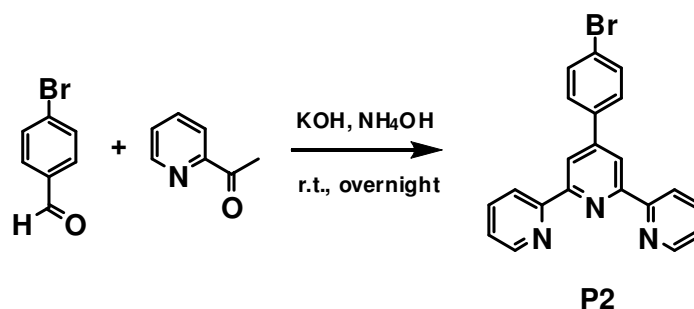
¹H NMR

(250 MHz, CDCl₃) δ [ppm] = 1.5 (br, 6H Cy), 2.2 (s, 12H, CH₃), 2.4 (br, 4H, Cy), 3.5 (br, 4H, NH₂), 6.9 (s, 4H, PhH).

¹³C NMR

(250 MHz, CDCl₃) δ [ppm] = 17.96 (CH₃), 23.00, 26.50, 37.33 (CH₂), 44.41 (C), 121.24, (C_{Ph}), 126.88 (CH_{Ph}), 138.72, 139.76 (C_{Ph}).

4'-(4-bromophenyl)-2,2'-6',2''-terpyridine (P2)¹⁷⁹



4-bromobenzaldehyde (10.6g, 57.0 mmol) was dissolved in 600 ml ethanol. KOH (15.4 g), NH₄OH (340 ml), and 2-acetyl pyridine (24.2g, 0.2 mol) were then added. Stirring was continued overnight. The white solid formed was filtered and dissolved in minimum amount of boiling chloroform and by a pipette slowly added to 300 ml of methanol which was vigorously stirred. The white precipitate so obtained was filtered and dried. Yield: 11.49 g, 52.0%.

C₂₁H₁₄BrN₃

388.26 g mol⁻¹

¹H NMR

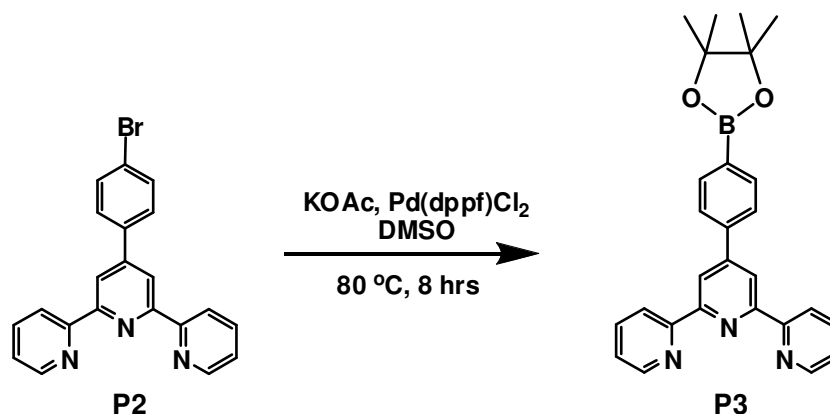
(130 °C) m/z (%) = 386.9 (100) $[M]^{+\bullet}$, 308.2 (59) $[M-Br]^{+\bullet}$.

(400 MHz, CDCl₃): δ [ppm] = 7.27 (dd, J_1 = 8.0 Hz, J_2 = 0.9 Hz, 2H, 5,5''-tpy), 7.57 (d, J = 8.7 Hz, 2H, PhH), 7.70 (d, J = 8.7 Hz, 2H, PhH), 7.82 (dd, J_1 = 8.0 Hz, J_2 = 0.9 Hz, 2H, 4,4''-tpyH), 8.59 (d, J = 8.0, 2H, 6,6''-tpy), 8.63 (s, 2H, 3',5'-tpy), 8.65 (dd, J_1 = 8.0 Hz, J_2 = 0.9 Hz, 2H, 3,3''-tpy).

¹³C NMR

(400 MHz, CDCl₃) δ [ppm] = 118.40, 121.28, 123.85, 128.78, 131.99, 136.81, 137.24, 148.86, 149.03, 155.93.

4'-(4-(4,4,5,5-tetramethyl-2-phenyl-1,3,2-dioxaborolane)phenyl)-2,2'-6',2''-terpyridine (P3) ¹⁷⁹



Potassium acetate (758 mg, 7.72 mmol), bis(pinacolatodiboron) (688 mg, 2.71 mmol), Pd(dppf)Cl₂ (56.6 mg, 17 μmol) and 4'-(4-bromophenyl)-2,2'-6',2''-terpyridine (1 g, 2.58 mmol) were added into argon bubbled DMSO (15 ml). The reaction mixture was stirred at 80 °C for 7 hours. After cooling down to room temperature 100 ml of toluene was added and the mixture was washed 3x200 ml water. Organic phase was dried at vacuo. Yield: 701 mg, 62%.

$$\text{C}_{27}\text{H}_{26}\text{BN}_3\text{O}_2$$
435.33 g mol⁻¹

MS (EI)

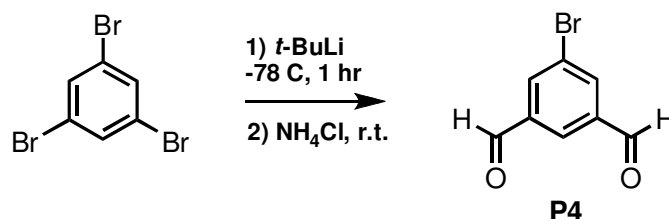
(130 °C) m/z (%) = 434.9 (100) $[M]^{+\bullet}$, 309.2 (7) $[M-(C_6H_{12}BO_2)]^{+\bullet}$.

¹H NMR

(400 MHz, CDCl₃) δ [ppm] = 7.29 (dd, J_1 = 7.9 Hz, J_2 = 1.8 Hz, 2H, 5,5''- tpy), 7.81 (dd, J_1 = 7.9 Hz, J_2 = 1.8 Hz, 2H, 4,4''-tpy), 7.86 (d, J = 5.9 Hz, 2H, PhH), 7.88 (d, J = 5.9 Hz, 2H, PhH), 8.60 (d, J = 7.9 Hz, 2H, 6,6''- tpy), 8.68 (dd, J_1 = 7.9 Hz, J_2 = 1.8 Hz, 2H, 3,3''-tpy), 8.69 (s, 2H, 3',5'-tpy).

^{13}C NMR (250 MHz, CDCl_3) δ [ppm] = 24.87, 83.93, 118.91, 121.39, 123.81, 126.53, 135.32, 136.90, 140.89, 149.03, 150.08, 155.86, 156.12.

5-bromoisophthalaldehyde (P4)¹⁸⁰



To a suspension of tribromobenzene (6.0 g, 19.1 mmol) in 200 ml dry ether was added 1.7 M tert-butyllithium in pentane (50 ml, 85 mmol) under argon atmosphere at -78°C . This mixture was stirred for 1 hour and keeping the temperature constant at -78°C DMF (4.4 ml, 57 mmol) was added. The solution was then allowed to warm to 10°C with stirring. Treating the reaction mixture with aqueous ammonium chloride (10 g) the organic products were extracted with ether. The extracts are combined, washed with brine, dried, filtrated, concentrated and applied on a silica column. Hexane/dichloromethane, 1:1. First band from the column is the mono aldehyde. The dialdehyde was collected as the fourth band, and dried to give a white solid. Yield: 2.0 g, 49 %.

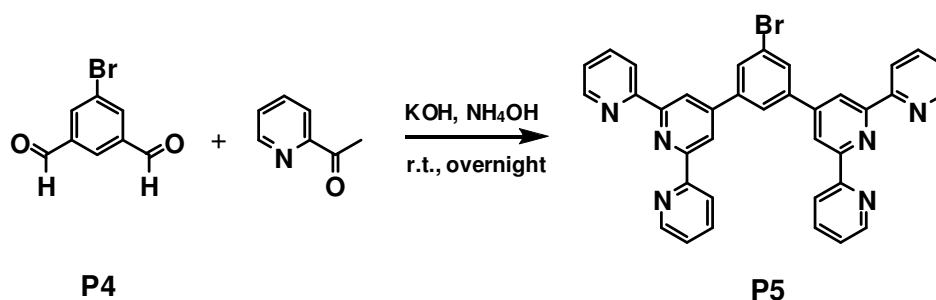
$\text{C}_8\text{H}_5\text{BrO}_2$ 213,03 g mol^{-1}

MS (EI) (40°C) m/z (%) = 212.0 (100) $[\text{M}]^{*+}$.

^1H NMR (250 MHz, CDCl_3) δ [ppm] = 8.23 (d, 2H, 4,6-isophth), 8.27 (t, 1H 2-isophth), 10.03 (s, 2H CHO).

^{13}C NMR (250 MHz, CDCl_3) δ [ppm] = 124.57 (5-isophth), 129.42 (2-isophth), 137.36 (4,6-isophth), 138.62 (1,3-isophth), 189.68 (CHO).

1-bromo 3,5-bis(2,2'-6',2''-terpyridine)benzene (P5)¹⁸¹



Step-wise procedure: 5-bromoisophthalaldehyde **P4** (1 g, 4.7 mmol) was dissolved in ethanol and 2-acetyl pyridine (2.53 g, 20.8 mmol) was added, followed after 2 min by aqueous NaOH (8.7 ml, 1M). After the solution was stirred at room temperature for 24 hours, the solvent was evaporated in vacuo and the oily substance left was added some water and extracted with dichloromethane. Collected extracts were washed with water as mentioned in the literature. However, this dissolves all the compound and there was nothing left in the organic phase. With basic extraction the intermediate was extracted into organic phase which was evaporated to yield an orange-brown solid. This solid was added then ammonium acetate (17 g) and glacial acetic acid (87 ml) and refluxed for 4 hours. After neutralization with Na₂CO₃ solution, greenish precipitate formed was washed with dichloromethane and the filtrate was evaporated and dried. Yield: 1.9 g, 65%.

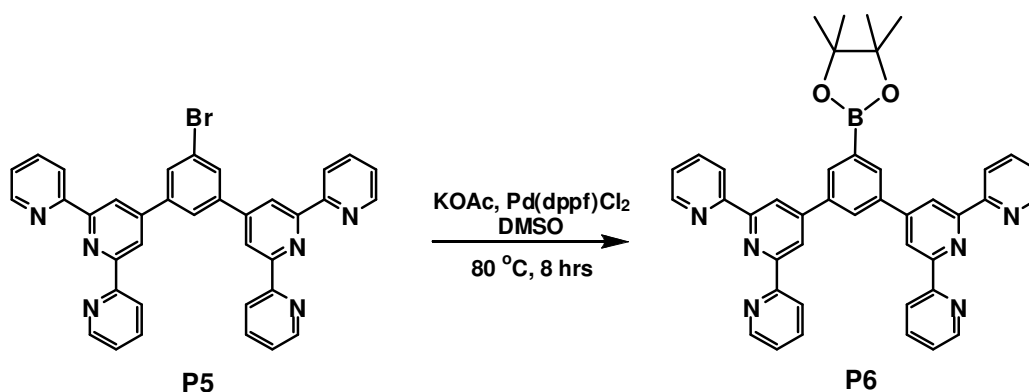
C₃₆H₂₃BrN₆ 619.51 g mol⁻¹

MS (EI) (220 °C) *m/z* (%) = 620.2 (81.4) [M]^{•+}, 540.3 (100) [M-Br]^{•+}.

¹H NMR (250 MHz, CDCl₃) δ [ppm] = 7.33 (dd, *J* = 6 Hz, 4H, 5,5''-tpy), 7.83 (dd, *J* = 8 Hz, 4,4''-tpy), 8.07 (s, 2H, 2,6-PhH) 8.31 (s, 1H, 4-PhH), 8.64 (d, *J* = 8 Hz, 4H, 3,3''-tpy), 8.70 (d, *J* = 5 Hz, 4H, 6,6''-tpy), 8.74 (s, 4H, 3',5'-tpy).

1-(4,4,5,5-tetramethyl-2-phenyl-1,3,2-dioxaborolane) benzene (P6)

3,5-bis(2,2'-6',2''-terpyridine)



Potassium acetate (56.9 mg, 0.579 mmol), bis(pinacolatodiboron) (51.6 mg, 0.203 mmol), Pd(dppf)Cl₂ (9.6 mg, 11.6 μmol) and 1-bromo 3,5-bis(2,2'-6',2''-terpyridine)benzene P5 (120 mg, 0.194 mmol) were added into argon bubbled DMSO (5 ml). The reaction mixture was stirred at 80 °C for 8 hours. After cooling down to room temperature 50 ml of toluene was added and the mixture was washed 3x100 ml water. Organic phase was dried at vacuo. Yield: 124 mg, 32%.

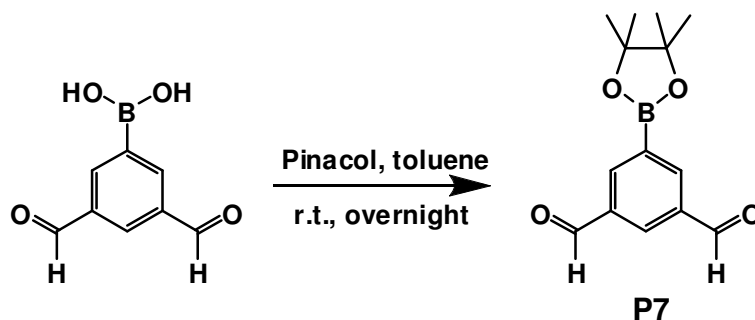
C₄₂H₃₅BrN₆O₂

666.58 g mol⁻¹

¹H NMR

(250 MHz, CDCl₃) δ [ppm] = 7.34 (dd, *J* = 6 Hz, 4H, 5,5''-tpy), 7.88 (dd, *J* = 8 Hz, 4,4''-tpy), 8.35 (s, 2H, 2,6-PhH) 8.39 (s, 1H, 4-PhH), 8.68 (d, *J* = 8 Hz, 4H, 3,3''-tpy), 8.70 (d, *J* = 5 Hz, 4H, 6,6''-tpy), 8.90 (s, 4H, 3',5'-tpy).

5-(4,4,5,5-tetramethyl-1,3,2-dioxaborolan-2-yl)isophthalaldehyde (P7)



3,5-diformylphenylboronic acid (531 mg, 2.98 mmol) was stirred with pinacol (355 mg, 3.03 mmol) in diethyl ether overnight and room temperature. (If any solid was still left, then it was filtered, and filtrate was taken). Solvent was evaporated and compound was dried well at vacuo. Yield quantitative.

C₁₄H₁₇BO₄

260.09 g mol⁻¹

MS (EI)

(40 °C) *m/z* (%) = 260.2 (79.8) [M]^{•+}, 245.3 (87.9) [M-CH₃]^{•+}.

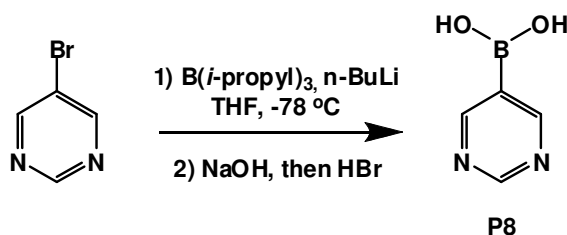
¹H NMR

(250 MHz, CDCl₃) δ [ppm] = 1.33 (s, 12H, CH₃), 8.40 (d, *J* = 1.9 Hz, 1H, 4-PhH), 8.49 (d, *J* = 1.9 Hz, 2H, 2,6-PhH), 10.07 (s, 2H, CHO).

¹³C NMR

(250 MHz, CDCl₃) δ [ppm] = 24.65, 84.51, 131.91, 136.16, 141.14, 191.00.

Pyrimidine-5-boronic acid (P8)¹⁸²



To a solution of 5-bromopyrimidine (5.50g, 34 mmol) and triisopropyl borate in 70 ml of THF, n-BuLi was added dropwise at -78 °C. The mixture was stirred for 4 hrs at -78 °C. Then 10 ml of water was added and the reaction was allowed to stir overnight at room temperature.

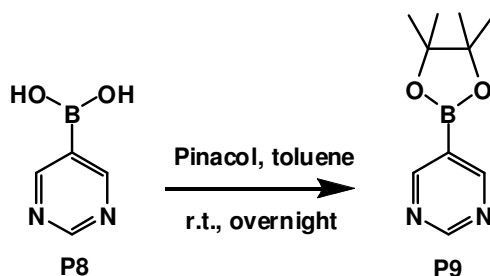
The organic solvents were removed in vacuo and the aqueous layer was added 5% NaOH solution to adjust the pH to 10. The organic impurities were removed by extracting into diethyl ether. The pH of the aqueous layer was then adjusted to 4 with HBr (48%) to precipitate the compound as white solid. Yield: 1.7 g, 40%.

C₄H₅BN₂O₂ 123,91 g mol⁻¹

MS (ESI-FTICR) m/z (%) = [M+H]⁺ (100) 125.0517.

¹H NMR (250 MHz, DMSO-d₆) δ [ppm] = 9.23 (s, 1H), 9.15 (s, 2H), 8.63 (s, 2H, OH).

5-(4,4,5,5-tetramethyl-2-phenyl-1,3,2-dioxaborolane)pyrimidine (P9)



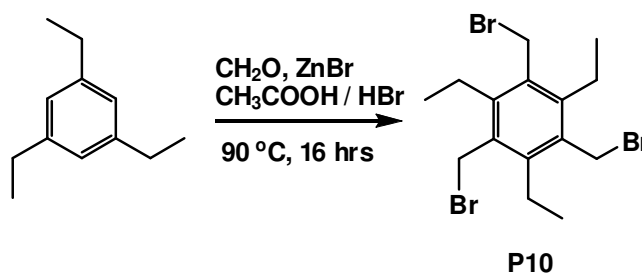
Obtained through the general pinacol ester synthesis from the boronic acid. Yield quantitative.

C₁₀H₁₅BN₂O₂ 206,05 g mol⁻¹

¹H NMR (250MHz, CDCl₃): δ [ppm] = 1.33 (s,12H), 8.99 (s, 2H), 9.24 (s, 1H).

¹³C NMR (250 MHz, CDCl₃): δ [ppm] = 24.65, 84.72, 159.99, 160.02, 162.40.

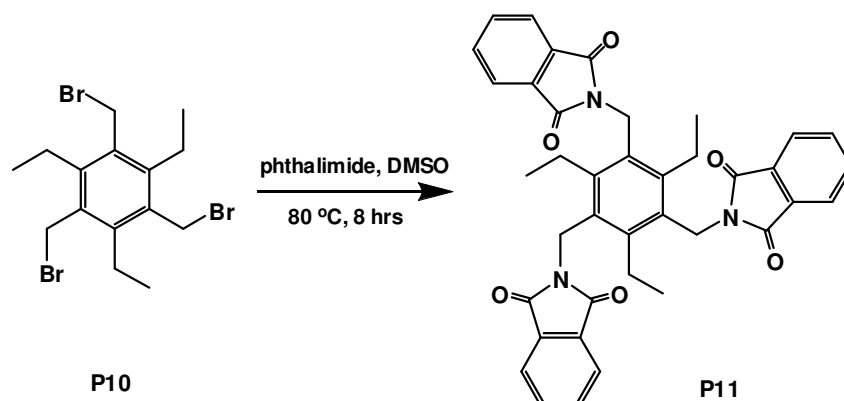
1,3,5-Tris(bromomethyl)-2,4,6-triethylbenzene (P10)¹⁸³



To the mixture of paraformaldehyde (6.7 g) and triethylbenzene (4 ml) in HBr/CH₃COOH (40 ml 30 wt%), zinc bromide (7.9 g, 6.9 mmol) was added slowly at room temperature. The mixture was heated for 16 hrs at 90 °C. White crystals that were formed were collected, washed with water and dried under vacuo to yield the product. Yield: 72%

C₁₅H₂₁Br₃	441,04 g mol ⁻¹
MS (EI)	<i>m/z</i> (%) = 439.9 (9) [M] ^{•+} , 360.9 (100) [M-Br] ^{•+} .
¹H NMR	(250 MHz, CDCl ₃) δ [ppm] = 4.56 (br, 6H), 2.92 (q, <i>J</i> = 7.3 Hz, 6H), 1.32 (t, <i>J</i> = 7.3 Hz, 9H).
¹³C NMR	(250 MHz, CDCl ₃) [ppm] = 15.40, 22.52, 28.34, 132.45, 144.79.

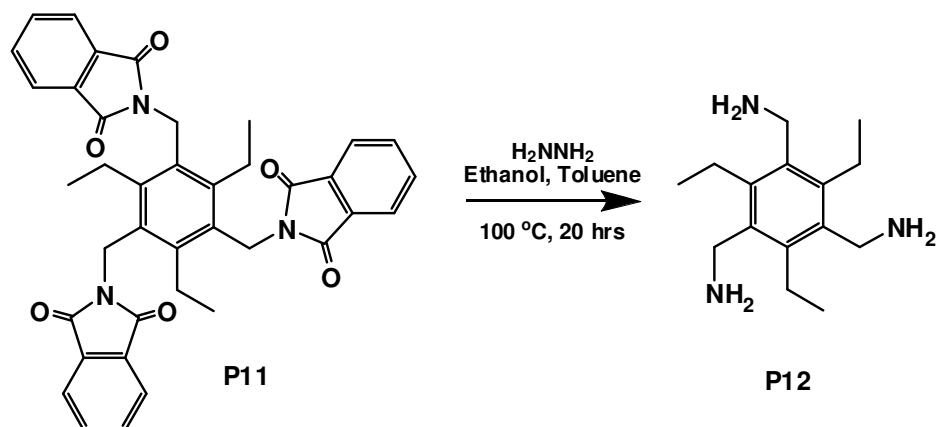
1,3,5-Tris(phthalimidomethyl)-2,4,6-triethylbenzene (P11)¹⁸⁴



1,3,5-Tris(bromomethyl) 2,4,6-triethylbenzene **P10** (2.5 g, 5.65 mmol) and phthalimide (4.2 g, 22.7 mmol) were mixed in dry DMSO and the reaction mixture was stirred at 80 °C for 8 hrs. After cooling to room temperature the solution was added water and extracted with dichloromethane, dried over sodium sulfate and concentrated at vacuo. The solid was applied on a column of silica, eluting with hexane/ethyl acetate (1:1). The first band was collected and dried. Yield: 24% (only the soluble part was columned) m.p. 236-238 °C.

C₃₉H₃₃N₃O₆	639,70 g mol ⁻¹
¹H NMR	(250 MHz, CDCl ₃) δ [ppm] = 7.80-7.64 (AA'BB' system, 12H), 4.93 (br, 6H), 3.06 (q, <i>J</i> = 7.3 Hz, 6H), 0.94 (t, <i>J</i> = 7.3 Hz, 9H).

1,3,5-Tris(aminomethyl)-2,4,6-triethylbenzene (P12)^{142e}



To a suspension of phthalimide derivative **P11** (320 mg, 0.5 mmol) in ethanol/toluene 2:1, (12 mL) hydrazine hydrate (0.1 mL, 3.08 mmol) was added at room temperature under argon atmosphere. The reaction was refluxed at 100 °C for 20 hrs during which a white solid was formed. This solid was dissolved in 40%, 80 mL KOH solution and extracted with chloroform (3x100 mL). Combined organic phases were dried over MgSO_4 and evaporated. Remaining pale yellow solid was dried at vacuo. Yield: 74% m.p. 138-140 °C.

$\text{C}_{15}\text{H}_{27}\text{N}_3$

249,39 g mol⁻¹

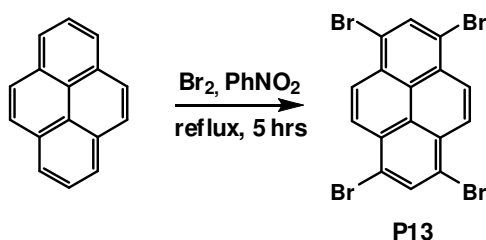
^1H NMR

(250 MHz, CDCl_3) δ [ppm] = 3.79 (br, 6H), 2.72 (q, J = 7.5 Hz, 6H), 2.27 (br, 6H), 1.15 (t, J = 7.5 Hz, 9H).

^{13}C NMR

(250 MHz, CDCl_3) δ [ppm] = 140.6, 137.1, 39.4, 22.7, 16.9.

1,3,6,8-tetrabromopyrene (P13)¹⁸⁵



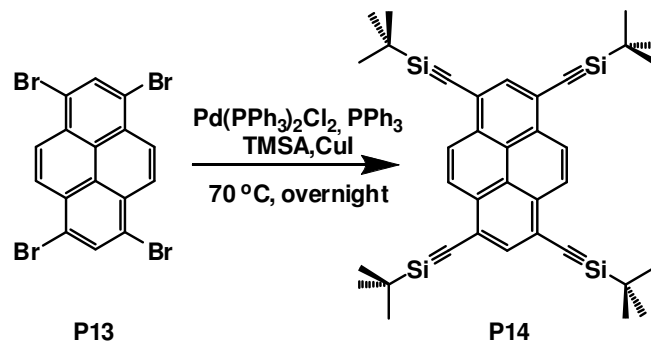
Pyrene (1 g, 4.9 mmol) in nitrobenzene (20 mL) was added dropwise bromine (3.5 g, 0.022 mol) with vigorous stirring. After 5 hrs, precipitated product was filtered and washed with ethanol. The light green product dried at high vacuum is insoluble in all common organic solvents and used without further purification. Yield quantitative. The compound was insoluble in the common organic solvents thus NMR spectra could not be obtained. Yield: 92%.

$\text{C}_{16}\text{H}_6\text{Br}_4$

517,83 g mol⁻¹

MS (EI) m/z (%) = 517.8 (100) $[M]^{\bullet+}$, 437.8 (28) $[(M-Br)]^{\bullet+}$, 357.9 (34) $[(M-2Br)]^{\bullet+}$.

1,3,6,8-tetra(trimethylsilylethynyl)pyrene (P14)¹⁸⁵



In a degassed solution of triethyl amine (20 ml) and dry THF (20 ml) 1,3,6,8-tetrabromopyrene **P13** (1g, 1.93 mmol), CuI (72.0 mg, 0.38 mmol), Pd(PPh₃)₂Cl₂ (267 mg, 0.380 mmol) and PPh₃ (199 mg, 0.760 mmol) were heated at 70⁰C overnight under argon. After the solvent was evaporated, crude product was applied on a silica column and eluted with hexane. The fluorescent band was collected and dried to yield the bright orange solid. Yield: 732 mg, 65%.

C₃₆H₄₂Si₄

587,06g mol⁻¹

¹H NMR

(250 MHz, CDCl₃) δ [ppm] = 0.37 (s, 36H), 8.27 (s, 2H), 8.53 (s, 4H).

¹³C NMR

(250 MHz, CDCl₃) δ [ppm] = -0.11, 100.16, 102.60, 118.38, 126.70, 131.75, 134.27.

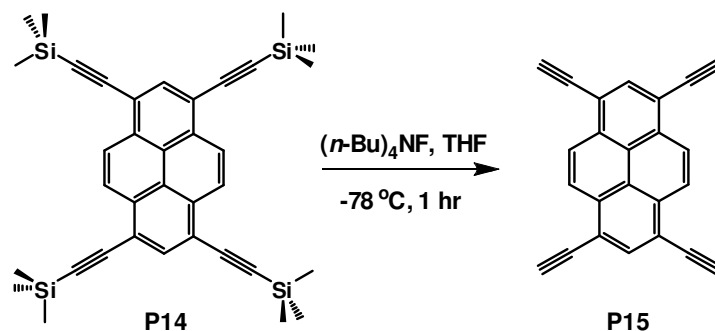
IR

(cm⁻¹) (C≡C) 2959.34.

MS (EI)

m/z (%) = 585.9 (100) $[M]^{\bullet+}$, 571 (15) $[(M-CH_3)]^{\bullet+}$, 490.0 (47) $[(M-C_5H_8Si)]^{\bullet+}$.

1,3,6,8-tetraethynylpyrene (P15)¹⁸⁶



To a solution of tetra(trimethylsilylacetylene)pyrene **P14** (200 mg, 0.34 mmol) in 8 ml degassed THF at -78 °C, tetra(n-butyl)ammonium fluoride (0.34 ml, 0.34 mmol) dissolved in 1 ml degassed THF was added dropwise under argon. After stirring for 1 hr at -78 °C, water was added and after warming the solution to room temperature, the mixture was extracted with dichloromethane, the organic layers were combined, washed with brine and dried over magnesium sulfate. After evaporation of the solvent, a yellow substance was obtained in 79% yield.

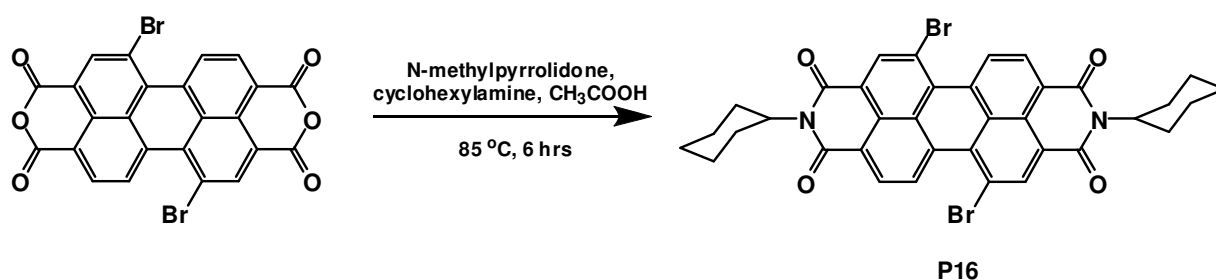
C₂₄H₁₀ 298.34 g mol⁻¹

¹H NMR (250 MHz, CDCl₃) δ [ppm] = 4.32 (s, 4H), 8.36 (s, 2H), 8.70 (s, 4H).

IR (cm⁻¹) (C≡CH) 3280.65.

MS (EI) *m/z* (%) = 298.1 (100) [M]⁺.

1,7-dibromoperylene-3,4,9,10-tetracarboxylic acid cyclohexylbisimide (**P16**)¹⁸⁷



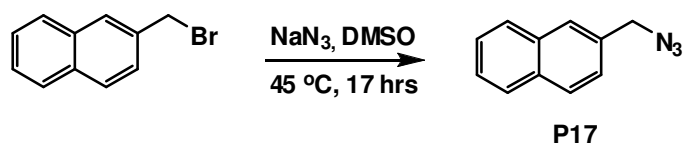
To a mixture of 1,7-dibromoperylene-3,4,9,10-tetracarboxylic dianhydride (3.95 g, 7.18 mmol) in 48 ml of N-methylpyrrolidone and 2.0 ml acetic acid, cyclohexylamine (2.2 ml, 19 mmol) was added dropwise with stirring. The mixture was heated under argon at 85 °C for 6 hrs. After cooling to room temperature, the precipitate was filtered, washed with methanol and dried at 100 °C under vacuum. The dried solid was applied on a silica column eluting with CH₂Cl₂. The orange-red solid was obtained after the evaporation of the light orange band with yellow fluorescence. 350 mg of substance was obtained from the purest fraction.

C₃₆H₂₈Br₂N₂O₄ 712.43 g mol⁻¹

MS (EI) *m/z* (%) = 712.1 (28) [M]⁺.

¹H NMR (250 MHz, CDCl₃) δ [ppm] = 1.15-1.95 (m, 12H, Cy), 2.43-2.60 (m, 8H, Cy), 4.89-5.05 (m, 2H, Cy), 8.60 (d, *J* = 8.3 Hz, 2H, Ar), 8.81 (s, 2H, ArH), 9.40 (d, *J* = 8.3 Hz, 2H, Ar).

2-(azidomethyl)naphthalene (P17)



2-(bromomethyl)naphthalene (1.1 g, 5 mmol) and sodium azide (2.6 g, 40 mmol) was heated in dry DMSO under argon atmosphere at 45 °C for 17 hrs. After cooling down to room temperature, 200 ml of water was added and the product was extracted into 3x100 ml dichloromethane. Combined organic phases was dried with MgSO₄, filtered and evaporated. A low-melting, solid was obtained. mp. 46-49 °C. Yield: 97%.

C₁₁H₉N₃ 183,21 g mol⁻¹

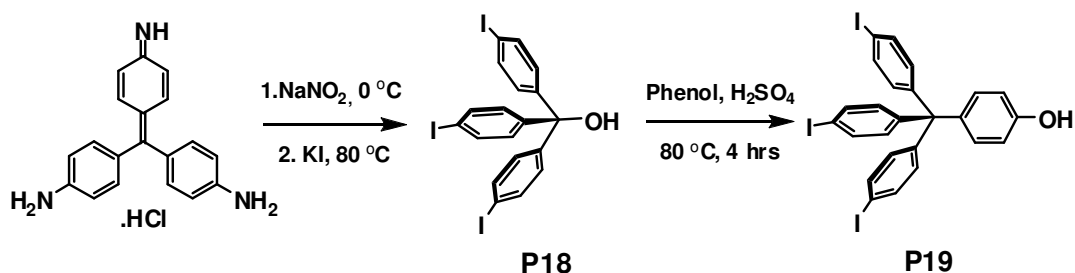
MS (EI) (30 °C) *m/z* (%) = 183.2 (66.6) [M]^{•+}, 141.2 (100) [M-N₃]^{•+}, 154.2 (47.8) [M-N₂]^{•+}.

¹H NMR (250 MHz, CDCl₃) δ [ppm] = 4.46 (s, 2H, CH₂), 7.40 (d, 3H, Ar_{naph}), 7.45- 7.53 (m, 6H, Ar_{naph}), 7.74 (s, 3H, Ar_{naph}), 7.81- 7.86 (m, 9H, Ar_{naph}).

¹³C NMR (400 MHz, CDCl₃) δ [ppm] = 55.06, 125.98, 126.46, 126.58, 127.27, 127.86, 128.06, 128.85, 128.86, 125.87, 132.93, 133.17, 133.34.

E.4.2. Stoppers syntheses

4-(tris(4-iodophenyl)methyl)phenol (P19)¹⁸⁸



Step 1: Parafuchsin hydrochloride (1.77 g, 5.46 mmol) in 10 ml water was added concentrated sulfuric acid (4 ml) and the mixture was cooled to 0 °C. A solution of sodium nitrite (1.24 g, 18 mmol) in 4 ml of water was added to the solution dropwise and the stirring was continued for 1 hr additional. Potassium iodide (10 g, 60 mmol) dissolved in 10 ml of water was then added and the reaction was first let to room temperature and then kept at 80 °C for 2 hours. The dark purple precipitate formed was filtered, washed with water and dried.

Column chromatography on silica gel eluting with dichloromethane yielded the pure product. $R_f = 0.8$. Yield: 2.80 g., 82%.

C₁₉H₁₃I₃O

638,02 g mol⁻¹

¹H NMR

(250 MHz, CDCl₃) δ [ppm] = 6.88 (d, $J = 8.7$ Hz, 6H), 7.54 (d, $J = 8.7$ Hz, 6H).

¹³C NMR

(250 MHz, CDCl₃) δ [ppm] = 81.6, 94.0, 129.9, 137.6, 145.8.

Step 2: Tris-(4-iodophenyl)-methanol **P18** obtained in the first step (5 g, 7.84 mmol) and phenol (4 g, 43 mmol) was added 10 drops of sulfuric acid and stirred under argon for 4 hours at 80 °C. After cooling down to room temperature 50 ml sodium hydroxide solution (10%) was added and the precipitate formed was filtered. Column chromatography on silica gel eluting with petroleum ether/ ethylacetate (5:1) yielded the pure product. $R_f = 0.7$. Yield: 4.25 g, 76%.

C₂₅H₁₇I₃O

714,12 g mol⁻¹

MS (EI)

(220 °C) m/z (%) = 714.3 [M]^{•+} (74), 511.2 [M-PhI]^{•+}

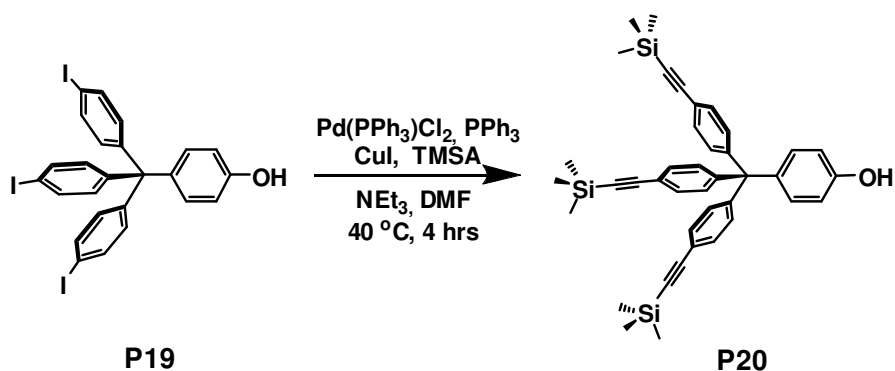
¹H NMR

(250 MHz, CDCl₃) δ [ppm] = 6.61 (d, $J = 8.8$ Hz, 2H), 6.82 (d, $J = 8.8$ Hz, 2H), 6.86 (d, $J = 8.6$ Hz, 6H), 7.60 (d, $J = 8.6$ Hz, 6H).

¹³C NMR

(250 MHz, CDCl₃) δ [ppm] = 62.9, 91.6, 114.3, 130.9, 132.2, 134.8, 136.1, 145.6, 155.3.

4-(tris(4-((trimethylsilyl)ethynyl)phenyl)methyl)phenol (**P20**)¹⁸⁸



Tris-(4-iodophenyl)-methylphenol **P19** (2.3 g, 3.22 mmol), trimethylsilylacetylene (2.75 ml, 19.5 mmol), bis(triphenylphosphine)palladium(II)dichloride (371 mg, 0.53 mmol) and

triphenylphosphine (338 mg, 1.29 mmol) was dissolved in 20 ml dry DMF and 90 ml dry triethylamine. The reaction mixture was kept at 40 °C for 4 hours. After all the solvent was evaporated at vacuum the residue was applied on a silica column eluting with petroleum ether/ ethyl acetate (5:1). R_f = 0.6 Yield: 0.8 g, 40%.

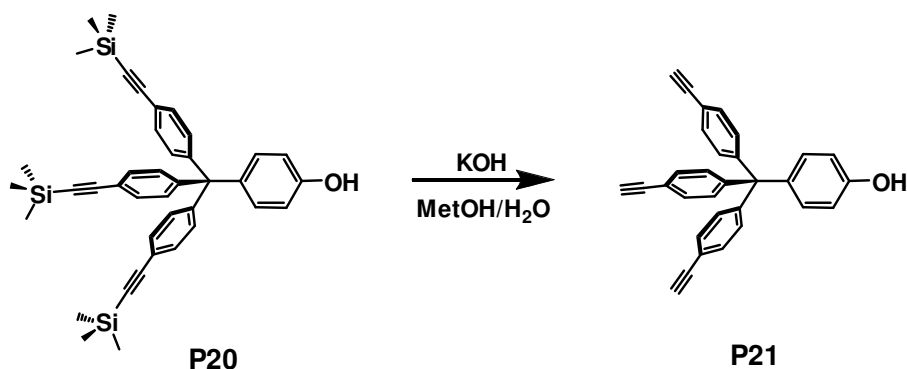
C₄₀H₄₄OSi₃ 625,03 g mol⁻¹

MS (EI) (220 °C) m/z (%) = 624.3 (100) [M]^{•+}.

¹H NMR (250 MHz, CDCl₃) δ [ppm] = 0.00 (s, 27H, CH₃), 4.77 (br, 1H, OH), 6.46 (d, J = 8.8 Hz, 2H), 6.71 (d, J = 8.8 Hz, 2H), 6.83 (d, J = 8.6 Hz, 6H), 7.10 (d, J = 8.6 Hz, 6H).

¹³C NMR (250 MHz, CDCl₃) δ [ppm] = 0.00, 64.2, 94.6, 104.8, 114.6, 121.0, 130.8, 131.3, 132.2, 137.8, 146.7, 153.9.

4-(tris(4-ethynylphenyl)methyl)phenol (P21)



4-(tris(4-((trimethylsilyl)ethynyl)phenyl)methyl)phenol **P20** (154 mg, 0.245 mmol) and potassium hydroxide (138 mg, 2.46 mmol) was stirred in a mixture of methanol and water (1:1) overnight. The mixture was neutralized by a few drops of HCl (conc) and the compound was extracted into dichloromethane, dried over MgSO₄, filtered and the solvent was evaporated. Yield: 85.4 mg, 85%. (When necessary, a short silica column was employed to further purification of the compound, eluting with dichloromethane).

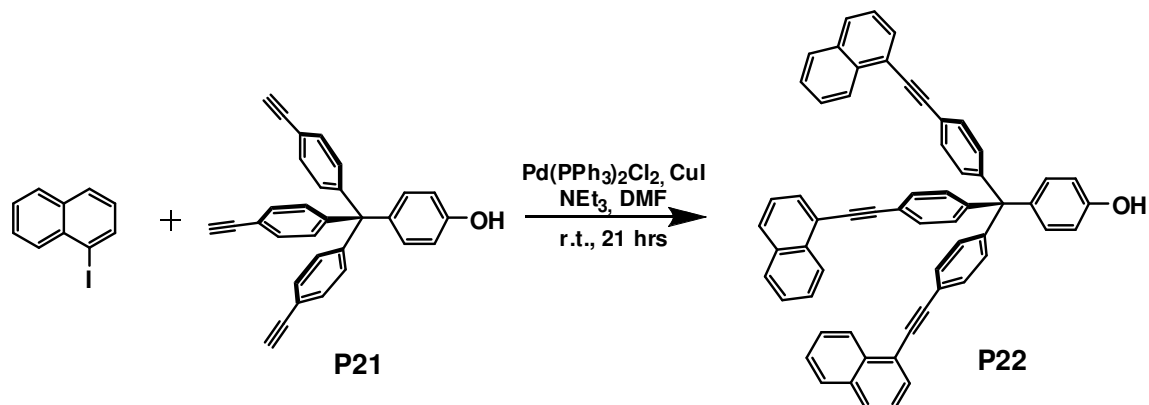
C₃₁H₂₀O 408,49 g mol⁻¹

MS (ESI-FTICR) m/z (%) = 407.15 (100) [M-H]⁻, 815.30 (5) [2M-H]⁻.

¹H NMR (250 MHz, CDCl₃) δ [ppm] = 3.05 (s, 3 H), 6.64 (d, J = 9 Hz, 2H, Ph_{phenol}), 6.85 (d, J = 9 Hz, 2H, Ph_{phenol}), 7.04 (d, J = 8.3 Hz, 2H, PhH), 7.28 (d, J = 8.3 Hz, 2H, PhH).

^{13}C NMR (400 MHz, CDCl_3) δ [ppm] = 64.24, 83.39, 99.98, 114.75, 120.07, 130.87, 131.58, 132.19, 137.64, 147.02, 154.09.

4-(tris(4-(naphthalen-1-ylethynyl)phenyl)methyl)phenol (P22)



4-(tris(4-ethynylphenyl)methyl)phenol **P21** (98 mg, 0.24 mmol), 1-iodonaphthalene (198 mg, 0.78 mmol), copper iodide (28.5 mg) and $\text{Pd(PPh}_3)_2\text{Cl}_2$ (35 mg) in 10 ml DMF was added dry NEt_3 (10 ml) and the reaction mixture was stirred under argon for 21 hrs by which time the reaction was complete. The solvents were evaporated at vacuum and the residue was applied on a silica column eluting with dichloromethane. The product was obtained after excess iodonaphthalene (first band) as the second band from the column. $R_f = 0.7$. Yield: 56 %.

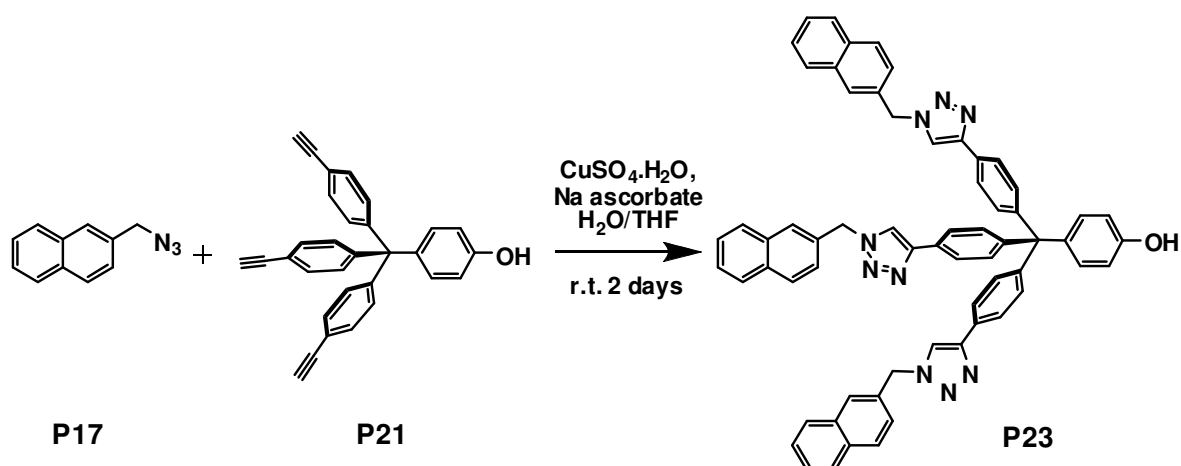
$\text{C}_{61}\text{H}_{38}\text{O}$ 786,95 g mol^{-1}

MS (EI) (300 $^\circ\text{C}$) m/z (%): 786.3 (32) $[\text{M}]^{+\bullet}$.

^1H NMR (250 MHz, CDCl_3) δ [ppm] = 6.77 (d, 2H, $J = 8.3$ Hz, $\text{PhH}_{\text{phenol}}$), 7.12 (d, $J = 8.3$ Hz, 2H, $\text{PhH}_{\text{phenol}}$), 7.30 (d, $J = 9$ Hz, 6H, PhH), 7.42-7.62 (m, 9H, Ar_{naph}), 7.74-7.88 (m, 9H, Ar_{naph}), 8.43 (d, $J = 7.7$ Hz, 3H, PhH).

^{13}C NMR (400 MHz, CDCl_3) δ [ppm] = 64.44, 87.92, 94.16, 114.84, 120.95, 121.35, 125.39, 126.30, 126.54, 126.90, 128.42, 128.89, 130.49, 131.09, 131.15, 132.30, 133.29, 133.36, 137.90, 146.84, 154.20.

4-(tris(4-(1-(naphthalen-2-ylmethyl)-1H-1,2,3-triazol-4-yl)phenyl)methyl)phenol (P23)



2-(azidomethyl)naphthalene **P17** (143 mg, 0.78 mmol), 4-(tris(4-ethynylphenyl)methyl)phenol **P21** (100 mg, 0.245 mmol), copper sulfate pentahydrate (1.84 mg, 7.35 μmol) and sodium ascorbate (7.28 mg, 36.8 μmmol) were stirred in THF/H₂O (1:1) at room temperature for 2 days by which time the reaction mixture became clearer and dispersed product mixture separated from the aqueous phase as a yellow liquid by letting the suspension wait without stirring. The product is extracted into 20 ml dichloromethane, washed well with 2x50 ml water, dried with MgSO₄, filtered and evaporated. The yellow residue was applied on a silica column and eluted first with pure dichloromethane to remove the impurities. Then the eluent was changed to CH₂Cl₂/MeOH (1:1) to obtain the product. Yield: 88%.

C₆₄H₄₇N₉O

958,12 g mol⁻¹

MS (ESI-TOF)

$m/z = 958.41 [\text{M}+\text{H}]^+, 980.39 [\text{M}+\text{Na}]^+$.

¹H NMR

(250 MHz, CDCl₃) δ [ppm] = 5.60 (s, 6H, CH₂), 6.55 (d, 2H, $J=9$ Hz, PhH_{phenol}), 6.87 (d, $J=9$ Hz, 2H, PhH_{phenol}), 7.11 (d, $J=8.3$ Hz, 6H, PhH), 7.24 (d, 3H, Ar_{naph}), 7.37- 7.43 (m, 6H, Ar_{naph}), 7.48 (d, $J=8.3$ Hz, 6H, PhH), 7.63 (s, 3H, CH), 7.65 (s, 3H, Ar_{naph}), 7.68-7.74 (m, 9H, Ar_{naph}).

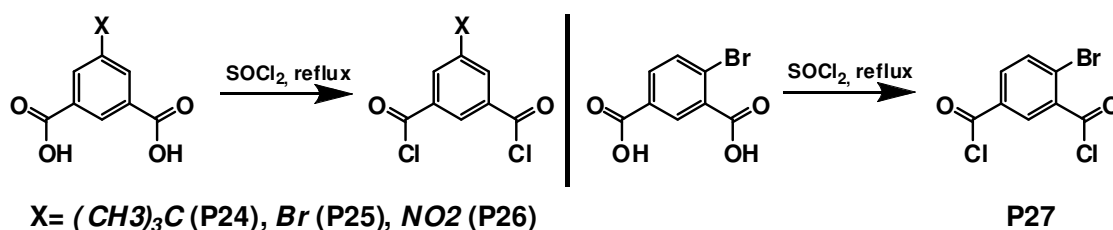
¹³C NMR

(250 MHz, CDCl₃) δ [ppm] = 54.40, 63.9, 120.26, 124.86, 125.16, 126.71, 127.32, 127.72, 127.89, 129.13, 131.38, 131.86, 131.96, 133.16, 133.19, 137.03, 147.04, 147.81.

E.4.3. Functionalized Macrocycles, Catenanes and Rotaxanes through Coupling Reactions

General procedure for isophthaloyl dichloride synthesis¹⁸⁹

Corresponding isophthalic acids (3 g) were refluxed with a large excess of SOCl_2 and one drop of DMF for 8 hours. The acid chlorides were obtained as a yellow liquid after evaporation of the thionyl chloride. And purified as given in separate procedures.



5-*tert*-butyl isophthaloyl dichloride hydrochloride (P24)

The compound was recrystallized from few milliliters of petroleum ether. Obtained colorless crystals were dried at high vacuum. Yield: 80-85%.

5-bromo isophthaloyl dichloride hydrochloride (P25)

Obtained liquid was carefully dried at high vacuum with heating at 40°C and used without further purification. Yield: quantitative.

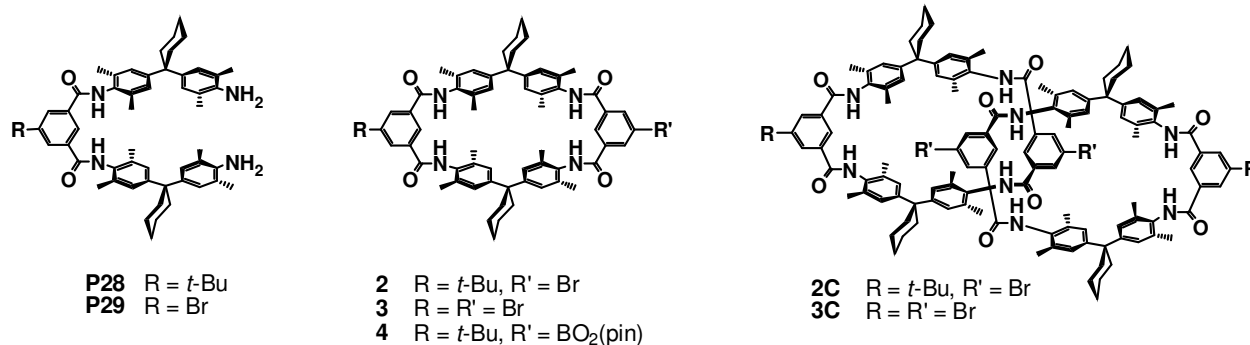
5-nitro isophthaloyl dichloride hydrochloride (P26)

Obtained solid was carefully dried at high vacuum with heating at 40°C and used without further purification. Yield: quantitative.

4-bromo isophthaloyl dichloride hydrochloride (P27)

Obtained liquid was carefully dried at high vacuum with heating at 40°C and used without further purification. Yield: quantitative.

Synthesis of precursor macrocycles



5-bromo-*N,N'*-Bis[4-{1'-(4''-amino-3'',5''-dimethylphenyl)cyclohexyl}-2,6-dimethylphenyl] isophthalic acid amide (P29)

A solution of 1,1-bis(4'-amino-3',5'-dimethylphenyl)cyclohexane (11.0 g, 0.034 mol) in dry dichloromethane (150 ml) and triethylamine (2 ml) was placed in a 250 ml flask. After purging the solution with argon for 5 minutes, with vigorous stirring at room temperature, 5-bromo isophthalic acid dichloride hydrochloride **P25** (1.6 g, 5.7 mmol, 0.9 ml) dissolved in 6 ml of dry dichloromethane was then added in six portions via a syringe over 1 hour. After stirring overnight, solvents were evaporated under reduced pressure. The residue was subjected to column chromatography on silica eluting with dichloromethane/ethyl acetate (76:8). 3.11 g of white product was obtained. Yield: 64%.

C₅₂H₆₁BrN₄O₂ 853,97 g mol⁻¹

MS (ESI-FTICR) m/z (%) = 853.90 (100) [M+H]⁺.

¹H NMR (400 MHz, DMSO-d₆) δ [ppm] = 1.46 (br, 12H, Cy), 2.04 (s, 12 H, PhCH₃), 2.12 (s, 12H, PhCH₃), 2.19 (br, 8H, Cy), 4.30 (br, 4H, NH₂), 6.75 (s, 4H, PhH), 6.98 (s, 4H, PhH), 8.28 (s, 2H, 4,6-isophth), 8.47 (s, 1H, 2-isophth), 9.84 (s, 2H, NH).

¹³C NMR (400 MHz, DMSO-d₆) δ [ppm] = 18.60, 18.88 (CH₃); 23.06, 26.36, 36.90 (CH₂); 122.15, 126.48, 126.62, 134.97 (CH); 44.49, 120.88, 126.39, 132.14, 133.06, 135.59, 137.34, 141.61, 148.59 (Cq) 163.62 (CO).

11'-bromo-29'-*tert*-butyl-5',17',23',35',38',40',43',45'-octamethyldispiro[cyclohexan-1,2'-7',15',25',33'-tetraazaheptacyclo[32.2.2.2.^{3',6'}.2^{16',19'}.2^{21',24'}.1^{9',13'}.1^{27',31'}] hexatetraconta-3',5',9',11',13'(44'),16',18',21',23',27',29',31'(39'),34',36',37',40',42',45'-octadecaen-20',1''-cyclohexan]-8',14',26',32'-tetraon, "bromo macrocycle" (2)¹⁹⁰

A solution of 5-*tert*-butyl isophthalic acid chloride **P28** (0.26 g, 1 mmol) in dry dichloromethane (250 ml) and a mixture of 2 and triethylamine (2 ml) in dry dichloromethane (250 ml) were simultaneously added dropwise to dry dichloromethane (1200 ml) by an automatic solvent pump over 12 hours, while the system was kept under argon atmosphere. The blurry solution was then stirred at room temperature overnight. The solvent was subsequently evaporated under reduced pressure. The residue was subjected to column on silica eluting with a mixture of dichloromethane, ethyl acetate first 15:1 to elute the catenane

which forms as a by-product and then using 6:1. The macrocycle was obtained as a white solid from the second fraction. $R_f = 0.83$. Yield: 20%

C₆₄H₇₁BrN₄O₄	1040,18 g mol ⁻¹
¹H NMR	(400 MHz, DMSO-d ₆) δ [ppm] = 1.36 (s, 9H, CH ₃), 1.46-1.67 (br, 12H, Cy), 2.08 (s, 12H PhCH ₃), 2.09 (s, 12H PhCH ₃), 2.32 (br, 8H, Cy), 7.01 (s, 8H, PhH), 8.05 (s, 2H, 4,6-(<i>t</i> -Bu isophth), 8.15 (s, 2H, 4,6-(bromo isophth), 8.39 (s, 1H, 2-(<i>t</i> -Bu isophth), 8.52 (s, 1H, 2-bromo isophth), 9.16 (s, 2H, NH), 9.36 (s, 2H, NH).

11',29'-dibromo-5',17',23',35',38',40',43',45'-octamethyldispiro[cyclohexan-1,2'-7',15',25',33'-tetraazaheptacyclo[32.2.2.2^{3',6'}.2^{16',19'}.2^{21',24'}.1^{9',13'}.1^{27',31'}]hexatetraconta-3',5',9',11',13'(44'),16',18',21',23',27',29',31'(39'),34',36',37',40',42',45'-octadecaen-20',1''-cyclohexan]-8',14',26',32'-tetraon, “dibromo macrocycle” (3)

Same as 2. Bromo extended diamine P29 was used in the reaction. After the solvent was evaporated, the residue was subjected to column by column chromatography on silica gel eluting with a mixture of dichloromethane/ethyl acetate (5:1). $R_f = 0.88$. 159 mg of white solid was obtained. Yield, 15%.

C₆₀H₆₂Br₂N₄O₄	1062,97 g mol ⁻¹
MS (ESI-FTICR)	m/z (%) = 1061.33 (100) [M+H] ⁺ .
¹H NMR	(400 MHz, DMF-d ₆) δ [ppm] = 1.48-1.69 (br, 12H, Cy), 2.24 (s, 24H PhCH ₃), 2.37 (br, 8H, Cy), 7.21 (s, 8H, PhH), 8.40 (s, 4H, 4,6-isophth), 8.71 (s, 1H, 2- <i>t</i> -Bu isophth), 8.52 (s, 1H, 2-bromo isophth), 9.16 (s, 2H, NH), 9.36 (s, 2H, NH).
¹³C NMR	(400 MHz, DMSO-d ₆) δ [ppm] = 14.31, 18.99, 19.35, 31.9, 45.35, 60.77, 70.50, 72.53, 122.35, 126.63, 132.61, 133.17, 135.45, 137.39, 147.35, 163.64.

10'-bromo-29'-tert-butyl-5',17',23',35',38',40',43',45'-octamethyldispiro[cyclohexan-1,2'-7',15',25',33'-tetraazaheptacyclo[32.2.2.2^{3',6'}.2^{16',19'}.2^{21',24'}.1^{9',13'}.1^{27',31'}]hexatetraconta-3',5',9',11',13'(44'),16',18',21',23',27',29',31'(39'),34',36',37',40',42',45'-octadecaen-20',1''-cyclohexan]-8',14',26',32'-tetraon, "3-bromomacrocycle" (2')

Synthesis is same as for the macrocycle 2. 4-bromo isophthalic acid was used in the reaction. After the solvent was evaporated, the residue was subjected to column by column chromatography on silica gel eluting with a mixture of dichloromethane, ethyl acetate (5:1). R_f = 0.88. 159 mg of white solid was obtained. Yield: 29%.

C₆₄H₇₁BrN₄O₄	1040,18 g mol ⁻¹
MS(ESI-TOF) ¹⁹¹	m/z = 1039.46 [M-H] ⁻ .
MS(ESI-TOF)	m/z = 1063.46 [M+Na] ⁺ , 1079.43 [M+K] ⁺ .
¹H NMR	(250 MHz, CDCl ₃ + CD ₃ OD) δ [ppm] = 1.37 (s, 9H, CH ₃), 1.47-1.58 (br, 12H, Cy), 2.08 (s, 6H, CH ₃), 2.13 (s, 18H, CH ₃), 2.26-2.38 (s, 8H, Cy), 6.83 (s, 2H, Ph), 6.88 (s, 2H, Ph), 6.91 (s, 2H, Ph), 6.96 (s, 2H, Ph), 7.68 (d, J = 6.25 Hz, 1H, 5-bromo isophth), 7.81 (d, J = 6.25 MHz, 1H, 6-bromo isophth), 7.93 (s, 1H, 2-isophth), 8.11 (s, 1H, 2-isophth), 8.18 (s, 2H, 4,6- <i>t</i> -Bu isophth).
¹³C NMR	(250 MHz, CDCl ₃ + CD ₃ OD) δ [ppm] = 13.9, 18.7, 20.7, 22.7, 26.1, 29.4, 30.6, 30.8, 31.0, 35.1, 35.7, 36.2, 44.9, 45.2, 60.2, 122.4, 122.9, 126.1, 126.3, 126.4, 126.7, 128.5, 128.6, 129.2, 130.4, 130.8, 131.0, 131.1, 131.3, 134.3, 134.6, 136.7, 146.7, 147.8, 147.9, 149.0, 153.5, 162.4, 164.4, 164.9, 165.2, 165.4, 171.0.

11'-tert-butyl-29'-(4,4,5,5-tetramethyl-2-phenyl-1,3,2-dioxaborolane)-5',17',23',35',38',40',43',45'-octamethyldispiro[cyclohexan-1,2'-7',15',25',33'-tetraazaheptacyclo[32.2.2.2^{3',6'}.2^{16',19'}.2^{21',24'}.1^{9',13'}.1^{27',31'}]hexatetraconta-3',5',9',11',13'(44'),16',18',21',23',27',29',31'(39'),34',36',37',40',42',45'-octadecaen-20',1''-cyclohexan]-8',14',26',32'-tetraon, "boronic ester macrocycle" (4)

Bromo macrocycle **2** (360 mg, 0.345 mmol), bispinacolato diboron (92.4 mg, 0.362 mmol), PddppfCl₂ (14.1 mg, 0.0173 mmol) and well-dried potassium acetate (101.7 mg, 1.035 mmol) was added to dried and argon bubbled 10 ml DMSO. The mixture was kept at 80 °C overnight

under argon atmosphere. After cooling to room temperature 20 ml CH₂Cl₂ and 20 ml of water were added and the product is extracted into the organic phase which was washed well three times with 20 ml of water. The separated organic phase was dried in vacuo and the residue was examined with TLC. Showing no starting bromo macrocycle on the TLC plate, the residue was applied on a 10 cm silica column and eluted with dichloromethane/ ethyl acetate, 1:1. The only band was collected and dried. Yield: 82%.

C₇₀H₈₃BN₄O₆	1087,242 g mol ⁻¹
MS (ESI-FTICR)	m/z (%) = 1087.56 (100) [M+H] ⁺ , 1109.54 (30) [M+Na] ⁺ , 1125.51 (46) [M+K] ⁺ .
¹H NMR	(250 MHz, CDCl ₃) δ [ppm] = 1.35 (s, 12H, CH ₃ pinacol) 1.40 (s, 9H, CCH ₃), 1.45-1.69 (b, 12H, Cy), 2.14 (s, 12H, PhCH ₃), 2.16 (s, 12H, PhCH ₃), 2.38 (b, 8H, Cy), 6.94 (s, 8H, PhH), 7.94 (s, 1H, 2-isophth), 8.19 (s, 2H, 4,6-isophth), 8.31 (s, 1H, 2-isophth), 8.51 (s, 2H, 4,6-isophth).
¹³C NMR	(250 MHz, CDCl ₃) δ [ppm] = 18.72, 22.73, 24.65, 26.17, 29.45, 30.98, 35.21, 45.00, 121.94, 126.23, 128.43, 128.78, 130.82, 134.20, 134.47, 136.47, 147.84, 153.66, 165.29.

General procedure to increase the yield of the catenanes in the macrocycle synthesis:

The yield of the by-product catenanes was found to be increased when triethylamine was added after additions of the two reactants were completed. Further stirring for 1 day and evaporating the solvents increased the amount of catenanes obtained from the usual syntheses by values of 30-110% depending on the type of extended diamine used in the reaction.

[2]-{11'-bromo-29'-tert-butyl-5',17',23',35',38',40',43',45'-octamethyldispiro [cyclohexan-1,2'-7',15',25',33'-tetraazaheptacyclo[32.2.2.2^{3',6'}.2^{16',19'}.2^{21',24'}.1^{9',13'}.1^{27',31'}] hexatetraconta-3',5',9',11',13'(44'),16',18',21',23',27',29',31'(39'),34',36',37',40',42',45'-octadecaen-20',1''-cyclohexan]-8',14',26',32'-tetraon}-catenane (2C)

The residue obtained through the general procedure for catenane synthesis was then applied on a silica column eluting with a mixture of dichloromethane, ethyl acetate (15:1) to yield the catenane as a white solid. *R_f* = 0.95. Yield: 7.2%.

C₁₂₈H₁₄₂Br₂N₈O₈	2080,35 g mol ⁻¹
---	-----------------------------

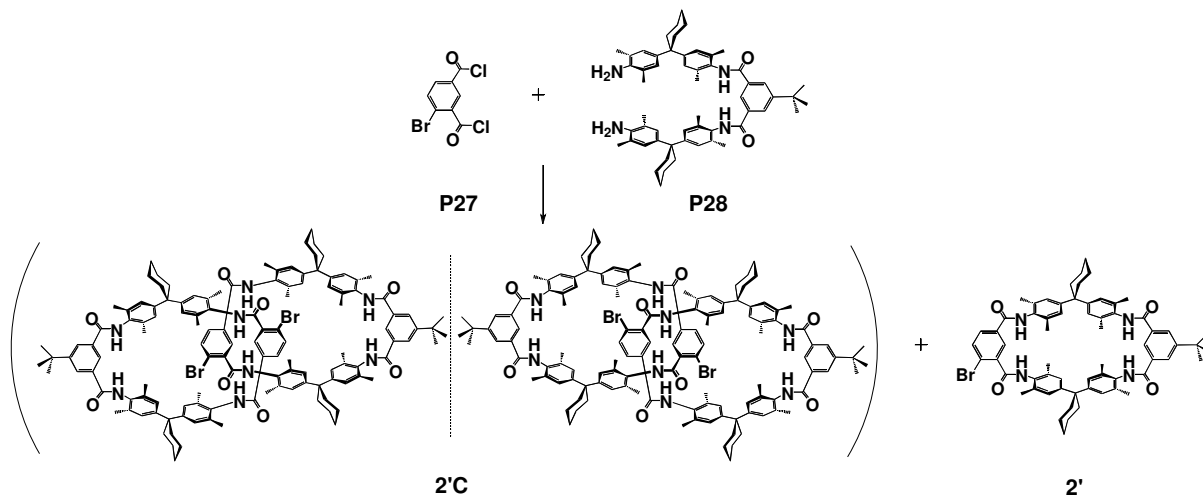
MS(ESI-FTICR)	$m/z = 2078.00 [M+H]^+, 2100.03 [M+Na]^+, 2115.97 [M+K]^+.$
MS/MS	(excitation of $[M+H]^+$) shows 1039.38 $[M+H-(\text{macrocycle})]^+.$
^1H NMR	(250 MHz, DMSO- d_6) Incredibly complicated!

[2]-{11',29'-dibromo-5',17',23',35',38',40',43',45'-octamethyldispiro[cyclohexan-1,2'-7',15',25',33'-tetraazaheptacyclo[32.2.2.2^{3',6'}.2^{16',19'}.2^{21',24'}.1^{9',13'}.1^{27',31'}]hexatetraconta-3',5',9',11',13'(44'),16',18',21',23',27',29',31'(39'),34',36',37',40',42',45'-octadecaen-20',1''-cyclohexan]-8',14',26',32'-tetraon}-catenane (3C)

The residue obtained through the general procedure for catenane synthesis was then applied on a silica column eluting with a mixture of dichloromethane, ethyl acetate (5:1) to yield the catenane as white solid. $R_f = 0.95$. Yield: 152 mg, 7.2%.

$\text{C}_{120}\text{H}_{124}\text{Br}_4\text{N}_8\text{O}_8$	2125,93 g mol ⁻¹
MS (ESI-FTICR)	$m/z = 2121.57 [M+H]^+.$
MS/MS	(excitation of $[M+H]^+$) shows 2103.19 $[M+H-H_2O]^+$, 1059.20 $[M+H-\text{dibromo macrocycle}]^+.$
^1H NMR	(400 MHz, DMSO- d_6) δ [ppm] = 0.74 (s, 6H, PhCH ₃), 1.06 (s, 6H, PhCH ₃), 1.20-1.48, (br, 24H, CH ₂ of Cy), 1.77 (s, 12H PhCH ₃), 2.13 (s, 12H, PhCH ₃), 1.64 (br, 8H, Cy), 1.96(br, 8H, Cy), 6.52, 6.76, 7.00 (all s, 16H, PhH), 7.19 (s, 4H, 4,6-isophth), 8.22 (s, 4H, 4,6-isophth), 7.76 (s, 2H, 2-isophth), 8.73 (s, 2H, 2-isophth), 9.30, 9.38, 9.71, 10.1 (all s, 8H, NH).
^{13}C NMR	not possible because of low solubility of the compound in common solvents.

**[2]-{10'-bromo-29'-tert-butyl-5',17',23',35',38',40',43',45'-octamethyldispiro
[cyclohexan-1,2'-7',15',25',33'-tetraazaheptacyclo[32.2.2.2^{3',6'}.2^{16',19'}.2^{21',24'}.1^{9',13'}.1^{27',31'}]
hexatetraconta-3',5',9',11',13'(44'),16',18',21',23',27',29',31'(39'),34',36',37',40',42',45'-
octadecaen-20',1''-cyclohexan]-8',14',26',32'-tetraon}-catenane (2'C)**



The usual macrocycle synthesis was modified to have more catenane. The yield was increased by adding triethyl amine after additions were completed and the mixture was allowed to stir overnight. Further stirring for 1 day and evaporating the solvents produces a residue which is then applied on a silica column of the same type to yield the catenane as a white solid. $R_f = 0.95$. Yield: 1.2-8.0 %.

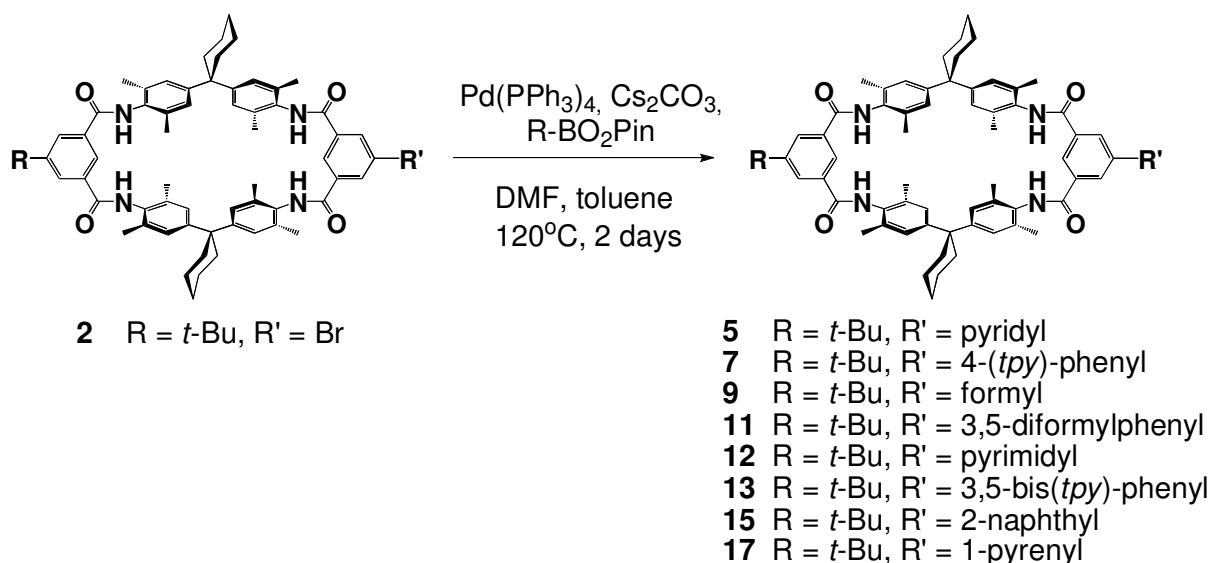
C₁₂₈H₁₄₂Br₂N₈O₈	2080,35 g mol ⁻¹
MS (ESI-FTICR)	$m/z = 2078.00 [M+H]^+, 2100.03 [M+Na]^+, 2115.97 [M+K]^+$
MS/MS	(excitation of $[M+H]^+$) shows 1039.38 $[M+H-(\text{macrocycle})]^+$
¹H NMR	(250 MHz, DMSO-d ₆) Incredibly complicated!

General procedure for Suzuki coupling on bromo macrocycle (2):

a) Preparation of pinacol boronic esters¹⁹²: The not-commercially available boronic esters were prepared from their boronic acids in a reaction with 1.1 eq of pinacol in toluene, adding drops of acetic acid when needed and stirring overnight. The solvent was evaporated and the formed pinacol ester was dried at high vacuum.

b) Suzuki coupling¹⁹³: Corresponding boronic acid pinacol esters (0.120 mmol) was poured into a argon-purged mixture of bromo macrocycle 2 (100 mg, 0.096 mmol), Pd(PPh₃)₄ (3.45 mg, 0.003 mmol), Cs₂CO₃ (46.9, 0.144 mmol) in 20 ml of dry toluene and dry DMF (1:1) at 100 °C. Then it was kept at 120-130 °C for 2 days under argon. Solvents were evaporated at

reduced pressure to dryness. Each compound was separately purified on silica columns with appropriate solvent mixtures.



11'-*tert*-butyl-29'-(4-pyridyl)-5',17',23',35',38',40',43',45'-octamethyldispiro [cyclohexan-1,2'-7',15',25',33'-tetraazaheptacyclo[32.2.2.2^{3',6'}.2^{16',19'}.2^{21',24'}.1^{9',13'}.1^{27',31'}] hexatetraconta-3',5',9',11',13'(44'),16',18',21',23',27',29',31'(39'),34',36',37',40',42',45'-octadecaen-20',1''-cyclohexan]-8',14',26',32'-tetraon, "pyridine macrocycle" (5)

After column chromatography on silica eluting with dichloromethane/methanol (95:5) pyridine macrocycle was obtained as a white powder. R_f = 0.20 Yield: 83.2 mg, 83.4%. m.p.>300 °C.

C₆₉H₇₅N₅O₄

1038,36 g mol⁻¹

MS (ESI-FTICR)

m/z (%) = 1038.60 (100) [M+H]⁺

¹H NMR

(400 MHz, DMSO-*d*₆) δ [ppm] = 1.35 (s, 9H, CH₃), 1.38-1.69 (br, 12H, Cy), 2.11 (s, 24H PhCH₃), 2.26 (br, 8H, Cy), 6.93 (s, 8H, PhH), 7.52 (d, J = 2H, H_{pyr}), 7.73 (s, 2H, 4,6-*t*-Bu isophth H), 7.82 (s, 1H, 2-*t*-Bu isophth H), 7.95 (s, 1H, NH), 8.12 (s, 2H, 4,6-isophth), 8.31 (s, 2H, NH), 8.36 (s, 2H, 2-isophth), 8.57 (s, 1H, NH).

¹³C NMR

(250 MHz, CDCl₃) δ [ppm] = 18.95, 19.02(CH₃); 22.94, 24.70, 26.38, 31.13, 31.28, 35.38 (CH₂); 121.74, 126.45, 128.51, 129.85, 150.33 (CH); 36.47, 45.17, 131.15, 134.72, 134.86, 135.70 (Cq) 162.64, 164.68 (CO).

11'-tert-butyl-29'-(4'-(4-(2,2'-6',2''-terpyridyl))-5',17',23',35',38',40',43',45'-octamethyldispiro[cyclohexan-1,2'-7',15',25',33'-tetraazaheptacyclo[32.2.2.2^{3',6'}.2^{16',19'}.2^{21',24'}.1^{9',13'}.1^{27',31'}]hexatetraconta-3',5',9',11',13'(44'),16',18',21',23',27',29',31'(39'),34',36',37',40',42',45'-octadecaen-20',1''-cyclohexan]-8',14',26',32'-tetraon, "terpyridine macrocycle" (7)

After column chromatography on neutral alumina eluting with 1% methanol in dichloromethane terpyridine macrocycle was obtained as a white powder. $R_f = 0.88$. Yield: 80.2 mg, 66%. m.p.>300 °C.

C₈₅H₈₅N₇O₄

1268,63 g mol⁻¹

MS (FT-ICR)

m/z (%) = 1267.993 (100) [M+H]⁺, 1289.948 (44) [M+Na]⁺, 1305.912 [(4) [M+K]⁺.

¹H NMR

(400 MHz, CDCl₃) δ [ppm] = 1.35 (s, 9H, CH₃), 1.40-1.65 (br, 12H, Cy), 2.07 (s, 12H PhCH₃), 2.09 (s, 12H, PhCH₃), 2.26 (br, 8H, Cy), 6.92 (s, 8H, PhH), 7.26 (m, 2H, 5,5''-tpy), 7.74 (d, $J = 8.3$ Hz, 2H, PhH), 7.78 (m, 2H, 4,4''-tpy), 7.91 (d, $J = 8.3$ Hz, 2H, PhH), 8.09 (s, 2H, 4,6-*t*-Bu isophth), 8.13 (s, 1H, 2-*t*-Bu isophth), 8.17 (s, 2H, 4,6-isophth), 8.37 (s, 1H, 2-isophth), 8.43 (s, 4H, NH), 8.54 (d, $J = 8$ Hz, 2H, 3,3''-tpy), 8.64 (d, $J = 4.6$ Hz, 2H, 6,6''-tpy), 8.71 (s, 2H, 3',5'-tpy).

¹³C NMR

(400 MHz, CDCl₃/CD₃OD (4:1)) δ [ppm] = 18.57, 22.91, 26.34, 31.10, 35.24, 36.61, 45.15, 118.83, 121.85, 123.66, 124.15, 126.24, 127.72, 127.86, 128.50, 128.60, 128.72, 129.53, 130.89, 131.38, 131.50, 131.87, 131.95, 132.32, 134.19, 135.03, 135.21, 137.40, 138.03, 140.02, 142.06, 148.01, 148.10, 148.93, 149.66, 153.43, 155.91, 156.04, 163.05, 166.40, 166.78.

11'-tert-butyl-29'-(4-formylphenyl)-5',17',23',35',38',40',43',45'-octamethyldispiro [cyclohexan-1,2'-7',15',25',33'-tetraazaheptacyclo[32.2.2.2^{3',6'}.2^{16',19'}.2^{21',24'}.1^{9',13'}.1^{27',31'}] hexatetraconta-3',5',9',11',13'(44'),16',18',21',23',27',29',31'(39'),34',36',37',40',42',45'-octadecaen-20',1''-cyclohexan]-8',14',26',32'-tetraon, "aldehyde macrocycle" (9)

After column chromatography on silica eluting with CH₂Cl₂/CH₃OH (7:1) aldehyde macrocycle was obtained as a white powder, 85.8 mg. *R_f* = 0.88. Yield: 84%. m.p.>300 °C.

C₇₁H₇₆N₄O₅

1065,39 g mol⁻¹

MS (ESI-FTICR)

m/z (%) = 1166.65 (100) [M+HNEt₃]⁺.

¹H NMR

(400 MHz, CDCl₃) δ [ppm] = 1.37 (s, 9H, CH₃), 1.47-1.70 (br, 12H, CH₂ of Cy), 2.12 (s, 24H PhCH₃), 2.31 (br, 8H, CH₂ of Cy), 6.97 (s, 8H, PhH), 7.48 (br, 4H, NH), 7.68 (d, *J* = 10.3 Hz, 2H, PhH), 7.75 (d, *J* = 10.3 Hz, 2H, PhH), 7.99 (s, 1H, 2-isophth), 8.14 (s, 2H, 4,6-isophth), 8.25 (s, 1H, 2-isophth), 8.37 (s, 2H, 4,6-isophth), 9.93 (s, 1H, CHO).

¹³C NMR

(400 MHz, CDCl₃) δ [ppm] = 15.33, 19.06, 23.03, 26.44, 30.80, 31.29, 35.45, 45.32, 65.92, 122.73, 126.66, 126.74, 127.98, 128.59, 130.07, 130.41, 130.92, 131.14, 134.63, 134.78, 134.94, 135.10, 135.21, 135.33, 135.92, 141.91, 144.97, 148.14, 148.39, 154.07, 164.94, 165.83, 192.08.

11'-tert-butyl-29'-(3,5-diformylphenyl)-5',17',23',35',38',40',43',45'-octamethyldispiro [cyclohexan-1,2'-7',15',25',33'-tetraazaheptacyclo[32.2.2.2^{3',6'}.2^{16',19'}.2^{21',24'}.1^{9',13'}.1^{27',31'}] hexatetraconta-3',5',9',11',13'(44'),16',18',21',23',27',29',31'(39'),34',36',37',40',42',45'-octadecaen-20',1''-cyclohexan]-8',14',26',32'-tetraon, "1,3-bisformyl benzene macrocycle" (11)

After column chromatography on silica eluting with CH₂Cl₂/CH₃OH (9:1) aldehyde macrocycle was obtained as a white powder, 89.2 mg. *R_f* = 0.4. Yield: 85%. Product is labile to oxidation on contact with air-MS spectra showed the oxidized product.

C₇₂H₇₆N₄O₆

1093,40 g mol⁻¹

¹H NMR

(250 MHz, CDCl₃) δ [ppm] = 1.35 (s, 9H CCH₃), 1.40-1.68 (b, 12H, Cy), 2.13 (s, 24H, PhCH₃), 2.30 (b,8H, Cy), 6.96 (s,8H, PhH), 7.55 (s, 2H, 4,6-isophth), 7.91 (s, 1H, 2-isophth), 8.05

(br, 4H, NH), 8.16 (s, 2H 4,6-isophth), 8.32 (s, 1H, 2-isophth), 8.40 (s, 2H, 4,6-PhH), 8.46 (s, 1H, 2-PhH), 10.06 (CHO).

11'-tert-butyl-29'-(5-pyrimidyl)-5',17',23',35',38',40',43',45'-octamethyldispiro [cyclohexan-1,2'-7',15',25',33'-tetraazaheptacyclo[32.2.2.2^{3',6'}.2^{16',19'}.2^{21',24'}.1^{9',13'}.1^{27',31'}] hexatetraconta-3',5',9',11',13'(44'),16',18',21',23',27',29',31'(39'),34',36',37',40',42',45'-octadecaen-20',1''-cyclohexan]-8',14',26',32'-tetraon, "pyrimidine macrocycle" (12)

To a mixture of bromo macrocycle 2 (208 mg, 0.200), Pd(PPh₃)₄ (6.93 mg, 6.0 μmol), Cs₂CO₃ (97.8 mg, 0.300 mmol) in dry toluene (10 ml) and dry DMF (10 ml) was added pyrimidine boronic acid pinacol ester (51.5 mg, 0.250 mmol) under argon. The reaction was continued at 120 °C for 2 days. All solvents were evaporated and the crude product was applied on a silica column, eluting with 5% methanol in CH₂Cl₂. The product obtained as the second band from the column was dried at high vacuum. Yield: 166 mg, 83%.

C₆₈H₇₄N₆O₄

1039,35 g mol⁻¹

MS (ESI-FTICR)

m/z (%) = 1039.579 [M+H]⁺ (100).

¹H NMR

(250 MHz, CDCl₃) δ [ppm] = 1.38 (s, 9H CCH₃), 1.42-1.65 (br, 12H, Cy), 2.14 (s, 24H, PhCH₃), 2.34 (br, 8H, Cy), 6.97 (s, 8H, PhH), 7.96 (s, 2H, NH), 8.15 (s, 1H, 2-isophth), 8.19 (s, 2H, 4,6-isophth), 8.40 (s, 2H 4,6-isophth), 8.56 (s, 2H, NH), 8.64 (s, 1H, 2-isophth), 9.04 (s, 2H, pyH), 9.16 (s, 1H, pyH). (The spectrum always showed that there are two equivalents of DMF associated with the macrocycle, even after extensive drying of the compound).

¹³C NMR

(250 MHz, CDCl₃) δ [ppm] = 18.70, 18.80, 22.64, 26.09, 29.45, 30.60, 31.02, 35.12, 36.20, 44.82, 122.90, 125.89, 126.14, 128.20, 128.39, 128.53, 129.69, 131.07, 131.27, 131.38, 131.54, 131.91, 132.84, 134.24, 134.47, 134.74, 135.69, 147.69, 148.15, 153.61, 154.79, 157.51, 162.40, 164.34, 165.50.

11'-tert-butyl-29'-(3,5-bis(2,2'-6',2''-terpyridinyl)benzyl))-5',17',23',35',38',40',43',45'-octamethyldispiro[cyclohexan-1,2'-7',15',25',33'-tetraazaheptacyclo[32.2.2.2^{3',6'}.2^{16',19'}.2^{21',24'}.1^{9',13'}.1^{27',31'}]hexatetraconta-3',5',9',11',13'(44'),16',18',21',23',27',29',31'(39'),34',36',37',40',42',45'-octadecaen-20',1''-cyclohexan]-8',14',26',32'-tetraon, "bisterpyridine benzene macrocycle" (13)

To a mixture of boronic ester macrocycle 4, (70 mg, 0.052), Pd(PPh₃)₄ (1.8 mg, 1.6 μmol), Cs₂CO₃ (25 mg, 0.078 mmol) in dry toluene (7 ml) and dry DMF (7 ml) was added 1-bromo 3,5-bis(4'-terpyridyl) benzene (32.0 mg, 0.052 mmol) under argon. The reaction was continued at 120 °C for 2 days. All solvents were evaporated and the crude product was applied on an alumina column, eluting with 2% methanol in CH₂Cl₂. Yield: 72%.

C₁₀₀H₉₄N₁₀O₄

1499,88 g mol⁻¹

MS (ESI-FTICR)

m/z (%) = 1500.799 (30) [M+H]⁺, 1000.861 (3) [2M+3H⁺]³⁺, 750.883 (100) [M+2H]²⁺.

¹H NMR

(250 MHz, CDCl₃) δ [ppm] = 1.38 (s, 9H CCH₃), 1.45-1.63 (br, 12H, Cy), 2.11 (s, 12H, PhCH₃), 2.14 (s, 12H, PhCH₃), 2.30 (br, 8H, Cy), 6.96 (s, 8H, PhH), 7.29 (m, 4H, 5,5''-tpy), 7.80 (m, 4H, 4,4''-tpy), 8.30 (s, 1H, 2-isophth), 8.35 (s, 1H, 2-isophth), 8.38 (s, 2H, 4,6-isophth), 8.55 (s, 2H, 4,6-isophth), 8.58 (d, *J* = 3.8 Hz, 4H, 3,3''-tpy), 8.65 (d, *J* = 3.8 Hz, 4H, 6,6''-tpy), 8.79 (s, 4H, 3',5'-tpy).

¹³C NMR

(250 MHz, CDCl₃) δ [ppm] = 18.98, 22.80, 26.30, 31.27, 36.40, 44.96, 119.40, 121.44, 123.01, 123.91, 125.48, 126.26, 126.90, 128.42, 128.52, 128.86, 130.34, 131.21, 131.64, 131.71, 131.75, 131.83, 132.00, 134.31, 134.93, 134.98, 135.40, 136.91, 140.56, 141.11, 142.19, 147.86, 148.12, 149.08, 149.84, 153.54, 155.96, 156.13, 165.38, 165.66.

**11'-tert-butyl-29'-(2-naphthyl)-5',17',23',35',38',40',43',45'-octamethyldispiro
[cyclohexan-1,2'-7',15',25',33'-tetraazaheptacyclo[32.2.2.2.^{3',6'}.2.^{16',19'}.2.^{21',24'}.1.^{9',13'}.1.^{27',31'}]
hexatetraconta-3',5',9',11',13'(44'),16',18',21',23',27',29',31'(39'),34',36',37',40',42',45'-
octadecaen-20',1''-cyclohexan]-8',14',26',32'-tetraon, "naphthalene macrocycle" (15)**

After column chromatography on silica eluting with dichloromethane/ethyl acetate (6:1) naphthalene macrocycle was obtained as the first band from the column was dried at high vacuum. Yield: 80.0 mg, 76%.

C₇₄H₇₈N₄O₄

1087,44 g mol⁻¹

MS (ESI-FTICR)

m/z (%) = 1088.61 (100) [M+H⁺]⁺, 544.31 (52) [M+2H⁺]²⁺.

¹H NMR

(500 MHz, CDCl₃+ 2 drops CD₃OD) δ [ppm] = 1.32 (s, 9H CCH₃), 1.40-1.62 (br, 12H, Cy), 2.09 (s, 12H PhCH₃), 2.11 (s, 12H, PhCH₃), 2.27 (br, 8H, Cy), 6.93 (s, 8H, PhH), 7.45 (m, 3H, Ar_{naph}), 7.80 (m, 4H, Ar_{naph}), 8.09 (s, 1H, 2-isophth), 8.12 (s, 2H, 4,6-isophth), 8.24 (s, 1H, 2-isophth), 8.44 (s, 2H 4,6-isophth), 8.62 (s, 2H, NH), 8.80 (s, 2H, NH).

¹³C NMR

(250 MHz, CDCl₃+ 2 drops CD₃OD) δ [ppm] = 18.37, 22.66, 26.11, 30.87, 34.88, 34.98, 44.86, 124.74, 125.91, 126.04, 126.28, 127.36, 128.06, 128.16, 128.53, 129.56, 131.13, 132.72, 133.30, 133.88, 134.86, 142.46, 147.72, 153.14, 166.43, 166.06.

**11'-tert-butyl-29'-(2-pyrenyl)-5',17',23',35',38',40',43',45'-octamethyldispiro
[cyclohexan-1,2'-7',15',25',33'-tetraazaheptacyclo[32.2.2.2.^{3',6'}.2.^{16',19'}.2.^{21',24'}.1.^{9',13'}.1.^{27',31'}]
hexatetraconta-3',5',9',11',13'(44'),16',18',21',23',27',29',31'(39'),34',36',37',40',42',45'-
octadecaen-20',1''-cyclohexan]-8',14',26',32'-tetraon, "pyrene macrocycle" (17)**

After column chromatography on silica eluting with dichloromethane/ethyl acetate (8:1) pyrene macrocycle was obtained as the second band from the column and dried at high vacuum. Yield: 87%.

C₈₀H₈₀N₄O₄

1161,52 g mol⁻¹

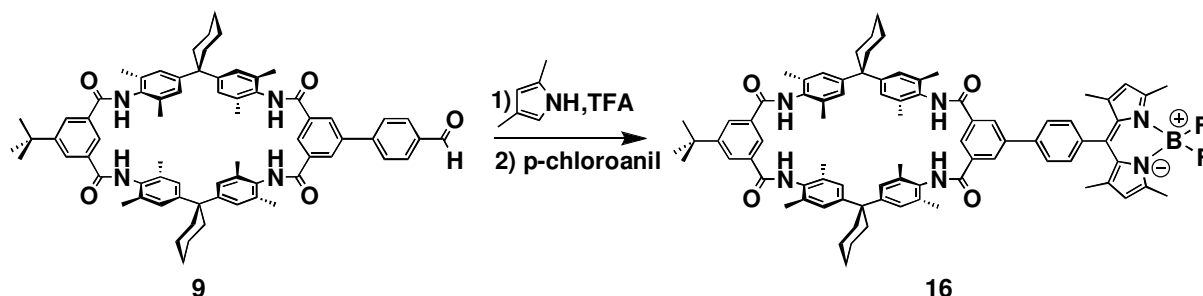
¹H NMR

(500 MHz, CD₂Cl₂) δ [ppm] = 1.44 (s, 9H CCH₃), 1.51-1.70 (br, 12H, Cy), 2.20 (s, 12H PhCH₃), 2.24 (s, 12H, PhCH₃), 2.40 (br, 8H, Cy), 7.09 (s, 8H, PhH), 7.44 (s, 2H, 4,6-isophth), 7.59 (s, 2H, 4,6-isophth), 8.03-8.30 (m, Ar_{pyre}), 8.37 (s, 4H, NH).

¹³C NMR

(250 MHz, CDCl₃) δ [ppm] = 18.48, 19.13, 23.02, 26.41, 31.31, 35.50, 45.31, 58.52, 124.48, 124.79, 124.84, 124.98, 125.29, 125.59, 126.29, 126.62, 126.73, 127.42, 127.61, 128.03, 128.38, 128.51, 128.70, 130.93, 131.03, 131.33, 131.50, 133.09, 134.65, 134.76, 134.97, 135.27, 135.42, 143.79, 148.22, 154.11, 165.34, 165.72.

11'-tert-butyl-29'-(4-BODIPY-phenyl)-5',17',23',35',38',40',43',45'-octamethyldispiro [cyclohexan-1,2'-7',15',25',33'-tetraazaheptacyclo[32.2.2.2^{3',6'}.2^{16',19'}.2^{21',24'}.1^{9',13'}.1^{27',31'}] hexatetraconta-3',5',9',11',13'(44'),16',18',21',23',27',29',31'(39'),34',36',37',40',42',45'-octadecaen-20',1''-cyclohexan]-8',14',26',32'-tetraon, "BODIPY macrocycle" (16)



2,4-dimethyl pyrrole (19 mg, 0.2 mmol, 17 μL) and aldehyde macrocycle **9** (106.5 mg, 0.1 mmol) were dissolved in 15 ml dry and CH₂Cl₂ (argon was bubbled for 10 min) under argon atmosphere. One drop of TFA was added and the solution was stirred at room temperature 4 hours. A solution of *p*-chloroanil (24.5 mg, 0.1 mmol) in 5 ml dry CH₂Cl₂ was added, stirring was continued for 30 min. The reaction mixture was washed three times with water and dried over MgSO₄. The solvent was evaporated and the residue was purified by silica gel column chromatography eluting with CH₂Cl₂. Yield: 62%.

C₈₃H₈₉BF₂N₆O₄

1283,44 g mol⁻¹

MS (ESI-FTCIR)

m/z (%) = 1306.723 (28) [M+Na]⁺, 1321.862 (100) [M+K]⁺, 1384.854 (18) [M+HNEt₃]⁺.

¹H NMR

(250 MHz, CDCl₃) δ [ppm] = 1.39 (s, 9H CCH₃), 1.41 (s, 6H, CH₃_{BODIPY}), 1.45-1.65 (br, 12H, Cy), 2.30 (br, 8H, Cy), 2.47 (s, 24H PhCH₃), 2.52 (s, 6H, CH₃(BODIPY)), 5.97 (s, 2H, PyH_{BODIPY}), 6.97 (s, 8H, PhH), 7.38 (d, *J* = 7.7, 2H, PhH), 7.38 (d, *J* = 7.7, 2H, PhH), 7.96 (s, 1H, 2-isophth), 8.20 (s, 2H, 4,6-isophth), 8.30 (s, 1H, 2-isophth), 8.49 (s, 2H 4,6-isophth). The spectrum always

showed three equivalents of DMF associated with the macrocycle even after extensive drying).

¹³C NMR

(250 MHz, CDCl₃) δ [ppm] = 14.39, 18.75, 22.64, 30.75, 31.04, 35.12, 36.22, 44.76, 121.09, 126.08, 127.84, 128.50, 131.15, 131.27, 134.24, 134.47, 134.54, 134.72, 135.05, 162.38.

11'-tert-butyl-29'-(3-pyridyl)-5',17',23',35',38',40',43',45'-octamethyldispiro [cyclohexan-1,2'-7',15',25',33'-tetraazaheptacyclo[32.2.2.2.2^{3',6'}.2^{16',19'}.2^{21',24'}.1^{9',13'}.1^{27',31'}] hexatetraconta-3',5',9',11',13'(44'),16',18',21',23',27',29',31'(39'),34',36',37',40',42',45'-octadecaen-20',1''-cyclohexan]-8',14',26',32'-tetraon, "3-pyridine macrocycle" (5')

Procedure same as for 5. 4-bromo macrocycle 2' was used in coupling. The residue was purified by a column chromatography on silica eluting with 95:5 dichloromethane:methanol. The product was obtained from the third fraction as a light tan solid. Yield: 30 %.

C₆₉H₇₅N₅O₄

1038,36 g mol⁻¹

MS (ESI-TOF)¹⁹¹

m/z (%) = 1038.59 (100) [M+H]⁺, 1060.57 (37) [M+Na]⁺.

¹H NMR

(250 MHz, DMF-d₇) δ [ppm] = 1.55 (s, 9H), 1.74 (br, 12H), 2.35 (s, 24H), 2.60 (br, 8H), 7.35 (s, 8H), 8.00 (d, 2H, H_{py}), 8.35 (m, 4H, 4,5-isophth), 8.73 (s, 1H, 2-isophth), 8.82 (s, 1H, isophth), 8.88 (d, 2H, H_{py}), 9.36 (s, 1H, NH), 9.65 (s, 1H, NH), 9.74 (s, 1H, NH), 9.90 (s, 1H, NH).

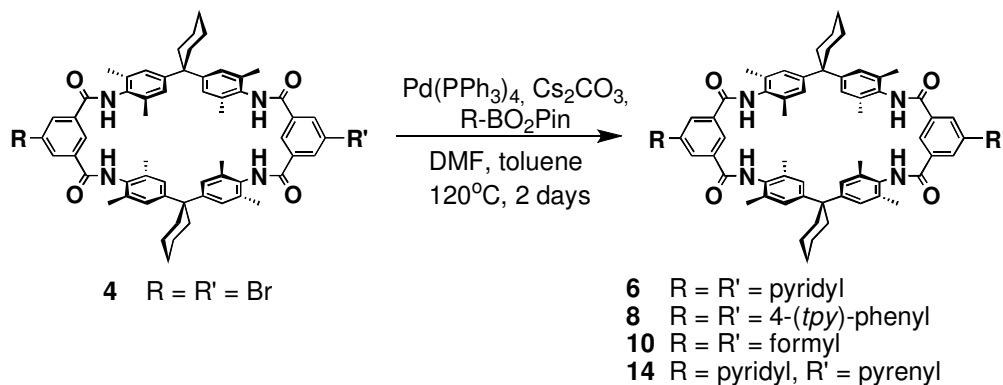
¹³C NMR

(250 MHz, DMF-d₇) δ [ppm] = 14.0, 18.8, 19.2, 23.5, 25.2, 26.7, 26.8, 31.3, 32.4, 35.9, 41.1, 45.5, 45.7, 71.0, 73.0, 74.2, 122.0, 124.0, 125.3, 126.4, 125.5, 126.8, 127.0, 128.4, 128.5, 129.3, 129.4, 130.5, 131.3, 132.3, 132.6, 134.7, 135.0, 135.1, 135.3, 135.5, 135.6, 135.7, 137.3, 141.4, 145.4, 148.1, 150.3, 151.3, 153.0, 164.7, 164.8, 165.4, 165.6, 165.7, 166.8, 166.9.

General procedure for Suzuki coupling on dibromo macrocycle (3)

a) Preparation of boronic esters: The not-commercially available bisboronic esters were prepared from their bisboronic acids in a reaction with 2.2 eq of pinacol in toluene, by addition of drops of acetic acid when needed, by stirring overnight. The solvent was evaporated and the formed pinacol ester was dried at high vacuum.

b) Suzuki coupling: Corresponding boronic acid pinacol ester (0.240 mmol) was poured into a oxygen-free mixture of dibromo macrocycle 3 (100 mg, 0.094 mmol), Pd(PPh₃)₄ (6.90 mg, 0.006 mmol), Cs₂CO₃ (93.8 mg, 0.288 mmol) in 20 ml of dry toluene and dry DMF (1:1) at 100 °C. Then it was kept at 120-130 °C for 2 days under argon. Solvents were evaporated at reduced pressure to dryness. Each compound was separately purified on silica columns with appropriate solvent mixtures.



11',29'-bis(4-pyridyl)-5',17',23',35',38',40',43',45'-octamethyldispiro[cyclohexan-1,2'-7',15',25',33'-tetraazaheptacyclo[32.2.2.2^{3',6'}.2^{16',19'}.2^{21',24'}.1^{9',13'}.1^{27',31'}]hexatetraconta-3',5',9',11',13'(44'),16',18',21',23',27',29',31'(39'),34',36',37',40',42',45'-octadecaen-20',1''-cyclohexan]-8',14',26',32'-tetraon, "bispyridine macrocycle" (6)

After column chromatography on alumina eluting with 5% methanol in dichloromethane bispyridine macrocycle was obtained as a pale yellow-to-white solid. (Even when eluting from the column, the compound was obtained as a suspension in the eluent.) Yield 62%. It was found that the compound is not soluble in the common organic solvents.

C₇₀H₇₀N₆O₄

1059,34 g mol⁻¹

MS (ESI-FTICR)

m/z (%) = 1059.55 (86) [M+H]⁺, 530.28 (100) [M+2H]²⁺.

¹H NMR

(250 MHz, DMF-d₇) δ [ppm] = 1.48-1.65 (br, 12H, Cy), 2.20 (s, 24H PhCH₃), 2.32 (br, 8H, Cy), 7.02 (s, 8H, PhH), 7.55 (d, *J*=3.8 Hz, H_{pyr}), 7.66 (s, 1H, 2- isophth), 8.35 (s, 4H, 4,6- isophth), 8.49 (d, *J*= 3.8, H_{pyr}), 8.65 (br, 4H, NH).

11',29'-bis(4-(2,2'-6',2''-terpyridyl)phenyl)-5',17',23',35',38',40',43',45'-octamethyl dispiro[cyclohexan-1,2'-7',15',25',33'-tetraazaheptacyclo[32.2.2.2^{3',6'}.2^{16',19'}.2^{21',24'}.1^{9',13'}.1^{27',31'}]hexatetraconta-3',5',9',11',13'(44'),16',18',21',23',27',29',31'(39'),34',36',37',40',42',45'-octadecaen-20',1''-cyclohexan]-8',14',26',32'-tetraon, "bisterpyridine macrocycle" (8)

After column chromatography on alumina eluting with 5% methanol in dichloromethane bisterpyridine macrocycle 8 which was collected as the first and second bands that are close to each other, was obtained as a pale yellow solid. (The third band was found out to be the hydroxyl derivative of the boronic ester compound.) Yield: 51%.

C₁₀₂H₉₀N₁₀O₄	1519,87 g mol ⁻¹
MS (FT-ICR)	m/z (%) = 760.87 (100) [M+2H] ²⁺
MS (ESI)	m/z = 1519.76 [M+H] ⁺ , 1541.75 [M+Na] ⁺ , 1558.72 [M+K] ⁺ .
MS (FAB)	m/z = 1520.9 (67) [M+H] ⁺ , 1542.2 (100) [M+Na] ⁺ .
MS (EI)	(320°C) m/z (%) = 1519.6 (20) [M] ⁺ .
¹H NMR	(250 MHz, pyridine-d ₅) δ [ppm] = 1.55-1.68 (br, 12H, Cy), 2.32 (s, 24H PhCH ₃), 2.46 (br, 8H, Cy), 7.34 (s, 8H, PhH), 7.39 (m, 4H, 5,5'-tpy), 7.92 (m, 4H, 4,4'-tpy), 8.08 (s, 1H, 2- isophth), 8.89 (d, J = 3.4 Hz, 4H, 6,6'-tpy), 8.93 (s, 4H, 3',5'-tpy), 8.97 (d, J = 5.8 Hz, 4H, 2,2'-tpy), 8.98 (s, 4H, 4,6-isophth), 9.11 (s, 4H, NH).

11',29'-bis(4-formylphenyl)-5',17',23',35',38',40',43',45'-octamethyldispiro[cyclohexan-1,2'-7',15',25',33'-tetraazaheptacyclo[32.2.2.2^{3',6'}.2^{16',19'}.2^{21',24'}.1^{9',13'}.1^{27',31'}]hexatetra conta-3',5',9',11',13'(44'),16',18',21',23',27',29',31'(39'),34',36',37',40',42',45'-octa decaen-20',1''-cyclohexan]-8',14',26',32'-tetraon, "bisaldehyde macrocycle" (10)

After column chromatography on silica eluting with 5% methanol in dichloromethane bisaldehyde macrocycle 10 was obtained as a pale yellow-to-white solid. It was found that that the compound is always associated with the mono- and bis-acid forms even after purification. Yield: 60%.

C₇₄H₇₂N₄O₆	1113,39 g mol ⁻¹
MS (ESI-FTICR)	m/z (%) = 1214.67 (100) [M+HNEt ₃] ⁺ .

¹H NMR (250 MHz, CDCl₃) δ [ppm] = 1.48-1.69 (br, 12H, Cy), 2.14 (s, 24H PhCH₃), 2.33 (br, 8H, Cy), 6.81 (s, 8H, PhH), 8.18 (s, 4H, 4,6-isophth), 8.23 (s, 1H, 2-isophth), 8.22 (br, 4H, NH), 9.85 (s, 2H, CHO).

¹³C NMR (500 MHz, CDCl₃) δ [ppm] = 18.09, 22.54, 23.14, 34.83, 47.91, 125.85, 126.74, 126.99, 134.67, 134.81, 138.01, 138.84, 142.10, 142.92, 166.41.

11'-pyrenyl-29'-(4-pyridyl)-5',17',23',35',38',40',43',45'-octamethyldispiro[cyclohexan-1,2'-7',15',25',33'-tetraazaheptacyclo[32.2.2.2.^{3',6'}.2.^{16',19'}.2.^{21',24'}.1.^{9',13'}.1.^{27',31'}]hexatetraconta-3',5',9',11',13'(44'),16',18',21',23',27',29',31'(39'),34',36',37',40',42',45'-octadecaen-20',1''-cyclohexan]-8',14',26',32'-tetraon, "pyrene-pyridine macrocycle" (14)

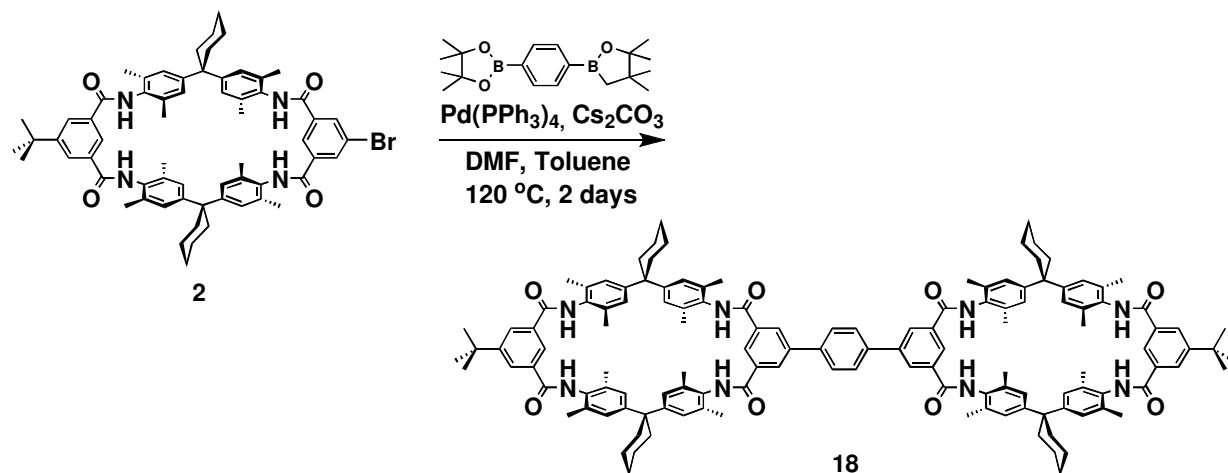
Simultaneous Suzuki coupling with both 1-pyrene boronic acid pinacol ester and 4-pyridine boronic acid pinacol ester. 4-pyridine boronic acid pinacol ester (42.4 mg, 0.207 mmol) and 1-pyrene boronic acid pinacol ester (67.9, 0.207 mmol) were poured into a oxygen-free mixture of dibromo macrocycle 7 (183 mg, 0.172 mmol), Pd(PPh₃)₄ (5.96 mg, 5.16 μmol), Cs₂CO₃ (168 mg, 0.516 mmol) in 20 ml of dry toluene and dry DMF (1:1) at 100 °C. Then it was kept at 120-130 °C for 2 days under argon. Solvents were evaporated at reduced pressure to dryness. After column chromatography on silica gel eluting with 2% methanol in dichloromethane, the desired product was separated from the pyrene-pyrene and pyridine-pyridine macrocycles which are the by-products of the reaction. Yield: 25%.

C₈₁H₇₅N₅O₄ 1182,49 g mol⁻¹

MS (ESI-FTICR) *m/z* (%) = 1182.58 (100) [M+H]⁺.

¹H NMR (250 MHz, CDCl₃) δ [ppm] = 1.08 (s, 9H, CCH₃), 1.47 (br, 12H, Cy), 2.08 (s, 12H, PhCH₃), 2.10 (s, 12H, PhCH₃), 2.20 (br, 8H), 6.87 (s, 8H), 7.42 (d, *J* = 6.44, 2H, H_{py}), 7.86-8.22 (m, 8H, Ar_{pyrene}), 7.96 (s, 2H, 4,6-isophth), 8.42 (s, 1H, 2-isophth), 8.48 (s, 2H, 4,6-isophth), 8.64 (d, *J* = 6.44, 2H, H_{py}).

1,4- bis {11'-*tert*-butyl-5',17',23',35',38',40',43',45'-octamethyldispiro[cyclohexan-1,2'-7',15',25',33'-tetraazaheptacyclo[32.2.2.2^{3',6'}.2^{16',19'}.2^{21',24'}.1^{9',13'}.1^{27',31'}]hexatetraconta-3',5',9',11',13'(44'),16',18',21',23',27',29',31'(39'), 34',36',37',40',42',45'-octadecaen-20',1''-cyclohexan]-8',14',26',32'-tetraon-29-yl} benzene “bismacrocycle benzene” (18)



To a mixture of bromo macrocycle (208 mg, 0.200 mmol), $\text{Pd(PPh}_3)_4$ (7.0 mg, 6.0 μmol), Cs_2CO_3 (97.8 mg, 0.300 mmol) in dry toluene (10 ml) and dry DMF (10 ml) was added 1,4 benzene diboronic acid pinacol ester (33.0 mg, 0.100 mmol) under argon. The reaction was continued at 120 °C for 1 day. All solvents were evaporated and the crude product was applied on a silica column, eluting with 10:1, CH_2Cl_2 : Methanol. The product obtained as the first band from the column was dried at high vacuum. Yield: 92%

$\text{C}_{134}\text{H}_{146}\text{N}_8\text{O}_8$

1996,64 g mol⁻¹

MS (ESI-FTICR)

m/z (%): 1996.15 (100) $[\text{M}+\text{H}]^+$, 998.057 (98) $[\text{M}+2\text{H}]^{2+}$.

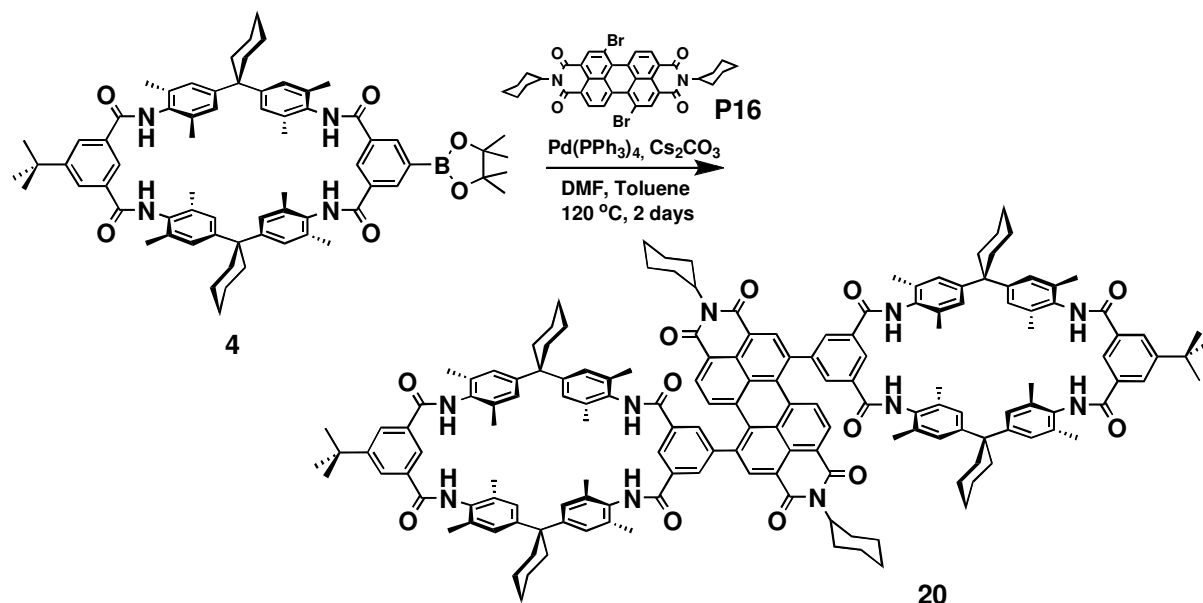
^1H NMR

(500 MHz, $\text{CDCl}_3/\text{CD}_3\text{OD}$, (2:1)) δ [ppm] = 1.39 (s, 18H, CCH_3), 1.45-1.65 (br, 24H, Cy), 2.16 (s, 24H, PhCH_3), 2.18 (s, 24H, PhCH_3), 2.31 (br, 16H, Cy), 6.98 (s, 16H, PhH), 7.86 (s, 2H, Ar_{benz}), 8.16 (s, 4H, 4,6-isophth), 8.17 (s, 2H, 2-isophth), 8.37 (s, 2H 4,6-isophth), 8.43 (s, 4H, 4,6-isophth).

^{13}C NMR

(250 MHz, $\text{CDCl}_3/\text{CD}_3\text{OD}$, (2:1)): δ [ppm] = 17.92, 22.44, 25.88, 30.48, 34.69, 34.81, 44.67, 15.79, 127.34, 128.06, 128.16, 128.35, 129.13, 130.96, 131.36, 131.52, 132.02, 133.65, 134.64, 141.63, 147.57, 147.67, 152.89, 160.67, 166.34, 166.74.

1,7- bis {11'-*tert*-butyl-5',17',23',35',38',40',43',45'-octamethyldispiro[cyclohexan-1,2'-7',15',25',33'-tetraazaheptacyclo[32.2.2.2^{3',6'}.2^{16',19'}.2^{21',24'}.1^{9',13'}.1^{27',31'}]hexatetraconta-3',5',9',11',13'(44'),16',18',21',23',27',29',31'(39'), 34',36',37',40',42',45'-octadecaen-20',1''-cyclohexan]-8',14',26',32'-tetraon-29-yl}perylene-3,4,9,10-tetracarboxylic acid cyclohexylbisimide "bismacrocycle perylene" (20)



To a mixture of boronic acid pinacol ester macrocycle **4** (219.5 mg, 0.2 mmol), Pd(PPh₃)₄ (6.93 mg, 6.0 μmol), Cs₂CO₃ (97.8 mg, 0.3 mmol) in dry toluene (10 ml) and dry DMF (10 ml) was added to 1,7-dibromoperylene-3,4,9,10-tetracarboxylic acid cyclohexylbisimide (71.2 mg, 0.1 mmol) under argon. The reaction was continued at 120 °C for 2 days. All solvents were evaporated and the crude product was applied on a silica column, eluting with 5% methanol in CH₂Cl₂. The product obtained was analyzed by ¹H NMR and ESI-MS and was found out to be contaminated with bismacrocycle (homocoupling). Thus a second column was employed with same solvent but a longer column. Yield: 45% (after second column).

C₁₆₄H₁₇₀N₁₀O₁₂

2473,16 g mol⁻¹

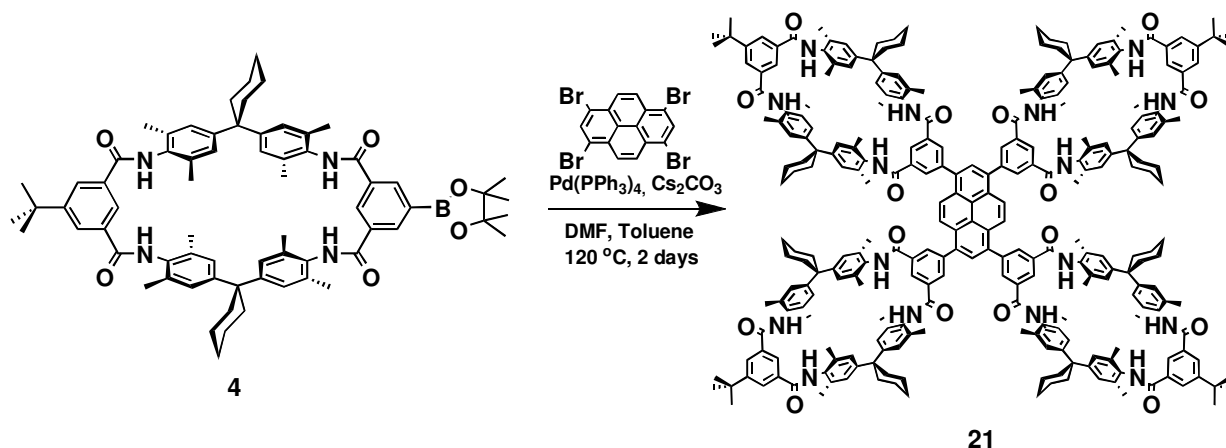
MS (ESI-FTICR)

m/z (%): 2574.44 (6) [M+HNEt₃]⁺.

¹H NMR

(250 MHz, CDCl₃: CD₃OD) δ [ppm] = 1.32 (s, 18H, CCH₃), 1.40-1.55 (br, 24H, Cy), 2.07 (s, 48H, PhCH₃), 2.23 (br, 8H, Cy), 6.88 (s, 16H, PhH), 8.02 (s, 2H, 2-isophth), 8.05 (s, 4H, 4,6-isophth), 8.10 (s, 4H, 4,6-isophth), 8.23 (s, 2H, 2-isophth), 8.40 (d, *J* = 8.3 Hz, 2H, Ar_{pery}), 8.51 (s, 2H, Ar_{pery}), 8.62 (d, *J* = 8.3 Hz, 2H, Ar_{pery}).

1,3,6,8-tetrakis[11'-*tert*-butyl-5',17',23',35',38',40',43',45'-octamethyldispiro[cyclohexan-1,2'-7',15',25',33'-tetraazaheptacyclo[32.2.2.2.2^{3',6'}.2^{16',19'}.2^{21',24'}.1^{9',13'}.1^{27',31'}]hexatetraconta-3',5',9',11',13'(44'),16',18',21',23',27',29',31'(39'),34',36',37',40',42',45'-octadecaen-20',1''-cyclohexan]-8',14',26',32'-tetraon-29-yl]pyrene, "tetramacrocycle pyrene" (21)



To a mixture of macrocycle boronic acid pinacol ester **4** (100 mg, 0.0920), Pd(PPh₃)₄ (2.55 mg, 2.21 μmol), Cs₂CO₃ (36.0 mg, 0.110 mmol) in dry toluene (7 ml) and dry DMF (7 ml) was added 1,3,6,8-tetrabromopyrene (9.56 mg, 0.0184 mmol) under argon. The reaction was continued at 120 °C for 2 days by which time a blue fluorescence from the reaction mixture under UV light was observed. All solvents were evaporated and the crude product was applied on a silica column, eluting with 5% methanol in CH₂Cl₂. The product obtained was analyzed by ¹H NMR and ESI-MS and was found out to be contaminated with trismacrocyclepyrene and bismacrocycle (homocoupling). Thus PTLC was applied and the products obtained were separately subjected to ESI-MS to check their identities. Yield: 60% (after first column).

C₂₇₂H₂₉₀N₁₆O₁₆

4039,31 g mol⁻¹

MS (ESI-FTICR)

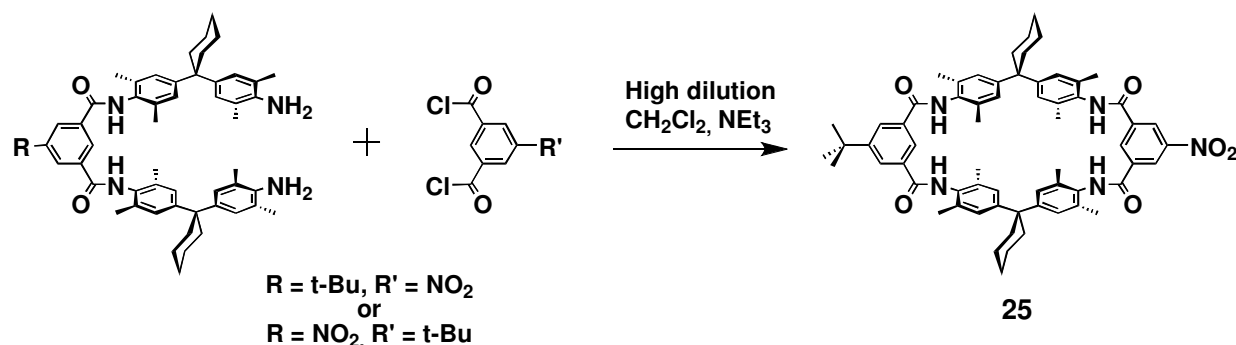
m/z (%) = 4139.331 (12) [M+HNEt₃⁺]⁺, 2120.232 (100) [M+2HNEt₃⁺]²⁺.

¹H NMR

(250 MHz, CDCl₃/CD₃OD) δ [ppm] = 1.35 (s, 36H, CCH₃), 1.40-1.60 (br, 48H, Cy), 2.11 (s, 96H, PhCH₃), 2.27 (br, 32H, Cy), 6.92 (s, 32H, PhH), 8.07 (s, 4H, 2-isophth), 8.14 (s, 8H, 4,6-isophth), 8.40 (s, 4H, Ar_{pyre}), 8.44 (s, 2H, Ar_{pyre}).

E.4.4. Functionalized Macrocycles by other methods than coupling reactions

11'-*tert*-butyl-29'-nitro-5',17',23',35',38',40',43',45'-octamethyldispiro[cyclohexan-1,2'-7',15',25',33'-tetraazaheptacyclo[32.2.2.2^{3',6'}.2^{16',19'}.2^{21',24'}.1^{9',13'}.1^{27',31'}]hexatetraconta-3',5',9',11',13'(44'),16',18',21',23',27',29',31'(39'),34',36',37',40',42',45'-octadecaen-20',1''-cyclohexan]-8',14',26',32'-tetraon, “nitro macrocycle”, (25)



A solution of *t*-butyl extended diamine **P28** (831 mg, 1.00 mmol) and triethyl amine (2 ml) in 250 ml of dry dichloromethane and a solution of nitro isophthalic acid dichloride **P26** (248 mg, 1 mmol) in 250 ml of dry dichloromethane were separately dropped 8 hours via a solvent pump into a flask containing 1.2 L of dry dichloromethane under argon with continuous stirring at room temperature. After the additions were complete, the reaction was continued one more day at room temperature. Then the solvent was completely evaporated and the residue was applied on a column of silica gel using dichloromethane/ethyl acetate (6:1). After the first band which is the catenane, macrocycle was collected as the second band, evaporated and dried. (To obtain larger amounts of the cycle with lower costs, the reaction was done four times and the crude products were combined and applied on a large column to save time, silica gel and solvent.) Yield: 250 mg, 25%.

C₆₄H₇₁N₅O₆

1005,54 g mol⁻¹

MS (ESI-FTICR)

m/z (%) = 1006.54 [M+H]⁺ (100).

¹H NMR

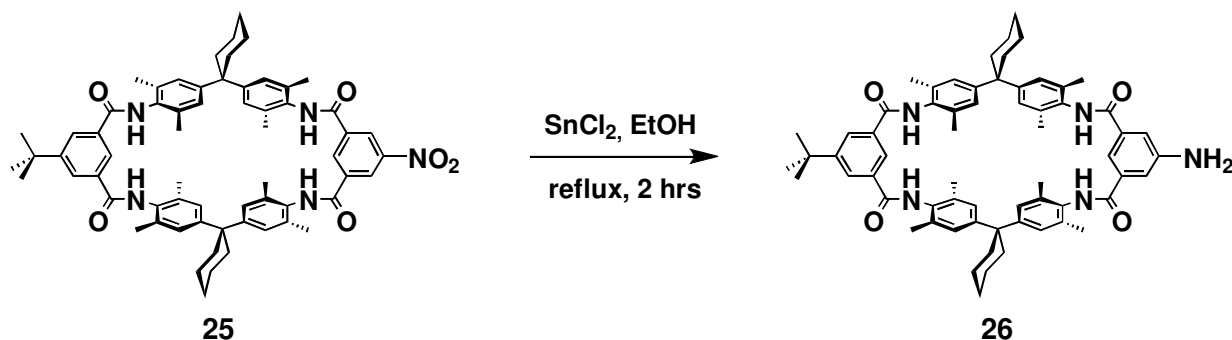
(250 MHz, CDCl₃/CD₃OD, (7:1)): δ [ppm] = 1.34 (s, 9H, CH₃C), 1.35-1.61 (br, 12H, CH₂ of Cy), 1.96 (s, 24 H, PhCH₃), 2.27 (br, 8H, CH₂ of Cy), 6.91 (s, 4H, PhH), 6.93 (s, 4H, PhH), 8.06 (s, 2H, 4,6-isophth), 8.11 (s, 1H, 2-isophth), 8.66 (s, 2H, 4,6-isophth), 8.90 (s, 1H, 2-isophth).

¹³C NMR

(250 MHz, CDCl₃/CD₃OD, (7:1)) δ [ppm] = 13.81 (CH₃C), 18.39 (CH₃Ph), 22.75 (CH₂), 26.18 (CH₂), 30.96 (CH₂), 34.94

(CCH₃), 45.00 (C_{Cy}), 125.41 (CH_{Ph} 2-*t*-Bu-isophth), 125.97 (CH_{Ph}), 126.00 (CH_{Ph}), 128.13 (CH 4,6-nitro-isophth), 130.85 (CH 4,6-*t*-Bu-isophth), 131.25 (CH 2-nitro-isoph), 134.00 (CH 4,6-*t*-Bu-isoph), 134.82 (C_{Ph}), 134.93 (C_{Ph}), 136.12 (C 5-*t*-bu-isophth), 147.74 (C_{Ph}), 148.13 (C_{Ph}), 153.19 (C 5-nitro-isoph), 163.83 (CO), 166.48 (CO).

11'-amino-29'-*tert*-butyl-5',17',23',35',38',40',43',45'-octamethyldispiro[cyclohexan-1,2'-7',15',25',33'-tetraazaheptacyclo[32.2.2.2.2^{3',6'}.2^{16',19'}.2^{21',24'}.1^{9',13'}.1^{27',31'}]hexatetraconta-3',5',9',11',13'(44'),16',18',21',23',27',29',31'(39'),34',36',37',40',42',45'-octadecaen-20',1''-cyclohexan]-8',14',26',32'-tetraon, “amino macrocycle” (**26**)



Nitro macrocycle **25** (100 mg, 0.1 mmol) was dissolved in 25 ml of ethanol and at room temperature tin(II) chloride (90 mg, 0.4 mmol) was added. The mixture was refluxed for two hours monitored with TLC and when almost all the nitro macrocycle turned into amino macrocycle, cooled to room temperature. 1 M NaOH solution was added until the pH was 10. Then the precipitate was filtered with 20 ml of dichloromethane and applied on a silica gel column eluting with dichloromethane/ethanol (9:1). 50 mg of white compound was obtained. (Application on silica gel as stated in the literature, was found out to reduce yields significantly. If the products of the next step could be separated easily column chromatography should be avoided at this step).

C₆₄H₇₃N₅O₄

976,30 g mol⁻¹

MS (ESI-FTICR)

m/z (%) = 976.55 (11) [M+H]⁺, 1952.04 (100) [2M+H]⁺.

¹H NMR

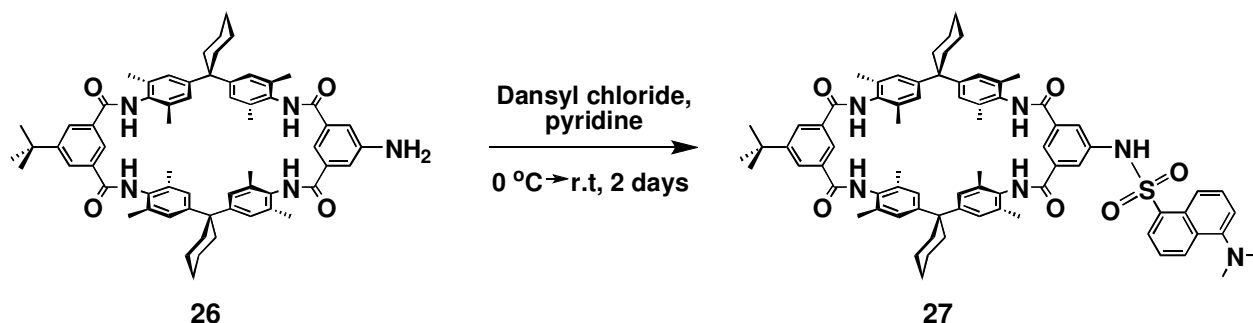
(250 MHz, CDCl₃/CD₃OD, 7:1) δ [ppm] = 1.42 (s, 9H, CH₃C), 1.50-1.65 (br, 12H, CH₂ of Cy), 2.16 (s, 12 H, PhCH₃), 2.18 (s, 12 H, PhCH₃), 2.33 (br, 8H, CH₂ of Cy), 6.99 (s, 8H,

PhH), 7.39 (s, 2H, 4,6-isophth), 7.63 (s, 1H, 2-isophth), 8.14 (s, 1H, 2-isophth), 8.20 (s, 2H, 4,6-isophth), 8.61 (s, 4H, NH).

¹³C NMR

(250 MHz, CDCl₃/CD₃OD, 7:1): δ [ppm] = 18.29, 22.57, 26.03, 29.37, 30.83, 44.84, 116.63, 125.89, 126.10, 128.12, 131.03, 131.11, 131.22, 133.92, 134.82, 135.17, 147.76, 153.14, 164.26.

11'-tert-butyl-29'-(5-(dimethylamino)naphthalene-1-sulfonamide)-5',17',23',35',38',40',43',45'-octamethyldispiro[cyclohexan-1,2'-7',15',25',33'-tetraazaheptacyclo[32.2.2.2.2^{3',6'}.2^{16',19'}.2^{21',24'}.1^{9',13'}.1^{27',31'}]hexatetraconta-3',5',9',11',13'(44'),16',18',21',23',27',29',31',(39'),34',36',37',40',42',45'-octadecaen-20',1''-cyclohexan]-8',14',26',32'-tetraon, "dansyl macrocycle" (27)



Amino macrocycle **26** (50 mg, 0.05 mmol) in dry pyridine (5 ml) was added to the solution of dansyl chloride (27.6 mg, 0.1 mmol) in dry pyridine (15 ml) at 0°C in four portions under argon. The mixture was allowed to react for two days at room temperature. Pyridine was evaporated and the residue was applied on a column. CH₂Cl₂/Methanol (95:5). *R_f* = 0.5. The product collected was evaporated and dried. Yield: 54.4 mg, 90%.

C₇₆H₈₄N₆O₆S

1209,58 g mol⁻¹

MS (FAB)

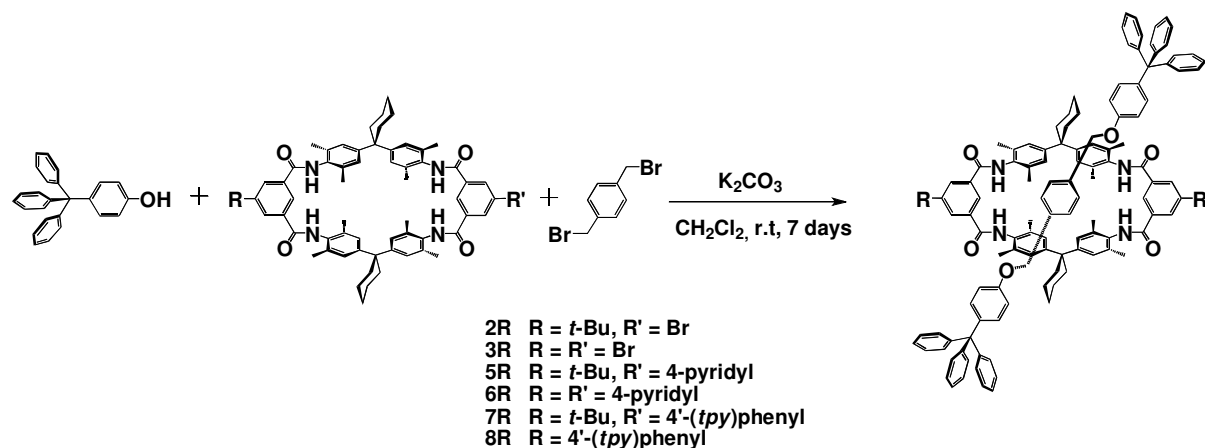
m/z = 1208.7 [M]⁺.

¹H NMR

(500 MHz, DMSO-*d*₆) δ [ppm] = 1.35 (s, 9H, CH₃C), 1.45-1.65 (br, 12H, Cy), 2.02 (s, 12 H; PhCH₃), 2.08 (s, 12 H, PhCH₃), 2.30 (br, 8H, Cy), 6.98 (s, 4H, PhH), 6.99 (s, 4H, PhH), 7.26 (d, 1H, *J* = 7.3 Hz), 7.61 (t, 2H, *J* = 7.7 Hz), 7.66 (t, 2H, *J* = 7.7 Hz), 7.72 (s, 2H, 4,6-isophth), 8.03 (s, 2H, 4,6-isophth), 8.16 (s, 1H, 2-isophth), 8.24 (d, 1H, *J* = 7.3 Hz), 8.37 (d, 1H, *J* = 8.7 Hz), 8.42 (s, 1H, 2-isophth), 8.47 (d, 1H, 8.4 Hz), 9.16 (s, 4H, NH), 9.22 (s, 4H, NH) .

¹³C NMR

(250 MHz, CDCl₃) δ [ppm] = 14.10, 18.87, 18.98, 22.67, 22.70, 22.92, 29.34, 29.63, 29.68, 31.18, 31.24, 31.90, 35.29, 45.29, 65.32, 126.45, 126.96, 127.57, 127.97, 128.47, 128.49, 129.33, 131.14, 134.65, 137.42.

E.4.5. Rotaxanes**E.4.5.1 Functionalized rotaxanes through classical rotaxane synthesis**

[2]-{1,4-bis((4-tritylphenoxy)methyl)benzene}-{11'-bromo-29'-*tert*-butyl-5',17',23',35',38',40',43',45'-octamethyldispiro[cyclohexan-1,2'-7',15',25',33'-tetraazaheptacyclo[32.2.2.2^{3',6'}.2^{16',19'}.2^{21',24'}.1^{9',13'}.1^{27',31'}]hexatetraconta-3',5',9',11',13'(44'),16',18',21',23',27',29',31'(39'),34',36',37',40',42',45'-octadecaen-20',1''-cyclohexan]-8',14',26',32'-tetraon} rotaxan, "bromo rotaxane" (2R)

Dibenzo[18]crown-6 (13.0 mg, 0.036 mmol), bromo macrocycle **2** (150 mg, 0.144 mmol), potassium carbonate (198 mg, 1.44 mmol), α,α' -dibromoparaxylene (38.0 mg, 0.144 mmol) and tritylphenol (96.9 mg, 0.288 mmol) were stirred in 20 ml dry dichloromethane for a week. The solvent was then evaporated and the residue was eluted on a silica column with 2% methanol in dichloromethane. Second band was collected as the pure rotaxane. R_f = 0.5. Yield: 100 mg, 38%.

C₁₂₂H₁₁₇BrN₄O₆

1815,16 g mol⁻¹

MS (ESI-FTICR)

m/z (%) = 1914.956 (100) [M+HNEt₃]⁺.

¹H NMR

(250 MHz, CDCl₃) δ [ppm] = 1.27 (s, 9H, CCH₃), 1.40-1.65 (br, 12H, Cy), 1.81 (s, 12H PhCH₃), 1.83 (s, 12H PhCH₃), 2.26 (br, 8H, Cy), 4.22 (s, 4H, OCH₂), 5.98 (s, 4H, PhH_{axle}), 6.34 (d, J = 4.5 Hz, PhH_{stopper}), 6.96 (s, 8H, PhH), 6.98 (d, J = 4.5 Hz,

PhH_{stopper}), 7.07-7.18 (m, 30 H, PhH_{stopper}), 7.46 (s, 1H, 2-isophth), 7.63 (s, 1H, 2-isophth), 8.05 (s, 2H, 4,6-isophth), 8.14 (s, 2H 4,6-isophth).

¹³C NMR

(250 MHz, CDCl₃ +2 drops of CD₃OD) δ [ppm] = 18.30, 30.79, 34.98, 4.03, 110.48, 112.87, 113.12, 125.56, 125.81, 126.39, 126.45, 127.11, 127.17, 127.26, 127.42, 130.47, 130.61, 130.66, 130.80, 132.33, 134.66, 134.77, 135.86, 140.78, 140.31, 161.62.

[2]-{1,4-bis((4-tritylphenoxy)methyl)benzene}-{11',29'-dibromo-5',17',23',35',38',40',43',45'-octamethyldispiro[cyclohexan-1,2'-7',15',25',33'-tetraazaheptacyclo[32.2.2.2.2^{3',6'}.2^{16',19'}.2^{21',24'}.1^{9',13'}.1^{27',31'}]hexatetraconta-3',5',9',11',13'(44'),16',18',21',23',27',29',31'(39'),34',36',37',40',42',45'-octadecaen-20',1''-cyclohexan]-8',14',26',32'-tetraon} rotaxan, “dibromo rotaxane” (3R)

Dibenzo[18]crown-6 (31.1 mg, 0.0863 mmol), dibromo macrocycle **3** (367 mg, 0.345 mmol), potassium carbonate (476 mg, 3.45 mmol), α,α'-dibromoparaxylene (91.0 mg, 0.345 mmol) and tritylphenol (232 mg, 0.690 mmol) were stirred in 20 ml dry dichloromethane for a week. The solvent was then evaporated and the residue was eluted on a silica column with 2% methanol in dichloromethane. Second band was collected as the pure rotaxane. *R_f* = 0.85. Yield: 35%.

C₁₁₈H₁₀₈Br₂N₄O₆

1837,95 g mol⁻¹

MS (ESI-FTICR)

m/z (%) = 1869.61 (100) [M+Cl]⁻.

¹H NMR

(250 MHz, CDCl₃) δ [ppm] = 1.40-1.71 (br, 12H, Cy), 1.83 (s, 24H PhCH₃), 2.30 (br, 8H, Cy), 4.33 (s, 4H, OCH₂), 5.84 (s, 4H, PhH_{axle}), 6.44 (d, *J* = 9.0 Hz, PhH_{stopper}), 6.98 (s, 8H, PhH), 7.04 (d, *J* = 9.0 Hz, PhH_{stopper}), 7.08-7.25 (m, 30 H, PhH_{stopper}), 7.63 (s, 1H, 2-isophth), 8.22 (s, 2H, 4,6-isophth).

[2]-{1,4-bis((4-tritylphenoxy)methyl)benzene}-{11'-*t*-butyl-29'-pyridyl-5',17',23',35',38',40',43',45'-octamethyldispiro[cyclohexan-1,2'-7',15',25',33'-tetraazaheptacyclo[32.2.2.2^{3',6'}.2^{16',19'}.2^{21',24'}.1^{9',13'}.1^{27',31'}]hexatetraconta-3',5',9',11',13'(44'),16',18',21',23',27',29',31'(39'),34',36',37',40',42',45'-octadecaen-20',1''-cyclohexan]-8',14',26',32'-tetraon} rotaxan, "pyridine rotaxane" (**5R**)

Dibenzo[18]crown-6 (31.1 mg, 0.0863 mmol), pyridine macrocycle **5** (367 mg, 0.345 mmol), potassium carbonate (476 mg, 3.45 mmol), α,α' -dibromoparaxylene (91.0 mg, 0.345 mmol) and tritylphenol (232 mg, 0.690 mmol) were stirred in 20 ml dry dichloromethane for a week. The solvent was then evaporated and the residue was eluted on a silica column with 2% methanol in dichloromethane. Second band was collected as the pure rotaxane. $R_f = 0.23$. Yield: 82%.

C₁₂₇H₁₂₁N₅O₆

1813,35 g mol⁻¹

MS (ESI-FTICR)

m/z (%) = 1915.06 (100) [M+HNEt₃]⁺, 1851.90 (20) [M+K]⁺, 1834.93 (12) [M+Na]⁺, 1813.94 (4) [M+H]⁺.

¹H NMR

(250 MHz, CDCl₃) δ [ppm] = 1.40 (s, 9H, CCH₃), 1.49-1.72 (br, 12H, Cy), 1.88 (s, 24H, PhCH₃), 2.32 (br, 8H, Cy), 4.34 (s, 4H, OCH₂), 5.89 (s, 4H, PhH_{axle}), 6.38 (d, $J = 9.1$ Hz, PhH_{stopper}), 6.96 (d, $J = 9.1$ Hz, PhH_{stopper}), 7.00 (s, 8H, PhH), 7.01-7.22 (m, 30 H, PhH_{stopper}), 7.36 (s, 2H, 4,6-isophH), 7.53 (d, $J = 6.4$, 2H, H_{pyr}), 7.82 (s, 1H, 2-isophth), 8.17 (s, 1H, 2-isophth), 8.37 (s, 2H, 4,6-isophth). 8.59 (d, $J = 6.4$ Hz, 2H, H_{pyr}).

¹³C NMR

(250 MHz, CDCl₃ + 2 drops of CD₃OD) δ [ppm] = 18.36, 22.72, 29.41, 30.83, 35.33, 45.09, 64.02, 70.26, 113.10, 122.49, 125.87, 126.51, 127.29, 128.88, 130.68, 130.82, 131.91, 132.37, 132.59, 134.72, 134.82, 135.55, 140.87, 146.29, 148.50, 148.91, 153.37, 160.59, 165.93.

[2]-{1,4-bis((4-tritylphenoxy)methyl)benzene}-{11',29'-dipyridyl-5',17',23',35',38',40',43',45'-octamethyldispiro[cyclohexan-1,2'-7',15',25',33'-tetraazaheptacyclo[32.2.2.2^{3',6'}.2^{16',19'}.2^{21',24'}.1^{9',13'}.1^{27',31'}]hexatetraconta-3',5',9',11',13'(44'),16',18',21',23',27',29',31'(39'),34',36',37',40',42',45'-octadecaen-20',1''-cyclohexan]-8',14',26',32'-tetraon} rotaxan, "bispyridinerotaxane" (6R)

Dibenzo[18]crown-6 (8.75 mg, 0.024 mmol), bispyridine macrocycle 6 (103 mg, 0.097 mmol), potassium carbonate (134 mg, 0.97 mmol), α,α' -dibromoparaxylene (25.7 mg, 0.097 mmol) and tritylphenol (65.3 mg, 0.194 mmol) were stirred in 10 ml dry dichloromethane for a week. The solvent was then evaporated and the residue was eluted on a silica column with 2% methanol in dichloromethane. Second band was collected as the pure rotaxane. $R_f = 0.7$. Yield: 45%.

C₁₂₈H₁₁₆N₆O₆

1834,33 g mol⁻¹

MS (ESI-FTICR)

m/z (%) = 1831.899 [M-H]⁻.

¹H NMR

(250 MHz, CDCl₃) δ [ppm] = 1.50-1.72 (br, 12H, Cy), 1.87 (s, 24H, PhCH₃), 2.32 (br, 8H, Cy), 4.38 (s, 4H, OCH₂), 5.89 (s, 4H, PhH_{axle}), 6.45 (d, $J = 9.0$ Hz, PhH_{stopper}), 6.97 (d, $J = 4.4$ Hz, PhH_{stopper}), 7.01 (s, 8H, PhH), 7.05-7.22 (m, 30 H, PhH_{stopper}), 7.52 (d, $J = 6.4$, 2H, H_{pyr}), 7.82 (s, 1H, 2-isophth), 8.36 (s, 2H, 4,6-isophth). 8.63 (d, $J = 6.4$, 2H, H_{pyr}).

¹³C NMR

(250 MHz, CDCl₃) δ [ppm] = 18.25, 22.62, 25.94, 35.21, 45.01, 48.25, 48.94, 63.98, 68.09, 69.45, 70.03, 113.14, 121.13, 121.70, 125.50, 125.73, 126.43, 127.05, 127.17, 127.40, 129.89, 130.61, 130.66, 130.74, 132.25, 134.68, 134.74, 135.19, 135.57, 139.51, 140.64, 146.29, 146.56, 146.81, 148.52, 149.37, 155.53, 165.19, 165.33. MS-ESI: m/z = 1935.03 [M+HNEt₃]⁺ (100).

[2]-{1,4-bis((4-tritylphenoxy)methyl)benzene}-{11'-*t*-butyl-29'-(2,2'-6',2''-terpyridyl) -5', 17',23',35',38',40',43',45'-octamethyldispiro[cyclohexan-1,2'-7',15',25',33'-tetraaza heptacyclo[32.2.2.2^{3',6'}.2^{16',19'}.2^{21',24'}.1^{9',13'}.1^{27',31'}]hexatetraconta-3',5',9',11',13'(44'),16', 18',21',23',27',29',31'(39'),34',36',37',40',42',45'-octadecaen-20',1''-cyclohexan]-8',14', 26',32'-tetraon}rotaxan, "terpyridine rotaxane" (7R)

Dibenzo[18]crown-6 (13.0 mg, 0.036 mmol), terpyridine macrocycle **7** (150 mg, 0.144 mmol), potassium carbonate (198 mg, 1.44 mmol), α,α' -dibromoparaxylene (38.0 mg, 0.144 mmol) and tritylphenol (96.9 mg, 0.288 mmol) were stirred in 20 ml dry dichloromethane for a week. The solvent was then evaporated and the residue was eluted on an alumina column with 2% methanol in dichloromethane. Second band was collected as the pure rotaxane. Yield: 100 mg, 38%.

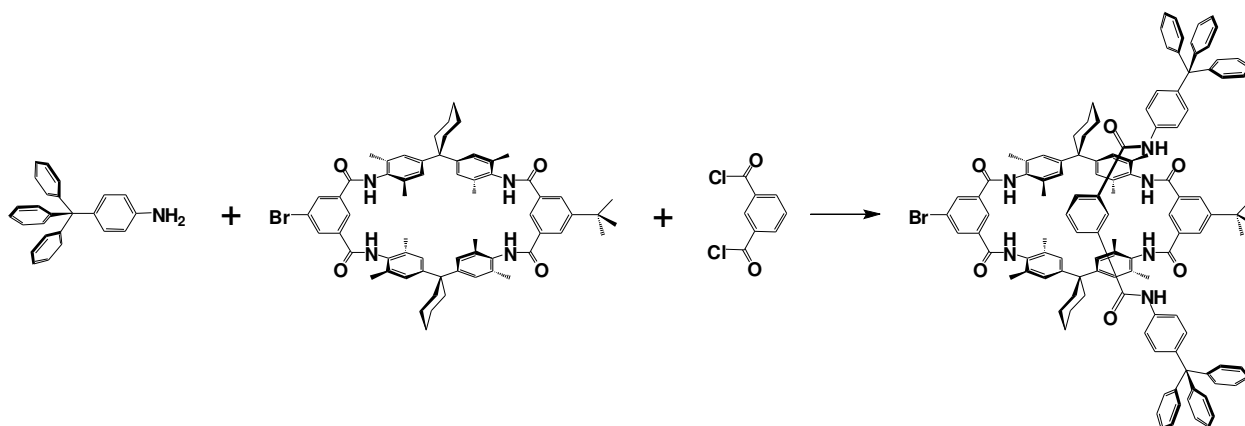
¹H NMR (250 MHz, CDCl₃) δ [ppm] = 1.31 (s, 9H CCH₃), 1.50-1.70 (br, 12H, Cy), 1.88 (s, 12H PhCH₃), 1.90 (s, 12H, PhCH₃), 2.33 (br, 8H, Cy), 4.36 (s, 4H, OCH₂), 5.89 (s, 4H, PhH_{axle}), 6.40 (d, J = 4.5 Hz, PhH_{stopper}), 6.99 (d, J = 4.5 Hz, PhH_{stopper}), 7.02 (s, 8H, PhH), 7.09-7.25 (m, 30 H, PhH_{stopper}), 7.31 (d, J = 7.7 Hz, 2H, 5,5''-tpy), 7.54 (s, 1H, 2-isophth), 7.75 (s, 1H, 2-isophth), 7.76 (d, J = 8.3 Hz, 2H, PhH), 7.87 (t, J = 7.7 Hz, 2H, 4,4''-tpy), 7.97 (d, J = 8.3 Hz, 2H, PhH), 8.14 (s, 2H, 4,6-isophth), 8.42 (s, 2H 4,6-isophth), 8.86 (d, J = 7.7 Hz, 2H, 3,3''-tpy), 8.73 (d, J = 7.7 Hz, 2H, 6,6''-tpy), 8.78 (s, 2H, 3,5'-tpy).

¹³C NMR (250 MHz, CDCl₃): δ [ppm] = 18.65, 23.05, 26.34, 31.16, 35.74, 45.40, 64.27, 70.85, 113.38, 118.77, 121.38, 121.69, 123.11, 123.84, 126.11, 126.90, 127.53, 127.81, 127.92, 129.15, 130.45, 130.95, 131.03, 131.17, 132.69, 134.60, 135.11, 135.40, 135.72, 136.85, 138.44, 139.47, 141.23, 142.86, 146.54, 149.05, 149.16, 149.21, 149.49, 154.22, 155.73, 156.09, 156.24, 165.16, 165.75.

MS (ESI-FTICR) m/z (%): 2043.02 (100) [M+H]⁺, 2144.14 (40) [M+HNEt₃]⁺.

E.4.5.2 Amide-axle rotaxanes

[2]-{*N*¹,*N*³-bis(4-tritylphenyl)isophthalamide}-{11'-bromo-29'-*tert*-butyl-5',17',23',35',38',40',43',45'-octamethyldispiro[cyclohexan-1,2'-7',15',25',33'-tetraazaheptacyclo[32.2.2.2^{3',6'}.2^{16',19'}.2^{21',24'}.1^{9',13'}.1^{27',31'}]hexatetraconta-3',5',9',11',13'(44'),16',18',21',23',27',29',31'(39'),34',36',37',40',42',45'-octadecaen-20',1''-cyclohexan]-8',14',26',32'-tetraon} rotaxan, "amide rotaxane" (2R')



Bromo macrocycle **2** (200 mg, 0.193 mmol) and isophthalic acid dichloride (39.2 mg, 0.193 mmol), in 10 ml dry dichloromethane were added trityl aniline (129 mg, 0.385 mmol) and triethylamine (0.2 ml) dropwise and stirred for a week. The solvent was then evaporated and the residue was eluted on a silica column with 40:1, CH₂Cl₂/CH₃OH. Third band was collected as the pure rotaxane. Yield: 65%.

C₁₂₂H₁₁₅BrN₆O₆

1841,16 g mol⁻¹

MS (ESI-FTICR)

m/z (%) = 1864.80 (20) [M+Na]⁺, 2144.14 (100) [M+HNEt₃]⁺.

¹H NMR

(250 MHz, CDCl₃:CD₃OD, 5:1) δ [ppm] = 1.19 (s, 9H CCH₃), 1.45-1.53 (br, 12H, Cy), 1.79 (s, 24H PhCH₃), 2.19 (br, 8H, Cy), 6.81 (s, 8H, PhH), 6.82 (d, PhH_{stopper}), 7.05-7.10 (m, 3H, 4,5,6-isophth_{axle}), 7.17 (m, 38 H, PhH_{stopper}), 7.36 (s, 1H, 2-isophth), 7.48 (s, 1H, 2-isophth), 7.68 (s, 1H, 2-isophth_{axle}), 7.74 (s, 2H, 4,6-isophth), 8.01 (s, 2H 4,6-isophth), 8.37 (s, 2H, NH), 8.69 (s, 2H, NH), 9.56 (s, 2H, NH_{axle})

*N*¹,*N*³-bis(4-tritylphenyl)isophthalamide

Obtained as a by-product of the threading reaction. Collected as the second band from the column as a white solid. Yield: 20%.

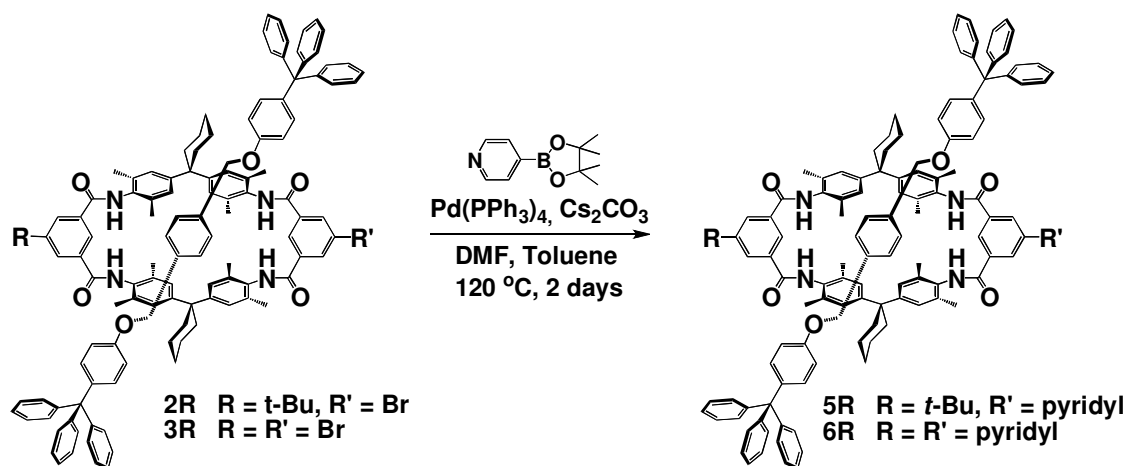
C₅₈H₄₄N₂O₂

800,98 g mol⁻¹

¹H NMR

(250 MHz, DMSO-*d*₆) δ [ppm] = 7.10-7.32 (m, 38H, PhH_{stopper}), 7.70 (d, *J* = 8.8 Hz, 2H, 4,6-isophth), 8.11 (d, *J* = 8.8 Hz, 1H, 5-isophth), 8.47 (s, 1H, 2-isophth), 10.44 (s, 2H, NH).

E.4.5.3 Suzuki coupling on rotaxanes



[2]-{1,4-bis((4-tritylphenoxy)methyl)benzene}-{11'-*t*-butyl-29'-pyridyl-5',17',23',35',38',40',43',45'-octamethyldispiro[cyclohexan-1,2'-7',15',25',33'-tetraazaheptacyclo[32.2.2.2^{3',6'}.2^{16',19'}.2^{21',24'}.1^{9',13'}.1^{27',31'}]hexatetraconta-3',5',9',11',13'(44'),16',18',21',23',27',29',31'(39'),34',36',37',40',42',45'-octadecaen-20',1''-cyclohexan]-8',14',26',32'-tetraon} rotaxan, "pyridine rotaxane" (**5R**)

(Post-functionalization of bromo rotaxane **2R**) To a mixture of bromo rotaxane **2R** (80 mg, 0.044), $\text{Pd(PPh}_3)_4$ (1.53 mg, 1.32 μmol), Cs_2CO_3 (21.5, 0.066 mmol) in dry toluene (5 ml) and dry DMF (5 ml) was added pyridine boronic acid pinacol ester (11.3 mg, 0.055 mmol) under argon. The reaction was continued at 120 °C for 2 days. All solvents were evaporated and the crude product was applied on a silica column, eluting with 2% methanol in CH_2Cl_2 . The product obtained as the third band from the column was dried at high vacuum. Yield: 6%. (major products were free axle 1st band and functionalized macrocycle (4th band))

(data given above)

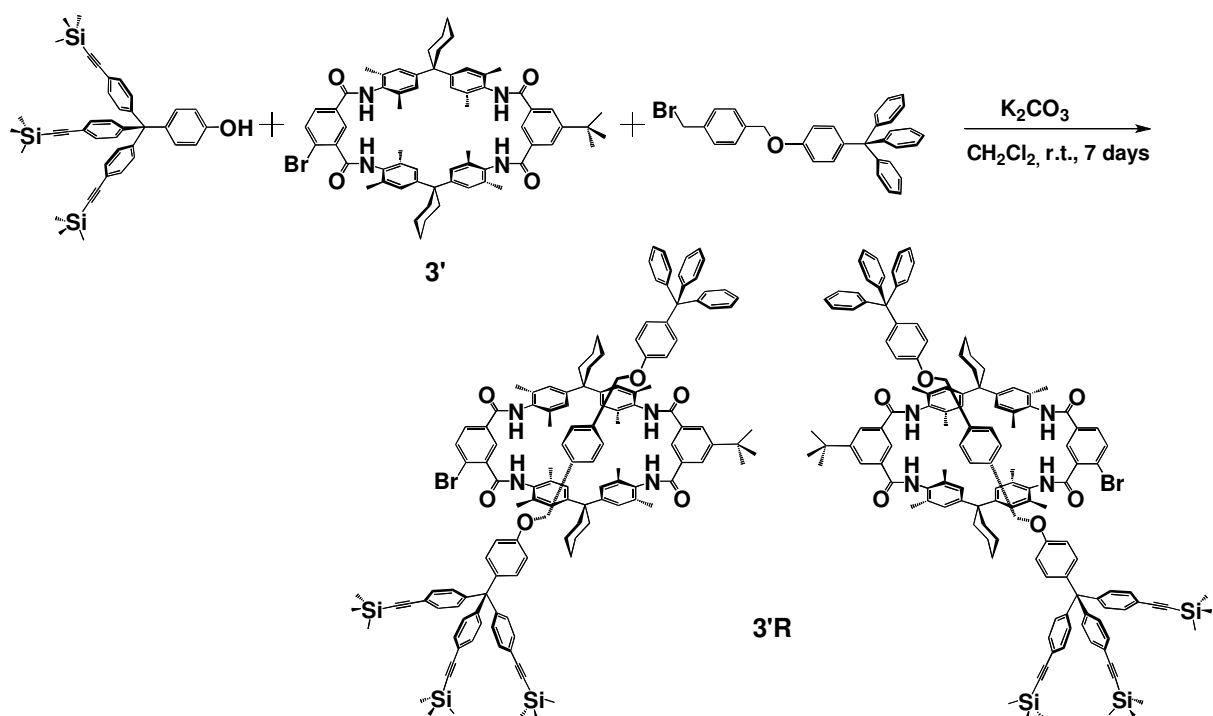
[2]-{1,4-bis((4-tritylphenoxy)methyl)benzene}-{11',29'-dipyridyl-5',17',23',35',38',40',43',45'-octamethyldispiro[cyclohexan-1,2'-7',15',25',33'-tetraazaheptacyclo[32.2.2.2.^{3',6',2^{16',19'},2^{21',24'},1^{9',13'},1^{27',31'}]}hexatetraconta-3',5',9',11',13'(44'),16',18',21',23',27',29',31'(39'),34',36',37',40',42',45'-octadecaen-20',1''-cyclohexan]-8',14',26',32'-tetraon} rotaxan, “bispyridinerotaxane” (6R)

(Post-functionalization of dibromo rotaxane **3R**) To a mixture of dibromo rotaxane **3R** (20 mg, 0.011), Pd(PPh₃)₄ (0.76 mg, 0.60 μmol), Cs₂CO₃ (10.8 mg, 0.33 mmol) in dry toluene (5 ml) and dry DMF (5 ml) was added pyrimidine boronic acid pinacol ester (5.6 mg, 0.028 mmol) under argon. The reaction was continued at 120 °C for 2 days. All solvents were evaporated and the crude product was applied on a silica column, eluting with 2% methanol in CH₂Cl₂. The product obtained as the third band from the column was dried at high vacuum. Yield: 8%.

(data given above)

E.4.5.4 Enantiomeric rotaxanes

[2]-{4-{4'- [Tris (4''-trimethylsilylethynylphenyl) methyl] phenyloxymethyl}- (4'''-tri phenylmethyl) phenyloxymethyl}-benzol}- {10'-bromo-29'-*tert*-butyl - 5',17',23',35',-38', 40',43',45'- octamethyldispiro [cyclohexan-1,2',7',15',25',33'- tetraazaheptacyclo-[32.2. 2.23',6'.216',19'.221',24'.19',13'.127',31'] hexatetraconta- 3',5',9',11',13'(44'),16',18',21',-23',27', 29',31'(39'),34',36',37',40',42',45'-octadecaen-20',1''-cyclohexan]- 8',14',26',32'- tetraon}rotaxan



Dibenzo[18]crown-6 (13.0 mg, 0.036 mmol), 4-bromo macrocycle **2'** (150 mg, 0.144 mmol), potassium carbonate (199 mg, 1.44 mmol), ((4-(4-(bromomethyl)benzyloxy)phenyl)methanetriyl)tribenzene (74.9 mg, 0.144 mmol) and trimethylsilylethynyl stopper (90.1 mg, 0.144 mmol) were stirred in 50 ml dry dichloromethane for a week. The solvent was then evaporated and the residue was eluted on a silica column with 2% methanol in dichloromethane. Second band was collected as the pure rotaxane. Yield: 85%.

C₁₃₇H₁₄₁BrN₄O₆Si₃

2103,77 g mol⁻¹

MS (ESI-FTICR)

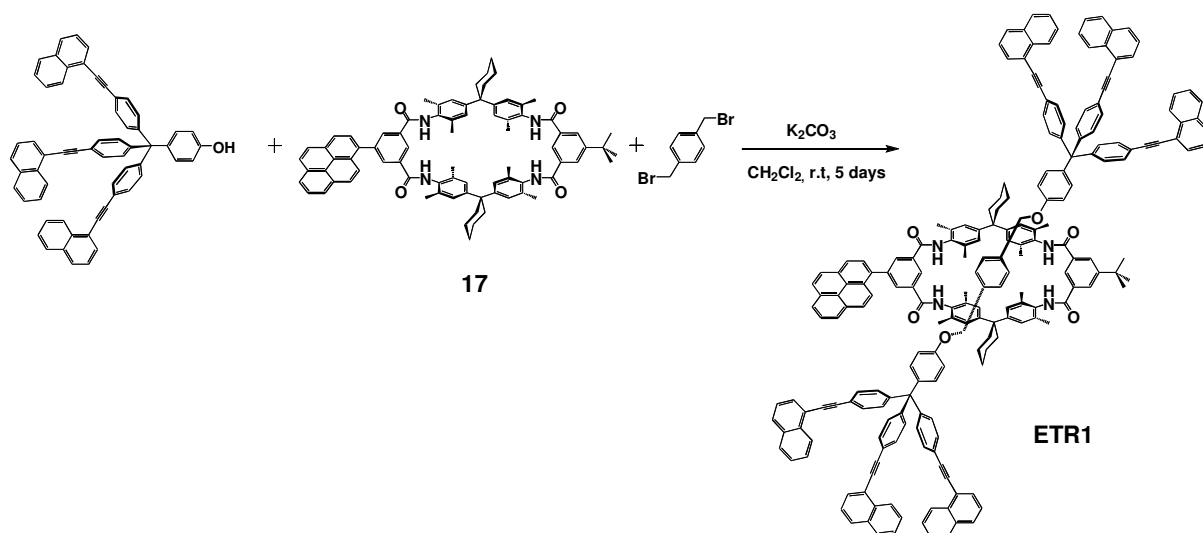
m/z (%) = 2102.94 (42) [M+H]⁺.

¹H NMR

(250 MHz, CDCl₃) δ [ppm] = 0.23 (s, 27H, SiCH₃), 1.19 (s, 9H CCH₃), 1.50-1.65 (br, 12H, Cy), 1.80 (s, 6H PhCH₃), 1.85 (s, 6H PhCH₃), 1.88 (s, 6H PhCH₃), 1.93 (s, 6H PhCH₃), 2.32 (br, 8H, Cy), 6.01 (s, 4H, Ph_{axle}), 6.34 (d, *J* = 9 Hz, PhH_{stopper}), 6.97 (s, 2H, PhH), 6.98 (s, 2H, PhH), 6.99 (s, 2H, PhH), 7.02 (s, 2H, PhH), 6.89-7.35 (m, 35H, PhH_{stopper}), 7.42 (s, 1H, 2-isophth), 7.58 (d, *J* = 3.8 Hz, 1H, 5-isophth), 7.60 (d, *J* = 3.8 Hz, 1H, 6-isophth), 7.84 (s, 1H, 2-isophth), 8.22 (s, 2H 4,6-isophth).

E.4.6. Syntheses of energy-transfer rotaxanes

[2]-{1,4-bis((4-(tris(4-(naphthalen-1-ylethynyl)phenyl)methyl)phenyloxy)methyl)benzene}-{10'-*t*-butyl-29'-pyrenyl-5',17',23',35',38',40',43',45'-octamethyldispiro[cyclohexan-1,2'-7',15',25',33'-tetraazaheptacyclo[32.2.2.2^{3',6'}.2^{16',19'}.2^{21',24'}.1^{9',13'}.1^{27',31'}]hexa tetraconta-3',5',9',11',13'(44'),16',18',21',23',27',29',31'(39'),34',36',37',40',42',45'-octa decaen-20',1''-cyclohexan]-8',14',26',32'-tetraon}rotaxan (ETR1)



Dibenzo[18]crown-6 (3.9 mg, 0.011 mmol), pyrene macrocycle **17** (20.0 mg, 0.017 mmol), potassium carbonate (23.5 mg, 0.17 mmol), α,α'-dibromoparaxylene (4.49 mg, 0.017 mmol) and 4-(tris(4-(naphthalen-1-ylethynyl)phenyl)methyl)phenol (27.2 mg, 0.034 mmol) were stirred in 10 mL dry dichloromethane for a week. The solvent was then evaporated and the residue was eluted on a silica column with dichloromethane. Second band was collected as the pure rotaxane. Yield: 82%.

C₂₁₀H₁₆₂N₄O₆

2837,56 g mol⁻¹

MS (ESI-FTICR)

m/z (%) = 1520.75 (22) [M+2HNEt₃]²⁺, 2939.34 (18) [M+HNEt₃]⁺.

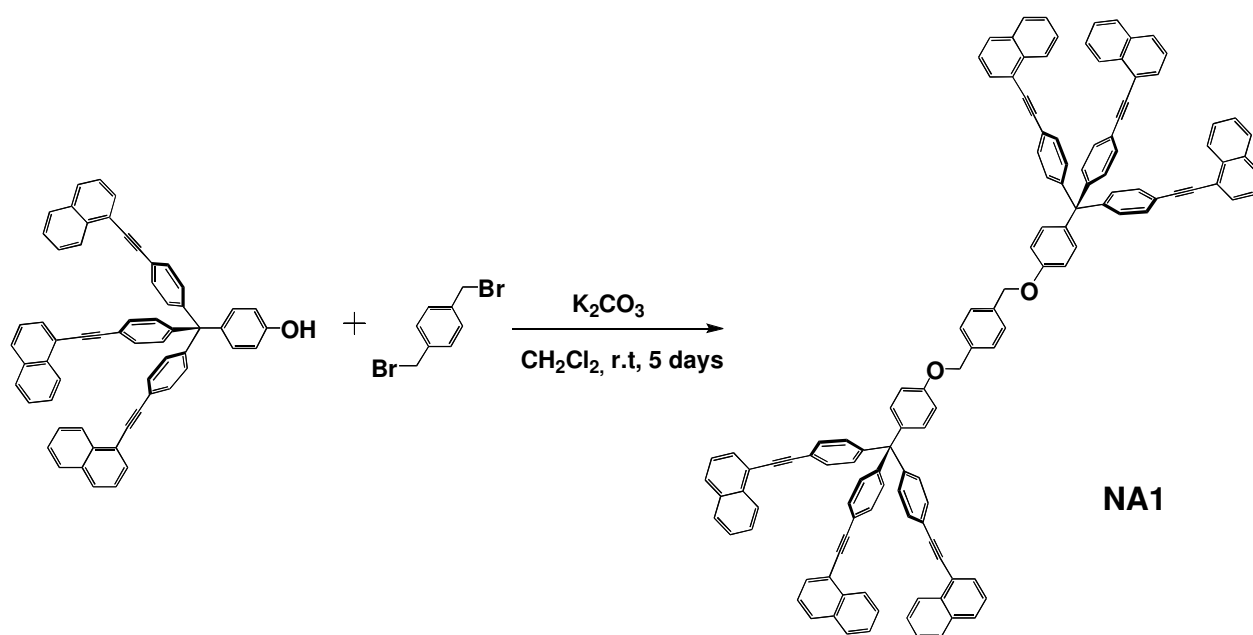
¹H NMR

(250 MHz, CDCl₃) δ [ppm] = 1.32 (s, 9H, CCH₃), 1.45-1.70 (br, 12H, Cy), 1.93 (s, 12H PhCH₃), 1.96 (s, 12H PhCH₃), 2.32 (br, 8H, Cy), 4.44 (s, 4H, OCH₂), 5.93 (s, 4H, PhH_{axle}), 6.52 (d, J = 8.3 Hz, 4H, PhH_{stopper}), 7.05 (s, 8H, PhH), 7.10 (d, J = 8.3 Hz, 4H, PhH_{stopper}), 7.19-8.17 (m, 93H, ArH), 8.38 (d, 12H, 2-Naph).

¹³C NMR

(250 MHz, CDCl₃) δ [ppm] = 14.19, 18.82, 22.77, 23.10, 26.38, 29.43, 29.74, 31.22, 31.99, 35.41, 35.78, 45.49, 64.38, 71.07, 88.23, 93.87, 113.84, 120.81, 121.71, 124.86, 125.35, 126.22, 126.53, 126.90, 127.02, 127.07, 127.84, 127.86, 128.10, 128.25, 128.35, 128.40, 128.46, 128.96, 129.29, 130.54, 130.60, 130.95, 131.10, 131.24, 131.34, 131.59, 132.65, 133.28, 133.32, 133.97, 134.71, 135.01, 135.15, 135.18, 135.68, 140.14, 146.23, 156.23, 165.37, 165.85.

1,4-bis((4-(tris(4-(naphthalen-1-ylethynyl)phenyl)methyl)phenoxy)methyl)benzene (NA1)



This was obtained as the by-product of the rotaxane synthesis. R_f = 0.9. Yield 5%.

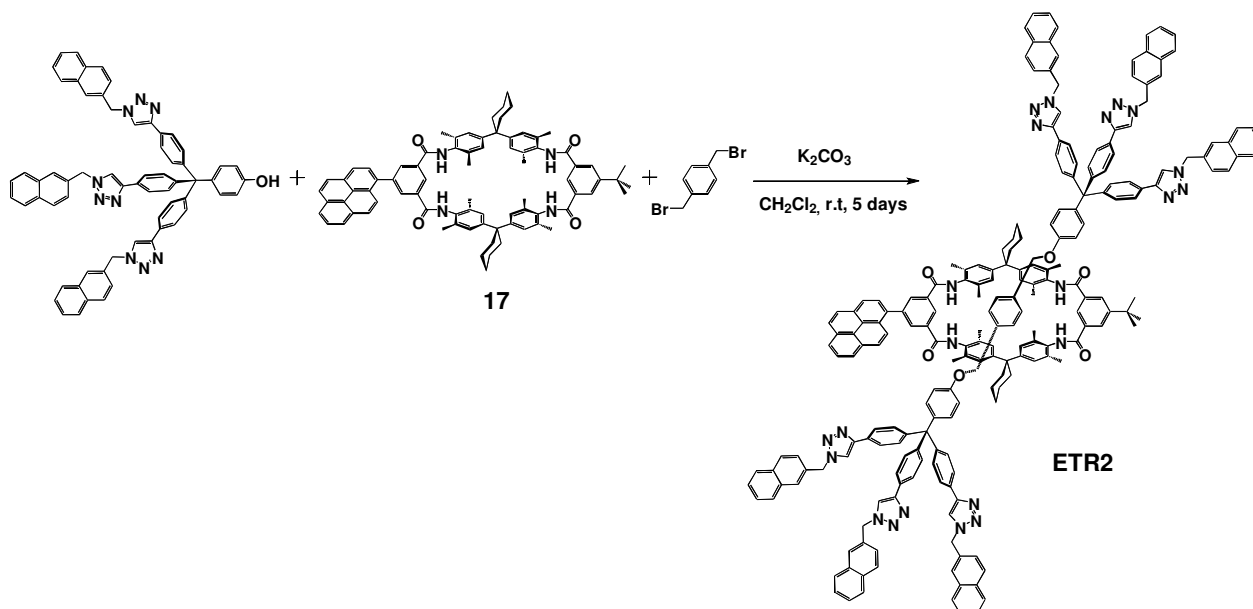
C₁₃₀H₈₂O₂

1676,04 g mol⁻¹

¹H NMR

(250 MHz, CDCl₃) δ [ppm] = 4.96 (s, 4H, CH₂), 6.81 (d, *J* = 7.0 Hz, 2H, PhH), 7.06 (d, *J* = 7.0 Hz, 2H, PhH), 7.18 (d, *J* = 6.8 Hz, 6H, PhH), 7.46 (d, *J* = 6.8 Hz, 6H, PhH), 7.31-7.74 (m, 36 H, Naph), 8.31 (d, *J* = 6.5 Hz, 6H, 2-Naph).

[2]-{1,4-bis((4-(tris(4-(1-(naphthalen-2-ylmethyl)-1H-1,2,3-triazol-4-yl)phenyl)methyl)phenoxy)methyl)benzene}-{10'-*t*-butyl-29'-pyrenyl-5',17',23',35',38',40',43',45'-octamethyldispiro[cyclohexan-1,2'-7',15',25',33'-tetraazaheptacyclo[32.2.2.2.2^{3',6'}.2^{16',19'}.2^{21',24'}.1^{9',13'}.1^{27',31'}]hexatetraconta-3',5',9',11',13'(44'),16',18',21',23',27',29',31'(39'),34',36',37',40',42',45'-octadecaen-20',1''-cyclohexan]-8',14',26',32'-tetraon}rotaxan (ETR2)



Dibenzo[18]crown-6 (3.9 mg, 0.011 mmol), pyrene macrocycle **17** (50 mg, 0.043 mmol), potassium carbonate (59 mg, 0.43 mmol), α,α'-dibromoparaxylene (11.0 mg, 0.043 mmol) and 4-(tris(4-(1-(naphthalen-2-ylmethyl)-1H-1,2,3-triazol-4-yl)phenyl)methyl)phenol (82 mg, 0.086 mmol) were stirred in 10 ml dry dichloromethane for a week. The solvent was then evaporated and the residue was eluted on a silica column with 20:1 dichloromethane/methanol. First band was collected as the pure rotaxane. Yield: 85%.

C₂₁₆H₁₈₀N₂₂O₆

3179,88 g mol⁻¹

MS (ESI-FTICR)

m/z (%): 1691.71 (100) [M+2HNEt₃]²⁺.

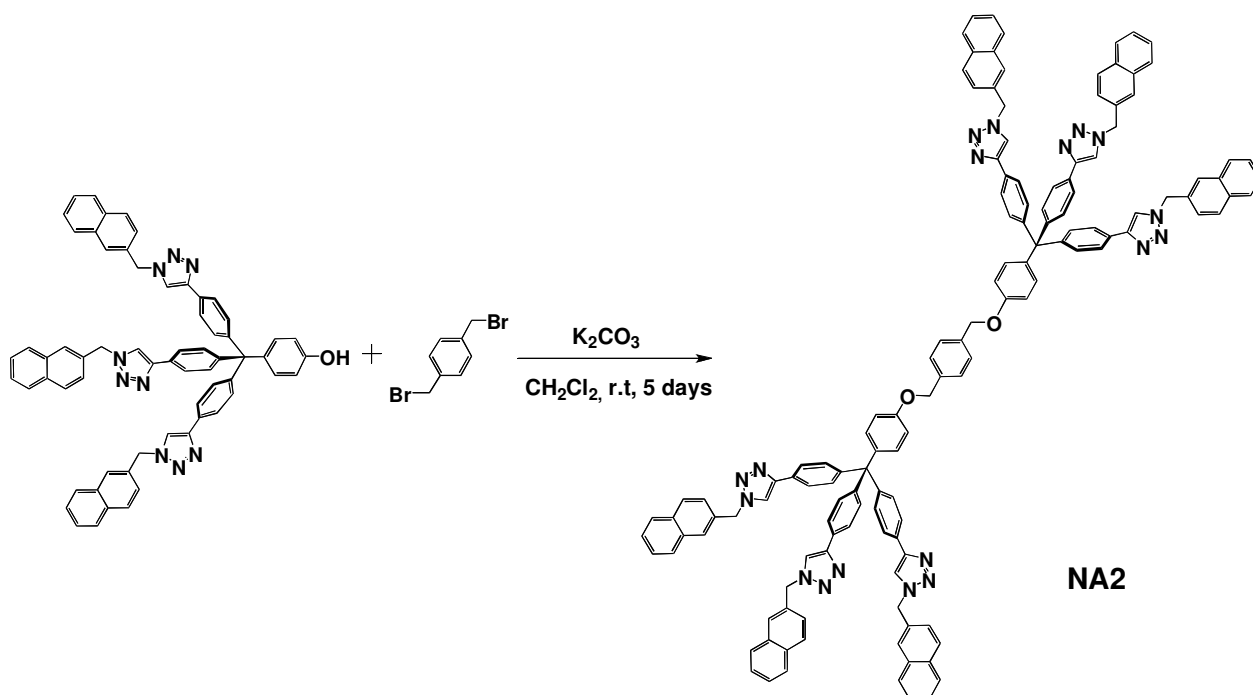
¹H NMR

(250 MHz, CDCl₃+CD₃OD, 5:1) δ [ppm] = 1.11 (s, 9H, CCH₃), 1.40-1.52 (br, 12H, Cy), 1.77 (s, 24H, PhCH₃), 2.11 (br, 8H, Cy), 4.20 (s, 4H, OCH₂), 5.57 (s, 12H, CH₂), 5.91 (s, 4H, PhH_{axle}), 6.34 (d, *J* = 8.3 Hz, 4H, PhH_{stopper}), 6.96 (s, 8H, PhH), 7.00 (d, *J* = 8.3 Hz, 4H, PhH_{stopper}), 7.11-8.02 (m, 99H, ArH), 7.92 (s, 2H, 4,6-isophth), 8.11 (s, 1H, 2-isophth).

¹³C NMR

(250 MHz, CDCl₃) δ [ppm] = 14.04, 18.65, 22.66, 22.93, 29.33, 29.65, 30.95, 31.91, 35.15, 45.30, 53.47, 54.42, 63.93, 70.43, 113.67, 120.09, 124.73, 124.97, 125.06, 125.13, 125.17, 125.19, 126.73, 127.31, 127.34, 127.74, 127.76, 127.83, 127.89, 127.91, 127.95, 128.18, 128.23, 129.02, 129.17, 131.02, 131.10, 131.28, 131.33, 131.38, 131.83, 131.89, 132.39, 133.17, 133.19, 133.21, 134.23, 134.87, 135.06, 135.77, 140.22, 146.35, 146.82, 147.67, 147.86, 166.35, 167.07.

1,4-bis((4-(tris(4-(1-(naphthalen-2-ylmethyl)-1H-1,2,3-triazol-4-yl)phenyl)methyl)phenoxy)methyl)benzene (NA2)



This was obtained as a by-product of the rotaxane synthesis. However, the yield of the compound was quite poor (less than 3%) so it was produced in a separate reaction. The stopper 4-(tris(4-(1-(naphthalen-2-ylmethyl)-1H-1,2,3-triazol-4-yl)phenyl)methyl)phenol (29.0 mg, 0.030 mmol), K₂CO₃ (21 mg, 0.15 mmol), Dibenzo[18]crown-6 (1.35 mg, 0.375

μmol) and α,α' -dibromoparaxylene (3.96 mg, 0.015 mmol) were dissolved in 10 ml of CH_2Cl_2 . The resulting mixture was allowed to stir 2 days by which time the reaction was complete. The only product was filtered through silica on a 10 cm column with dichloromethane. $R_f = 0.9$. Yield: 87%.

$\text{C}_{136}\text{H}_{100}\text{N}_{18}\text{O}_2$

2018,37 g mol⁻¹

^1H NMR

(250 MHz, CDCl_3) δ [ppm] = 4.12 (s, 4H, OCH_2), 5.70 (s, 4H, PhH), 6.70 (d, $J = 8.8$ Hz, 4H, $\text{PhH}_{\text{stopper}}$), 7.00 (d, $J = 8.3$ Hz, 4H, $\text{PhH}_{\text{stopper}}$), 7.19-7.73 (m, 66H, ArH), 7.63 (s, 2H, $\text{CH}_{\text{triazide}}$).

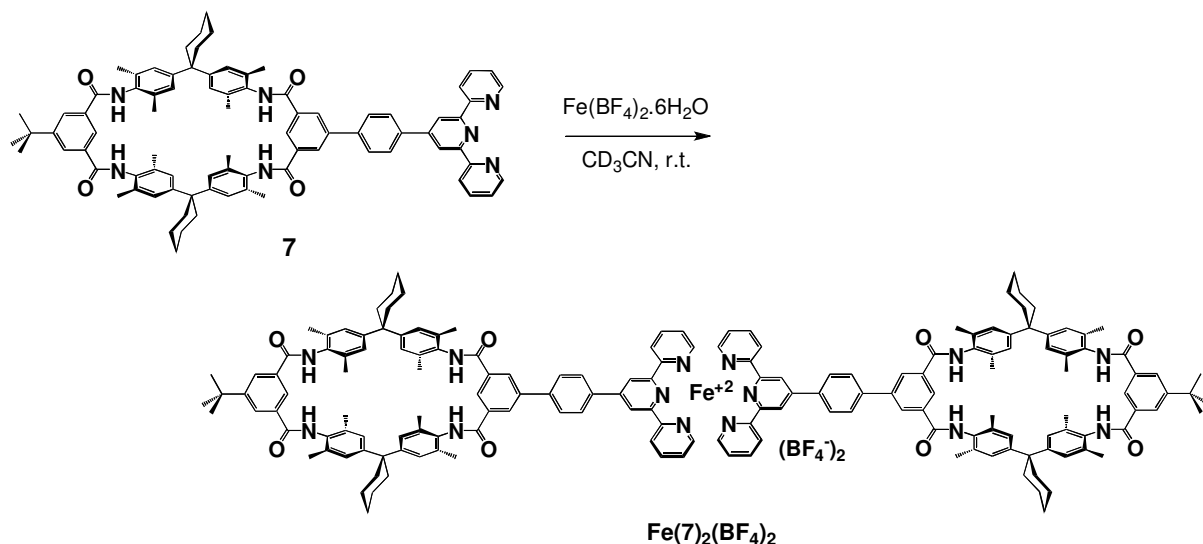
E.4.7. Assemblies and Metal Complexes

Covalent self-assembly of 1,3,5-tris(aminomethyl)benzene (P12) and aldehyde macrocycle (9)

Aldehyde macrocycle **9** (79.0 mg, 0.075 mmol) was dissolved in 0.7 ml of CDCl_3 . This solution was added on solid tris(aminomethyl)benzene (6.24 mg, 0.025 mmol). ^1H NMR shows the vanishing of the aldehyde peak and complete formation of imine. The spectrum is complicated because of the cis and trans isomers in the final architecture.

Synthesis of metal complexes of macrocycles and rotaxanes

Bis[11'-*tert*-butyl-29'-(4'-(4-(2,2'-6',2''-terpyridyl)))-5',17',23',35',38',40',43',45'-octa
methyldispiro[cyclohexan-1,2'-7',15',25',33'-tetraazaheptacyclo[32.2.2.2.2^{3',6'}.2^{16',19'}.2^{21',24'}
1^{9',13'}.1^{27',31'}]hexatetraconta-3',5',9',11',13'(44'),16',18',21',23',27',29',31'(39'),34',36',
37',40',42',45'-octadecaen-20',1''-cyclohexan]-8',14',26',32'-tetraon} iron(II)tetrafluoro
borate (Fe(7)₂(BF₄)₂)



Terpyridine macrocycle **7** (30.0 mg, 0.0116 mmol) in CD₃CN was introduced a metal solution containing half equivalent of metal ion from a stock solution separately prepared from Fe(BF₄)₂·6H₂O in CD₃CN. The mixture was added 2 drops of CD₃OD (without which the NMR spectra seem to be overwhelmingly broad in this case). The resulting mixture was stirred for 30 min to yield the desired complex in quantitative yield and examined with ¹H-NMR and MS (ESI-FTICR).

C₁₇₀H₁₇₀B₂F₈FeN₁₄O₈

2766,71 g mol⁻¹

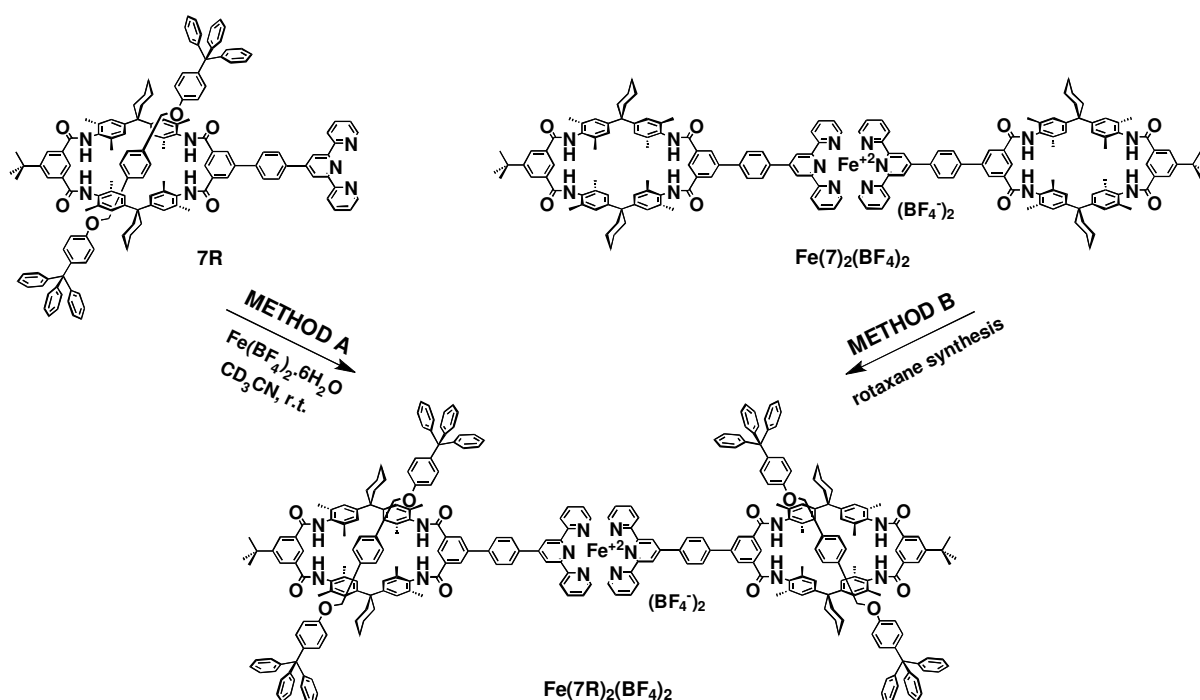
MS (ESI-FTICR)

m/z (%) = 1296.14 (100) [M-2BF₄⁻]²⁺.

¹H NMR

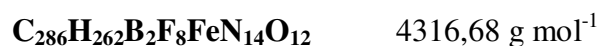
(500 MHz, CD₃CN+2 drops CD₃OD) δ [ppm] = 1.40 (s, 18H, *t*-Bu), 1.53-1.70 (b, 24H, Cy), 2.17 (s, 24H, CH₃), 2.22 (s, 24H, CH₃), 2.45 (b, 16H, CH₂ Cy), 7.11 (br, 4H, 2,2''-tpy), 7.18 (s, 16H, Ph), 7.22 (br, 4H, 3,3''-tpy), 7.53 (d, *J* = 6.2 Hz, 4H, Ph), 7.60 (d, *J* = 6.2 Hz, 4H, Ph), 7.63 (s, 4H, 4,6-isophth), 7.93 (t, *J* = 6.2 Hz, 4H, 4,4''-tpy), 8.18 (s, 4H, 4,6-isophth), 8.24 (s, 2H, 2-isophth), 8.47 (b, 4H, 5,5''-tpy), 8.50 (s, 2H, 2-isophth), 8.60 (s, 4H, 3',5'-tpy), 9.24 (s, 8H, NH).

Bis{[2]-{1,4-bis((4-tritylphenoxy)methyl)benzene}-{11'-*t*-butyl-29'-(2,2'-6',2''-terpyridyl)-5',17',23',35',38',40',43',45'-octamethyldispiro[cyclohexan-1,2'-7',15',25',33'-tetraazaheptacyclo[32.2.2.2^{3',6'}.2^{16',19'}.2^{21',24'}.1^{9',13'}.1^{27',31'}]hexatetraconta-3',5',9',11',13'(44'),16',18',21',23',27',29',31'(39'),34',36',37',40',42',45'-octadecaen-20',1''-cyclohexan]-8',14',26',32'-tetraon}rotaxan}iron(II)tetrafluoroborate (Fe(7R)₂(BF₄)₂)



Method A: *Post-threading synthesis starting with terpyridine rotaxane.* Terpyridine rotaxane **7R** (16.0 mg, 7.83 μmol) in CDCl_3 was introduced a metal solution containing half equivalent of metal ion from a stock solution separately prepared from $\text{Fe}(\text{BF}_4)_2 \cdot 6\text{H}_2\text{O}$ in CD_3CN . The mixture was added 2 drops of CD_3OD (without which the NMR spectra seem to be overwhelmingly broad in this case). The resulting mixture was stirred for 1 hour to yield the desired complex in quantitative yield and examined with ^1H -NMR and MS (ESI-FTICR).

Method B: *Post-complexation synthesis starting with iron complex of terpyridine macrocycle.* Terpyridine macrocycle **7** (15 mg, 5.4 μmol), trityl phenol (7.3 mg, 0.022 mmol), α, α' -dibromoparaxylene (2.86 mg, 0.008 mmol), K_2CO_3 (14.7 mg, 0.108 mmol) and dibenzo[18]crown-6 (1.0 mg, 0.0027 mmol) were stirred in dry dichloromethane for 1 week. The reaction mixture was examined with ESI-FTICR and it was found out that the reaction leads to the desired rotaxane metal complex.



MS (ESI-FTICR)

m/z (%) = 2071.49 (100) $[M-2BF_4]^{2+}$, 1682.80 (47) $[M-axle-2BF_4]^{2+}$.

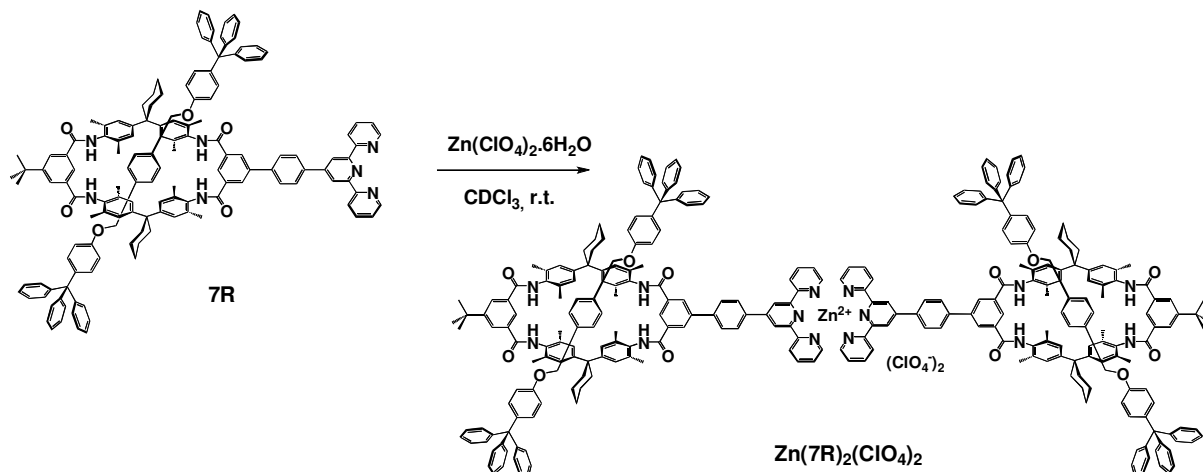
 1H NMR

(500 MHz, (CDCl₃, 2 drops CD₃OD) δ [ppm] = 1.17 (s, 18H, t-Bu), 1.32-1.60 (b, 24H, Cy), 1.73 (s, 24H, CH₃), 1.79 (s, 24H, CH₃), 2.19 (br, 16, Cy), 4.06 (s, 8H, OCH₂), 6.16 (s, 8H, PhH_{axle}), 6.27 (d, 8H, J = 8.65 Hz, PhH_{stopper}), 6.87 (d, 8H, J = 8.65 Hz, PhH_{stopper}), 6.89 (s, 8H, PhH), 6.85-6.92 (m, 8H, 6,6''; 3,3''-tpy) 6.95-7.17 (m, 60H, PhH_{stopper}), 7.24 (s, 2H, 2-isophth), 7.48 (s, 4H, 4,6-isophth), 7.73 (t, J = 7.15 Hz, 4H, 5,5''-tpy), 7.80 (s, 2H, 2-isoph), 7.88 (t, J = 7.15 Hz, 4H, 4,4''-tpy), 7.94 (s, 4H, 4,6-isophth), 8.25 (d, J = 7.05 Hz, 4H, PhH), 8.29 (s, 4H, 3',5'-tpy), 8.51 (d, J = 7.05 Hz, 4H, Ph), 9.09 (s, 4H, NH).

 ^{13}C NMR

(500 MHz, (CDCl₃, 2 drops CD₃OD) δ [ppm] = 18.50, 22.89, 26.23, 29.51, 30.93, 35.10, 35.32, 45.14, 64.22, 69.64, 117.3, 122.07, 122.62, 125.76, 125.93, 126.49, 127.30, 127.37, 127.47, 127.80, 128.40, 128.71, 129.98, 130.80, 130.86, 131.26, 131.35, 132.20, 134.23, 135.08, 135.15, 135.35, 135.95, 140.11, 141.35, 141.41, 146.75, 148.16, 148.51, 153.58, 156.01, 157.79, 160.23, 166.17.

Bis[2]-{1,4-bis((4-tritylphenoxy)methyl)benzene}-{11'-*t*-butyl-29'-(2,2'-6',2''-terpyridyl)-5',17',23',35',38',40',43',45'-octamethyldispiro[cyclohexan-1,2'-7',15',25',33'-tetraazaheptacyclo[32.2.2.2^{3',6'}.2^{16',19'}.2^{21',24'}.1^{9',13'}.1^{27',31'}]hexatetraconta-3',5',9',11',13'(44'),16',18',21',23',27',29',31'(39'),34',36',37',40',42',45'-octadecaen-20',1''-cyclohexan]-8',14',26',32'-tetraon}rotaxan} zinc(II) perchlorate (Zn(7R)₂(BF₄)₂)



Terpyridine rotaxane **7R** (12.0 mg, 5.87 μmol) in CDCl_3 was introduced a metal solution containing half equivalent of metal ion from a stock solution separately prepared from $\text{Zn}(\text{ClO}_4)_2 \cdot 6\text{H}_2\text{O}$ in CD_3CN . The mixture was added 2 drops of CD_3OD (without which the NMR spectra seem to be overwhelmingly broad in this case). The resulting mixture was stirred for 5 days to yield the desired complex.

C₂₈₆H₂₆₂Cl₂N₁₄O₂₀Zn

4351,54 g mol⁻¹

MS (ESI-FTICR)

m/z (%) = 2153.05 (100) $[\text{M}-2\text{ClO}_4+\text{HCOO}]^+$.

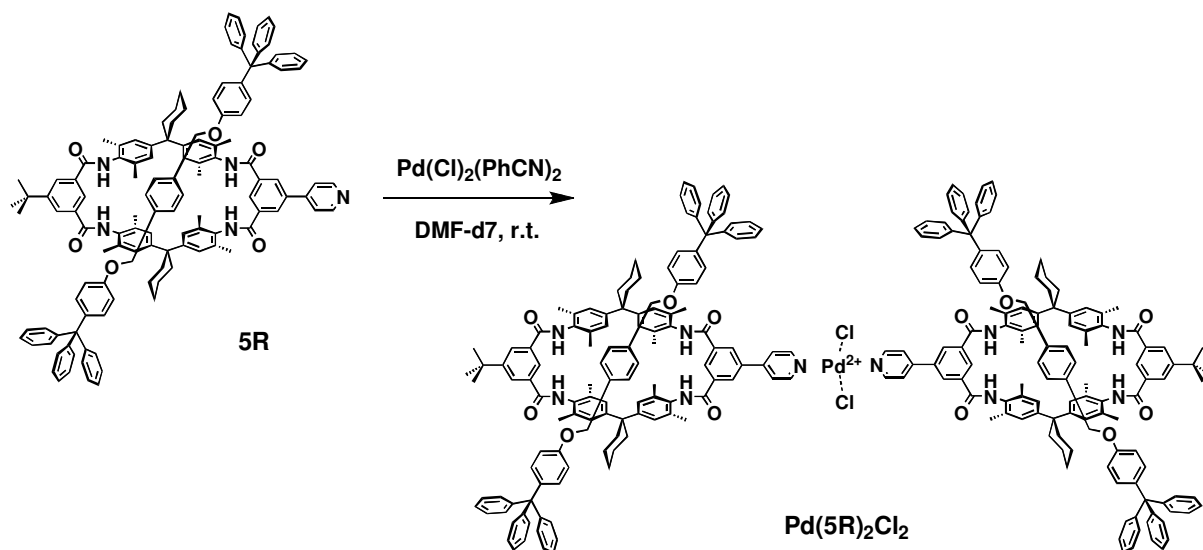
¹H NMR

(500 MHz, (CDCl_3 , 2 drops CD_3OD) δ [ppm] = 1.27 (s, 18H, *t*-Bu), 1.34-1.65 (b, 24H, Cy), 1.84 (s, 48H, CH₃), 2.57 (br, 16, Cy), 4.35 (s, 8H, OCH₂), 6.18 (s, 8H, PhH_{axle}), 6.43 (d, 8H, J = 8.65 Hz, PhH_{stopper}), 6.90 (d, 8H, J = 8.65 Hz, PhH_{stopper}), 6.99 (s, 8H, PhH), 6.85-6.92 (m, 8H, 6,6''; 3,3''-tpy) 7.02-7.11 (m, 60H, PhH_{stopper}), 7.30 (s, 2H, 2-isophth), 7.41 (s, 4H, 4,6-isophth), 7.60 (t, J = 7.15 Hz, 4H, 5,5''-tpy), 7.70 (s, 2H, 2-isoph), 7.83 (t, J = 7.15 Hz, 4H, 4,4''-tpy), 7.97 (s, 4H, 4,6-isophth), 8.12 (d, J = 7.05 Hz, 4H, PhH), 8.38 (s, 4H, 3',5'-tpy), 8.61 (d, J = 7.05 Hz, 4H, Ph), 8.85 (s, 4H, NH). (The spectrum shows approximately 1/9 uncomplexed rotaxane).

¹³C NMR

(500 MHz, (CDCl₃, 2 drops CD₃OD) δ [ppm] = 18.10, 22.49, 25.82, 29.13, 30.54, 34.72, 34.95, 44.78, 63.81, 69.36, 112.93, 116.35, 120.01, 120.95, 122.61, 125.53, 126.10, 127.06, 127.25, 127.47, 127.84, 128.05, 128.34, 129.55, 130.43, 130.89, 131.85, 133.80, 134.68, 134.74, 134.93, 135.51, 139.77, 141.02, 141.12, 146.33, 147.18, 147.30, 147.78, 148.19, 149.28, 153.26, 155.60, 165.49, 165.88.

Bis{[2]-{1,4-bis((4-tritylphenoxy)methyl)benzene}-{11',29'-dipyridyl-5',17',23',35',38',40',43',45'-octamethyldispiro[cyclohexan-1,2'-7',15',25',33'-tetraazaheptacyclo[32.2.2.2^{3',6'}.2^{16',19'}.2^{21',24'}.1^{9',13'}.1^{27',31'}]hexatetraconta-3',5',9',11',13'(44'),16',18',21',23',27',29',31'(39'),34',36',37',40',42',45'-octadecaen-20',1''-cyclohexan]-8',14',26',32'-tetraon} rotaxan palladium(II) chloride (Pd(5R)₂Cl₂)



Pyridine rotaxane **5R** (6.30 mg, 3.47 μmol) in DMF-d7 was introduced a metal solution containing half equivalent of metal ion from a stock solution separately prepared from PdCl₂ in DMF-d7. The resulting mixture was stirred for 1 hour to yield the desired complex. The mixture was examined with ¹H-NMR and MS (ESI-FTICR) and it was seen that complex forms quantitatively.

C₂₅₄H₂₄₂Cl₂N₁₀O₁₂Pd

3804,03 g mol⁻¹

MS (ESI-FTICR)

m/z (%) = 3826.60 (88) [M+Na]⁺.

¹H NMR

(500 MHz, DMF-d7) δ [ppm] = 1.37 (s, 9H, *t*-Bu), 1.38-1.65 (br, 12H, Cy), 1.91 (s, 12H, PhCH₃), 1.93 (s, 12H, PhCH₃), 2.43 (br, 8H, Cy), 4.09 (s, 4H, OCH₂), 6.54 (d, *J* = 9.0 Hz,

PhH_{stopper}), 7.05 (s, 4H, PhH_{axle}), 7.08 (d, $J = 9.0$ Hz, PhH_{stopper}), 7.24 (s, 8H, PhH), 7.25-7.32 (m, 30 H, PhH_{stopper}), 7.88 (d, $J = 7.7$ Hz, 2H, H_{pyr}), 8.61 (s, 1H, 2-isophth), 8.44 (s, 2H, 4,6-isophth), 8.81 (d, $J = 6.4$, 2H, H_{pyr}), 9.03 (s, 2H, NH), 9.31 (s, 2H, NH).

Preparation of assemblies pyridine macrocycle (5) and Pd(dpp)(OTf)₂⁵⁷

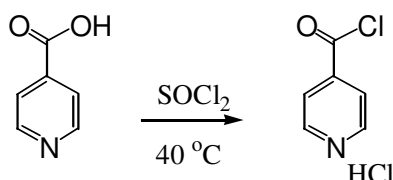
An equimolar DMF-d₇ mixture of pyridine macrocycle (5) and the corner molecule Pd(dpp)(OTf)₂ was stirred overnight. Without isolation, a sample from the mixture was diluted to 30 μ M and subjected to analysis with ESI-FTICR. The results are discussed in the Result and Discussion part.

E.4.8. Frechet Dendrimers (Part II)

All dendrimers of Part II were synthesized, purified, and characterized according to well-established procedures published previously¹⁹⁴.

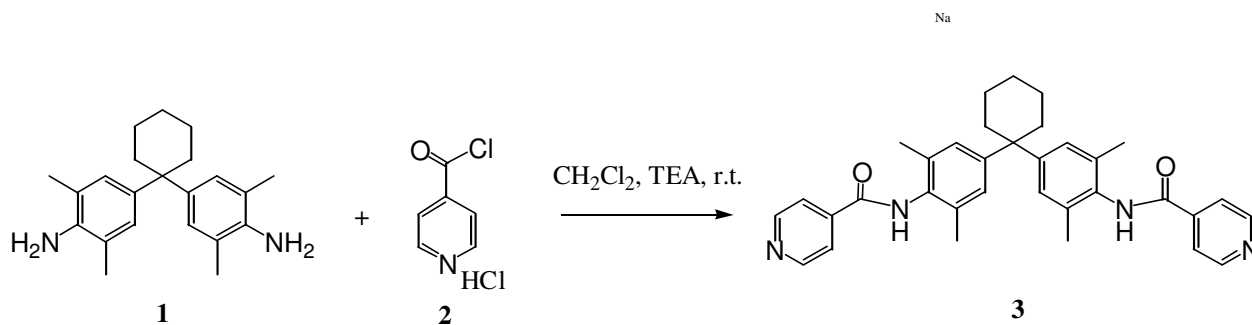
E.4.9. Hunter Ligand and Related Control Compounds (Part III)

Isonicotinoyl chloride hydrochloride:



6 ml of SOCl₂ was slowly added onto a one drop of dimethylformamide and 2.46 g. of isonicotinic acid at r.t. The reaction mixture is stirred at 40 °C for 30 minutes. Afterwards, excess SOCl₂ was carefully removed using water aspirator pump. The white product is put into 100 ml of dry diethyl ether and filtered using a glass filter, washed using another 100 ml of dry diethyl ether. The product is then dried under vacuum. Yield: 98%.

N,N'-(4,4'-(cyclohexane-1,1-diyl)-bis(2,6-dimethyl-4,1-phenylene)) diisonicotinamide 3:



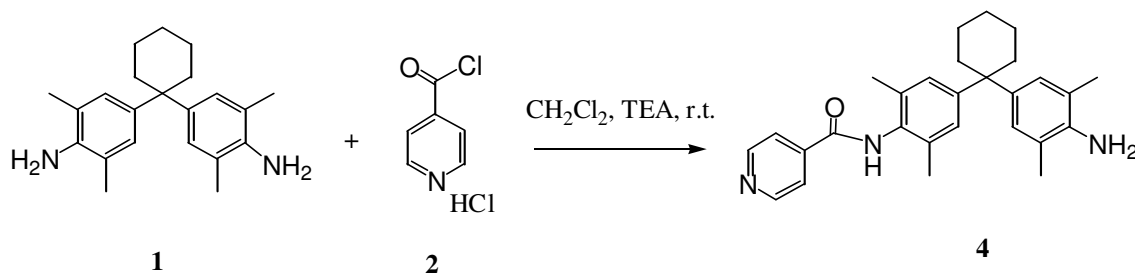
Hunter's diamine (2.5 g , 7.8 mmol) is placed in a 500 ml three-necked round bottomed reaction flask and filled with dry CH_2Cl_2 (260 mL) under argon atmosphere. Triethylamine (3.2 mL) was added into this solution. Afterwards, of isonicotinoyl chloride (4.14 g) was added into the reaction flask in six portions in one hour. The reaction was allowed to stir at room temperature overnight. The content was transferred into an extraction funnel and washed with 3x200 ml of water. The organic phase was then dried over MgSO_4 (anhydrous). The MgSO_4 was filtered and CH_2Cl_2 is removed using a rotary evaporator and the residue was purified by column chromatography using silica and CH_2Cl_2 : MeOH (9:1) as an eluent. To have a chloride free ligand, small amount of the pure product was columned with basic Al_2O_3 using the same solvent system given above. White solid. Yield: 75%. $R_f = 0.54$. m.p. 185 °C.

^1H NMR (400 MHz, DMSO-d_6) δ (ppm) = 9.71 (s, 2H, H_{amide}), 8.69 (d, 4H, $\text{H}_{\text{pyridine}(\alpha)}$), 7.84 (d, 4H, $\text{H}_{\text{pyridine}(\beta)}$), 7.01 (s, 4H, H_{phenyl}).

^{13}C NMR (100 MHz, CD_3OD) δ (ppm) = 166.5, 151.8, 149.7, 148.6, 144.8, 136.6, 132.2, 128.4, 127.0, 46.8, 38.2, 27.6, 24.2, 18.9.

MS (ESI-FTICR) m/z = 533.3 $[\text{M}+\text{H}]^+$, 555.28 $[\text{M}+\text{Na}]^+$, 1065.6 $[\text{M}_2+\text{H}]^+$ dimer, 1598.96 $[\text{M}_3+2\text{H}]^+$ trimer.

N-(4-(1-(4-amino-3,5-dimethylphenyl)cyclohexyl)-2,6-dimethylphenyl) isonicotinamide 4:



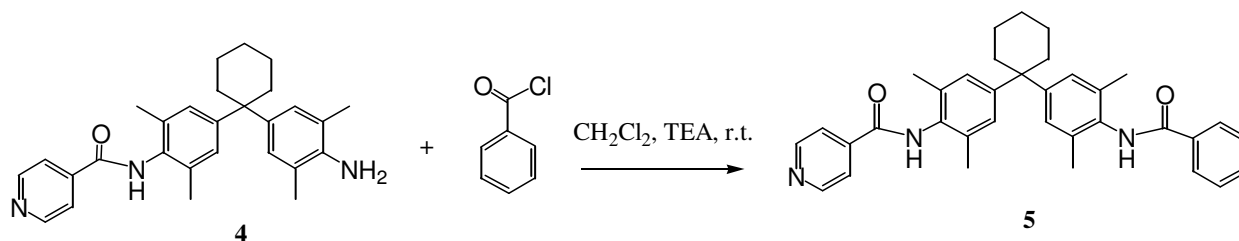
Hunter's diamine (4.06 g , 12.6 mmol) is placed in a 100 mL three-necked round bottomed reaction flask and filled with dry CH₂Cl₂ (50 mL) under argon atmosphere. Triethylamine (7.0 ml) was added into this solution. Afterwards, isonicotinoyl chloride (1.87 g) was added into the reaction flask. The reaction was allowed to stir at room temperature overnight. The content was transferred into an extraction funnel and washed with 3x200 ml of water. The organic phase was then dried over MgSO₄ (anhydrous). The MgSO₄ was filtered and CH₂Cl₂ is removed using a rotary evaporator and the residue was purified by column chromatography using silica and CH₂Cl₂:MeOH (5:1) as an eluent. White solid. Yield: 70 %. *R_f* = 0.45. m.p. 215 °C.

¹H NMR (400 MHz, DMSO-d₆) δ (ppm) = 9.91 (s, 1H, H_{amide}), 8.77 (d, 2H, H_{pyridine(α)}), 7.86 (d, 2H, H_{pyridine(β)}), 7.01 (s, 2H, H_{phenyl}), 6.76 (s, 2H, H_{phenyl}), 4.32 (b, 2H, H_{amine}), 2.17 (b, 4H, H_{aliphatic}), 2.12 (s, 6H, CH₃), 2.04 (s, 6H, CH₃), 1.46 (b, 6H, H_{aliphatic}).

¹³C NMR (100 MHz, CD₃OD) δ (ppm) = 164.00, 150.89, 150.86, 148.77, 142.01, 141.95, 135.58, 135.12, 132.01, 126.66, 126.58, 121.93, 120.81, 44.58, 36.98, 23.17, 21.27, 18.91, 18.76, 14.60.

MS (ESI-TOF) *m/z* = 428.27 [M+H]⁺, 450.25 [M+Na]⁺, 466.23[M+K]⁺.

N-(4-(1-(4-benzamido-3,5-dimethylphenyl)cyclohexyl)-2,6-dimethylphenyl)isonicotinamide 5:



Mono-pyridine compound **4** (0.36 g , 0.84 mmol) is placed in a 100 ml three-necked round bottomed reaction flask and filled with dry CH₂Cl₂ (50 ml) under argon atmosphere. Triethylamine (0.70 ml) was added onto this solution. Afterwards, benzoyl chloride (0.39 g) was added into the reaction flask in six portions in one hour. The reaction was allowed to stir at room temperature overnight. The content was transferred into an extraction funnel and washed with 3x200 ml of water. The organic phase was then dried over MgSO₄ (anhydrous). The MgSO₄ was filtered and CH₂Cl₂ is removed using a rotary evaporator and the residue was purified by column chromatography using silica and CH₂Cl₂:MeOH (9:1) as an eluent. To

have a chloride free ligand, small amount of the pure product was columned with basic Al₂O₃ using the same solvent system given above. White solid. Yield: 72%. *R_f* = 0.6. m.p. 175 °C.

¹H NMR (400 MHz, DMSO-d₆) δ (ppm) = 9.92 (s, 1H, H_{amide}), 9.61 (s, 1H, H_{amide}), 8.77 (d, 2H, H_{pyridine(α)}), 7.95 (t, 2H, H_{benzene}), 7.86 (d, 2H, H_{pyridine(β)}), 7.51 (m, 4H, H_{benzene}), 7.11 (s, 2H, H_{phenyl}), 7.09 (s, 2H, H_{phenyl}), 2.28 (b, 6H, H_{aliphatic}, CH₂), 2.15 (b, 12H, CH₃), 1.52 (b, 6H, H_{aliphatic}, CH₂).

¹³C NMR (100 MHz, CD₃OD) δ (ppm) = 165.5, 163.9, 150.9, 141.9, 135.63, 135.47, 134.94, 133.11, 132.39, 129.78, 129.09, 128.96, 127.93, 126.70, 126.57, 121.91, 45.53, 21.57, 21.28, 19.00, 18.93.

MS (ESI-TOF) *m/z* = 532.3 [M+H]⁺, 554.3 [M+Na]⁺, 570.3 [M+K]⁺.

Syntheses of assemblies, **7a,b**, **8a,b**, and vesicles **11a,b** and **11a',b'**

7a and **7b**, and metal to ligand complexes: an equimolar amounts of (dppp)M(OTf)₂ complex (M = Pd(II) (**6a**) or M = Pt(II) (**6b**)) and of the ligand **3** were mixed in dichloromethane and the mixture is stirred for 2 hours. Finally, slow addition of diethyl ether to the reaction mixture resulted in a white precipitate of **7a** and **7b**, with a yield of 95% and 90%, respectively. Compounds **8a** and **8b** were synthesized similarly.

Assembly (**7a**)

White solid. Yield: 95%.

¹H NMR (400 MHz, DMF-d₇) δ (ppm) = 9.92 (s, 2H, H_{amide}), 9.14 (b, 4H, H_{pyridine}), 7.87-7.82 (m, 16H, H_{dppp-meta} + H_{pyridine}), 7.63 (b, 5H, H_{dppp-para}), 7.52 (m, 10H, H_{dppp-ortho}), 7.20 (s, 4H, H_{phenyl}), 3.30 (b, 6H, H_{dppp}), 2.32 (b, 8H, CH₂ H_{cyclohexyl}), 2.18 (s, 12H, CH₃), 1.53 (b, 8H, CH₂ H_{cyclohexyl}).

¹³C NMR (100 MHz, DMSO-d₆) δ (ppm) = 155.07, 151.39, 147.52, 139.18, 137.36, 136.01, 136.62, 133.57, 130.53, 130.00, 129.55, 127.71, 126.80, 124.24, 49.04, 40.39, 30.12, 26.87, 25.78, 25.44, 21.97.

³¹P NMR (202 MHz, DMF-d₇) δ (ppm) = 11.16, 5.67.

¹⁹F NMR (470 MHz, DMF-d₇) δ (ppm) = -79.06.

MS (ESI-FTICR) $m/z = 1199.4$ Da $[\text{ML}(\text{OTf})]^+$, and $[\text{M}_2\text{L}_2(\text{OTf})]^{2+}$.

Assembly (7b)

White solid. Yield: 90%.

^1H NMR (400 MHz, DMF- d_7) δ (ppm) = 9.96-9.91 (m, 2H, H_{amide}), 9.26 (b, 4H, $\text{H}_{\text{pyridine}}$), 8.83 (d, $\text{H}_{\text{pyridine-free}}$), 7.85 (m, 14H, $\text{H}_{\text{dppp-meta}} + \text{H}_{\text{pyridine}}$), 7.55 (m, 5H, $\text{H}_{\text{dppp-para}}$), 7.48 (m, 10H, $\text{H}_{\text{dppp-ortho}}$), 7.22-7.19 (m, 4H, H_{phenyl}), 2.32 (b, 6H, $\text{CH}_2 \text{H}_{\text{cyclohexyl}}$), 2.15 (s, 6H, CH_3), 2.13 (s, 6H, CH_3), 1.53 (b, 8H, $\text{CH}_2 \text{H}_{\text{cyclohexyl}}$).

^{13}C NMR (100 MHz, DMSO- d_6 , 25 °C) δ (ppm) = 168.40, 166.73, 166.25, 165.74, 165.66, 156.08, 155.64, 155.33, 151.95, 148.38, 148.23, 148.05, 146.28, 139.94, 139.64, 138.10, 136.68, 136.28, 136.11, 131.21, 129.42, 126.29, 40.99, 30.62, 27.48, 25.79, 23.29, 23.24, 23.07, 22.08, 13.54.

^{31}P NMR (202 MHz, DMF- d_7) δ (ppm) = -14.05 (open assemblies (L_2M), ^{195}Pt satellites $^1J_{\text{Pt-P}} = 3041$ Hz), -11.82 (mono metal coordination, (LM); -10.7 (Stang's free corner, ^{195}Pt satellites $^1J_{\text{Pt-P}} = 3646$ Hz), -9.47 (cyclic assemblies, L_2M_2).

^{19}F NMR (470 MHz, DMF- d_7) δ (ppm) = -79.09. MS (ESI-FTICR, acetone): $m/z = 1288.4$ Da $[\text{ML-OTf}]^+$ and $[\text{M}_2\text{L}_2\text{-OTf}]^{2+}$.

MS (ESI-FTICR) $m/z = 1288.5$ Da $[\text{ML}(\text{OTf})]^+$, and $[\text{M}_2\text{L}_2(\text{OTf})]^{2+}$.

Assembly (8a)

Yellow solid. Yield: 98%.

^1H NMR (400 MHz, DMF- d_7) δ (ppm) = 9.92 (s, 2H, H_{amide}), 9.60 (s, 2H, H_{amide}), 9.10 (b, 4H, $\text{H}_{\text{pyridine}}$), 8.09 (d, 4H, $\text{H}_{\text{pyridine}}$), 7.85 (b, 20H, $\text{H}_{\text{dppp-pmeta}}$), 7.65 (b, 10H, $\text{H}_{\text{dppp-para}}$), 7.55 (m, 20H, $\text{H}_{\text{dppp-ortho}}$), 7.22 (s, 4H, H_{phenyl}), 7.19 (s, 4H, H_{phenyl}), 3.25 (b, 6H, $\text{CH}_2 \text{H}_{\text{dppp}}$), 2.34 (b, 10H, CH_2), 2.25 (s, 12H, CH_3), 2.19 (s, 12H, CH_3), 1.55 (b, 12H, $\text{CH}_2 \text{H}_{\text{cyclohexyl}}$).

^{13}C NMR (100 MHz, CD_3OD) δ (ppm) = 165.54, 151.23, 147.59, 146.84, 143.88, 135.46, 135.19, 133.59, 133.19, 132.73, 131.96, 131.49, 129.68, 128.55, 127.69, 126.62, 126.39, 125.85, 124.02, 123.17, 119.97, 45.07, 36.47, 26.33, 26.20, 22.95, 18.23, 18.03.

^{31}P NMR (202 MHz, DMF- d_7) δ (ppm) = 15.55.

¹⁹F NMR	(470 MHz, DMF-d ₇) δ (ppm) = -78.51.
MS (ESI-FTICR)	m/z = 532.3 Da [LH] ⁺ , 1063.6 Da [L ₂ H] ⁺ , 1198.3 Da [ML(OTf)] ⁺ , 1728.6 Da [ML ₂ (OTf)] ⁺ .

Assembly (8b)

Pink solid. Yield: 96%.

¹H NMR	(400 MHz, DMF-d ₇) δ (ppm) = 9.98 (s, 1H, H _{amide}), 9.94 (s, 1H, H _{amide}), 9.60 (d, 2H, H _{pyridine}), 9.27 (d, 2H, H _{pyridine}), 9.05 (d, 2H, H _{pyridine}), 8.08 (d, 4H, H _{pyridine}), 8.03-7.41 (b, 50H, H _{pyridine} + H _{dppp-meta} + H _{dppp-para} + H _{dppp-ortho}), 7.32-7.19 (m, 8H, H _{phenyl}), 3.24 (b, 6H, CH ₂ H _{dppp}), 2.34 (b, 10H, CH ₂ H _{cyclohexyl}), 2.23 (s, 12H, CH ₃), 2.17 (s, 12H, CH ₃), 1.55 (b, 12H, CH ₂ H _{cyclohexyl}).
¹³C NMR	(100 MHz, CD ₃ OD) δ (ppm) = 165.54, 151.30, 146.83, 144.57, 135.45, 135.18, 133.61, 133.19, 131.78, 131.51, 129.56, 128.56, 127.68, 126.64, 126.39, 123.18, 121.10, 119.98, 45.06, 36.47, 26.21, 26.19, 22.94, 18.22, 18.04, 18.03.
³¹P NMR	(202 MHz, DMF-d ₇) δ (ppm) = -13.34 (L ₂ M, ¹⁹⁵ Pt satellites ¹ J _{Pt-P} = 3053 Hz), -11.08 (LM), -9.93 (Stang's free corner, ¹⁹⁵ Pt satellites ¹ J _{Pt-P} = 3649 Hz).
¹⁹F NMR	(470 MHz, DMF-d ₇) δ (ppm) = -78.68.
MS (ESI-FTICR)	m/z = 1287.3 Da [ML(OTf)] ⁺ , 1818.5 Da [ML ₂ (OTf)] ⁺ .

E.5. TEM experiments

(Part III) Samples were prepared as follows: Approach-I: 2mg/ml aqueous solution of **7a** or **7b** were first dissolved in methanol and then doubly distilled water was added dropwise by stirring to get a suspension in 40% aqueous methanol solution of **11a** or **11b**. The suspension was additionally sonicated for 15 minutes. Approach-II: **11a'** and **11b'** were prepared by dissolving 1:1 stoichiometric amounts of **3** and **6a** or **6b** in methanol firstly, and double distilled water was added dropwise to get a 40% aqueous suspension of **11a'** or **11b'** and the suspension was additionally sonicated for 15 minutes. The same sample was used for Cryo-TEM analysis. A droplet (5 μl) of the suspensions were placed on hydrophilized (60 s plasma treatment at 8 W using a BALTEC MED 020 device) copper grids G-400 mesh coated with 0.5 % collodium film evaporated with a carbon layer. Excess fluid was blotted off after 60 s.

Staining was not necessary for the Pd(II) and Pt(II) vesicles since these metal ions produced enough contrast.

Summary

Bottom-to-top approach has lately gained more attention in nanotechnology for building new functional materials. However, the gap between the well-studied supramolecular architectures with promising features and the functional nano-materials is still a challenge for the chemists. Molecular machinery, which is a part of nanotechnological research, requires building blocks that are easily achievable, tuneable and working with high efficiency. Moreover, the assembly of these building blocks in specially designed ways is needed to achieve complex architectures. Macrocycles and rotaxanes have been well investigated as components of molecular machines so far by others. Even though there are uncountable examples of such systems with possible use in nanotechnology, the above mentioned gap is still present for them. In the first part of this work, not only different functional groups are incorporated in tetralactam macrocycles and rotaxanes in a straightforward way to obtain various different architectures but also ways to assemble them into higher structures are shown. The various possible uses of these architectures are stated and as an example, energy transfer systems are synthesized. In the second part, Fréchet dendrimers are investigated by a powerful analytical tool for supramolecular chemistry, electrospray ionization mass spectrometry. In this study, the defects that result from syntheses of these dendrimers are analysed. Then, an interesting and novel fragmentation pattern encountered in collision induced dissociation experiments is presented, to which several mechanisms are proposed and discussed. The last part of the thesis is another approach to functional supramolecular architectures: Self-assembled nano-spheres. The study is the display of a discovery of a previously-not-known way of building up nano-spheres from coordination polymers of simple organic ligands and metal complexes.

Zusammenfassung

Um funktionelle Materialien aufzubauen, hat der "Bottom-to-Top"-Ansatz in der letzten Zeit mehr Aufmerksamkeit in der Nanotechnologie gewonnen. Allerdings ist die Lücke zwischen gut bekannten supramolekularen Architekturen mit vielversprechenden Eigenschaften und funktionellen Nanomaterialien immer noch eine Herausforderung für Chemiker. Molekulare Maschinen, ein Teil der Forschung auf dem Gebiet der Nanotechnologie, benötigt Bausteine, die leicht zu machen und zu modifizieren sind und mit hoher Effizienz arbeiten. Ferner ist eine definierte, planbare Anordnung der molekularen Bausteine notwendig, um komplexe Architekturen zu erreichen. Makrozyklen und Rotaxane sind bereits von anderen als Komponenten von molekularen Maschinen studiert worden. Auch wenn es schon unzählbare Beispiele für solche Systeme mit einer möglichen Anwendung in der Nanotechnologie gibt, ist dennoch die oben erwähnte Lücke auch für diese vorhanden. Im ersten Teil der Arbeit werden nicht nur verschiedene funktionelle Gruppen in Tetralactammakrozyklen und -rotaxanen direkt inkorporiert um verschiedene von einander unterschiedliche Architekturen zu erhalten, sondern auch verschiedene Wege aufgezeigt, diese zu höheren Strukturen zu arrangieren. Die mannigfaltigen denkbaren Strukturen werden dargelegt. Als Beispiel wurden Energietransfersysteme synthetisiert. Im zweiten Teil der Arbeit wird die Analyse von Fréchetdendrimeren mit einem leistungsstarken Werkzeug der supramolekularen Chemie, der Elektrospraymassen-spektrometrie, dargestellt. In dieser Studie werden zunächst die Defekte resultierend aus der Synthese der Dendrimere untersucht. Anschließend wird ein neues und interessantes Fragmentationmuster beschrieben, zu dem verschiedene Mechanismen vorgeschlagen und diskutiert werden. Der letzte Teil zeigt eine weitere Annäherung auf dem Weg zu funktionellen, supramolekularen Strukturen auf: Selbstorganisierte Nanosphären. Der bis vor kurzem unentdeckte Ansatz, Nanosphären aus Koordinationspolymeren, die aus einfachen organischen Liganden und Metallkomplexen bestehen, aufzubauen, wird gezeigt.

References and Notes

- ¹ Feynman, R. P. "There's a Plenty of Room at the Bottom" *Engineering and Science*, American Physical Society Annual Meeting at Caltech, 1960.
- ² Nanotechnology as a term was first coined by Norio Taniguchi in 1974 to describe semiconductor processes such as thin film deposition and ion beam milling exhibiting characteristic control on the order of a nanometer: "'Nano-technology' mainly consists of the processing of separation, consolidation, and deformation of materials by one atom or one molecule." Taniguchi, N. *Proc. Intl. Conf. Prod. Eng. Tokyo*, Part II, Japan Society of Precision Engineering, **1974**.
- ³ Drexler, K. E. *Nanosystems: molecular machinery, manufacturing, and computation*, Wiley Interscience, **1992**.
- ⁴ www.imm.org Institute for Molecular Manufacturing website.
- ⁵ In this text "nanomachine,, is used synonymous with "molecular machine". For a review: Khuong, T.-A. V.; Nuñez, J. E.; Godinez, C. E.; Garcia-Garibay, M. A. *Acc. Chem. Res.* **2006**, *39*, 413-422.
- ⁶ Pedersen, C.J. *J. Am. Chem. Soc.* **1967**, *89*, 7017-7036
- ⁷ Curtis, N.F. *Coord. Chem. Rev.* **1968**, *3*, 3-47.
- ⁸ Schalley, C. A.; Weilandt, T.; Brüggemann, J.; Vögtle, F. *Topic in Current Chemistry*, **2004**, *248*, 141–200.
- ⁹ Schalley, C. A. *J. Phys. Org. Chem.* **2004**, *17*, 967-972.
- ¹⁰ De Silva, A. P.; Gunaratne, H. Q. N.; McCoy, C. P. *Nature*, **1993**, *364*, 42-44; b) Ghosh, P.; Bharadwaj, P. K.; Poy, J.; Ghosh, S. *J. Am. Chem. Soc.* **1997**, *119*, 11903-11909; c) Feldheim, D. L.; Keating, C. D. *Chem. Soc. Rev.* **1998**, *27*, 1-12. d) Barigelletti F.; Flamigni L. *Chem Soc. Rev.* **2000**, *29*, 1-12.
- ¹¹ Collings, A. F.; Chritchley, C. (eds) *Artificial Photosynthesis*, Wiley-VCH, Weinheim, **2005**.
- ¹² a) Schalley C. A.; Beizai, K.; Vögtle, F. *Acc. Chem. Res.* **2001**, *34*, 465-476; b) Collin, J. P.; Dietrich-Buchecker, C.; Gavina, P.; Jimenez-Molero, M. C.; Sauvage, J.-P. *Acc. Chem. Res.* **2001**, *34*, 477-487; c) Shipway, A. W.; Willner, I. *Acc. Chem Res.* **2001**, *34*, 421-432; d) Pease A. R.; Jeppesen, J. O.; Stoddart, J. F.; Luo, Y.; Collier, C. P. Heath, J. R. *Acc. Chem. Res.* **2001**, *34*, 433-444; e) Ballardini, R.; Balzani, V.; Credi, A.; Gandolfi, M. T.; Venturi, M. *Acc. Che. Res.* **2001**, *34*, 445-455; f) Felder, T.; Schalley, C. A. *Artificial Rotary Motors Based on Rotaxanes: Highlights in Bioorganic Chemistry*, Wennemers, H.; Schmuck, C. (eds) Wiley-VCH, Weinheim, **2004**, 526-539.
- ¹³ Sauvage, J.-P.; Dietrich-Buchecker (eds) *Catenanes, Rotaxanes and Knots, A Journey Through World of Molecular Topology*, Wiley-VCH, **1999**.
- ¹⁴ Upon aesthetics in supramolecular chemistry: Schummer, J. *Foundation of Chemistry*, **2006**, *8*, 53-72.
- ¹⁵ First molecular shuttle: Anelli, P. L.; Spencer, N.; Stoddart J. F. *J. Am. Chem. Soc.* **1991**, *113*, 5131 – 5133. Selected recent examples: a) Mateo-Alonso, A.; Fioravanti, G.; Marcaccio, M.; Paolucci, F.; Jagesar, D. C.; Brouwer, A. M., Prato, M. *Org. Lett.* **2006**, *8*, 5173-5176; b) Crowley, J. D.; Leigh, D. A.; Lusby, P. J.; McBurney, R. T.; Perret-Aebi, L.-E.; Petzold, C.; Slawin, A. M. Z.; Symes, M. D. *J. Am. Chem. Soc.* **2007**, *129*, 15085-15090.
- ¹⁶ Some examples of light driven shuttles: a) Armarolli, N.; Balzani, V.; Collin, J.P.; Gavina, P.; Sauvage, J.-P.; Ventura, B. *J. Am. Chem. Soc.* **1999**, *121*, 4397-4408; b) Brouwer, A. M.; Frochot, C.; Gatti, F. G.; Leigh, D. A.; Mottier, L.; Paolucci, F.; Roffia, S.; Wurfel, G. W. H. *Science* **2001**, *291*, 2124-2128; c) Silvi, S.; Arduini, A.; Pochini, A.; Secchi, A.; Tomasulo, M.; Raymo, F. M., Barancini, M.; Credi, A. *J. Am. Chem.*

- Soc. **2007**, 129, 13378-13379; d) Raymo, F. M. *Angew. Chem. Int. Ed.* **2006**, 24, 5249-5251; e) Saha, S.; Stoddart, J. F. *Chem. Soc. Rev.* **2007**, 36, 77-92.
- 17 Some examples of oxidation/reduction shuttles: a) Asakawa, M.; Ashton, P. R.; Balzani, V.; Credi, A.; Hamers, C.; Mattersteig, G.; Montalti, M.; Shipway, A. N.; Spencer, N.; Stoddart, J. F.; Tolley, M. S.; Venturi, M.; White, A. J. P.; Williams, D. J. *Angew. Chem. Int. Ed.* **1998**, 37, 333-337. b) Livoreil, A.; Sauvage, J.-P.; Armaroli, N.; Balzani, V.; Flamigni, L.; Ventura, B. J. *Am. Chem. Soc.* **1997**, 119, 12114-12124. c) Iijima, T.; Vignon, S. A.; Tseng, H.-R.; Jarroson, T.; Sanders, J. K. M.; Marchioni, F.; Venturi, M.; Apostoli, E.; Balzani, V.; Stoddart, J. F. *Chem. Eur. J.* **2004**, 10, 6375-6392. d) Saha, S.; Flood, A. H.; Impellizzeri, S.; Silvi, S.; Venturi, M.; Credi, A. *J. Am. Chem. Soc.* **2007**, 129, 12159-15171. e) Aprahamian, I.; Dichtel, W. R.; Ikeda, T.; Heath, J. R.; Stoddart, J. F. *Org. Lett.* **2007**, 9, 1287-1290.
- 18 Some examples of shuttles switched by chemical inputs: a) Balzani, V.; Gomez-Lopez, M.; Stoddart, J. F. *Acc. Chem. Res.* **1998**, 31, 405-414; b) Collin, J. P.; Dietrich-Buchecker, C.; Gavin, P.; Jimenez-Molero, M. C.; Sauvage, J.-P. *Acc. Chem. Res.* **2001**, 34, 477-487; c) Sindelar, V.; Silvi, S.; Kaifer, A. E. *Chem. Commun.* **2006**, 2185-2187; d) Kelly, T. R.; Cai, X.; Damkaci, F.; Panicker, S. B.; Tu, B.; Bushell, S. M.; Cornelly, I.; Piggott, M. J.; Salives, R.; Caverio, M.; Zhao, Y.; Jasmin, S. *J. Am. Chem. Soc.* **2007**, 129, 376-386.
- 19 a) Harada, A. *Acc. Chem. Res.* **2001**, 34, 456-464; b) Kelly, T. R.; *Acc. Chem. Res.* **2001**, 34, 514-522. c) Ballardini, R.; Balzani, V.; Credi, A.; Gandolfi, M. T. Venturi, M. *Acc. Chem. Res.* **2001**, 34, 445-455.
- 20 Feringa, B. L. *Acc. Chem. Res.* **2001**, 34, 504-513.
- 21 Recent reviews: a) Anslyn, E. V. *J. Org. Chem.* **2007**, 72, 687-699; b) Rogers, C. W.; Wolf, M. O. *Coord. Chem. Rev.* **2002**, 341-350; c) Valeur, B.; Leray, I. *Coord. Chem. Rev.* **2000**, 3-40.
- 22 a) de Silva, A.P.; McClenaghan, N. D. *J. Am. Chem. Soc.* **2000**, 122, 3965-3966; b) Magri, D. C.; Brown, G. J., McClean, G. D., de Silva, A. P. *J. Am. Chem. Soc.* **2006**, 128, 4950-4951; c) Credi, A.; Balzani, V.; Langford, S. J., Stoddart, J. F. *J. Am. Chem. Soc.*, **1997**, 119, 2679-2681; d) Margulies, D.; Melman, G.; Shanzer, A. *J. Am. Chem. Soc.* **2006**, 128, 4865-4871.
- 23 Bustamante, C.; Keller, D.; Oster, G. *Acc. Chem. Res.* **2001**, 34, 412-420.
- 24 Schalley, C. A.; Beizai, K.; Vögtle, F. *Acc. Chem. Res.* **2001**, 34, 465-476.
- 25 Ghosh, P.; Federwisch, G.; Kogej, M.; Schalley, C. A.; Haase, D.; Saak, W.; Lützen, A.; Gschwind, R. M. *Org. Biomol. Chem.* **2005**, 3, 2691-2700.
- 26 Ashton, P. R.; Ballardini, R.; Balzani, V.; Credi, A.; Dress, K. R.; Ishow, E.; Kleverlaan, C. J.; Kocian, O.; Preece, J. A.; Spencer, N.; Stoddart, J. F.; Venturi, M.; Wenger, S. A. *Chem. Eur. J.* **2000**, 6, 3558-3574.
- 27 a) Hernandez, R.; Tseng H.-R.; Wong, J. W.; Stoddart, J. F.; Zink, J. I. *J. Am. Chem. Soc.* **2004**, 126, 3370-3371. b) Nguyen, T. D.; Liu, Y.; Saha, S.; Leung, K. C.-F.; Stoddart, J. F.; Zink, J. I. *J. Am. Chem. Soc.* **2007**, 129, 626-634.
- 28 Badjić, J. D.; Balzani, V.; Credi, A.; Silvi, S.; Stoddart, J. F. *Science* **2004**, 303, 1845-1849.
- 29 Feringa, B. L.; van Delden, R. A. *Angew. Chem. Int. Ed.* **1999**, 38, 3418-3438.
- 30 a) Schill, G. *Catenanes, Rotaxanes and Knots*. Academic Press, New York, **1971**. b) Dietrich-Buchecker, C.; Sauvage, J. P. *Chem Rev.* **1987**, 87, 795-810; c) Jäger, R.; Vögtle, F. *Angew. Chem.* **1997**, 109, 966-980. *Angew Chem Int. Ed. Engl.* **1997**, 36, 930-944; d) Nepogoeiev, S. A.; Stoddart, J. F. *Chem. Rev.* **1998**, 98, 1959-1976; e) *Molecular Catenanes, Rotaxanes and Knots*, Sauvage, J.-P.; Dietrich-Buchecker, C. (eds) Wiley-VCH: Weinheim, **1999**. f) Linnartz, P.; Schalley, C. A. in *Rotaxanes and*

- Pseudorotaxanes: Encyclopedia of Supramolecular Chemistry*, Atwood, J. L. Steed, J. W. (eds) Dekker: New York, **2004**.
- 31 Pease, A. R.; Jeppesen, J. O.; Stoddart, J. F.; Luo, Y.; Collier, C. P.; Heath, J. R. *Acc. Chem. Res.* **2001**, *34*, 433-444.
- 32 a) Gimzewski, J. K.; Joachim, C.; Schlitter, R. R.; Langais, V.; Tang, H.; Johannsen, I. *Science* **1998**, *281*, 531; b) Shipway, A. N.; Willner, I. *Acc. Chem. Res.* **2001**, *34*, 421-432.
- 33 Agam, G.; Zilkha, A. *J. Am. Chem. Soc.* **1976**, *98*, 5214-5216.
- 34 Schalley, C. A.; Baytekin, H. T.; Baytekin, B. in: *Macrocyclic Chemistry: Current Trends and Future*, K. Gloe (Ed.), Springer, Heidelberg **2005**, 37-52.
- 35 a) Hamann, C.; Kern, J.-M.; Sauvage, J.-P. *Dalton Trans.* **2003**, 3770-3775. b) Prikhod'ko, A. I.; Durola, F.; Sauvage, J.-P. *J. Am. Chem. Soc.* **2008**, *130*, 448-449. c) Buchecker-Dietrich C.; Sauvage, J.-P. *Chem. Rev.* **1987**, *87*, 795-810. d) Sauvage, J.-P. *Acc. Chem. Res.*, **1990**, *23*, 319-330.
- 36 a) Nepogodiev, S. A.; Stoddart, J. F. *Chem. Rev.* **1998**, *98*, 1959-1976. b) Raymo, F. M.; Stoddart, J.F. *Chem. Rev.* **1999**, *99*, 1643-1664.
- 37 Yin, Z.; Zhang, Y.; He, J.; Cheng, J.-P. *Chem. Commun.* **2007**, 2599-2601.
- 38 a) Kolchinski, A. G.; Busch, D. H.; Alcock, N. W. *J. Chem. Soc., Chem. Commun.* **1995**, 1289-1291; b) Ashton, P. R.; Collins, A. N.; Fyfe, M. C. T.; Menzer, S. Stoddart, J. F.; Williams, D. J. *Angew. Chem.* **1997**, *109*, 760-763., *Angew. Chem. Int. Ed.* **1997**, *36*, 735-738. c) Gatti, F.G.; Leigh, D. A.; Nepogodiev, S. A.; Slawin, A. M. Z.; Teat, S. J.; Wong, J. K. Y. *J. Am. Chem. Soc.* **2001**, *123*, 5983-5989.
- 39 a) Schalley, C. A.; Reckien, W.; Peyerimhoff, S.; Baytekin, B.; Vögtle, F. *Chem. Eur. J.* **2004**, *10*, 4777-4789; b) Seel, C.; Parham.; Safarowsky, O.; Hübner, G. M.; Vögtle, F. *J. Org. Chem.* **1999**, *64*, 7236-7242; c) Heim, C.; Affeld, A.; Nieger, M.; Vögtle, F. *Helvetica Chimica Acta*, **1999**, *82*, 746-759; d) Jäger, R.; Vögtle, F. *Angew. Chem.* **1997**, *109*, 966-980., *Angew. Chem. Int. Ed.* **1997**, *36*, 930-944; e) Leigh, D. A., Moody, K.; Smart, J. P.; Watson, K. J.; Slawin, A. M. Z. *Angew. Chem.* **1996**, *108*, 326-331, *Angew. Chem. Int. Ed.* **1996**, *35*, 306-310.
- 40 Recent representative examples: a) Beer, P. D.; Sambrook, M. R.; Curiel, D. *Chem. Commun.* **2006**, 2105-2117; b) Ng, K.-Y.; Cowley, A. R.; Beer, P. D. *Chem. Commun.* **2006**, 3676-3678. Special issue of phenol templated rotaxanes: c) Hübner, G. M.; Gläser, J.; Seel, C.; Vögtle, F. *Angew. Chem.* **1999**, *111*, 395-398. *Angew. Chem. Int. Ed.* **1999**, *38*, 383-386; d) Seel, C.; Vögtle, F. *Chem. Eur. J.* **2000**, *6*, 21-24; e) Reuter, C.; Vögtle, F. *Org. Lett.* **2000**, *2*, 593-595; f) Hübner, G. M.; Reuter, C.; Seel, C.; Vögtle, F. *Synthesis*, **2000**, 103-108; g) Ghosh, P.; Mermagen, O.; Schalley, C. A. *Chem. Commun.* **2002**, 2628-2629; h) Schalley, C. A.; Silva, G.; Nising, C. F.; Linnartz, P. *Helv. Chim. Acta* **2002**, 1578-1596; i) Lankshear, M. D.; Beer, P. D. *Acc. Chem. Res.* **2007**, *40*, 657-668.
- 41 Bernhardt, P. V.; Moore, E.G. *Aust. J. Chem.* **2003**, *56*, 239-258.
- 42 Some interesting recent examples of vast variety of functionalizations on calixarenes: a) Bew, S. P.; Brimage, R. A.; L'Hermite, N.; Sharma, S. V. *Org Lett.* **2007**, *9*, 3713-3716; b) Cao, Y.; Vysotsky, M. O.; Böhmer, V. *J. Org. Chem.* **2006**, *71*, 3429-3434.
- 43 Some examples of resorcinarene functionalized with ligands: a) Pinalli, R.; Cristini, V.; Sottili, V.; Geremia, S.; Campagnolo, M.; Caneshi, A.; Dalcanale, E. *J. Am. Chem. Soc.* **2004**, *126*, 6516-6517; b) Jude, H.; Sicclair, D. J.; Das, N.; Sherburn, M. S.; Stang, P. J. *J. Org. Chem.* **2006**, *71*, 4155-4163; c) Aakeröy, C. B.; Schultheiss, N.; Desper, J. *Org. Lett.* **2006**, *8*, 2607-2610.
- 44 Ahman, A.; Luostrarinen, M.; Schalley C. A.; Nissinen, M.; Rissanen, K. *Eur. J. Org. Chem.* **2005**, 2783-2801.

45 For reviews and examples: a) Imamura, T.; Fukushima, K. *Coord. Chem Rev.* **2000**,
198, 133-156. b) Wojaczynski, J.; Latos-Grazynski, L. *Coord. Chem. Rev.* **2000**, 204,
113-171. c) Satake A.; Kobuke Y. *Tetrahedron*, **2005**, 61, 13-41. d) Rucareanu, S.;
46 Schuwey, A.; Gossauer, A. *J. Am. Chem. Soc.* **2006**, 128, 3396-3413.
Kamada, T.; Aratani, N.; Ikeda, T.; Shibata, N.; Higuchi, Y.; Wakamiya, A.;
Yamaguchi, S.; Kim, K. S.; Yoon, Z. S.; Kim, D.; Osuka, A. *J. Am. Chem. Soc.* **2006**,
128, 7670-7678.
47 Fujimura, F.; Kimura, S. *Org. Lett.* **2007**, 9, 793-796.
48 A drastical difference in changing the sequence of functionalization-assembly formation
is displayed in: Mynar, J. L.; Yamamoto, T.; Kosaka, A.; Fukushima, T.; Ishii, N.; Aida,
T. *J. Am. Chem. Soc.* **2008**, 130, 1530-1531.
49 a) Tominaga, M.; Suzuki, K.; Murase, T.; Fujita M. *J. Am. Chem. Soc.*, **2005**, 127,
11950-11951. b) Tominaga, M.; Suzuki, K.; Kawano, M.; Kusukawa, T.; Ozeki, T.;
Sakamoto, S.; Yamaguchi, K.; Fujita, M. *Angew. Chem. Int. Ed.*, **2004**, 43, 5621-5625
50 Lukin, O.; Vögtle, F. *Angew. Int. Ed.* **2005**, 44, 1456-1477.
51 Lukin, O.; Yoneva, A.; Vögtle, F. *Eur. J. Org. Chem.* **2004**, 69, 1236-1238.
52 Actually, the terms exo- and endo- are not new and one may refer to the following
example for such a use in supramolecular structures: Hilmey, D. G.; Paquette, L. A. *J.*
Org. Chem. **2004**, 69, 3262-3270.
53 a) Lee S. J.; Lin, W. *J. Am. Chem. Soc.*, **2002**, 124, 4554-4555; b) Würthner, F.; Sautter,
A. *Chem. Commun.*, **2000**, 445-446; c) Würthner, F.; Sautter, A.; Schmid, D.; Weber, P.
J. A. *Chem. Eur. J.* **2001**, 7, 894-902; d) You, C.-C.; Würthner, F. *J. Am. Chem. Soc.*
2003, 125, 9716-9725.
54 Takanashi, K.; Yamamoto, K. *Org. Lett.* **2007**, 9, 5151-5154.
55 Böhmer, A.; Brüggemann, J.; Kaufmann, A.; Yoneva, A.; Müller, S.; Müller, W. M.;
Müller, U.; Vergeer, F. W.; Chi, L.; De Cola, L.; Fuchs, H.; Chen, X.; Kubota, T.;
Okamoto, Y.; Vögtle, F. *Eur. J. Org. Chem.* **2007**, 45-52.
56 Loeb, S. J. *Chem. Soc. Rev.* **2007**, 36, 226-235.
57 Baytekin, H. T.; Sahre, M.; Engeser, M.; Rang, M.; Schulz, A.; Schalley, C. A. *Small*,
accepted.
58 Jiménez, C.; Dietrich-Buchecker, C.; Sauvage, J.-P. *Angew. Chem. Int. Ed.* **2000**, 39,
3284-3287.
59 Berná, J.; Leigh, D. A.; Lubomska, M.; Mendoza, S. M.; Pérez, E. M.; Rudolf, P.;
Teobaldi, G.; Zerbetto, F. *Nature Materials*, **2005**, 4, 704-710.
60 Yang, , H.-B.; Ghosh, K.; Northrop, B. H.; Zheng, Y.-R.; Lyndon, M. M.; Muddiman,
D. C.; Stang, P. J. *J. Am. Chem. Soc.* **2007**, 129, 14187-14189.
61 Excluding an example to understand the axle reactivity of a rotaxane towards chemical
reactions: Parham, A. H.; Windisch, B.; Vögtle, F. *Eur. J. Org. Chem.* **1999**, 1233-1238.
62 Thomas, J.A. *Chem. Soc. Rev.*, **2007**, 36, 856-868.
63 Hofstadter, D. *I am a Strange Loop*, Basic Books, **2007**.
64 Blau, W.J., Fleming, A.J. *Science* **2004**, 304, 1457-1458.
65 Curtis, N.F. *Coord. Chem. Rev.* **1968**, 3, 3-47.
66 General reviews on self-assembly: a) Glotzer S. C. *Science* **2004**, 306, 419-420. b)
Whitesides, G. M.; Mathias, J. P.; Seto, C. T. *Science* **1991**, 254, 1312-1319. c) Philp,
D.; Stoddart, J. F. *Angew. Chem.* **1996**, 108, 1242-1286; *Angew. Chem. Int. Ed.* **1996**,
35, 1154-1196. d) Lehn, J.-M. *Science* **2002**, 295, 2400-2403. e) Vriezema, D. M.;
Aragone`s, M. C.; Elemans, J. A. A. W.; Cornelissen, J. J. L. M.; Rowan, A. E.; Nolte,
R. J. M. *Chem. Rev.* **2005**, 1445-1489.

- 67 a) Orgel, L. E. *Nature* **1992**, 358, 203-209; b) Wintner, E. A.; Conn, M. M.; Rebek Jr, J. *Acc. Chem. Res.* **1994**, 27, 198-203; c) Li, T.; Nicolaou, K. C. *Nature* **1994**, 369, 218-224. d) Kassianidis, E.; Pearson, R. J.; Philp, D. *Chem. Eur. J.* **2006**, 12, 8798-8812.
- 68 Weimann, D. P.; Schalley, C. A. *Supramol. Chem.* **2008**, 20, 117-128
- 69 A recent review on supramolecular nanotubes: Shimizu, T.; Masuda, M.; Minamikawa, H. *Chem. Rev.* **2005**, 105, 1401-1443.
- 70 Selected examples of self-assembled vesicles: a) Discher, D. E.; Eisenberg, A. *Science* **2002**, 297, 967-973. b) Antonietti, M.; Förster, S. *Adv. Mater.* **2003**, 15, 1323-1333. c) Opsteen, J. A.; Cornelissen, J. J. L. M.; Hest, J. C. M. V. *Pure Appl. Chem.* **2004**, 76, 1309-1319. d) Tian, L.; Nguyen, P.; Hammond, P. T. *Chem. Commun.* **2006**, 3489-3491. e) Jin, B.; Chen, X.; Wang, X.; Yang, C.; Xie, Y.; Qui, H. *Chem. Eur. J.* **2007**, 13, 9137-9142. f) Vriezema, D. V.; Hoogboom, J.; Velonia, K.; Takazawa, K.; Christianen, P. C. M.; Maan, J. C.; Rowan, A. E.; Nolte, R. J. M. *Angew. Chem.* **2003**, 115, 796-800, *Angew. Chem. Int. Ed.* **2003**, 42, 772-776. g) Ghoroghchian, P. P.; Frail, P. R.; Susumu, K.; Blessington, D.; Brannan, A. K.; Bates, F. S.; Chance, B.; Hammer, D. A.; Therien, M. J. *Proc. Natl. Acad. Sci.*, **2005**, 102, 2922-2927. h) Li, X.; Li, Y.; Li, H.; Liu, S.; Wang, S.; Gan, H.; Li, J.; Wang, N.; He, X.; Zhu, D. *Angew. Chem.* **2006**, 118, 3721-3725, *Angew. Chem. Int. Ed.* **2006**, 45, 3639-3643. i) Gohy, J.-F.; Lohmeijer, B. G.; Décamps, B.; Leroy, E.; Boileau, S.; Broek, J. A. V. D.; Schubert, D.; Haase, W.; Schubert, U. S. *Polym. Int.* **2003**, 52, 1611-1618. j) Constable, E. C.; Meier, W.; Nardin, C.; Mundweiler, S. *Chem. Commun.* **1999**, 1483-1484. k) Wackerly, J. W.; Moore, J. S. *Macromolecules*, **2006**, 39, 7269-7276. l) Baytekin, H. T.; Baytekin, B.; Schulz, A.; Schalley, C. A. *Small*, **2008**, submitted.
- 71 For reviews on polynuclear, self-assembling metal complexes, see: (a) Fujita, M. *Self-assembled Macrocycles, Cages, and Catenanes Containing Transition Metals in Their Backbones*, in: Comprehensive Supramolecular Chemistry, vol. 9, Atwood, J. L.; Davies, J. E. D.; MacNicol, D. D.; Vögtle, F.; Lehn, J.-M.; Sauvage J.-P.; Hosseini M. W. (eds.), Pergamon, Oxford **1996**, 253-282. (b) Fredericks, J. R.; Hamilton, A. D. Metal Template Control of Self-Assembly in Supramolecular Chemistry in: Supramolecular Control of Structure and Reactivity - Perspectives in Supramolecular Chemistry, vol. 3, Hamilton, A. D. (eds.), Wiley, New York, **1996**, 1-39. (c) Fujita, M.; Ogura, K. *Coord. Chem. Rev.* **1996**, 148, 249-264. (d) Fujita, M.; Ogura, K. *Bull. Chem. Soc. Jpn.* **1996**, 69, 1471-1482. (e) Piguet, C.; Bernardinelli, G.; Hopfgartner, G. *Chem. Rev.* **1997**, 97, 2005-2062. (f) Stang, P. J.; Olenyuk, B. *Acc. Chem. Res.* **1997**, 30, 502-518. (g) Albrecht, M. *Chem. Soc. Rev.* **1998**, 27, 281-287. (h) Jones, C. J. *Chem. Soc. Rev.* **1998**, 27, 289-299. (i) Fujita, M. *Chem. Soc. Rev.* **1998**, 27, 417-425. (j) Slone, R. V.; Benkstein, K. D.; Bélanger, S.; Hupp, J. T.; Guzei, I. A.; Rheingold, A. L. *Coord. Chem. Rev.* **1998**, 171, 221-243. (k) Piguet, C. J. *Inclusion Phenom. Macrocyc. Chem.* **1999**, 34, 361-391. (l) Caulder, D. L.; Raymond, K. N. *Acc. Chem. Res.* **1999**, 32, 975-982. (m) Leininger, S.; Olenyuk, B.; Stang, P. J. *Chem. Rev.* **2000**, 100, 853-908. (n) Fujita, M.; Umemoto, K.; Yoshizawa, M.; Fujita, N.; Kusukawa, T.; Biradha, K. *Chem. Commun.* **2001**, 509-518. (o) Holliday, B. J.; Mirkin, C. A. *Angew. Chem.* **2001**, 113, 2076-2097; *Angew. Chem. Int. Ed.* **2001**, 40, 2022-2043. (p) Albrecht, M. *Chem. Rev.* **2001**, 101, 3457-3498. (q) Johnson, D. W.; Raymond, K. N. *Supramol. Chem.* **2001**, 13, 639-659. (r) Swiegers, G. F.; Malfetse, T. J. *J. Inclusion Phenom. Macrocyc. Chem.* **2001**, 40, 253-264. (s) Cotton, F. A.; Lin, C.; Murillo, C. A. *Acc. Chem. Res.* **2001**, 34, 759-771. (t) Sun, S.-S.; Lees, A. J. *Coord. Chem. Rev.* **2002**, 230, 171-192. (u) Würthner, F.; You, C.-C.; Saha-Möller, C. R. *Chem. Soc. Rev.* **2004**, 33, 133-146. (v) Hofmeier, H.; Schubert, U. S. *Chem. Soc. Rev.* **2004**, 33, 373-399. (w) Fujita, M.; Tominaga, M.; Hori, A.; Therrien, B. *Acc. Chem. Res.* **2005**, 38, 371-380. (x) Cronin, L.

- Annu. Rep. Prog. Chem. Sect. A* **2005**, *101*, 348-374. (y) Gianneschi, N. C.; Masar III, M. S.; Mirkin, C. A. *Acc. Chem. Res.* **2005**, *38*, 825-837. (z) Kaiser, A.; Bäuerle, P. *Top. Curr. Chem.* **2005**, *249*, 127-201. (aa) You, C.-C.; Dobrawa, R.; Saha-Möller, C. R.; Würthner, F. *Top. Curr. Chem.* **2005**, *258*, 39-82. (bb) Crowley, J. D.; Bosnich, B. *Eur. J. Inorg. Chem.* **2005**, 2015-2025. (cc) Amijs, C. H. M.; van Klink, G. P. M.; van Koten, G. *Dalton Trans.* **2006**, 308-327. (dd) Huang, W.; Zhu, H.-B.; Gou, S.-H. *Coord. Chem. Rev.* **2006**, *250*, 414-423. (ee) Iengo, E.; Zangrando, E.; Alessio, E. *Acc. Chem. Res.* **2006**, *39*, 841-851. (ff) Nitschke, J. R. *Acc. Chem. Res.* **2007**, *40*, 103-112. (gg) Crookson, J.; Beer, P. D. *Dalton Trans.* **2007**, 1459-1472. (hh) Albrecht, M.; Fröhlich, R. *Bull. Chem. Soc. Jpn.* **2007**, *80*, 797-808. (ii) Georgiev, I. G.; MacGillivray, L. R. *Chem. Soc. Rev.* **2007**, *36*, 1239-1248. (jj) Gunnlaugsson, T.; Stomeo, F. *Org. Biomol. Chem.* **2007**, *5*, 1999-2009.
- 72 Bonnet, S.; Collin, J.-P.; Koizumi, M.; Mobian, P.; Sauvage, J.-P. *Adv. Mater.* **2006**, *18*, 1239-1250 and references therein.
- 73 Chichak, K.; Walsh, M. C.; Branda, N. R. *Chem. Commun.* **2000**, 847-848
- 74 Davidson, G. J. E.; Loeb S. J. *Dalton Trans.* **2003**, 4319-4323.
- 75 Davidson, G. J. E.; Loeb S. J.; Passanati, P.; Silvi, S.; Credi, A. *Chem Eur. J.* **2006**, *12*, 3233.
- 76 Bonnet, S.; Collin, J.-P.; Koizumi, M.; Mobian, P.; Sauvage, J.-P. *Adv. Mater.* **2006**, *18*, 1239-1250.
- 77 Li, X.-y.; Illigen, J.; Nieger, M.; Michel, S.; Schalley, C. A. *Chem Eur. J.* **2003**, *9*, 1332-1347.
- 78 Cabrera, D. G.; Koivisto, B. D.; Leigh, D. A. *Chem Commun.* **2007**, 4218-4220.
- 79 Marlin, D. S.; Cabrera, D. G.; Leigh, D. A.; Slawin, A. M. Z. *Angew. Chem. Int. Ed.* **2006**, *45*, 1385-1390.
- 80 Lehn, J.-M. *Chem. Eur. J.* **1999**, *5*, 2455-2463.
- 81 A very detailed review on dynamic covalent chemistry: Rowan, S. J.; Cantrill, S. J.; Cousins, G. R. L.; Sanders, J. K. M.; Stoddart, J. F. *Angew. Chem. Int. Ed.* **2002**, *41*, 898-952.
- 82 Some representative examples are: a) Hamilton, D. G.; Feeder, N.; Teat, S. J.; Sanders, J. K. M. *New J. Chem.* **1998**, 1019-1021. b) Kidd, T. J.; Leigh, D. A.; Wilson, A. J. J. *Am. Chem. Soc.* **1999**, *121*, 1599-1600. c) Cantrill, S. J.; Rowan, S. J.; Stoddart, J. F. *Org. Lett.* **1999**, *1*, 1363-1366. d) Rowan, S. J.; Stoddart, J. F. *Org. Lett.* **1999**, *1*, 1913-1916. e) Glink, P. T.; Oliva, A. I.; Stoddart, J. F.; White, A. J. P.; Williams, D. J. *Angew. Chem.* **2001**, *113*, 1922-1927; *Angew. Chem. Int. Ed.* **2001**, *40*, 1870-1875. f) Y. Furusho, T. Hasegawa, A. Tsuboi, N. Kihara, T. Takata *Chem. Lett.* **2000**, 18-19. g) Haussmann, P. C.; Khan, S. I.; Stoddart, J. F. *J. Org. Chem.* **2007**, *72*, 6708-6713. h) Hodačová, J.; Buděšinský, M. *Org. Lett.* **2007**, *9*, 5641-5643.
- 83 a) Rowan, S. J.; Cantrill, S. J.; Stoddart, J. F.; White, A. J. P.; Williams, D. J. *Org Lett.* **2000**, *2*, 759-762. b) Guidry, E. N.; Li, J.; Stoddart, J. F.; Grubbs, R. H. *J. Am. Chem. Soc.* **2007**, *129*, 8944-8945.
- 84 a) Northrop, B. H.; Aricó, F.; Tangchiavang, N.; Badjić, J. D.; Stoddart, J. F. *Org. Lett.* **2006**, *8*, 3899-3902. b) Leung, K. C.-F.; Arico, F.; Cantrill, S. J.; Stoddart, J. F. *J. Am. Chem. Soc.* **2005**, *127*, 5808-5810. c) Williams, A. R.; Northrop, B. H.; Chang, T.; Stoddart, J. F. White, A. J. P.; Williams, D. J. *Angew. Chem.* **2006**, *118*, 6817-6821.
- 85 Kidd, T. J.; Loontjens, T. J. A.; Leigh, D. A.; Wong, J. K. Y. *Angew. Chem. Int. Ed.* **2003**, *42*, 3379-3383.
- 86 Mohry, A.; Schwierz, H.; Vögtle F. *Synthesis* **1999**, *10*, 1753-1758.
- 87 Closson, W.; Frisch, H. L.; Wassermann E. J. *J. Am. Chem. Soc.* **1961**, *83*, 3789-3795.

- 88 a) Mitchell, D. K.; Sauvage, J.-P. *Angew. Chem.* **1988**, *100*, 985-987. *Angew Chem Int. Ed. Eng.* **1988**, *27*, 930-931. b) Nierengarten, J.-F.; Dietrich-Buchecker, C.; Sauvage, J.-P. *J. Am. Chem. Soc.* **1994**, *116*, 375-376.
- 89 Sauvage, J.-P.; Dietrich-Buchecker, C. *Molecular Topology: Catenanes, Rotaxanes and Knots*, VCH: Weinheim, **1999**.
- 90 Mohry, A.; Vögtle, F.; Nieger, M.; Hupfer, H. *Chirality*, **2000**, *12*, 76-83.
- 91 Xu, Z.-X.; Zhang, C.; Zheng, Q.-Y.; Chen, C.-F.; Huang, Z.-T. *Org. Lett.* **2007**, *9*, 4447-4450.
- 92 Lukin, O.; Kubota, T.; Okamoto, Y.; Kaufmann, A.; Vögtle, F. *Chem. Eur. J.* **2004**, *10*, 2804-2810.
- 93 Recent example: Theil, A.; Mauve, C.; Adeline, T.; Marinetti, A.; Sauvage, J.-P. *Angew. Chem. Int. Ed.* **2006**, *45*, 2104-2107.
- 94 a) Yamamoto, C.; Okamoto, Y.; Schmidt, T.; Jäger, R.; Vögtle, F. *J. Am. Chem. Soc.* **1997**, *119*, 10547-19548. b) Reuter, C.; Pawlitzki, G.; Wörsdörfer, U.; Plevvoets, M.; Mohry, A.; Kubota, T.; Okamoto, Y.; Vögtle, F. *Eur. J. Org. Chem.* **2000**, 3059-3067.
- 95 McArdle, C. P.; Van, S.; Jennings, M. C.; Puddephatt, R. J. *J. Am. Chem. Soc.* **2002**, *124*, 3959-3965.
- 96 Loren, J. C.; Gantzel, P.; Linden, A.; Siegel, J. S. *Org. Biomol. Chem.* **2005**, *3*, 3105-3116.
- 97 a) Burchell, T.J.; Eisler, D. J.; Puddephatt, R. J. *Dalton Trans.* **2005**, 268-272. b) Habermehl, N. C.; Jennings, M. C.; McArdle, C. P.; Mohr, F.; Puddephatt, R. J. *Organometallics*, **2005**, *24*, 5004-5014.
- 98 Chui, S. S.-Y.; Chen, R.; Che, C.-M. *Angew. Chem Int. Ed.* **2006**, *45*, 1621-1624.
- 99 a) An interesting example with energy transfer: Koizumi, M.; Dietrich-Buchecker, C.; Sauvage, J.-P. *Eur. J. Org. Chem.* **2004**, 770-775. b) Ashton, P. R.; Heiss, A. M.; Pasini, D.; Raymo, F. M.; Shipway, A. N.; Stoddart, J. F.; Spencer, N. *Eur. J. Org. Chem.* **1999**, 995-1004. c) Vignon, S. A.; Wong, J.; Tseng, H.-R.; Stoddart, J. F. *Org. Lett.* **2004**, *6*, 1095-1098. An interestingly achiral catenane: d) Chambron, J. -C.; Sauvage, J. -P. *J. Am. Chem. Soc.* **1997**, *119*, 9558-9559.
- 100 Hori, A.; Akasaka, A.; Biradha, K.; Sakamoto, S.; Yamaguchi, K.; Fujita, M. *Angew. Chem. Int. Ed.* **2002**, *41*, 3269-3272.
- 101 a) Makita, Y.; Kihara, N.; Nakakoji, N.; Takata, T.; Inagaki, S.; Yamamoto, C.; Okamoto, Y. *Chemistry Letters*, **2007**, *36*, 162-163; b) Hattori, G.; Hori, T.; Miyake, Y.; Nishibayashi, Y. *J. Am. Chem. Soc.* **2007**, *129*, 12930-12931.
- 102 Kameta, N.; Nagawa, Y.; Karikomi, M.; Hiratani, K. *Chem Commun.*, **2006**, 3714-3716.
- 103 Reuter, C.; Mohry, A.; Sobanski, A.; Vögtle, F. *Chem. Eur. J.* **2000**, *6*, 1674-1682.
- 104 Liu, Y.; Bonvallet, P. A.; Vignon, S. A.; Khan, S. I.; Stoddart, J. F. *Angew. Int. Ed.* **2005**, *44*, 3050-3055.
- 105 Bogdan, A.; Vysotsky, M. O.; Ikai, T.; Okamoto, Y.; Böhmer, V. *Chem. Eur. J.* **2004**, *10*, 3324-3330.
- 106 For reviews on FRET theory and applications: a) Wu, P.; Brand, L. *Anal. Biochem.* **1994**, *218*, 1-13. b) Szöllösi, J.; Damjanovich, S.; Matyus, L. *Cytometry*, **1998**, *34*, 159-179.
- 107 Castellano, R. K.; Craig, S. L.; Nuckolls, C.; Rebek, Jr., J. *J. Am. Chem. Soc.* **2000**, *122*, 7876-7882.
- 108 Tamura, M.; Ueno, A. *Chem. Lett.* **1998**, 369-370.
- 109 For related examples where a macrocycle itself quenches a donor: a) Giro, G.; Cocchi, M.; Fattori, V.; Gadret, G.; Ruani, G.; Cavallini, M.; Bicarini, F.; Zamboni, R.; Loontjens, T.; Thies, J.; Leigh, D. A.; Morales, A. F.; Mahrt, R. F. *Synth. Met.* **2001**,

- 122, 27-29. b) Perez, E. M.; Dryden, D. T. F.; Leigh, D. A.; Teobaldi, G.; Zerbetto, F. *J. Am. Chem. Soc.* **2004**, *126*, 12210-12211.
- 110 For examples of energy/electron transfer a) Armaroli, N.; Diederich, F.; Dietrich-Buchecker, C. O.; Flamigni, L.; Marconi, G.; Nierengarten, J.-F.; Sauvage, J.-P. *Chem. Eur. J.* **1998**, *4*, 406-416. b) Ishow, E.; Credi, A.; Balzani, V.; Spadola, F.; Mandolini, L. *Chem. Eur. J.* **1999**, *5*, 984-989. c) Andersson, M.; Linke, M.; Chambron, J.-C.; Davidsson, J.; Heitz, V.; Hammarström, L.; Sauvage, J.-P. *J. Am. Chem. Soc.* **2002**, *124*, 4347-4362. d) Watanabe, N.; Kihara, N.; Furosho, Y.; Takata, T.; Araki, Y.; Ito, O. *Angew. Chem. Int. Ed.* **2003**, *42*, 681- 683, *Angew. Chem.* **2003**, *115*, 705-707. e) Li, K.; Bracher, P. J.; Guldi, D. M.; Herranz, M. A.; Echegoyen, L.; Schuster, D. I. *J. Am. Chem. Soc.* **2004**, *126*, 9156-9157. f) Hiratani, K.; Kaneyama, M.; Nagawa, Y.; Koyama, E.; Kanesato, M. *J. Am. Chem. Soc.* **2004**, *126*, 13568-13569. g) Sandanayaka, A. S. D.; Sasabe, H.; Araki, Y.; Furusho, Y.; Ito, O.; Takata, T. *J. Phys. Chem. A* **2004**, *108*, 5145-5155. h) Onagi, H.; Rebek, Jr., J. *Chem Commun.* **2005**, 4604-4606.
- 111 Energy transfer in a supramolecular knot: Passanati, P.; Ceroni, P.; Balzani, V.; Lukin, O.; Yoneva, A.; Vögtle, F. *Chem. Eur. J.* **2006**, *12*, 5685-5690.
- 112 Two interesting examples of shuttling of a rotaxane by light: a) Zhou, W.; Chen, D.; Li, J.; Xu, J.; Lv, J.; Liu, H.; Li, Y. *Org. Lett.* **2007**, *9*, 3929-3932. b) Tomatsu, I.; Hashidzume, A.; Harada, A. *Angew. Chem.* **2006**, *118*, 4721-4724.
- 113 FRET was discovered by Theodor Förster. The distance between two counterparts of the transfer is named after him as "Förster radius".
- 114 Li, Y.; Li, H.; Liu, H.; Wang, S.; He, X.; Wang, N.; Zhu, D. *Org. Lett.* **2005**, *7*, 4835-4838.
- 115 Tominaga, M.; Suzuki, K.; Kawano, M.; Kusukawa, T.; Ozeki, T.; Sakamoto, S.; Yamaguchi, K.; Fujita, M. *Angew. Chem. Int. Ed.*, **2004**, *43*, 5621-5625
- 116 Miyaura, N.; Suzuki A. *Chem. Rev.* **1995**, *95*, 2457-2483.
- 117 Click reaction is simply a 1,3-cyclo-addition of azides with terminal acetylenes using a Cu catalyst at room temperature discovered concurrently and independently by the groups of K. Barry Sharpless and Morten Meldal. This was an improvement over the same reaction first popularized by Rolf Huisgen in the 1970s, albeit at elevated temperatures in the absence of water and without a Cu catalyst. a) Kolb, H. C.; Finn, M. G.; Sharpless, K. B. *Angew. Chem. Int. Ed.* **2001**, *40*, 2004-2021, *Angew. Chem.* **2001**, *113*, 2056-2075. b) Torne, C. W.; Christensen, C.; Meldal M. *J. Org. Chem.* **2002**, *67*, 3057-3064,
- 118 Ishiyama, T.; Murata, M.; Miyaura, N. *J. Org. Chem.* **1995**, *60*, 7508-7510.
- 119 Schalley, C. A.; Ghosh, P.; Engeser, M. *Int. J. Mass Spectrom.* **2004**, 232-233.
- 120 Ishiyama, T.; Itoh, Y.; Kitano, T.; Miyaura, N. *Tetrahedron Lett.* **1997**, *38*, 3447-3450.
- 121 a) Goodall, W.; Wild, K.; Arm, K. J.; Williams, J. A. G. *J. Chem. Soc., Perkin Trans.* **2002**, 1669-1681. b) Aspley, C. J.; Williams, J. A. G. *New J. Chem.* **2001**, *25*, 1136-1147.
- 122 Multivalency is a hot topic in supramolecular chemistry. For recent reviews: a) Badjić, J. D.; Nelson, A.; Cantrill, S. J.; Turnbull, W. B.; Stoddart, J. F. *Acc. Chem. Res.*, **2005**, *38*, 723 -732. b) Ludden, M. J. W.; Reinhoudt, D. N.; Huskens, J. *Chem Soc. Rev.* **2006**, *35*, 1122-1134. c) Baldini, L.; Casnati, A.; Sansone, F.; Ungaro, R. *Chem Soc. Rev.* **2007**, *36*, 254-266. d) Badjić, J. D.; Nelson, A.; Cantrill, S. J.; Turnbull, W. B.; Stoddart, J. F. *Acc. Chem. Res.*, **2005**, *38*, 723 -732. e) Hayashida, O.; Uchiyama, M. *J. Org. Chem.* **2007**, *72*, 610-616.
- 123 Kaufmann, L. *Synthese neuer multivalenter Wirtmoleküle*, Freie Universität Berlin, **2007**.

- 124 a) Goze, C.; Ulrich, G.; Mallon, L. J.; Allen, B. D.; Harriman, A.; Ziessel, R. *J. Am. Chem. Soc.* **2006**, *128*, 10231-10239. b) Yu, Y.-H.; Descalzo, A. B.; Shen, Z.; Röhr, H.; Liu, Q.; Wang, Y.-W.; Spieles, M.; Li, Y.-Z.; Rurack, K.; You, X.-Z. *Chem. Asian. J.* **2006**, *1-2*, 176-187. c) Harriman, A.; Mallon, L. J.; Stewart, B.; Ulrich, G.; Ziessel, R. *Eur. J. Org. Chem.* **2007**, 3191-3198. d) Loudet, A.; Burgess, K. *Chem. Rev.* **2007**, *107*, 4891-4932.
- 125 a) Turfan, B.; Akkaya, E. U. *Org. Lett.* **2002**, *4*, 2857-2859. b) Coskun, A.; Baytekin, B. T.; Akkaya, E. U. *Tetrahedron Lett.* **2003**, *44*, 5649-5651.
- 126 Baggerman, J.; Jagesar, D.; Vallée, R. A. L.; Hofkens, J.; de Shryver, F. C.; Schelhase, F.; Vögtle, F.; Brouwer, A. M. *Chem. Eur. J.* **2007**, *13*, 1291-1299.
- 127 Brusilowskij, B. *Synthese cis/trans-divalenter Palladiumkomplexe als potentielle makrocyclische Wirte*, Free University Berlin, **2006**.
- 128 Weimann, D. [2] *Rotaxanes with Dendritic Stoppers via Click Chemistry*, Free University Berlin, **2007**.
- 129 Baytekin, H. T. *Fluorescent Sensing of Cations, Anions and Neutral Molecules Towards Information Processing at Molecular Level*, The Graduate School of Natural and Applied Sciences of Middle East Technical University, Ankara, **2002**.
- 130 Brusilowskij, B. unpublished results.
- 131 An antenna system is a special FRET system with many donor units corresponding to one acceptor. Some examples of covalent and non-covalent antennae for light-harvesting: a) Tamura, M.; Gao, D.; Ueno, A. *Chem. Eur. J.* **2001**, *7*, 1390-1397. b) Yilmaz, M. D.; Bozdemir, O. A.; Akkaya, E. U. *Org. Lett.* **2006**, *8*, 2871-2873. c) Kodis, G.; Terazono, Y.; Liddell, P. A.; Andreasson, J.; Garg, V.; Hambourger, M.; Moore, T. A.; Moore, A. L.; Gust, D. *J. Am. Chem. Soc.* **2006**, *128*, 1818-1827.
- 132 Weber, E.; Seichter, W.; Skobridis, K.; Alivertis, D.; Theodorou, V.; Bombicz, P.; Csöreg, I. *J. of Inc. Phen. and Mac. Chem.*, **2006**, 131-149.
- 133 a) Affeld, A.; Hübner, G. M.; Seel, C.; Schalley, C. A. *Eur. J. Org. Chem.* **2001**, 2877-2890. b) Linnartz, P.; Bitter, S.; Schalley, C. A. *Eur. J. Chem.* **2003**, 4819-4829. c) Heim, C.; Affeld, A.; Nieger, M.; Vögtle, F. *Helv. Chim. Acta* **1999**, *82*, 746-759.
- 134 Some inspiring examples are: a) Such, G. K.; Quinn, J. F.; Quinn, A.; Tjipto, E.; Caruso, F. *J. Am. Chem. Soc.* **2006**, *128*, 9318-9319. b) Isobe, H.; Cho, K.; Solin, N.; Werz, D. B.; Seeberger, P. H.; Nakamura, E. *Org. Lett.* **2007**, *9*, 4611-4611. c) Bew, S. P.; Brimage, R. A.; L'Hermite, N.; Sharma, S. *Org. Lett.* **2007**, *9*, 3713-3716. d) Liu, Y.; Ke, C.-F.; Zhang, H.-Y.; Cui, J.; Ding, F. *J. Am. Chem. Soc.* **2008**, *130*, 600-605.
- 135 Thummel, R. P.; Jahng, Y. *Inorg. Chem.* **1986**, *25*, 2527-2534.
- 136 Meier, M. A. R.; Lohmeijer, B. G. G.; Schubert, U. S. *J. of Mass. Spec.* **2003**, *38*, 510-516.
- 137 Dobrawa, R.; Lysetska, M.; Ballester, P.; Grüne, M.; Würthner, F. *Macromolecules* **2005**, *38*, 1315-1325.
- 138 Beves, J. E.; Chapman, B. E.; Kuchel, P. W.; Lindoy, L. F.; McMurtrie, J.; McPartlin, M.; Thordarson, P.; Wei, G. *Dalton Trans.* **2006**, 744-750.
- 139 Schalley, C. A.; Müller, T.; Linnartz, P.; Witt, M.; Schäfer, M.; Lützen, A. *Chem. Eur. J.* **2002**, *8*, 3538-3551.
- 140 Beves, J. E.; Chapman, B. E.; Kuchel, P. W.; Lindoy, L. F.; McMurtrie, J.; McPartin, M.; Thordarson, P.; Wei, G. *Dalton Trans.*, **2006**, 744-750.
- 141 Kilway, K. V.; Siegel, J. S. *Tetrahedron*, **2001**, *57*, 3615-3627.
- 142 a) Tam-Chang, S.-W.; Stehouwer, J. S.; Hao, J. *J. Org. Chem.* **1999**, *64*, 334-335. b) O'Leary, B. M.; Szabo, T.; Svenstrup, N.; Schalley, C. A.; Lützen, A.; Schäfer, M.; Rebek Jr., J. *J. Am. Chem. Soc.* **2001**, *123*, 11519-11533. c) Hennich, G.; Anslyn, E. *Chem. Eur. J.* **2002**, *8*, 2219-2224. d) Schmuck, C.; Schwegmann, M. *J. Am. Chem. Soc.*

- 2005**, *127*, 3373-3379. e) Francesconi, O.; Ienco, A.; Moneti, G.; Nativi, C.; Roelens, S. *Angew. Chem.* **2006**, *118*, 6845-6848.
- 143 a) Nadai, C. De; Whelan, C.M.; Perollier, C.; Clarkson, G.; Leigh, D.A.; Caudano, R.; Rudolf, P. *Surf. Sci.* **2000**, *112*, 454-456. b) Weber, N.; Hamann, C.; Kern, J.-M.; Sauvage, J.-P. *Inorg. Chem.* **2003**, *42*, 6780-6792. c) Coronado, E.; Forment-Aliaga, A.; Gavina, P.; Romero, F. M *Inorg. Chem.* **2003**, *42*, 6959-5961. d) Moulin, J. F.; Kengne, J. C.; Kshirsagar, R.; Cavallini, M.; Biscarini, F.; Leon, S.; Zerbetto, F.; Bottari, G.; Leigh, D. A. *J. Am. Chem. Soc.* **2006**, *128*, 526-532 e) Whelan, C. M.; Gatti, F.; Leigh, D. A.; Rapino, S.; Zerbetto, F.; Rudolf, P. *J. Phys. Chem. B* **2006**, *110*, 17076-17081.
- 144 There are no examples of rotaxanes on surface by layer-by-layer self-assembly approach. On L-b-L of supramolecular architectures see following examples: a) Crespo-Biel, O.; Dordi, B.; Reinhoudt, D. N.; Huskens; J. *J. Am. Chem. Soc.* **2005**, *127*, 7594-7600. b) Lin, C.; Kagan, C. R. *J. Am. Chem. Soc.* **2003**, *125*, 336-337 c) Wanunu, M.; Vaskevich, A.; Cohen, S. R.; Cohen, H.; Arad-Yellin, R.; Shanzer, A.; Rubinstein, I. *J. Am. Chem. Soc.* **2005**, *127*, 17877-17887. d) Salditta, T.; Schubert, U. S.; *Reviews in Molecular Biotechnology*, **2002**, *90*, 55-70.
- 145 For recent reviews, see: a) Newkome, G. R.; Moorefield, C. N.; Vögtle, F. *Dendritic Molecules: Concepts, Synthesis, Perspectives*, Wiley-VCH, Weinheim **1996**; b) Zeng, F.; Zimmerman, S. C. *Chem. Rev.* **1997**, *97*, 1681-1712; c) Archut, A.; Vögtle, F. *Chem. Soc. Rev.* **1998**, *27*, 233-240; d) Smith, D. K.; Diederich, F. *Chem. Eur. J.* **1998**, *4*, 1351-1361; e) Fischer, M.; Vögtle, F. *Angew. Chem.* **1999**, *111*, 934-955; *Angew. Chem. Int. Ed.* **1999**, *38*, 884-905; f) Bosman, A. W.; Jansen, H. M.; Meijer, E. W. *Chem. Rev.* **1999**, *99*, 1665-1688; g) Newkome, G. R.; He, E.; Moorefield, C. N. *Chem. Rev.* **1999**, *99*, 1689-1746; h) Nierengarten, J.-F. *Chem. Eur. J.* **2000**, *6*, 3667-3670; i) Schlüter, A. D.; Rabe, J. P. *Angew. Chem.* **2000**, *112*, 860-880; *Angew. Chem. Int. Ed.* **2000**, *39*, 864-883; j) Newkome, G. R.; Moorefield, C. N.; Vögtle, F. *Dendrimers and Dendrons. Concepts, Syntheses, Applications*, Wiley-VCH, Weinheim **2001**; k) Haag, R. *Chem. Eur. J.* **2001**, *7*, 327-335; l) Hecht, S.; Fréchet, J. M. J. *Angew. Chem.* **2001**, *113*, 76-94; *Angew. Chem. Int. Ed.* **2001**, *40*, 74-91; m) Fréchet, J. M. J.; Tomalia, D. A. *Dendrimers and other dendritic polymers*, Wiley, New York **2001**; n) Grayson, S. M. G.; Fréchet, J. M. J. *Chem. Rev.* **2001**, *101*, 3819-3868.
- 146 Denning, J. *Top. Curr. Chem.* Dendrimers V, **2003**, *228*, 621-672.
- 147 a) Venturi, M.; Serroni, S.; Junis, A.; Campagna, S.; Balzani, V. **1998**, *197*, 193-228. b) Balzani, V.; Ceroni, P.; Maestri, M.; Saudan, C.; Vicinelli, V. *Top. Curr. Chem.* Dendrimers V, **2003**, *228*, 159-191.
- 148 Tomalia, D. A. *Aldrichimica Acta* **2004**, *37*, 39-57.
- 149 Representative examples for the analysis of defects through mass spectrometry: a) Hawker, C. J.; Fréchet, J. M. J. *J. Am. Chem. Soc.* **1990**, *112*, 7638-7647. b) Liu, M.; Fréchet, J. M. J. *Polymer Bull.* **1999**, *43*, 379-386; c) Wolter, E. K.; Cloninger, M. J. *Org. Lett.* **2002**, *4*, 7-10; d) Engel, G. D.; Gade, L. H. *Chem. Eur. J.* **2002**, *8*, 4319-4329; e) Zhang, W.; Tichy, S. E.; Pérez, L. M.; Maria, G. C.; Lindahl, P. A.; Simanek, E. E. *J. Am. Chem. Soc.* **2003**, *125*, 5086-5094; e) Zimmerman, S. C.; Zharov, I.; Wendland, M. S.; Rakow, N. A.; Suslick, K. S. *J. Am. Chem. Soc.* **2003**, *125*, 13504-13518; f) Dirksen, A.; Hahn, U.; Schwanke, F.; Nieger, M.; Reek, J. N. H.; Vögtle, F.; De Cola, L. *Chem. Eur. J.* **2004**, *10*, 2036-2047.
- 150 a) Juo, C. G.; Shiu, L. L.; Shen, C. K. F.; Luh, T. Y.; Her, G. R. *Rap. Commun. Mass Spectrom.* **1995**, *9*, 604; b) Coullerez, G.; Mathieu, H. J.; Lundmark, S.; Malkoch, M.; Magnusson, H.; Hult, A. *Surf. Interface Anal.* **2003**, *35*, 682-692.
- 151 See, for example: a) Kawaguchi, T.; Walker, K. L.; Wilkins, C. L.; Moore, J. S. *J. Am. Chem. Soc.* **1995**, *117*, 2159-2165; b) Schwartz, B. L.; Rockwood, A. L.; Smith, R. D.;

- Tomalia, D. A.; Spindler, R. *Rap. Commun. Mass Spectrom.* **1995**, *9*, 1552-1555; c) Leon, J. W.; Kawa, M.; Fréchet, J. M. J. *J. Am. Chem. Soc.* **1996**, *118*, 8847-8859; d) Wendland, M. S.; Zimmerman, S. C. *J. Am. Chem. Soc.* **1999**, *121*, 1389-1390; e) Rheiner, P. B.; Seebach, D. *Chem. Eur. J.* **1999**, *5*, 3221-3236; f) Bu, L.; Nonidez, W. K.; Mays, J. W.; Tan, N. B. *Macromolecules*, **2000**, *33*, 4445-4452; g) Zhou, L.; Russell, D. H.; Zhao, M.; Crooks, R. M. *Macromolecules* **2001**, *34*, 3567-3573; h) Chen, H.; He, M.; Cao, X.; Zhou, X.; Pei, J. *Rap. Commun. Mass Spectrom.* **2004**, *18*, 367-370.
- 152 Selected examples: a) Kallos, G. J.; Tomalia, D. A.; Hedstrand, D. M.; Lewis, S.; Zhou, J. *Rap. Commun. Mass Spectrom.* **1991**, *5*, 383-386; b) Hummelen, J. C.; van Dongen, J. L. J.; Meijer, E. W. *Chem. Eur. J.* **1997**, *3*, 1489-1493; c) Tolic, L. P.; Anderson, G. A.; Smith, R. D.; Brothers II, H. M.; Spindler, R.; Tomalia, D. A. *Int. J. Mass Spectrom.* **1997**, *165/166*, 405-418; d) Puapaboorn, U.; Taylor, R. T. *Rap. Commun. Mass Spectrom.* **1999**, *13*, 508-515; e) Watanabe, S.; Sato, M.; Sakamoto, S.; Yamaguchi, K.; Iwamura, M. *J. Am. Chem. Soc.* **2000**, *122*, 12588-12589; f) Cohen, S. M.; Petoud, S.; Raymond, K. N. *Chem. Eur. J.* **2001**, *7*, 272-279; g) Rio, Y.; Accorsi, G.; Nierengarten, H.; Rehspringer, J.-L.; Hönerlage, B.; Kopitkovas, G.; Chugreev, A.; Van Dorsselaer, A.; Armaroli, N.; Nierengarten, J.-F. *New J. Chem.* **2002**, *26*, 1146-1154; h) Iavarone, A. T.; Williams, E. R. *J. Am. Chem. Soc.* **2003**, *125*, 2319-2327; i) Luostarinen, M.; Laitinen, T.; Schalley, C. A.; Rissanen, K. *Synthesis* **2004**, *2*, 255-262.
- 153 a) Blais, J.-C.; Turrin, C.-O.; Caminade, A.-M.; Majoral, J.-P. *Anal. Chem.* **2000**, *72*, 5097-5105; b) Felder, T.; Schalley, C. A.; Fakhrnabavi, H.; Lukin, O. *Chem. Eur. J.*, submitted.
- 154 a) Weener, J.-W.; Dongen, J. L. J.; Meijer, E. W. *J. Am. Chem. Soc.* **1999**, *121*, 10346-10355; b) Puapaboorn, U.; Taylor, R. T.; Jai-nhuknan, J. *Rap. Commun. Mass Spectrom.* **1999**, *13*, 516-520; c) Koster, S.; Duursma, M. C.; Guo, X.; van Benthem, R. A. T. M.; de Koster, C. G.; Boon, J. J.; Heeren, R. M. A. *J. Mass. Spectrom.* **2002**, *37*, 792-802; d) Adhiya, A.; Wesdemiotis, C. *Int. J. Mass Spectrom.* **2002**, *214*, 75-88; e) Neubert, H.; Knights, K. A.; de Miguel, Y. R.; Cowan, D. A. *Macromolecules* **2003**, *36*, 8297-8303; f) Koster, S.; Duursma, M. C.; Boon, J. J.; Heeren, R. M. A.; Ingemann, S.; van Benthem, R. A. T. M.; de Koster, C. G. *J. Am. Soc. Mass Spectrom.* **2003**, *14*, 332-341; g) He, M.; McLuckey, S. A. *Rap. Commun. Mass Spectrom.* **2004**, *18*, 960-972. h) Schalley, C. A.; Baytekin, B.; Baytekin, H. T.; Engeser, M.; Felder, T.; Rang, A. *J. Phys. Org. Chem.* **2006**, *19*, 479-490.
- 155 Some selected examples for MS-detected self-assembly through hydrogen bonding: a) Corbin, P. S.; Lawless, L. J.; Li, Z.; Ma, Y.; Witmer, M. J.; Zimmerman, S. C. *Proc. Natl. Acad. Sci. USA* **2002**, *99*, 5099-5104. Through metal coordination: b) van Manen, H.-J.; van Veggel, F. C. J. M.; Reinhoudt, D. N. *Top. Curr. Chem., Dendrimers IV* **2001**, *217*, 121-162.
- 156 a) Ong, W.; Kaifer, A. E. *Angew. Chem.* **2003**, *115*, 2214-2217; *Angew. Chem. Int. Ed.* **2003**, *42*, 2164-2167; b) Yamada, T.; Ge, M.; Shinohara, H.; Kimura, K.; Mashiko, S. *Chem. Phys. Lett.* **2003**, *379*, 458-465; c) Broeren, M. A. C.; van Dongen, J. L. J.; Pittelkow, M.; Christensen, J. B.; van Genderen, M. H. P.; Meijer, E. W. *Angew. Chem.* **2004**, *116*, 3541-3646; *Angew. Chem. Int. Ed.* **2004**, *43*, 3557-3562.
- 157 a) Hawker, C. J.; Fréchet, J. M. J. *J. Am. Chem. Soc.* **1990**, *112*, 7638-7647; b) Hawker, C. J.; Fréchet, J. M. J. *J. Chem. Soc., Chem. Commun.* **1990**, 1010-1013.
- 158 Schalley, C. A.; Verhaelen, C.; Klärner, F. G.; Hahn, U.; Vögtle, F. *Angew. Chem. Int. Ed.* **2005**, *44*, 477-480.
- 159 For reviews, see: a) Lifshitz, C. *Acc. Chem. Res.* **1994**, *27*, 138-144. Also, see: b) Howe, I.; McLafferty, F. W. *J. Am. Chem. Soc.* **1971**, *93*, 99-105; c) Siegel, A. *J. Am. Chem.*

- Soc. **1974**, 96, 1251-1252; d) Traeger, J. C.; McLoughlin, R. G. *J. Am. Chem. Soc.* **1977**, 99, 7351-7352; e) Cone, C.; Dewar, M. J. S.; Landman, D. *J. Am. Chem. Soc.* **1977**, 99, 372-376; f) McLafferty, F. W.; Bockhoff, F. M. *Org. Mass Spectrom.* **1979**, 14, 181-184; g) Moon, J. H.; Choe, J. C.; Kim, M. S. *J. Phys. Chem. A* **2000**, 104, 458-463; h) Malow, M.; Penno, M.; Weitzel, K.-M. *J. Phys. Chem. A* **2003**, 107, 10625-10630.
- 160 This statement is only an approximation to the real situation. Large ions can emit IR photons and thus the internal energy is decreased. We cannot exclude that this occurs for the larger dendrons as well to some extent, but the absence of any signals of higher generation benzyl cations in the mass spectra indicates that this process does not significantly contribute so that our argument would be changed.
- 161 Buhleier, E.; Wehner, W.; Vögtle, F. *Synthesis* **1978**, 155-158.
- 162 a) Aoyagi, M.; Biradha, K.; Fujita, M. *J. Am. Chem. Soc.* **1999**, 121, 7457-7458. b) Kim, Y.; Mayer, M. F.; Zimmerman, S. C. *Angew. Chem.* **2003**, 115, 1153-1158; *Angew. Chem. Int. Ed.* **2003**, 42, 1121-1126. c) Tashiro, S.; Tominaga, M.; Kusukawa, T.; Kawano, M.; Sakamoto, S.; Yamaguchi, K.; Fujita, M. *Angew. Chem.* **2003**, 115, 5742-5745; *Angew. Chem. Int. Ed.* **2003**, 42, 3267-3270. d) Kim, D. H.; Karan, P.; Göring, P.; Leclaire, J.; Caminade, A.-M.; Majoral, J.-P.; Gösele, U.; Steinhart, M.; Knoll, W. *Small* **2005**, 1, 99-102. e) Yamaguchi, T.; Tashiro, S.; Tominaga, M.; Kawano, M.; Ozeki, T.; Fujita, M. *Chem. Asian J.* **2007**, 2, 468-476.
- 163 a) Yoshikawa, I.; Sawayama, J.; Araki, K. *Angew. Chem.* **2008**, 120, 1054-1057; *Angew. Chem. Int. Ed.* **2008**, 47, 1038-1041. b) Boerakker, M. J.; Hannink, J. M.; Bomans, P. H. H.; Frederik, P. M.; Nolte, R. J. M.; Meijer, E. M.; Sommerdijk, N. A. J. M. *Angew. Chem.* **2002**, 114, 4413-4415; *Angew. Chem. Int. Ed.* **2002**, 41, 4239-4241.
- 164 a) Kellermann, M.; Bauer, W.; Hirsch, A.; Schade, B.; Ludwig, K.; Böttcher, C. *Angew. Chem.* **2004**, 116, 3019-3022; *Angew. Chem. Int. Ed.* **2004**, 43, 2959-2962; b) Ryu, J. -H.; Kim, H.-J.; Huang, Z.; Lee, E.; Lee, M. *Angew. Chem.* **2006**, 118, 5430-5433; *Angew. Chem. Int. Ed.* **2006**, 45, 5304-5307. c) Yan, Y.; Besseling, N. A. M.; de Keizer, A.; Marcelis, A. T. M.; Drechsler, M.; Stuart, A. C. *Angew. Chem.* **2007**, 119, 1839-1841; *Angew. Chem. Int. Ed.* **2007**, 46, 1807-1809; d) Radowski, M. R.; Shukla, A.; von Berlepsch, H.; Böttcher, C.; Pickaert, G.; Rehage, H.; Haag, R. *Angew. Chem.* **2007**, 119, 1287-1292; *Angew. Chem. Int. Ed.* **2007**, 46, 1265-1269.
- 165 a) Discher, D. E.; Eisenberg, A. *Science* **2002**, 297, 967-973. b) Antonietti, M.; Förster, S. *Adv. Mater.* **2003**, 15, 1323-1333. c) Opsteen, J. A.; Cornelissen, J. J. L. M.; Hest, J. C. M. V. *Pure. Appl. Chem.* **2004**, 76, 1309-1319. d) Tian, L.; Nguyen, P.; Hammond, P. T. *Chem. Commun.* **2006**, 3489-3491.
- 166 a) Ghoroghchian, P. P.; Frail, P. R.; Susumu, K.; Blessington, D.; Brannan, A. K.; Bates, F. S.; Chance, B.; Hammer, D. A.; Therien, M. J. *Proc. Natl. Acad. Sci. USA* **2005**, 102, 2922-2927. b) Li, Y.; Li, X.; Li, Y.; Liu, H.; Wang, S.; Gan, H.; Li, J.; Wang, N.; He, X.; Zhu, D. *Angew. Chem.* **2006**, 118, 3721-3725; *Angew. Chem. Int. Ed.* **2006**, 45, 3639-3643.
- 167 a) Messerschmidt, C.; Draeger, C.; Schulz, A.; Rabe, J. P.; Fuhrhop, J.-H. *Langmuir*, **2001**, 17, 3526-3531. b) Gohy, J.-F.; Lohmeijer, B. G. G.; Schubert, U. S. *Macromolecules*, **2002**, 35, 4560-4563. c) Gohy, J.-F.; Lohmeijer, B. G. G.; Décamps, B.; Leroy, E.; Boileau, S.; van den Broek, J. A.; Schubert, D.; Haase, W.; Schubert, U. S. *Polym. Int.* **2003**, 52, 1611-1618.
- 168 a) Vriezema, D. V.; Hoogboom, J.; Velonia, K.; Takazawa, K.; Christianen, P. C. M.; Maan, J. C.; Rowan, A. E.; Nolte, R. J. M. *Angew. Chem.* **2003**, 115, 796-800; *Angew. Chem. Int. Ed.* **2003**, 42, 772-776. b) Liu, Y.; Xu, J.; Craig, S. L. *Chem. Commun.* **2004**, 1864-1865. c) Zou, J.; Tao, F.; Jiang, M. *Langmuir* **2007**, 23, 12791-12794. d) Jin, B.; Chen, X.; Wang, X.; Yang, C.; Xie, Y.; Qiu, H. *Chem. Eur. J.* **2007**, 13, 9137-9142. e)

- Wang, Y.; Ma, N.; Wang, Z.; Zhang, X. *Angew. Chem.* **2007**, *119*, 2881-2884; *Angew. Chem. Int. Ed.* **2007**, *46*, 2823-2826. f) Chiper, M.; Meier, M. A. R.; Wouters, D.; Hoepfner, S.; Fustin, C.-A.; Gohy, J.-F.; Schubert, U. S. *Macromolecules* **2008**, DOI: 10.1021/ma0718954.
- 169 Li, D.; Zhang, J.; Landskron, K.; Liu, T. *J. Am. Chem. Soc.* **2008**, *130*, 4226-4227.
- 170 a) Hunter, C. A. *J. Am. Chem. Soc.* **1992**, *114*, 5303-5311. b) Hunter, C. A.; Jones, P. S.; Tiger, P.; Tomas, S. *Chem. Eur. J.* **2002**, *8*, 5435-5446.
- 171 Hunter, C. A.; Low, C. M. R.; Rotger, C.; Vinter, J. G.; Zonta, C. *Proc. Natl. Acad. Sci. USA* **2002**, *99*, 4873-4876.
- 172 a) Constable, E. C.; Meier, W.; Nardin, C.; Mundwiler, S. *Chem. Commun.* **1999**, 1483-1484. b) Qin, Z.; Jennings, M. C.; Puddephatt, R. *Chem. Commun.* **2002**, 354-355. c) Burchell, T. J.; Eisler, D. J.; Puddephatt, R. J. *Chem. Commun.* **2004**, 944-945. d) Kim, H.-J.; Zin, W.-C.; Lee, M. *J. Am. Chem. Soc.* **2004**, *126*, 7009-7014. e) Wackerly, J. W.; Moore, J. S. *Macromolecules* **2006**, *39*, 7269-7276.
- 173 a) Stang, P. J.; Cao, D. H. *J. Am. Chem. Soc.* **1994**, *116*, 4981-4982. b) Stang, P. J.; Whiteford, J. A. *Organometallics* **1994**, *13*, 3776-3777. c) Stang, P. J.; Cao, D. H.; Saito, S.; Arif, A. M. *J. Am. Chem. Soc.* **1995**, *117*, 6273-6283. d) Olenyuk, B.; Whiteford, J. A.; Stang, P. J. *J. Am. Chem. Soc.* **1996**, *118*, 8221-8230. e) Chatterjee, B.; Noveron, J. C.; Resendiz, M. J. E.; Liu, J.; Yamamoto, T.; Parker, D.; Cinke, M.; Nguyen, C. V.; Arif, A. M.; Stang, P. J. *J. Am. Chem. Soc.* **2004**, *126*, 10645-10656.
- 174 a) Fujita, M.; Yazaki, J.; Yamaguchi, K.; Ogura, K. *J. Am. Chem. Soc.* **1990**, *112*, 5645-5647. b) Fujita, M.; Ibukura, F.; Yamaguchi, K.; Ogura, K. *J. Am. Chem. Soc.* **1995**, *117*, 4175-4176.
- 175 Bisson, A. P.; Carver, F. J.; Eggleston, D. S.; Haltiwanger, R. C.; Hunter, C. A.; Livingstone, D. L.; McCabe, J. F.; Rotger, C.; Rowan, A. E. *J. Am. Chem. Soc.* **2000**, *122*, 8856-8868.
- 176 Blokzijl, W.; Engberts, J. B. F. N. *Angew. Chem.* **1993**, *115*, 796-800; *Angew. Chem. Int. Ed.* **1993**, *32*, 1545-1579.
- 177 Böttcher, C.; Schade, B.; Ecker, C.; Rabe, J. P.; Shu, L.; Schlüter, A. D. *Chem. Eur. J.* **2005**, *11*, 2923-2928.
- 178 Procedure adapted from: C. A. Hunter, *J. Chem. Soc., Chem. Commun.* **1991**, 749-751.
- 179 a) Goodall, W.; Wild, K.; Arm, K. J.; Williams, J. A. G. *J. Chem. Soc., Perkin Trans.* **2002**, 1669-1681. b) Aspley, C. J.; Williams, J. A. G. *New J. Chem.* **2001**, *25*, 1136-1147.
- 180 Matsuda, K.; Nakamura, N.; Takahashi, K.; Inoue, K.; Koga, N.; Iwamura, H. *J. Am. Chem. Soc.* **1995**, *117*, 5550-5560.
- 181 a) Newkome, G. R.; Cho, T. J.; Moorefield, C. N.; Cush, R.; Russo, P. R.; Godinez, L. A.; Saunders, M. J.; Mohapatra, P. *Chem. Eur. J.* **2002**, *8*, 2946-2954. b) Wang, P.; Moorefield, C. N.; Newkome, G. R. *Org. Lett.* **2004**, *6*, 1197-1200. c) Newkome, G. R.; Cho, T. J.; Moorefield, C. N.; Mohapatra, P. P.; Godinez, L. A. *Chem. Eur. J.* **2004**, *10*, 1493-1500.
- 182 Saygili, N.; Batsanov, A. S.; Bryce, M. R. *Org. Biomol. Chem.* **2004**, *2*, 852-857.
- 183 Wallace, K. J.; Hanes, R.; Anslyn, E.; Morey, J.; Kilway, K. V.; Siegel, J. *Synthesis* **2005**, *12*, 2080-2083.
- 184 Vacca, A.; Nativi, C.; Cacciarini, M.; Pergoli, R.; Roelens, S. *J. Am. Chem. Soc.* **2004**, *126*, 16456-16465.
- 185 Venkataramana, G.; Sankararaman, S. *Eur. J. Org. Chem.* **2005**, 4162-4166.
- 186 Procedure adapted from a) Rausch, D.; Lambert, C. *Org. Lett.* **2006**, *8*, 5037-5040. b) Lüning, U.; Eggert, J. P. W.; Hagemann, K. *Eur. J. Chem.* **2006**, 2747-2752. (-78 °C must be used in order to obtain the product!)

- 187 Bohm, A.; Arms, H.; Henning, G.; Blaschka, P. BASF, German Patent No. DE
19547209A1, **1997**.
- 188 Illigen, J. *Design und Synthese von Rotaxanen fuer die Einzelmolekuel- Spektroskopie
und massenspektrometrische Untersuchungen von Guanosin- Quartetts* Mathematisch-
Naturwissenschaftlichen Fakultät der Rheinischen Friedrich-Wilhelms-Universität
Bonn, Bonn, **2006**.
- 189 Schwetlick, K. *Organikum* 22. Aufl., Wiley, Weinheim, **2004**.
- 190 Geertz, Y.; Muscat, D.; Müllen, K. *Macromol. Chem. Phys.* **1995**, 196, 3425-3435.
- 191 Ranta, J. *Tetralactam Macrocycles as Building Blocks for Molecular Machinery*,
Jyväskylä University /Finland, **2008**.
- 192 McKiernan, G. J.; Hartley, R. C. *Org. Lett.* **2003**, 5, 4389-4392.
- 193 Procedure adapted from a work on calix[4]arenes: Klein, C.; Graf, E.; Hosseini, M.W.;
De Cian, A.; Kyritsakas-Gruber, N. *Eur. J. Org. Chem.* **2003**, 395-399.
- 194 Compounds shown in part **2.1** were supplied by Dr. Uwe Hahn. Control compounds **C1-
C6**: Procedures for the dendrimers were adapted from the following references and
bromo dendrimers obtained this way were mixed with excess triethylamine in
acetonitrile to achieve the final triethylammonium salts. (by Dr. H. Tarik Baytekin) As
discussed before bromination with CBr₄ is the neat way to obtain defect-free
dendrimers. a) C. J. Hawker, J. M. J. Fréchet, *J. Am. Chem. Soc.* **1990**, 112, 7638-7647.
b) C. J. Hawker, J.M. J. Fréchet, *J. Chem. Soc., Chem. Commun.* **1990**, 1010-1013.

Publication List

- 1 *A Modular “Toolbox” Approach to Flexible Branched Multi-Macrocyclic Hosts as Precursors for Multiply Interlocked Architectures*
Baytekin, B.; Zhu, S. S.; Brusilowskij, B.; Illigen, J.; Ranta, J.; Huuskonen, J.; Russo, L.; Rissanen, K.; Schalley C. A. **2008**, accepted..
- 2 *Hierarchical Self-Assembly of Metallo-Supramolecular Nano-Spheres*
Baytekin, H. T.; Baytekin, B.; Schulz, A.; Schalley, C. A. *Small*, **2008**, accepted.
- 3 *Mass spectrometric studies of non-covalent compounds: why supramolecular chemistry in the gas phase?*
Baytekin, B.; Baytekin, H. T.; Schalley, C. A. *Org. Biomol. Chem.* **2006**, 4, 2825-2841
- 4 *Mass Spectrometry as a Tool in Dendrimer Chemistry: From Self-Assembling Dendrimers to Dendrimer Gas-Phase Host-Guest Chemistry*
Schalley, C. A.; Baytekin, B.; Baytekin, H. T.; Engeser, M.; Felder, T.; Rang, A. J. *Phys. Org. Chem.* **2006**, 19, 479-490.
- 5 *How useful is mass spectrometry for the characterization of dendrimers? “Fake defects” in the ESI and MALDI mass spectra of dendritic compounds*
Baytekin, B.; Werner, N.; Luppertz, F.; Engeser, M.; Brüggemann, J.; Bitter, S.; Henkel, R.; Felder, T.; Schalley, C. A. *Int. J. Mass Spec.* **2006**, 138-148, 249-250.
- 6 *Towards Functional Macrocycles: Self-Assembly and Template Strategies*
Schalley, C. A.; Baytekin, H. T.; Baytekin, B. *Macrocyclic Chemistry: Current Trends and Future*, K. Gloe (Ed.), Springer, Heidelberg **2005**, 37-52.
- 7 *Theory and Experiment in Concert: Templated Synthesis of Amide Rotaxanes, Catenanes, and Knots*
Schalley, C. A.; Reckien, W.; Peyerimhoff, S.; Baytekin, B. and Vögtle, F. *Chem. Eur. J.* **2004**, 10, 4777-4789
- 8 *Novel fluorescent chemosensor for anions via modulation of oxidative PET: a remarkable 25-fold enhancement of emission*
Coskun, A.; Baytekin, B. T.; Akkaya, E. U. *Tet. Lett.* **2003**, 5649-5651.
- 9 *Modulation of Boradiazaindacene Emission by Cation-Mediated Oxidative PET*
Turfan, B.; Akkaya, E. U. *Org. Lett.* **2002**, 4, 2857-2859.
- 10 *Thermoreversible Gelation of Isotropic and Liquid Crystalline Solutions of a “Sticky” Rodlike Polymer*
Schmidtke, S.; Russo, P.; Nakamatsu, J.; Buyuktanir, E.; Turfan, B.; Temyanko, E. *Macromolecules* **2000**, 33, 4427-4432.

Oral Presentations

- 1 *A Lego-Box of Macrocycles and Rotaxanes*, G3 Summit, Berlin, 2007.
- 2 *Searching for the Missing Benzylic Daughter Mass Spectrometric Study on Fréchet-type Dendrimers with Ammonium Cores*, G3 Summit, Aachen, 2006.
- 3 *ESI-FTICR Mass Spectrometric Study on Fréchet-type Dendrimers with Ammonium and Ruthenium-tris-phenanthroline Cores*, G3 Summit, Oldenburg, 2005.
- 4 *ESI-FTICR Mass Spectrometric Study on Fréchet-type Dendrimers with Ammonium and Ruthenium-tris-phenanthroline Cores*, 2nd Supraphone Meeting (Supramolecular Photonics Network in Europe), Dresden, May 5-7, 2005.

Poster Presentations

- 1 *Hierarchical Self-Assembly of Metallo-Supramolecular Spherical Assemblies and their Characterization by NMR, ESI-FTICR, and TEM*, Baytekin, H. T.; Baytekin, B.; Springer, A.; Schulz, A.; Schalley, C. A. Tag der Chemie, April 23-24, Berlin, 2008.
- 2 *Towards Complex Threaded Molecular Architectures- Functionalized Macrocycles and Rotaxanes Serving As A Toolbox* Zhu, S. S.; Baytekin, B.; Brusilowskij, B.; Schalley, C. A. 113th BASF International Summer Course, July 23-August 3, BASF, Ludwigshafen, 2007.
- 3 *Functionalized Macrocycles and Rotaxanes : A Toolbox for Supramolecular Assemblies*, Baytekin, B.; Brusilowskij, B.; Zhu, S. S.; Illigen, J.; Schalley, C. A. . SFB Tagung, Münster, 20074*Mechanistic Detective Story: Tandem ESI-FTICR Mass Spectrometric Study on Fréchet Type Dendrimers*, Baytekin, B.; Baytekin, H. T.; Reckien, W.; Kirchner, B.; Schalley, C. A. 1st European Chemistry Congress, Budapest, August 27-31, Budapest, 2006.
- 5 *Design and Synthesis of Novel Fluorescent Chemosensors Based on Electron and Energy Transfer Phenomena*, XVI Ulusal Kimya Kongresi, September 10-13, Konya, Turkey, 2002.
- 6 *Design and Synthesis of Novel Fluorescent Chemosensors Based on Electron and Energy Transfer Phenomena*, 6th International Conference on Calixarenes, May 29-June 2, Enschede, The Netherlands, 2001.

Acknowledgements

First of all, of course, I would like to thank Prof. Christoph A. Schalley for the chance he has given me to complete my studies under his supervision, encouraging me to discover my own ways throughout the work and supporting my sometimes-crazy ideas. I am grateful not only for his guidance in chemistry and especially in mass spectrometry but also for his friendship and sincerity.

I am in debt to all my labmates especially Mr. Boris Brusilowskij for the fruitful discussions, collaborations, starting material exchange but above everything, for an absolute friendship. My far but not too far labmates Mr. Ralf Troff and Mr. Dominik Weimann should also be mentioned, since they took part in all our discussions in the coffee room and exchanged experience. I am grateful to Ms. Jenni Ranta who reproduced the chiral catenane and the corresponding macrocycles with great effort. My old lab mates in Bonn should not be forgotten. Special thanks to the “macrocycle” group: Dr. Thorsten Felder, Dr. Micheal Kogej, Dr. Jens Illigen and particularly Mr. Shuxia S. Zu. My pretty-new lab mates Mr. Wei Jiang and Mr. Qi Wang are also thanked.

Without the helping hand of Ms. Andrea Schulz, things could have been not so straight. I would like to thank her for introducing me to the new department and for her care for all the time I was in FU.

I also would like to acknowledge the NMR departments of both Bonn and Berlin, especially Dr. Andreas Schäfer and Ms. Anja Peucker for helping me with the standard measurements and sometimes with my strange wishes. I am grateful to all the mass department people particularly to Berlin, and Dr. Andreas Springer for the quick and diligent measurements at the FTCIR.

And above all, I would like to thank my parents Ece Turfan (who also proof-read this thesis) and Mümtaz Turfan for their continuous uphold at all times and my aunt and my uncle Perizat and Aydin Efe for their support during times I was in Berlin. Finally, I express my endless gratitude to my husband Dr. Tarik Baytekin for his help in the lab, for the productive discussions and guidance, for his never-ending backing and patience through all these years.